

Energy performance of ventilation, heating and cooling systems integrated in sandwich panel of high performance concrete

Tomás Mikeska

PhD Thesis

**Department of Civil Engineering
2015**

DTU Civil Engineering Report R-330
Juli 2015



Energy performance of ventilation,
heating and cooling systems integrated in
sandwich panel of high performance
concrete

PhD Thesis

Tomas Mikeska

Department of Civil Engineering

Technical University of Denmark

2015

Preface

This doctoral thesis was written in partial fulfilment of the requirements of my PhD study at the Section of Building Physics of the Department of Civil Engineering at the Technical University of Denmark (DTU) under the supervision of Professor Svend Svendsen and co-supervision of Assistant Professor Christian Anker Hviid.

The work in this thesis includes the results of measurements and CFD calculations which were both carried out at the Technical University of Denmark.

The work is described in four scientific papers which have either been published, accepted for publication, or submitted for publication in ISI journals. The thesis is subdivided into two separate parts. Part I includes an introduction and summary of the research papers, and Part II includes the collection of full-length scientific papers.

Acknowledgements

I want to express my sincere gratitude to my supervisor, Professor Svend Svendsen, who made this work possible and who supported me over the course of my PhD study. I very much appreciate that Svend always found the time for discussion, pointed me in the right direction, and stayed positive in times when I was frustrated. His valuable suggestions certainly enriched this work. I would like to thank to my co-supervisor, Assistant Professor Christian Anker Hviid, for his fruitful discussions and comments. Many thanks are also due to Associate Professor Jianhua Fan who supported me during the CFD investigations. I especially appreciate his patience in times when I was losing focus.

I am very grateful to Connovate A/S for their partial financial support of my studies and for providing the test building where all my measurements were carried out. My appreciation goes especially to Karsten Bro for his help throughout the project. I also want to acknowledge the financial and academic support of the Technical University of Denmark.

I want to express my appreciation to all my colleagues in the Section of Building Physics and Services for creating a friendly environment and making my stay at DTU a nice experience.

Special thanks go to my close friend and PhD fellow, Martin Kotal, who gave me a lot of good advice during the course of my PhD study and who has read through and commented on this thesis.

I want also to thank to all the friends I have in Denmark who made my stay here joyful and interesting.

I extend my most sincere thanks to my sister and my parents who greatly contributed to making my PhD possible and have always been there for me.

My very special thanks are addressed to my girlfriend, Jana, who has been a great support for me in difficult life situations and has always been an inspiration for me.

Lyngby, June 2015

Abstract

Spaces with a high density of occupants have high internal heat gains and need relatively high air change rates to be able to deliver the required amount of fresh air to the space. Classrooms often have elevated concentrations of CO₂ mainly as a result of limited air change rates. Using traditional mechanical ventilation diffusers, it is a challenge to supply large amounts of fresh air to the space without creating local discomfort for occupants. This often leads to spaces with poor indoor air quality and problems with overheating, which have a negative influence on the comfort, performance, and health of occupants. One solution to this problem is to use a diffuse ceiling inlet that supplies fresh air in the room through a large area of perforated suspended ceiling, so that the air supplied has a low velocity. However, such ventilation systems have limited cooling ability, because the cooling capacity of outdoor air is considerably decreased during the summer. A promising solution to this problem is to use radiant cooling systems integrated into the inner structures of building elements. The ventilation system can supply fresh air and remove latent heat gains, while the radiant cooling system can remove large amounts of sensible heat gain. The large areas of internal surface available for radiant systems can give an increase in cooling capacity without compromising the comfort of occupants.

The aim of the research for this thesis was to design, optimize and contribute to the development of new concepts of cooling, heating, and ventilation systems integrated into the sandwich wall elements made of high performance concrete. The goal was to find solutions that would work well with respect to energy efficiency and the indoor environment, and that would minimise the cost of components in a new building system made of high performance concrete.

This thesis reports on the behaviour of wall elements made of high performance concrete with an integrated water-based radiant cooling and heating system which has been developed over the course of the PhD study and implemented in a full scale test building. The designed system of radiant cooling and heating is based on plastic capillary tubes cast in the inner layer of wall elements made of high performance concrete. The plastic capillary tubes represent a way of implementing a radiant cooling and heating system in a thin building structure. The temperature distribution around the integrated plastic capillary tubes was studied using numerical calculations. Measurements were made to evaluate the dynamic behaviour of the room equipped with a wall radiant cooling system combined with a diffuse ceiling inlet for ventilation. The proposed solution for ventilation is based on a diffuse ceiling inlet for mechanical ventilation made of perforated gypsum board with airtight connections utilizing the full potential of a diffuse layer without undesirable crack flow. Methods applied in this work included measurements and numerical simulations. Measurements were carried out in the full scale test building. The test room represented a classroom with a high density of occupants. Theoretical investigations were carried out with a CFD model of the test room. The aim of the development of the CFD model was to allow for a deeper understanding of the diffuse ceiling inlet and wall radiant system and to facilitate efficient and economical optimization of the design taking into account various parameters.

The results of the investigations presented show that a diffuse ceiling inlet can successfully ventilate and cool the room with a high density of occupants using supply air at an average temperature of 21 °C. The resulting cooling power was 23 W/m² at a flow rate of 5.8 l/s·m² of floor area. The average air temperature in the test room was 24.5 °C. The cooling power of 32 W/m² was available at a flow rate of 8.0 l/s·m² of

floor area, which resulted in an average air temperature in the test room of 24 °C. This creates a comfortable indoor environment without draughts. Sufficient mixing was obtained mainly as a result of the interaction of incoming air and heat sources situated in the test room. The diffuse ceiling inlet can therefore be considered a well-performing alternative to the traditional means of mechanical ventilation in spaces with a high density of occupants. The results also show that plastic capillary tubes integrated in a layer of high performance concrete can provide the energy needed for cooling between 29 W/m² and 59 W/m² of floor area with cooling water temperatures between 22 °C and 18 °C. This resulted in indoor air temperatures of 24.5 °C and 22 °C, respectively, and a draught-free indoor environment.

The relatively high reaction speed of the designed system of radiant cooling was achieved as a result of the slim construction of high performance concrete. Measured values were used to validate a developed CFD model, with the aim of achieving a precise CFD model which can be used to evaluate indoor comfort numerically. The results show that transient calculations using Large Eddy Simulation turbulent models can give a good prediction of temperatures and air flow velocity magnitude in a room ventilated using a diffuse ceiling inlet. However, steady-state turbulent models needed to be applied to obtain adequate predictions in the rooms equipped with a wall radiant cooling system.

Dansk resume

I rum hvor mange personer opholder sig, vil der være et stort internt varmetilskud og behov for et relativt stort luftskifte, for at levere den nødvendige mængde frisk luft. Klasselokaler har ofte høje Koncentrationer af CO₂ hvilket hovedsagligt skyldes, at luftskiftet er begrænset. Ved hjælp af traditionelle armaturer til mekanisk ventilation, kan det være en udfordring at øge lufttilførslen i et givent rum, uden at der opstår gener for brugerne. Dette resulterer i rum med ringe indendørs luftkvalitet og problemer med overophedning, hvilket har en negativ indflydelse på brugernes komfort, ydeevne og helbred. En løsning på problemet er at anvende diffus lufttilførsel, hvor frisk luft tilføres rummet gennem et stort perforeret område i et nedhængt loft, hvilket resulterer i en lavere lufthastighed i indblæsningsluften. Sådanne ventilationssystemer giver til gengæld mindre mulighed for at køle luften, da kølekapaciteten af udendørs luft er betydeligt begrænset om sommeren. En lovende metode til at opveje for dette, er at anvende strålings-kølesystemer, der kan integreres i de indvendige bygningskomponenter. Strålings-kølesystemer kan fjerne store mængder sensibel varme fra luften, mens ventilationen kan tilføre frisk luft og samtidig fjerne den latente varme der afgives fra personer i rummet. Hvis der er store indvendige overfladearealer tilgængelige til brug som stråleflader, kan dette give øget kølekapacitet uden at gå på kompromis med brugernes komfort.

Formålet med forskningen præsenteret i denne afhandling har været at designe, optimere og bidrage med udvikling af nye koncepter for kølings-, opvarmnings- og ventilationssystemer, der er integreret i sandwich-vægelementer lavet af højstyrkebeton. Målet har været at identificere gode løsninger, med henblik på energieffektivitet, indeklima og minimerede komponentomkostninger for det nye bygningssystem af højstyrkebeton.

Denne afhandling beskriver hvordan et vægelement af højstyrkebeton og med integrerede løsninger for vandbaseret strålevarme eller -køling, som er blevet udviklet i løbet af Ph.D. studiet, opfører sig. Derudover beskrives implementeringen af elementet i en fuldskala test bygning. Det designede system for strålevarme og -køling er baseret på plastik kapillarrør, der er indstøbt i det inderste lag af et vægelement af højstyrkebeton. Plastik kapillarrørene gør det muligt at implementere strålevarmesystemer og -kølesystemer i en tynd bygningskonstruktion. Temperaturfordelingen omkring de integrerede plastik kapillarrør er blevet studeret gennem numeriske beregninger. Målingerne blev foretaget for at evaluere den dynamiske udvikling i testrummet, som var udstyret med strålekølingssystem i væggen og diffust ventilationsluftindtag i loftet. Den foreslåede løsning med mekanisk ventilation var baseret på at ventilationsluften blev tilført gennem et loft bestående af perforerede gipsplader med lufttætte samlinger, hvorved den diffuse lufttilførsel udnyttedes til fulde, uden at der utilsigtet tilføres luft gennem sprækker mellem pladerne. Metoderne der er anvendt i dette arbejde inkluderer målinger og numeriske simuleringer. Målingerne er udført i fuldskala testbygningen. Testrummet repræsenterede et klasselokale med et stort antal brugere. De teoretiske undersøgelser er blevet udført med en CFD-model af testrummet. Målet med CFD-modellen var at skabe en dybere forståelse for den diffuse tilførsel af ventilationsluft gennem loftspladerne og strålesystemet i væggen, for at kunne tage flere parametre i betragtning ved den økonomiske og energimæssige optimering af designet.

Resultaterne af de undersøgelser der er foretaget i afhandlingen, viser at diffus ventilation gennem loftsplader giver en god ventilation og afkøling i testrummet med mange brugere, ved en gennemsnitlig

temperatur på 21 °C for indblæsningsluften, resulterende i et kølepotentiale på 23 W/m² og 32 W/m² ved luftskifter på henholdsvis 6,6 gange i timen og 9,1 gange i timen. Dette giver et behageligt indeklima med en operativ temperatur på 24,5 °C, uden at der opstår træk. Der blev opnået tilstrækkelig opblanding af luften i rummet, hovedsagligt som et resultat af samspillet mellem indblæsningsluften og varmekilderne, som var placeret i testrummet. Det diffuse luftindtag gennem loftet kan derfor betragtes som et velfungerende alternativ til traditionelle mekaniske ventilationsløsninger. Resultaterne viste også at plastik kapillarrørene, der blev integreret i et lag af højstyrkebeton, kan afgive en køleenergi på 55 W/m² per gulvareal uden at skabe gener, når der i testrummet med mange brugere blev anvendt en vandtemperatur på 16,5 °C. Resultaterne viste at lufttemperaturen i rummet kan holdes indenfor et komfortabelt område ved at bruge kølende vand med en temperatur som kun er 5 K lavere end lufttemperaturen. Den relativt korte reaktionstid der blev opnået for det designede strålekølingssystem er et resultat af den tynde højstyrkebeton-konstruktion. Resultaterne fra de målte værdier blev brugt til at validere den udviklede CFD model, med det formål at skabe en præcis CFD model, der kan bruges til at evaluere indeklimaet numerisk. Resultaterne har vist, at transiente beregninger der gør brug af Large Eddy Simulation turbulente modeller er velegnede til at forudsige temperaturer og hastigheden af luftflowet i rummet, der blev ventileret gennem diffus ventilation via loftspladerne. Det var dog nødvendigt at tilføje steady-state turbulente modeller for at opnå en forudsigelse for rum udstyret med strålekølingssystem indbygget i væggen.

Table of Contents

Preface.....	i
Acknowledgements	iii
Abstract	v
Dansk resume	vii
Table of Contents	ix
List of papers	xiii
Abbreviations	xv
1. Introduction	1
1.1 Objective	3
1.2 Hypothesis	4
1.2.1 Main hypothesis.....	4
1.2.2 Sub-hypothesis.....	4
1.3 Limitations	5
2. Background	7
2.1 Indoor climate.....	7
2.1.1 Indoor air	7
2.1.2 Carbon dioxide.....	7
1.1.1 Sick Building Syndrome.....	8
1.1.2 Indoor air quality in classrooms and work places.....	8
2.1.3 Economical considerations	10
2.2 Energy savings in buildings	10
3. State of the art literature.....	13
3.1 Ventilation in buildings	13
3.1.1 Ventilation principles.....	13
3.1.2 Diffuse ceiling inlet	15
3.1.3 Design methods for ventilation diffusers	17
3.2 Radiant heating and cooling systems	17
3.2.1 History and development of radiant systems.....	17
3.2.2 Advantages of radiant systems.....	18
3.2.3 Limitations and drawbacks of radiant systems.....	19
3.2.4 Coupling of radiant systems to ventilation system.....	20

4.	Product design and development.....	23
4.1	Development of new building system	23
4.2	Scope of product development in the thesis.....	23
4.2.1	Process of product development in the thesis:	24
5.	Testing facility	29
5.1	Full scale test building.....	29
5.2	Radiant cooling system	31
5.3	Air handling unit.....	34
5.4	Diffuse ceiling inlet	36
6.	Measurements	39
6.1	Measuring apparatus.....	39
6.1.1	Temperature measurements.....	39
6.1.2	Air velocity measurements	44
6.1.3	Tracer-gas measurements	44
6.1.4	Pressure drop.....	44
6.1.5	Thermo-graphic investigation.....	44
6.2	Measurement and evaluation methods	44
6.2.1	Indoor climate.....	44
6.2.2	Temperature measurements.....	45
6.2.3	Velocity measurements	47
6.2.4	Tracer-gas measurements	48
7.	Numerical simulations	49
7.1	Model of the test room.....	49
7.2	Boundary conditions.....	49
7.3	Grid creation	50
7.4	Turbulence modeling	51
7.4.1	Steady-state turbulence modeling	51
7.4.2	Transient turbulence modeling	51
7.5	Porous zone modeling	51
7.6	Solver settings.....	52
8.	Methods of investigation used in research papers	53
9.	Summary of the research papers.....	55
9.1	Paper I.....	55

9.1.1	Investigated setup	55
9.1.2	Results and discussion	56
9.1.3	Conclusion.....	63
9.2	Paper II	64
9.2.1	Investigated setup	64
9.2.2	Results and discussion	64
9.2.3	Conclusion.....	69
9.3	Paper III	70
9.3.1	Investigated setup	70
9.3.2	Results and discussion	71
9.3.3	Complementary CFD investigation of air flow in the test room using tracer-gas methods (not included in Paper III)	81
9.3.4	Conclusions	84
9.4	Paper IV.....	86
9.4.1	Investigated setup	86
9.4.2	Results and discussion	86
9.4.3	Complementary investigations (not included in Paper IV)	91
9.4.4	Conclusions	96
10.	Practical use of radiant cooling systems.....	97
10.1	Software tool	97
10.1.1	Limitations	97
10.2	Validation of the model in IDA ICE.....	97
10.3	Setting up realistic model	99
10.4	Parameter investigation on realistic model.....	100
10.4.1	Wall to floor ratio.....	100
10.4.2	Effect of condensation on operation of radiant cooling.....	103
10.4.3	Sun radiation influence	107
10.4.4	Temperature of supply water	108
10.4.5	Heat flux from the cooling surface	110
10.4.6	Heat loads variations	110
11.	Discussion on hypotheses.....	113
12.	Conclusions on hypotheses	121
13.	Recommendations for further work.....	123

Bibliography..... 125

List of papers

- I. Mikeska T. , Fan J., Full Scale Measurements and CFD Simulations of Diffuse Ceiling Inlet for Ventilation and Cooling of Densely Occupied Rooms, *Accepted for publication in Energy and Buildings Journal, 2015.*
- II. Mikeska T., Svendsen S., Study of thermal performance of capillary micro tubes integrated into the building sandwich element made of high performance concrete, *Published in Applied Thermal Engineering Journal 52 (2013) 576-584*
- III. Mikeska T., Fan J., Svendsen S., Full scale measurements and CFD investigations of wall radiant cooling system based on plastic capillary tubes in thin concrete walls, *Accepted with major revision to Energy and Buildings Journal, 2014.*
- IV. Mikeska T., Svendsen S., Dynamic behavior of radiant cooling system based on capillary tubes in walls made of high performance concrete, *Accepted with minor revision to Energy and Buildings Journal, 2014.*

Abbreviations

CFD	Computational Fluid Dynamics
CO ₂	Carbon Dioxide
EU	European Union
IAQ	Indoor Air Quality
PMV	Predicted mean vote
PPD	Predicted percentage of dissatisfied
SBS	Sick Building Syndrome
USA	United States of America

Part I

Introduction and summary of research

1. Introduction

The thermal insulating properties and air tightness of new and renovated buildings have improved considerably in recent decades. This has certainly decreased the energy consumption of these buildings, but has also contributed to problems with indoor environment because mechanical ventilation systems were not installed. Such serious omissions suggest that there was little focus at the time on indoor climate and indoor air quality (IAQ). Modern buildings often have poor IAQ as a result of the combined effect of airtight envelopes and either the lack of a ventilation system or the selection of the wrong type or design of ventilation. Indoor environment deserves much more attention than it used to get, because people spend most of their lifetime indoors, in some regions up to 90% [1]. For those concerned, the indoor environment is the most important environment for human health [2]. Allergies and asthma have increased worldwide in recent decades and have been associated with poor indoor air quality [2]. Classrooms, being spaces with a high density of occupants, have been repeatedly observed as having high concentrations of CO₂ mainly as a result of limited supply air flows and the overall bad design of ventilation systems. Consequently, many classrooms report health problems, often described as sick building syndrome, reduced concentration in students resulting in low educational performance, and reduced attendance. [3], [4], [5].

The focus on energy efficiency and energy savings in buildings is increasing globally as a result of the rather high prices of energy on worldwide markets. Energy consumption is increasing worldwide, and it is predicted that the world energy consumption will grow about 1.6% per year from 2011 to 2030 [6]. The European Union energy policy gives a high priority to energy savings and the use of renewable energy. A building sector is responsible for about 40% of our overall energy consumption. A very similar situation is found in the United States of America where the building sector consumes about 41% of the total energy [7]. The European Union requires its member states to lower the energy used in new buildings close to the level of “nearly zero energy” buildings by 2018 in the case of public buildings and by 2020 in the case of other buildings [8]. Buildings with such low energy use can be realized by using highly insulated building envelopes, high performance windows, high performance heating and cooling systems, and ventilation systems with heat recovery. The highly insulated sandwich wall element made of high performance concrete is an interesting alternative for the façades of future low energy buildings. It offers a way of implementing a thick insulation with a minimum of total wall thickness, because the thickness of the concrete plates is only a few centimetres. This is possible thanks to the use of concrete with high strength. The resulting wall element has better thermal performance characteristics than conventional products with the same thickness. A low weight of wall element is also a benefit, because savings are made on transport and lifting on the building site. Solutions made of high performance concrete are environmentally friendly since the low amount of concrete material used results in low CO₂ emissions during its production.

Regulatory institutions are becoming more aware about the importance of proper air exchange in buildings. Mechanical systems for ventilation need to become standard equipment for all new buildings because it is not possible to achieve the required low energy consumption in buildings using natural ventilation. In the case of mechanical ventilation, applying heat recovery can save energy that would otherwise be lost with natural ventilation. Traditional mixing and displacement ventilation diffusers are the most commonly used types of diffusers for installations in buildings occupied by humans. However, there are situations where traditional types of ventilation diffusers are not able to deliver the required amount of conditioned air in comfortable ways and are not able to remove large internal heat gains. Spaces with a high density of occupants are often difficult to ventilate using traditional ventilation diffusers. A diffuse ceiling inlet used as a supply diffuser seems to be a good alternative to traditional ventilation diffusers for spaces such as classrooms, meeting rooms and conference centres. A diffuse ceiling inlet is characterized by the activation of a large area of suspended ceiling as an inlet diffuser. The fresh air enters the space at very low velocity, and large amounts of fresh air can then be supplied to the space without a risk of creating draughts. The results of previous investigations have shown that a diffuse ceiling inlet is able to handle higher thermal loads and higher flow rates than five traditional ventilation systems [9]. Investigations into the cooling benefits of diffuse ceiling inlet have shown reduced hours of overheating in the room [10]. Investigations in this thesis show that a diffuse ceiling inlet can successfully ventilate and cool rooms with a high density of occupants with supply air at a temperature of 21 °C. The resulting cooling power was 23 W/m² for a flow rate of 5.8 l/s·m² of floor area. The average air temperature in the test room was 24.5 °C. A cooling power of 32 W/m² was obtained for a flow rate of 8.0 l/s·m² of floor area, which resulted in an average air temperature in the test room of 24 °C.

Spaces with a high density of occupants can experience overheating rather easily as a consequence of the effect of high internal heat gains and highly insulated building envelopes. It can become a challenge to cool such spaces with ventilation systems while keeping a comfortable indoor climate at the same time. Draught can be created as a result of large amounts of cold air being supplied to the space. Furthermore, the cooling ability of ventilation system is reduced during the summer because of the limited cooling capacity of outdoor air. One option to solve this problem is the installation of a radiant cooling system in conjunction with a ventilation system. Radiant cooling systems are integrated in the structure of the building, in the ceiling, floor or walls. The large areas of internal surface available for radiant cooling systems result in increased cooling capacity without compromising occupant comfort. Investigations in this thesis show that a wall radiant cooling system combined with a diffuse ceiling inlet can create a comfortable indoor climate in a classroom with a high density of occupants. The low temperature difference between the cooling water and the room air allows the use of natural sources of cold water such as ground and sea water. The results show that plastic capillary tubes integrated into a layer of high performance concrete can provide the energy needed for cooling between 29 W/m² and 59 W/m² of floor area with temperatures of cooling water between 22 °C and 18 °C. The indoor air temperature was 24.5 °C – 25 °C when a cooling power of 29 W/m² was used and 22 °C – 23 °C when a cooling power of 59 W/m² was used.

Among the methods applied in this research were measurements and numerical simulations. A test building specifically built for the purpose of testing proposed solutions for ventilation and cooling was used for measurements. The test room represented a classroom with a high density of occupants. Theoretical investigations were carried out using a CFD model of a test room developed in the software Ansys Fluent. The outputs from measurements were used for the specification of boundary conditions in a CFD model and to validate the model. The dynamic effects of the designed wall radiant cooling system were investigated by measuring the response times to changes in a control system. The indoor climate of a test room equipped with a wall radiant cooling system and a diffuse ceiling inlet was investigated under steady-state and transient situations. The validated CFD model was used for thorough parametrical analysis.

New solutions for the ventilation and cooling of buildings need to be designed and developed to create a comfortable indoor climate in an optimal way. The building sector is experiencing growing industrialization and the idea for the buildings of the future is that they will be composed of individual building components which have been produced industrially in production factories [11]. Product development methods will be applied during the design process to allow for maximal prefabrication of the products developed. The proposed solution for cooling is based on a fully prefabricated complete wall sandwich element with integrated cooling systems based on plastic capillary tubes cast in the inner layer of high performance concrete. The proposed solution for ventilation is based on a diffuse ceiling inlet for mechanical ventilation made of perforated gypsum boards.

To the best of the author's knowledge, no work has previously been done on an application where plastic capillary tubes have been installed in a layer of high performance concrete and used as a radiant cooling system. New knowledge about the performance of radiant cooling systems made of plastic capillary tubes cast in a thin layer of high performance concrete is presented in this thesis. The literature review did not reveal any case of a diffuse ceiling inlet based on acoustic ceiling gypsum boards with absolutely airtight connections distributing the supply air equally over the whole area of suspended ceiling.

1.1 Objective

The aim of the research was to analyse, optimize and contribute to the development of new concepts for cooling, heating, and ventilation systems integrated into sandwich elements made of high performance concrete. The aim was also to explore various possibilities for the integration of cooling and ventilation systems and to identify the challenges involved in the production of such systems.

The goal was to find solutions that work well with respect to energy efficiency and the indoor environment and that would minimise the total cost of the new building system made of high performance concrete.

The idea and effort behind the thesis was to present the knowledge on how new concepts of cooling and ventilation systems can be designed and developed as an integrated part of highly insulated building elements.

1.2 Hypothesis

1.2.1 Main hypothesis

Wall radiant cooling systems based on plastic capillary tubes integrated into a thin layer of high performance concrete can provide sufficient cooling and heating power in classrooms with high internal heat gains. A low temperature difference between cooling (heating) water and room air can be successfully used. When combined with a diffuse ceiling inlet for ventilation which supplies large amounts of fresh air into a room, this solution results in a comfortable indoor climate without any local discomfort.

1.2.2 Sub-hypothesis

Sub-hypothesis 1

“A diffuse ceiling inlet for ventilation of classrooms with a high density of occupants can work without local discomfort when supplying large amounts of fresh air, and give a good indoor climate.”

Sub-hypothesis 2

“Radiant heating and cooling systems based on plastic capillary tubes installed in a thin layer of high performance concrete can provide sufficient power to heat or cool the space using a low temperature difference between heating or cooling water and room air, and therefore allow the use of natural sources of energy, such as ground water and sea water for cooling and solar heat for heating.”

Sub-hypothesis 3

“A wall radiant cooling system combined with a diffuse ceiling inlet for ventilation can provide a comfortable indoor climate in classrooms with a high density of occupants and does not cause any discomfort in the form of draught.”

Sub-hypothesis 4

“The dynamic response of a wall radiant cooling system based on plastic capillary tubes installed in a thin layer of high performance concrete is fast enough to provide cooling capacity faster than the cooling load is developed, so that the operative temperature in the room remains in a comfortable range.”

Sub-hypothesis 5

“CFD can predict indoor environment with acceptable precision and therefore can be used in engineering practice to make the design process more efficient, especially in the first stages of a project and product development.”

Sub-hypothesis 6

“Radiant systems in the form of plastic capillary tubes can be cast in a layer of high performance concrete that is only 30 mm thick without the casting process itself significantly affecting the project financially.”

Sub-hypothesis 7

“The theoretical and measured findings from this work can be generalized in the way to be sufficient for the use as assessment of the radiant cooling systems in practice”

The hypotheses were investigated in the research for this thesis and the four appended papers.

Paper I describes how the 2D heat flow in the wall element made of the high performance concrete with integrated plastic capillary tubes for heating and cooling was investigated using the finite difference program HEAT2. Various configurations of plastic capillary tubes were investigated to give an idea about performance of such systems. The research question was whether radiant heating and cooling system based on plastic capillary tubes installed in a thin layer of high performance concrete can provide sufficient power to heat or cool the space, making use of the low temperature difference between heating or cooling water and room air and therefore allowing the use of natural sources of energy. **Paper I** gives useful information on the usability of very thin plastic capillary tubes in this project.

Paper II deals with a diffuse ceiling inlet which was used to ventilate a classroom with a high density of occupants. The investigation includes a comparison of measurements and calculations of its performance. The main interest was to answer the question of whether a diffuse ceiling inlet used for ventilation of classrooms with a high density of occupants can work without local imbalances, which would result in local discomfort when supplying large amounts of fresh air, and whether it is able to cool the room.

Paper III provides information on the performance of a wall radiant cooling system combined with diffuse ceiling ventilation to create an optimal indoor climate in a classroom with a high density of occupants. The research question was: Can activation of a wall radiant cooling system combined with a diffuse ceiling inlet for ventilation provide a comfortable indoor climate in classrooms with a high density of occupants? Also of interest was to find out whether the wall radiant cooling system would cause discomfort in the form of draught in the proximity of the cooled wall.

Paper IV deals with the investigation of the dynamic behaviour of the designed system for cooling. Special attention was paid to the situation when occupants enter the room and the system for radiant cooling is activated. The research question here was whether the dynamic response of a wall radiant cooling system based on capillary plastic tubes installed in a thin layer of high performance concrete would be fast enough to provide the cooling capacity faster than the cooling load developed, so that it could ensure a comfortable indoor climate.

1.3 Limitations

All the measurements took place in a test building situated in an outdoor environment. The boundary conditions for such a facility differ very much from laboratory conditions in which such measurements are usually made. Therefore the main limitation was a constantly changing outdoor environment influencing the heat loss through the façade of the test facility

2. Background

The main purpose of buildings has always been to create living environment which would be better than outdoor conditions. In early days this certainly included shielding against a rain and wind and a control of temperature.

During last decades a thermal performance of buildings has improved dramatically as a result of the use of thick layers of a thermal insulation in building envelopes and well-performing, airtight windows. The need for installation of ventilation system in such buildings was often not respected and omitted. This combination can result in buildings which are not favourable for living and occupants can experience various health issues. Allergies and asthma have increased worldwide over the last 30 years and they are associated to environmental exposures including stay in buildings with a poor IAQ [2].

This severe situation has therefore given impulses to a research in relevant fields in order to improve it. As a problem is rather complex it is still challenging nowadays to solve it in an optimal way. New systems for ventilation, heating and cooling of buildings need to be designed and developed in order to create a comfortable and healthy indoor climate in spaces with a high density of occupants in an optimal way.

2.1 Indoor climate

2.1.1 Indoor air

The importance of good indoor air quality is based on a fact that people spend substantial amount of time exposed to indoor air. According to statistical records from Canada and USA, people spend about 15-16 hours per day in indoor environment [12]. This does not include the time spent in other “enclosures” such as cars. In some regions people spend up to 90% indoors [1]. From presented findings it can be concluded that indoor environment is the most important environment concerning human health [2]. Indoor air is a rather complex composition containing except oxygen and CO₂ also nitrogen, water vapour, volatile organic compounds and other solid particles. The pollution of an indoor air can come partly from the outside environment and partly from indoor sources, including human beings, furniture, equipment and a building material [13].

2.1.2 Carbon dioxide

CO₂ concentration is often used to assess an IAQ. CO₂ concentration indicates human activity that is connected to a production of moisture, aerosols, dust particles and bioeffluents. This makes CO₂ concentration a good indicator of an indoor air quality in general [14]. It was Pettenkofer who started to use concentration of CO₂ as an indicator of IAQ already in the middle of 19th century [15]. He proposed that the value of CO₂ concentration of 1000 ppm should be used as a maximum for well ventilated spaces. It is worth mentioning that this value is still used in different regulations and standards today. Pettenkofer did not see CO₂ concentration itself to be of any harm, he rather connected it with other substances present in the air which created an odor leading subsequently to discomfort for occupants. An odor is created beside CO₂ also by aldehydes, esters and alcohols, generally called bioeffluents. Their concentration in the air is usually low to cause any harm to a human body [14]. A resulting odor can however weaken an immune system which is a main precondition for any following health issues [2]. The IAQ is usually classified based

on a perception of people entering a room. A percentage of people dissatisfied with an indoor air quality based on CO₂ concentration is a rather convenient way to assess an indoor air quality, see Figure 1 [14].

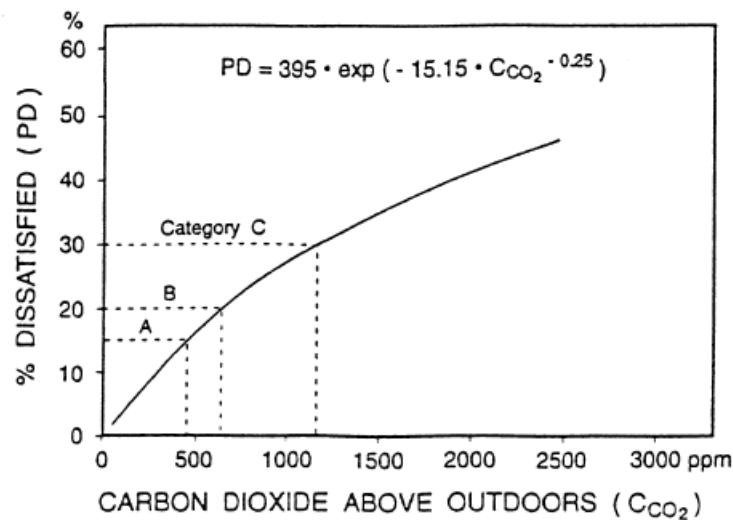


Figure 1: CO₂ as an indicator of human bioeffluents [14]

CO₂ is produced by humans proportionally to their metabolic rate [14]. CO₂ present in indoor air in small quantities is not harmful, as it is a natural compound of the outdoor air as well. The present average value of CO₂ concentration in the outside air outside of the city areas is about 370-380 ppm [16]. Presence in a space with a high concentration of CO₂ can however have negative effects on a human health and performance and can lead to problems very often described as a sick building syndrome (SBS) [17]. Pettenkofer recommended that rooms where people stay for longer period of time should have concentration of CO₂ lower than 700 ppm in order for people to feel comfortable.

1.1.1 Sick Building Syndrome

SBS can be defined by rather a large number of symptoms including a throat, eye and nose irritation, a tiredness, headaches, a dry skin, a cough and in extreme case also a nausea and dizziness [13], [18], [19]. In order to assign those symptoms to SBS, a statistically valid association of SBS symptoms with a particular building should be defined [18]. The main assumption, when assessing SBS, is that people being investigated do not have any symptoms when entering a building and they have the symptoms when leaving a building. This is the main precondition to association of SBS symptoms to a building. However, an assessment is rather complicated, since there are many other factors which can influence a development of symptoms in investigated people. Some of the factors are social interactions with other people in buildings, job relations and a general emotional state. A research on an influence between ventilation flow rates and SBS is very complicated due to complex relations, but it is evident that there is a link between an air change rate and prevalence of SBS [20].

1.1.2 Indoor air quality in classrooms and work places

Classrooms have generally rather poor indoor environment, which was found by many researchers in separate studies [3], [4]. It can be anticipated that reasons are bad choice of ventilation system and generally poor design of a building itself. Schools are typical places where it is relatively easy to observe a negative effect of an elevated concentration of CO₂ as a density of people in a classroom is usually high and

the learning tasks require a good concentration. Many studies about a CO₂ concentration effect on a human health and performance were therefore carried out in educational buildings. Furthermore, most of the schools are based in old buildings, where there is a high probability of an occurrence of elevated emissions from building materials and a mold growth which can further worsen an IAQ. It does not come then as a surprise that classrooms often report health problems very often described as a SBS and also reduced concentration of students resulting in a low educational performance.

Wargocki and Wyon observed an increased performance among students when an outdoor air supply was increased from 4 l/s to 10 l/s [3]. Seven independent field studies were done in five different schools with 380 children situated in Denmark and Sweden. According to authors can be performance of children in schools increased up to 30% in comparison to the performance of students in indoor climate of an average educational institution.

A large study in schools was carried out in Finland [4]. The results of questionnaire from 297 schools were used to assess an IAQ. A ventilation rate and thermal conditions were measured in sample of 56 schools. A measured mean ventilation flow rate per student was 5.7 l/s, which was rather high and close to standard requirements. Regardless good ventilation flow rates, some negative effects of an IAQ were reported. Weekly symptoms included a fatigue (7.7%), stuffy nose (7.3%) and headache (5.5%). The most often reported daily inconvenience was however a noise (11.0%).

Other types of spaces such as offices and call centers have also similar findings. Wyon in his experiment found that a poor IAQ can result in a decrease of office-work related performance by up to 9% [21]. Author also concluded that there is a linear relationship between a decreased performance of people and percentage of people dissatisfied with indoor climate. Wargocki et al. carried out investigations about a relation between a ventilation flow rate and effects of a SBS, perceived air quality and productivity in an office room with ventilation flow rates of 3 l/s, 10 l/s and 30 l/s per person [5]. This corresponded to an air change rate of 0.6 h⁻¹, 2 h⁻¹ and 6 h⁻¹. Authors found that productivity increased by 1.7% for every two-fold increase in a ventilation flow rate between 3 l/s and 30 l/s per person consistently for various tasks such as typing and proof-reading. At the same time the perceived air quality was improved and symptoms of SBS decreased when the ventilation flow rate was increased. This work had various advantages over similar studies carried out until that time. Firstly, the only changing variable was a ventilation flow rate. Other boundary conditions were kept the same for the whole time of experiments, which could be challenging in field studies. Secondly, the ventilation flow rates were measured with rather high precision. Thirdly, the air was mixed properly for each experiment. Fourthly, authors avoided the use of a traditional air handling unit as it could be very often a source of pollution for a building. The outdoor air was supplied into an office room by the use of axial fans mounted in a window, without the use of a filtration or air-conditioning [5].

Seppanen carried out a literature study of existing literature relating a work performance to ventilation air change rates in offices [22]. He found that an increase of performance was statistically significant when ventilation flow rates were increased up to 15 l/s per person. The results of his review stated that an increase in performance was 2% to 3.5% per 10 l/s per person in a ventilation range 6.5 l/s to 10 l/s per person, 1% to 2% in a ventilation range 10 l/s to 20 l/s per person and 0.5% to 1% in a ventilation range of 20 l/s to 40 l/s per person. Nearly a negligible increase of performance was related to ventilation flow rates over 45 l/s per person [22]. The health and performance benefits for occupant per additional unit of ventilation will be diminished at higher ventilation flow rates [20].

Seppanen did a review of 21 studies investigating association of CO₂ concentration with human responses in office buildings [20]. Firstly he found that 10 out of 15 buildings did not deliver a minimum ventilation flow rate for which ventilation systems were designed. He argues that the reason could be that codes and standards specify minimum ventilation flow rates for a design of a ventilation system, however not for an operation of a designed system. He suggests that new building codes should specify minimum ventilation flow rates during occupancy of buildings [20]. Author stated that all investigated studies found a statistically significant increase in SBS symptoms for ventilation flow rates below 10 l/s per person. The SBS symptoms were lowered with decreasing CO₂ concentrations below 800 ppm [20]. However a generally accepted level of CO₂ concentration in most of the typical buildings is 1000 ppm [13], [23].

The findings presented in the previous text rise a question if the generally accepted value of 1000 ppm of concentration of CO₂ in standards is not too high. Author of the study dealing with a direct effect of elevated CO₂ concentrations on a human health stated that people sense the decreased quality of air in a room when CO₂ concentration is 600 ppm and most people experience some of the symptoms described as a SBS in levels of 1000 ppm [16]. The same author stated that the toxic level of CO₂ concentration over a life-time exposure is 426 ppm [24]. Pettenkofer already in 19th century stated that a concentration of CO₂ should not rise above 700 ppm in rooms where people stay for longer time. As we already know, considerably large number of people living in western society spends nearly 90% of their time in artificial indoor environment including buildings and transportation [1]. As it was already mentioned, the concentration of CO₂ in reasonably well designed and maintained buildings is expected to be about 1000 ppm. The conclusion is very alarming since presented studies suggest that some people spend most of their lifetime in environment with unacceptably high concentrations of CO₂.

The study carried out by Shendell et al. focused on relation between CO₂ concentration and student attendance in 22 schools across states Washington and Idaho [25]. Authors found that an increase in indoor concentration of CO₂ 1000 ppm above outdoor concentration was linked to a 10% to 20% relative increase in student absence. Ventilation flow rates were less than required 7.5 l/s per person in at least 50% of investigated classrooms based on measurements of CO₂ concentration.

2.1.3 Economical considerations

The flow rates between 10 l/s and 20 l/s per person leads not only to improved health conditions, but also to increased productivity of people and lower absence rate, altogether having economic advantages [20]. Operating costs of air conditioning systems are less than 1% of labor costs [5]. However, a 10% increase in percentage of dissatisfied with indoor climate leads to a decrease in performance of office workers of 1% [1]. A payback time of investment into improved indoor climate is less than 2 years [13].

2.2 Energy savings in buildings

The focus on energy efficiency and energy savings in buildings is increasing globally. The safety of energy delivery is a motivator for governments to support energy savings and use of renewable sources of energy. If the "IDA Climate Plan 2050" is followed, Denmark could become independent on imports of fossil fuels by 2050 [26]. By the same time, Denmark can reduce its CO₂ emissions by 90% [26].

From economical point of view the high price of energy on worldwide markets is strong motivator not only for governments but also for the private sector to take the action. Energy consumption increases

worldwide and it is predicted that world energy consumption will grow 1.6% per year from 2011 to 2030 [6]. Population and income growth are main reasons behind growing energy consumption. The trend of growing prices of energy can be expected also in the near future. The EU energy policy gives high priority to energy savings and use of renewable energy. As the building sector is responsible for about 40% of overall energy consumption in the society, the need for appropriate action is understandable. The EU requires its member states to lower the energy use in new buildings close to level of “nearly zero energy” buildings by 2018 in case of public buildings and by 2020 in case of any other buildings [8]. The similar situation is in the USA where building sector consume about 41% of total energy [7] On the worldwide scale, the fraction of energy used for buildings is about 24% [27].

Owners of buildings are therefore motivated / directed to be more interested in innovative and technically advanced solutions without which it would be difficult to reach nearly zero energy buildings. The need for development of competitive energy efficient solutions for new generation of buildings motivates the research activities within this sector.

3. State of the art literature

The following chapters summarize the state of the art literature concerning ventilation in buildings and the use of radiant systems for heating and cooling in buildings.

3.1 Ventilation in buildings

As presented in section 2.2, the requirements for energy consumption in buildings constructed in the near future are rather strict. Mechanical systems for ventilation need to become standard equipment for all newly constructed buildings as it is not possible to keep required low energy consumption in buildings with use of natural ventilation. In case of mechanical ventilation, applying a heat recovery can save considerable amount of energy otherwise being lost with use of natural ventilation.

The main purpose of ventilation in buildings is to create healthy and comfortable indoor environment. This is done by supplying a fresh, outside air into the occupied space and removing polluted air out of the building. The air must be supplied into the designed space in the way that thermal comfort requirements are met and occupants experience healthy and comfortable IAQ. The special attention should be paid to draught-free design of occupied zone [28]. That can be rather challenging in certain types of spaces as will be discussed in more details in section 0. The requirements for ventilation in different types of buildings are usually set by each country on national level. However, the attempt of EU is to unite the requirements so those would become the same for whole EU [29], [14]. The importance of proper air exchange in buildings is becoming more and more known among regulatory institutions and building engineers. Poor ventilation of buildings may have an effect on various illnesses developed among people occupying such buildings, as described in section 1.1.1.

3.1.1 Ventilation principles

The ventilation principles can be divided into mechanical ventilation, natural ventilation and hybrid ventilation (which aims to combine benefits of the two). Until very recently, majority of residential buildings used natural ventilation principles to exchange the air in the building. The mechanical ventilation was used more often in offices, educational and representative buildings where there was a need for better air quality and/or air-conditioning. In the last decade mechanical ventilation became more common also in residential buildings as a result of energy saving intentions.

Concerning the distribution of the air in the room, different ventilation principles are known. There are three main principles of mechanical ventilation being used in most of the buildings nowadays. The most often used principle is mixing ventilation. Mixing ventilation works on principle of supplying the fresh air into the space with rather high velocity (high momentum) causing mixing of incoming air with air present in the room [30], see Figure 2 (where t_r is temperature of room air, t_i temperature of inlet air and t_u is temperature of used air). Special types of diffusers are usually installed to generate high momentum.

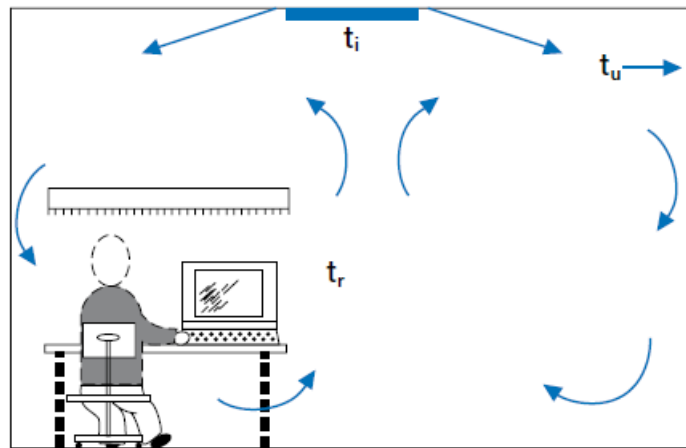


Figure 2: Mixing ventilation principle [30]

Second type commonly used is displacement ventilation working on principle of supplying an air into the room in low velocities and close to the floor surface, see Figure 3 (where t_r is temperature of room air, t_i temperature of inlet air and t_u is temperature of used air). The inlet air should have lower temperature than room air to ensure the proper distribution in the room. The movement of the air is then caused by buoyancy principles due to the heat sources situated in the room [30]. The old air is replaced with new, fresh air which results in higher ventilation efficiency. In most cases the heat sources are also pollution sources (occupants present in the room). The proper design of displacement ventilation system results in creation of a polluted air layer close to the ceiling and good IAQ in occupied zone.

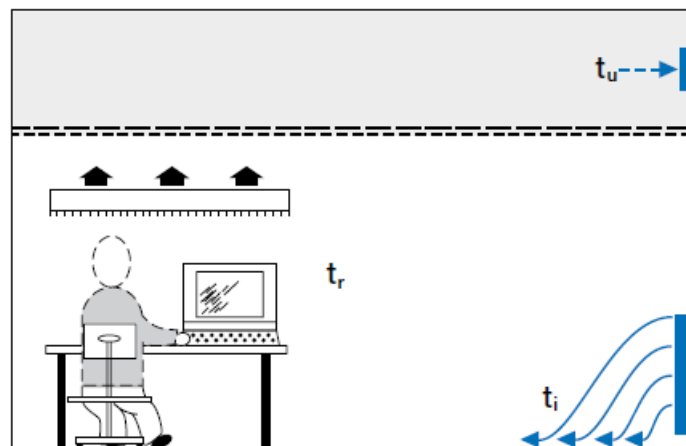


Figure 3: Displacement ventilation principle

Other type of ventilation is piston flow, where the air is supplied to the room through large area (fx. ceiling) and in large volumes resulting in very high ventilation effectiveness. This solution is usually used only in special spaces with very high hygienic demands, such as operating rooms in hospitals, since its design and operation are more expensive.

3.1.2 Diffuse ceiling inlet

A diffuse ceiling inlet combines mixing and piston flow principles. It uses a large surface area as supply diffuser, but it is supplying smaller amounts of air than the piston flow principle, resulting in creating a mixing of supplied and room air.

As already stated in previous section, the mixing and displacement ventilation diffusers are most often used types of diffusers for installations in buildings occupied by humans. However, there are situations where traditional types of ventilation diffusers are not able to deliver required amount of conditioned air in comfortable ways and are not able to remove large heat gains. This results in situation where such ventilation diffusers are not able to comply with relevant standards concerning indoor climate. Spaces representing this category include educational classrooms, theaters, meeting rooms and generally all the spaces with high occupancy density. A diffuse ceiling inlet offers an alternative to traditional ventilation diffusers for such cases.

Diffuse ceiling inlet ventilation is characterized by an activation of large area of ceiling as inlet ventilation diffuser. The air is then supplied into the space at very low velocity. The large amounts of fresh air can be supplied to the space without having a risk of creating any draughts. Due to low velocities, very low momentum is created in supplied air by ventilation system itself. Instead, the movement of the air in the room is enhanced by thermal sources due to buoyancy forces and moving elements situated inside the room.

In principle, the fresh outside air is supplied into the plenum, which is the space between the ceiling concrete deck and perforated suspended ceiling where it gets uniformly distributed, see Figure 22 in section 5.4. The incoming air can be pre-heated/pre-cooled in the plenum. After that, the pre-conditioned air comes into the room through the perforated suspended ceiling made of perforated gypsum boards. The over-pressure is kept in the plenum thanks to a sound absorbing material (an acoustic textile) being installed on top of the perforated gypsum boards. The over-pressure kept in plenum allows supplied air to be distributed equally through the whole area of the perforated suspended ceiling. This results in whole surface acting as a supply diffuser. Apart from gypsum, porous suspended ceiling can be created from other types of materials such as aluminium or shredded spruce wood mixed with cement investigated by Hvid [31], [32].

Chodor and Taradajko investigated in their thesis a diffuse ceiling inlet made of unspecified material covered with painting resulting in white plane surface of ceiling without any signs of presence of ventilation diffuser [33]. The work focused mainly on investigation of influence of position of heat sources on air flow pattern and overall indoor climate in the room. Authors concluded that position of heat loads had significant influence on performance of the system and that highest cooling capacity of a diffuse ceiling inlet was obtained under the situation where heat sources were equally distributed within a space [33]. Interestingly, the authors found that higher risk of draught creation was for situations where heat sources were distributed at height levels close to the floor surface. Authors further suggested to use the “most critical results of cooling capacity” as reference value for design in practice due to unpredictable position of future heat sources within the space. Furthermore, it was found that decreased area of a diffuse ceiling inlet resulted in lower cooling capacity.

A diffuse ceiling inlet is nowadays mainly known in livestock industry where it has been used as supply diffuser in agricultural buildings, particularly in Denmark [31], [34]. The experiences have shown a good overall performance. Applications in commercial buildings include administrative building for the head quarter of Novo Nordisk A/S [35], and renovated classrooms in Holland [36]. Jacobs in his work carried out investigations on mechanical ventilation equipped with a diffuse ceiling inlet installed in existing educational building [36]. Two different types of perforated ceiling with different sizes of perforation were investigated and compared with the results of supply diffuser situated on facade. Results have shown that lower energy consumption for fans and low noise levels were experienced by installing a diffuse ceiling inlet. An indoor environment was improved and better study performance of students was experienced as a result. Jacobs also claims that “installation set up has been realized at acceptable costs”. However, he also mentions, that this depends on possibilities of existing buildings [36]. A diffuse ceiling inlet installation can utilize an existing acoustic ceiling which would need to be installed in majority of spaces anyway, as the noise problems prevail in classrooms (described in section 1.1.2). Some savings can be therefore made on such installation as no additional air ducts and ventilation diffusers are needed. The potential for use of a diffuse ceiling inlet in public buildings is rather big as a diffuse ceiling inlet could be widely applied in spaces with high occupancy density such as classrooms, meeting rooms, theaters, cinemas etc.

Nielsen and Jakubowska in their study focused on performance of a diffuse ceiling inlet in office space with two manikins and basic office equipment [9]. Total heat gain in the room was 480 W, however for some experiments was raised up to 1060 W. The air change rate ranged from 2.75 h^{-1} to 10.45 h^{-1} . This study was more complex compared to other studies since larger variation of supply diffusers were tested, therefore interesting comparison of performance of each could be made. The performance of a diffuse ceiling inlet was compared with five other ventilation systems with different ventilation principles, including mixing and displacement. The authors of the report claim that a diffuse ceiling inlet had superior performance in comparison with other ventilation principles. The results of the investigation have shown that the diffuse ceiling inlet was able to handle highest thermal loads and higher flow rates for investigated full-scale room. The results are evaluated and presented with use of so-called “design chart” (described in section 0). Design chart was used to find the limits for maintaining an acceptable comfort level with small draught and low temperature gradients within the room. Results in design chart have shown dependence of velocities in the room on heat loads. The higher velocities were measured in the room when higher heat loads were introduced. However, according to authors, the draught in the occupied zone was independent of the flow rate to the room [9]. Authors mentioned in their report that “main part of the supply flow passes the ceiling in the suspension system of the acoustic elements”. This inclines to the fact that the whole area of the ceiling was not fully activated and therefore did not act as the diffuse ceiling inlet. Similar findings reported Hvid, who in his experiment realized that suspension construction had great influence on the flow to the room [31]. Hvid found that more air was coming from the plenum to the room through the attachment of perforated tile with suspension construction, instead of going directly through the perforation of the tiles. Similarly as in case of Nielsen, this suggests that suspended ceiling did not act as diffuse ceiling inlet. Hvid reported experiences with local discomfort in the room which could be an indication of draught feeling for occupants. The author also found that “significant preheating in the plenum as well as in the ceiling” has happened [31].

3.1.3 Design methods for ventilation diffusers

The design of traditional ventilation diffusers is usually done by use of measured data provided by producer of ventilation diffuser. Those data usually include information about pressure drop, sound level and air throw. The air throw is defined as the distance from center of ventilation diffuser to the point where supply air has a velocity 0.2 m/s [30]. This critical velocity should always be outside the occupied zone. Ventilation diffusers used for mixing ventilation are often limited by air throw as they are based on supply of air to the room with high momentum.

A diffuse ceiling inlet presented in this thesis is rather unusual type of ventilation diffuser. The use of general guidelines for design of such an installation is therefore very limited. The movement of the air in the room is governed by buoyancy in case of a diffuse ceiling inlet and therefore previously mentioned air throw cannot be applied as highest velocity in the space is dependent on size and position of heat sources in the room rather than velocity generated by diffuse ceiling inlet. The full-scale experiments and CFD calculations are usually used during design of such specific ventilation diffusers [28]. The full-scale experiments are however not very convenient in practice due to their higher time and financial requirements. The use of CFD calculations offers a good alternative to the experiments.

Nielsen tried to express the limits of ventilation diffusers by use of design chart [28]. The design chart expresses the limits of each diffuser concerning flow rates and temperature differences between supply and return air for specific designed space. This allows designers to choose proper air distribution device for concrete application and design it within the limits of healthy and comfortable indoor climate. Design chart is rather convenient way of presenting and comparing the performance of different supply diffusers investigated in the same full-scale room. The design chart method has its limitation as it is dependent on room size and layout. However CFD simulations can be used to predict the behavior of the air flow in the room and following creation of design chart [28].

3.2 Radiant heating and cooling systems

3.2.1 History and development of radiant systems

The use of radiant systems for heating has longer history than for cooling. The very first types of floor heating systems were constructed in Asia [37]. Those systems used exhaust air from the fireplace to heat up a stone floor. This was a reasonable idea as the heat generated during cooking would be wasted otherwise. The similar system was introduced in Europe by Romans probably at the end of 1st century B.C. [38]. First solutions using water as a carrier of energy were applied from beginning of 20th century. Bank of England is one example of building where copper pipes were cast in the building constructions for heating and also for cooling purposes. At those days the floor had to be very warm to be able to heat up the space as the houses were rather poorly insulated. This resulted in uncomfortable indoor climate [37].

The very beginnings of floor heating systems as we know them today go back to 1933 when Gibson and Fawcett developed polyethylene. This was the forerunner in development of cross-linked polyethylene (PEX) pipe which is being used nowadays for most applications of floor heating [37], [39]. The popularity of radiant systems is growing and about 30% to 50% of new residential buildings in Austria, Germany and Denmark are equipped with floor heating [38]. The installation of radiant heating systems into the floor construction is most popular for various reasons. One of them is a good, comfortable feeling on feet when

walking on heated floor surface and overall thermal comfort. Other reason has to do more with physics behind heat transfer, as the installation into the floor surface for heating results in higher heat transfer coefficient and therefore such installation is more efficient than walls or ceiling. One of the other factors positioning the floor surface as the most suitable for radiant systems is that it has usually highest view factor towards occupants resulting in better radiant heat transfer between floor surface and occupant [38].

Very first radiant cooling systems were encountering problems with condensation on the surface as a result of low surface temperature. It was in 1930s when radiant cooling systems began to be used together with ventilation systems, which helped to lower the risk of condensation on the cooled surfaces. Those installations were predecessors to modern radiant cooling systems combined with dedicated outdoor air systems [39]. Few applications of radiant cooling integrated as part of building construction are known. Those usually include floor applications in highly glassed buildings where the floor is exposed to direct solar radiation or floor applications originally designed mainly for heating purposes. Simmonds in his paper described development and performance of radiant cooled floor combined with displacement ventilation [40]. Investigated system created comfortable indoor climate with high thermal stratification in designed space. The need for amount of ventilated air was lowered and also overall energy consumption decreased [40]. Most of the known applications for radiant cooling installed in ceiling involve the use of ceiling radiant cooling panels which are installed in suspended ceiling [41], [42].

3.2.2 Advantages of radiant systems

In theory virtually all surfaces in the room can be activated for cooling, including walls, floor and ceiling. However many limitations can be posed during design process of building concerning availability of surfaces for cooling/heating. Ceiling is very often covered with perforated gypsum boards for purposes of acoustic regulation and floors often can be covered with materials such as carpet. In both cases, the heat transfer between the radiant surface and room would be dramatically decreased. Weitzman investigated the effect of acoustic ceiling on cooling capacity of thermo active building systems. He found that cooling capacity is around 70% of cooling capacity of totally uncovered ceiling when 83% of ceiling area is covered with material for acoustic regulation [43]. No results are however available for situation when the ceiling surface is covered by 100%. The heat transfer between wall and room can be influenced into certain degree by position of furniture, however into lesser degree than in case of floor and ceiling. Furthermore, it is relatively easy to adjust furniture position in the room. This implies that the wall could be regarded as most appropriate surface for radiant systems concerning the practicality and availability.

Large areas of internal surfaces available for radiant systems result in increase of cooling/heating capacity without compromising the comfort for occupants. Large internal surfaces also allow for use of higher temperatures of cooling water/lower temperatures of heating water. The fact that radiant systems optimally work with cooling/heating water temperature close to room temperature is favorable for use of low grade renewable heat sources such as geothermal energy and solar energy. Use of radiant cooling also increases the efficiency of cooling coil about 25% compare to conventional evaporator coils [44].

The small temperature difference between radiant surface and room air is also linked with ability of radiant system to regulate its power output. This self-regulation is possible due to the fact that heat transfer coefficient is dependent on temperature difference. In cooling scenario, the power output from cooled surface is increased if the temperature in room is increased. Even higher degree of self-regulation can be

achieved in case of radiant heating in low energy buildings, as the heat losses from such buildings are generally low, which results in higher temperatures of surfaces in the room. Heat flux from radiant heating system decrease as the indoor temperature increase, up to the point where heat transfer is totally diminished [45]. This self-regulation ability could mean that fewer elements are needed for active control of the system. This could make this solution also economically attractive.

Uniform thermal environment is established in room with use of radiant systems due to the radiant heat exchange between radiant surface and surrounding surfaces in the room. Improved comfort and overall indoor climate is often experienced in occupied space as radiant systems produce virtually no noise, which is often the case for convective systems [46]. Radiant systems also eliminate the air movement and transportation of dust in the room and therefore create healthy indoor environment. This can be especially important for somebody with allergies.

Radiant cooling systems decrease the temperature of surrounding surfaces which influence also operative temperature in the room. The air temperature can be kept higher as a result implying that supply air can have higher temperature as well. Principally the same but reversed situation is in the case of radiant heating systems which increase the temperature of surrounding surfaces [46]. This is especially true for modern low energy buildings with high thermal insulation of building envelope. The air in the room can be kept at lower temperature while keeping the same comfort for occupants in the room. This inevitably results in smaller ventilation heat losses and also in increased relative humidity of room air during winter having positive influence on occupant's health [38]. Higher surface temperatures also eliminate any condensation and mold growth. Furthermore, it was found that air with lower temperature is perceived by people as air having better quality [47].

Aesthetics of the room equipped with radiant systems are improved as those are integrated into the building construction and therefore are not visible. This is not the case for any other type of cooling systems.

Radiant systems are also favorable for zoning which can be easily created and also control in individual zones is considerably simpler and therefore cheaper compare to variable-air-volume ventilation systems.

3.2.3 Limitations and drawbacks of radiant systems

The cooling capacity of radiant systems may be limited by dew-point temperature, vertical air temperature difference, radiant asymmetry or minimum acceptable temperature of cooled surfaces [46].

One of the main drawbacks of radiant systems in general is slow response to the control system. The reaction time of conventional ventilation systems is much shorter. The changes are virtually at one moment as air has small thermal capacity and no thermal mass is activated. Thermal mass of construction is the main reason for slow response of regular installations of radiant systems as those are usually casted into rather thick layer of concrete being usually 70 mm and higher. This can become easily a problem especially in highly occupied spaces such as classrooms where fluctuations in presence of internal heat sources can be rather high. According to Weitzmann instantaneous cooling can become a problem in case where thick concrete slab is used as it is difficult to control it and uncomfortable temperatures in the room can be obtained as a result [48]. One possibility how to improve this situation is minimizing the amount of activated thermal mass. This means reduction of thickness of concrete layer where cooling pipes are

installed and eliminating the amount of water in the pipes. Rather slim construction of high performance concrete (30 mm) was designed in this project in combination with small plastic capillary tubes to carry the water to eliminate the negative effects during the control of the system.

The transmission heat loss of construction with integrated radiant systems is higher in comparison to the same construction without any radiant systems. This is caused by lower temperature of inner layer of cooled surface in case of cooling and higher temperature of inner layer of heated surface in case of heating. The heat loss increase can be as high as 20% [49]. On other hand, some energy savings are made on ventilation and transmission heat losses from surrounding constructions. This is due to the effect of radiant systems on operative temperature. The resulting increase of overall heat losses for the whole house was found to be 2.6% [49]. This can be considered as cost of increased comfort for occupants and it should be taken into consideration during design process of the building.

As radiant systems can remove only sensible heat loads, the additional system has to be designed to account for latent heat loads. Exception for this can be in some very dry climates, where latent cooling is theoretically not needed [44]. If the latent cooling is made by radiant cooling systems, one must count with resulting condensation on cooled surfaces. Latent heat loads are usually removed by ventilation system. As in most cases the ventilation air change rate is designed in relation to number of occupants, this air change rate is also sufficient to remove generated latent heat load in most cases [50]. This applies only for spaces where there are no other sources of latent heat load but occupants. The supply air should be designed in the way to remove all the latent heat generated by occupants and also by infiltration. Dehumidification of the supply air can be very often required in order to avoid the condensation of water vapour on cooled surfaces.

The installation cost of radiant systems can be higher than other conventional heating and cooling systems which can be regarded as a drawback of those systems and can discourage the investors from its use. However, the fact that that radiant systems use the same installation for heating and also cooling purposes could positively influence the economics of radiant systems.

3.2.4 Coupling of radiant systems to ventilation system

Low energy buildings can have higher cooling demands compared to conventional buildings, mainly as a result of increased thermal insulation of building envelope. Spaces with high occupant density result in overheating as a consequence of combined effect of high internal heat loads and highly insulated building envelopes. Classroom is a good example of spaces with high occupant density. It can become a challenge to cool down such spaces with air cooling systems while keeping comfortable indoor climate as draught can be created as a result of large amounts of supplied air. One option to solve this problem is installation of radiant systems in conjunction with ventilation system. The importance of ventilation systems in low energy buildings has already been discussed and it can therefore be assumed that it will become the standard equipment of buildings. Ventilation system can be used to supply required amount of fresh air, to cool incoming supply air and at the same time can be used to remove the whole latent gain from the room [44].

If the space is equipped with radiant system, large savings can be made on ventilation system as radiant systems can handle all the sensible heat gains. Only latent heat gains are covered by ventilation system and it can be therefore designed for much smaller air flow compare to full-air cooling systems based on

requirements of relevant standards concerning the health and comfort needs [51], [14]. Savings are made on space and material otherwise used for ventilation ducts as those can be dimensioned significantly smaller and also ventilation unit itself can be smaller.

As the amount of ventilated air is decreased significantly, savings about 10 - 30% are usually made on electricity otherwise used for running fans for full-air cooling systems [44], [50]. The installation cost is about 15% lower compare to full-air cooling systems [50]. The smaller requirements for preheating of supply air in heating season and for precooling in cooling season allow for smaller capacities of heater and cooler situated in ventilation unit which has inevitably the influence on its price and also size.

4. Product design and development

Product design and development methods include any procedures, techniques and tools being used during the process. It is believed that there are several reasons behind the need to improve traditional ways of working in design [52]. One of them is increasing complexity of a design of the new product. The products tend to be more advanced and complex since more pressure is on innovation. New demands arise for the designers as a result. Designers therefore need a systematic approach to be able to handle such complicated tasks. Furthermore, the risk of failure of designed product is usually high as most products are produced as mass production. High financial losses can therefore be experienced in case of failure in design together with loss of trust of customers which can be never built again. Many unnecessary, serious mistakes can be eliminated by applying systematic approach to the design.

There are two main approaches to systematic design including creative and rational methods [52]. The creative methods try to stimulate creative thinking and increase the flow of ideas. One of the modern and often used creative methods is brainstorming. The rational methods try to formalize the design procedure. This is done in an effort to make whole design process somehow more transparent and organised. It helps into certain degree to minimize the risk of failure. It is very suitable for more complex designs and therefore it supports the team work. The rational methods aim at better product development [52].

4.1 Development of new building system

The presented PhD study has been carried out as part of a larger project involving other PhD students and group of companies working on the common project under company Connovate A/S [53]. The vision of the Connovate group is to develop a new sustainable building system using high performance concrete for wall sandwich elements as a solution for building system which ensures modern living standards by improved indoor environment, decreased energy consumption, and increased living space [54]. To accomplish the sustainability of the system the goals such as low energy consumption, low material use, material recycling, and low CO₂ emissions through the whole life cycle must be reached. The new building system seeks to increase the prefabrication of its elements which should result in offering, along the lowered price, also increased quality of indoor climate and increased space for living. The objective of the Connovate is to develop, certify, and deliver the state of the art building elements for a new building system.

4.2 Scope of product development in the thesis

As a basis of a product development in this thesis was the need to develop new concepts for ventilation, heating and cooling systems for low energy buildings constructed from new building system in order to create comfortable indoor climate in optimal way. Product development methods discussed in previous chapters were used to bridge the gap between this challenging task and the final product solution.

In this project there have been following issues to be focused on:

- need to allow a full prefabrication of wall element with integrated radiant cooling and heating
- providing healthy and comfortable indoor environment
- allowing utilisation of low quality heat sources
- minimizing an influence of installed technical systems on the building design

- ensuring safety of installed technical services during the transport of fully prefabricated elements

Present requirements made by governments mean that buildings need to be adapted to the future energy requirement [8]. The solution needs to include (i) decrease of energy consumption in buildings and (ii) development of new solutions for building components and systems which will work well regarding the utilization of future energy sources. The system here refers to the “group of components” which when combined create the “system” for concrete function in building. In this project building system is represented by diffuse ceiling inlet, which is composed of building components such as ventilation inlet, acoustic regulation, space for installations and component with aesthetical function. In this case the building system combines also different building functions.

The building components should be made in a way to allow to meet new demands and to help to rationalize the building production. As a result, building components should have better quality at decreased cost. The building elements (components) such as floor, wall and roof can become building product, since the functional requirements are usually made for each building element opposed to whole building itself. This would differ to the situation nowadays where a building material is building product (instead of building component).

The production of building components can be done in the production facility as part of a prefabrication process, which can be then controlled in better way. That should result in more efficient production processes, higher quality, and lower price of buildings. Prefabrication process allows for time savings during whole process of building construction as various works can continue on building side during the time of prefabrication of various building components.

4.2.1 Process of product development in the thesis:

The client’s requirements were specified as a starting point of product development. Different stakeholders and decision makers had different requirements and wishes for the future product. Each stakeholder had also different relevance in a decision making process. It has shown to be the case that lifetime, space optimization, overall design, and indoor environment were having the highest importance. It is probable that the designed solution would not have a success on the market without meeting the mentioned demands.

The next step in product development was to specify the properties of new product which would ensure that it will work in the way clients require it to work. The design objectives needed to be specified and the objective tree method was used for those purposes. The main aim of objective tree method was to clarify the objectives and their relationship. On the left side of the objective tree are stated product attributes. By working through the objective tree towards the right side, it was explored **how** the desired product attributes can be accomplished. We are getting from the wishes to the real practical solutions. The lower-level objectives (situated on the right side of Figure 4) are a means of achieving higher-level objectives (situated on the left side of Figure 4). Going from the lower to the higher level of objective (from the right to the left side of Figure 4) one can realize **why** particular sub-objective is needed for design of the product. The objective tree method for the new types of cooling, heating, and ventilation systems is depicted in Figure 4.

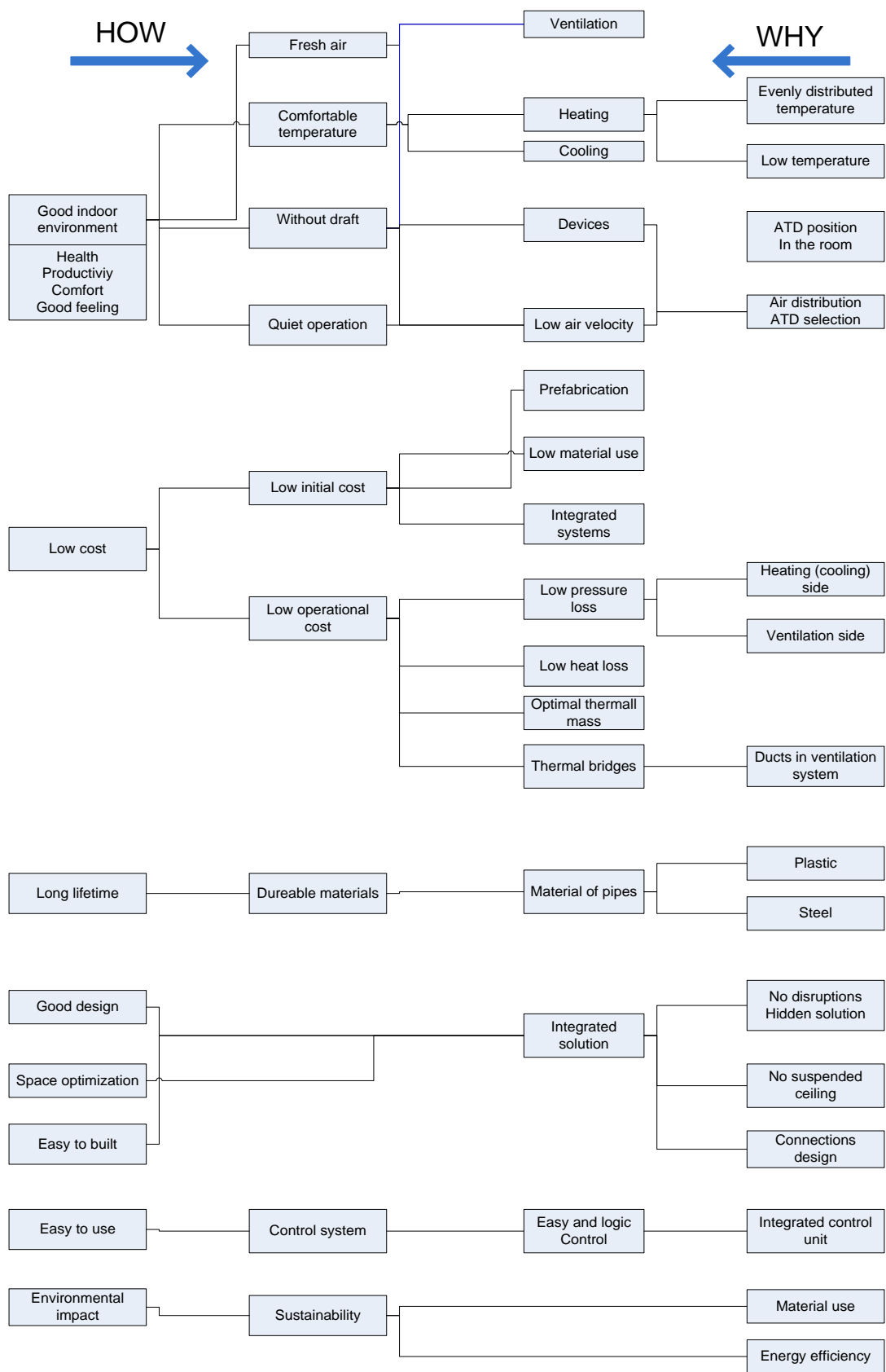


Figure 4: Objective tree method

The next step after defining the product attributes was to specify the engineering characteristics which will represent those product attributes. It was very important that product attributes were carefully translated into the engineering characteristics, without losing a direction towards required product to be developed. The basic idea was to come up with all the relevant engineering characteristics which specify all product attributes and can help the engineer to design the best possible solution of required product, therefore satisfy the customer’s needs. The matrix with engineering characteristics standing against product attributes was created and can be seen in Figure 5. The engineering characteristics relevant for heating system are highlighted with green color and for ventilation system with red color (on the left side of the matrix). The influence of each engineering characteristics on each product attributes was specified on scale from positive (green colour), through neutral influence (yellow colour) to negative influence (red colour). The matrix chart represents the visualisation of the relationship of the customer’s requirements and engineering characteristics, which are the main “tools” engineer is working with during the product development process. As we already know which product attributes have highest importance for the client, we can very much decide on which part of the matrix to focus the most.

Engineering characteristics	Product attributes					Environmental impact	Low operative cost	Long lifetime	Good indoor environment	Design	Space optimization
	Easy to produce	Cheap to produce	Easy to mount	Cheap to mount							
Evenly distributed surface temperature											
Low temperature of the surface											
Low power of the surface											
Proper connections of the loops											
High thermal mass											
Low energy consumption of the pump											
Low pressure loss- RHCS											
Type material of pipes											
Low material use_RHCS											
Air distribution (ATD selection)											
ATD position in the room											
Low pressure loss- DCV											
Low material use_DCV											
Prefabrication											
Integrated system											
Low heat loss											
Low thermal bridges											
Proper control system											
Energy efficiency											

Figure 5: Product attributes vs engineering characteristics

The possible solutions were now generated as a result of product development process. The alternative solutions were compared to each other in terms of satisfying customer’s requirements.

Proposed solution for cooling is based on a fully prefabricated complete wall sandwich element with integrated heating and cooling systems based on plastic capillary tubes casted into the inner layer of high performance concrete, see Figure 11. Proposed solution for ventilation is based on diffuse ceiling inlet made of perforated gypsum boards installed in suspended ceiling, see Figure 22 and Figure 23. The system of diffuse ceiling inlet is designed as integrated part of building. Whereas radiant cooling system based on plastic capillary tubes is designed as integrated part of building component.

The solution for a diffuse ceiling inlet as an integrated part of building component was also designed, but was not approved for further development by company Connovate A/S. The origin of this solution is in ceiling cooling element depicted in Figure 6, which has concrete ribs inside the element. The idea for an element with a diffuse ceiling inlet was to move the ribs out of the element, more precisely at bottom side of element, see Figure 7. The space between neighboring ribs was covered with use of perforated gypsum boards. The resulting space called plenum is used for distribution of inlet air within the element. The resulting ceiling element with a diffuse ceiling inlet can be seen in Figure 8. The plastic capillary tubes were cast into the concrete layer situated in the plenum and incoming air could be therefore pre-cooled or pre-heated depending on the current needs.

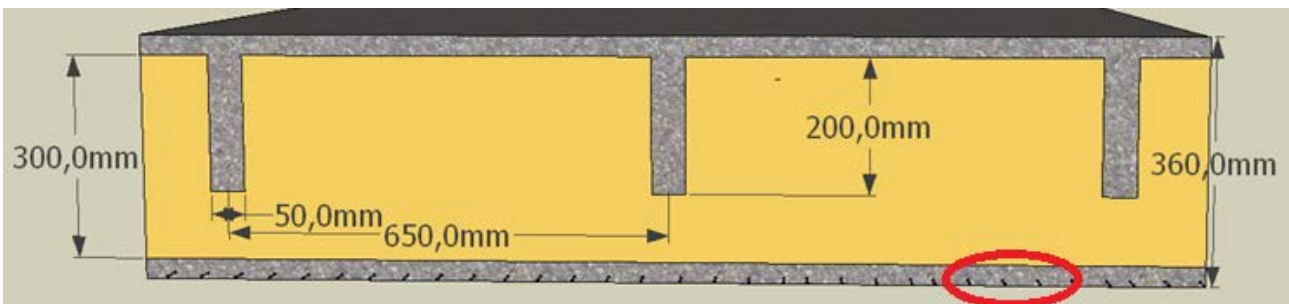


Figure 6: Ceiling cooling element made of high performance concrete

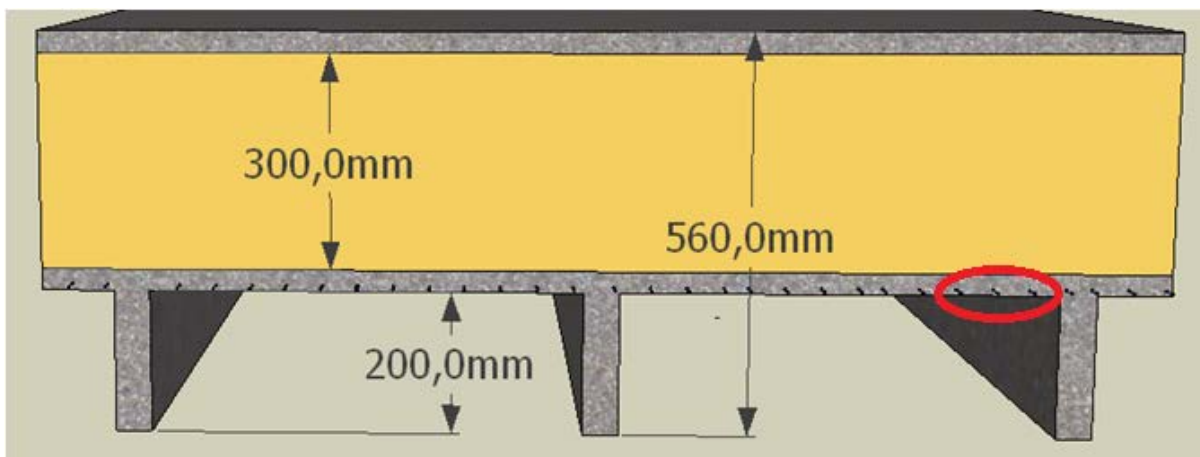


Figure 7: Creation of space for plenum between the exposed ribs

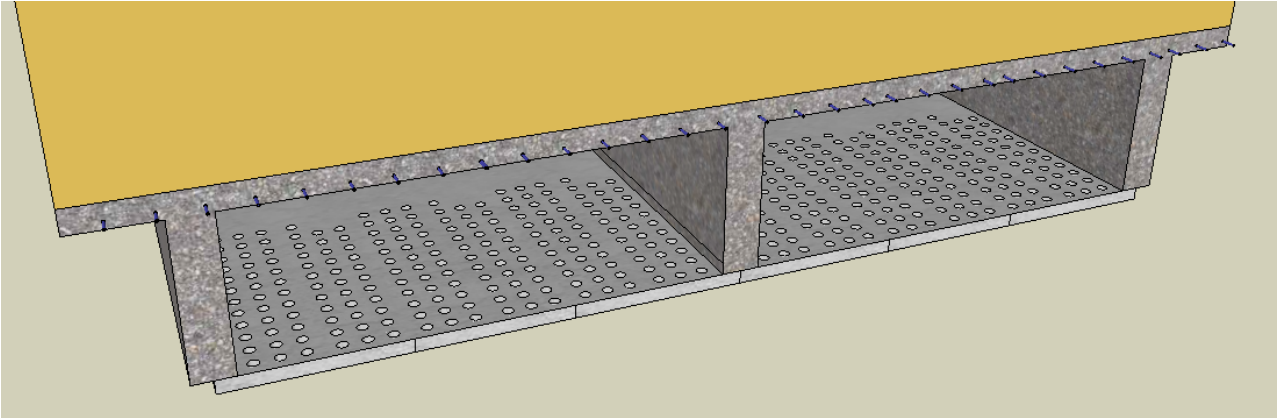


Figure 8: A diffuse ceiling inlet as building component made of high performance concrete

The solution for diffuse wall inlet was also designed in similar way as previous solution and is shown in Figure 9. The difference is in depth of the plenum dependent on the size of the used ribs. Similarly as previous case also this solution was not approved for further development. In both cases only part of ceiling/wall area can be activated for ventilation as it is divided by the ribs.

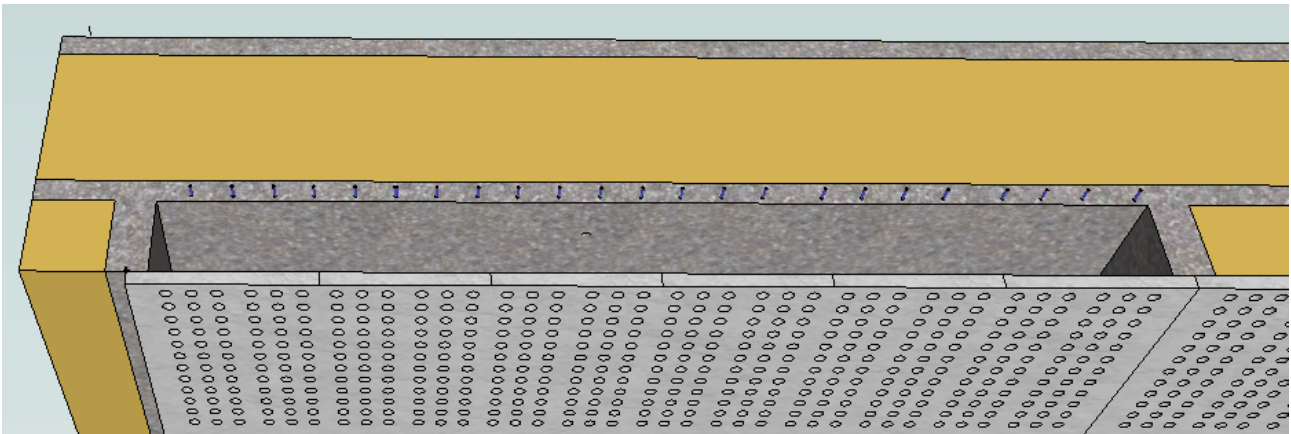


Figure 9: Diffuse wall inlet

5. Testing facility

5.1 Full scale test building

Based on the results of a product development from the initial phase of PhD study it was decided to build a full scale testing facility in a campus of Technical University of Denmark. A decision to build a test building was also based on needs and interests of other PhD students and company Connovate A/S® involved in the project developing a new building system based on high performance concrete [53]. The test building was built in summer 2013 in order to allow all interested parties to investigate relevant topics. The test house was designed and built as a two storeys building as can be seen from Figure 10. The first storey of the test house was reserved for investigations of high performance concrete concerning its behaviour when exposed to thermal changes. The second floor was dedicated to investigation of radiant heating and cooling systems and a diffuse ceiling inlet used for ventilation. The entrance to the upper floor is on an externally situated staircase placed on a north-east side of the test house.



Figure 10: Test House after its construction

The test house was built from sandwich wall elements made of two layers of high performance concrete and thermal insulation in the middle, see Figure 11. The outer layer of high performance concrete is 20 mm, inner layer of high performance concrete is 30 mm and thermal insulation is 300 mm thick. The ribs with dimensions of 100 mm x 50 mm having a loadbearing function were placed close to the inner wall in a distance of 1200 mm. The ceiling decks in both storeys were made of pre-stressed concrete hollow core elements with thickness of 200 mm.

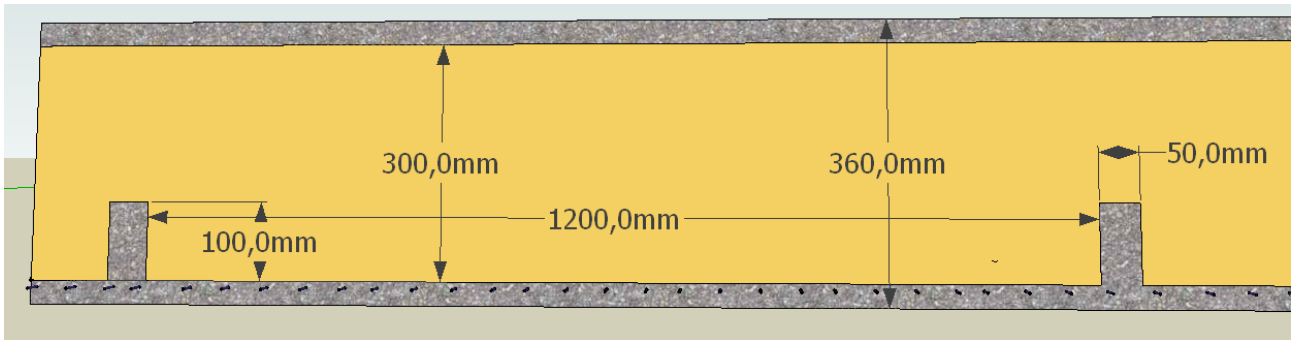


Figure 11: Drawing of sandwich wall element made of high performance concrete

The upper floor was further divided into a test room and a technical room, as depicted in Figure 12. A test room represented the main room to be investigated and was equipped with two windows, a ventilation unit, and a suspended ceiling made of perforated gypsum boards. The height of the testing room after installation of a suspended ceiling was 2.65 m. The test room was 6.05 m long and 3.25 m wide and a resulting area of floor was 19.66 m². Two windows with dimensions 2.5 m x 1.1 m were installed in a wall facing north-west resulting in an overall area of 5.5 m². The technical room was used for different kinds of measuring equipment, including mainly data loggers and a computer. The technical room was also used for all the installations connected with radiant systems, such as flow meters, closing valves etc. The partition wall separating the testing room from the technical room was made of a wood structure and gypsum. Its purpose was to separate the two spaces in terms of an air flow, in order to avoid any disruptions during measurements when somebody enter the building. No thermal insulation was used as the volume of the technical room was also heated/cooled. The dimension of the technical room was 3.25 m x 1.00 m.

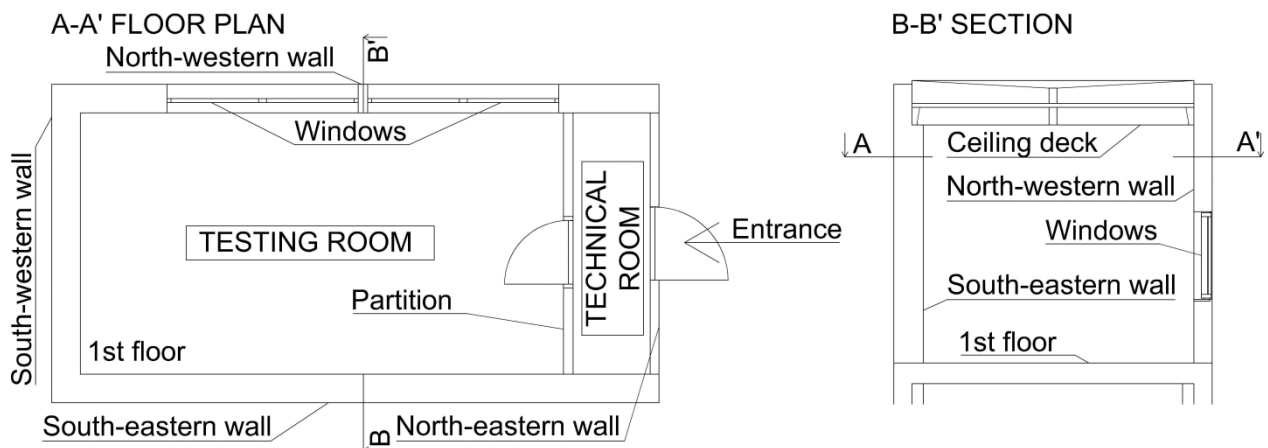


Figure 12: Design of Test House

The room was equipped with basic furniture for a classroom including 6 tables with dimensions 1.2 m x 0.7 m and height 0.7 m, 12 chairs accommodating the occupants represented by 12 metal barrels simulating sedentary occupants. Metal barrels were painted black and the heat was generated by light bulbs situated inside of the barrels. Furniture equipment of the test room can be seen in Figure 32. Four lighting units with fluorescent tubes (type T5) with power output of 28 W/unit and 2600 lumens/unit were installed 0.2 m

below the diffuse ceiling inlet and their position is shown in Figure 13. The lamps were installed in parallel to longer walls as it was believed that such a positioning will ensure more even light distribution throughout the test room.

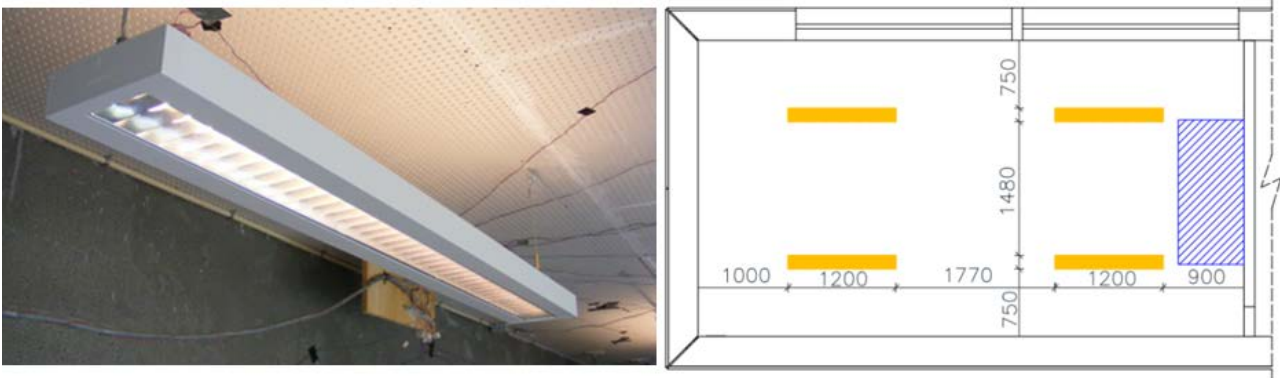


Figure 13: Photo and layout with positions of lighting fixtures

A rather unfortunate installation of a drainage pipe was done in the test room. A plastic pipe with a diameter of 110 mm was installed just below a suspended ceiling as can be seen in Figure 14. Such an installation could possibly influence measurements in two ways. Firstly, the pipe created a thermal bridge and therefore an influence on thermal losses could be expected. Secondly, the pipe could have an influence on an air flow in the test room. A more appropriate position for such an installation would be outside of the building taking into account that the aim was for a low energy building.



Figure 14: Drainage pipe situated below suspended ceiling

5.2 Radiant cooling system

An investigated radiant cooling system was based on a plastic capillary tube made of polypropylene material cast into a 30 mm inner layer of a high performance concrete wall element. The casting took place in a production factory and a resulting element was the prefabricated sandwich wall element with already installed radiant systems. Casting process is depicted in Figure 15. The outer diameter of a capillary plastic tube was 4.3 mm, thickness of a wall of plastic capillary tube was 0.8 mm and a resulting inner diameter

was 2.7 mm. The capillary plastic tubes were assembled into the capillary mats with dimensions of 2.7 m x 1.0 m (L x B) with a 30 mm (A) spacing between plastic capillary tubes as shown in Figure 16. Capillary mats represent a way of implementing radiant cooling systems into a thin construction. Two walls were used for installation of radiant systems as shown by the blue lines in Figure 47, together containing 10 pieces of capillary mats providing a radiant area of 27 m². The designed system is using water as cooling medium. All the capillary mats contain 4.32 l of cooling water. The plastic capillary tubes run in parallel in a distance of 30 mm to each other. This is optimal for an even distribution of temperature on surface of cooled walls. The plastic capillary tubes run in parallel from a top part of the wall to a bottom and then back to the top of the wall as can be seen from Figure 16. Therefore the supply and also exhaust pipe connections are situated at the top of the wall element in a space between ceiling concrete deck and suspended ceiling. The capillary mats are connected to the polypropylene manifold pipes by use of the flexible hoses with a diameter of 10 mm as shown in Figure 17. The manifold pipes had an outer diameter of 20 mm and were used to run cooling water from the technical room into the plenum. The connections were situated in a space above the suspended ceiling and therefore were not visible from the test room. Further equipment for a radiant system including water pumps, water flow meters, safety valves etc. was placed in the technical room. A cooling loop was a closed system separated by a plate heat exchanger from a source of cold water, which was a tap water in our investigations.



Figure 15: Casting of CPTs in the HPC wall element

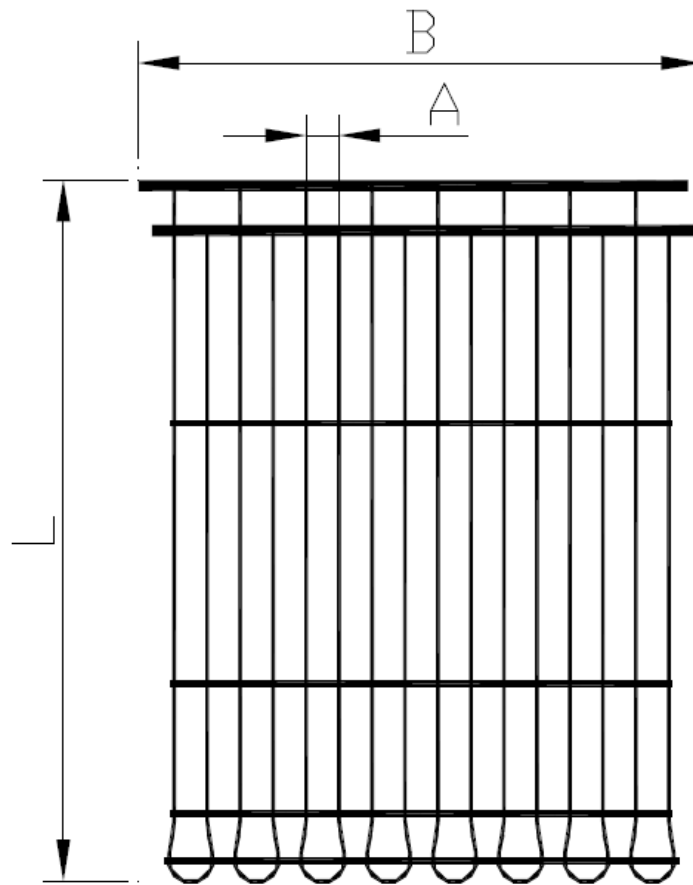


Figure 16: Capillary mat made of plastic capillary tube



Figure 17: Connection of capillary mats with manifold pipes

Practical challenges were experienced during a casting of capillary mats into a layer of high performance concrete. The capillary mats were delivered from producer “twisted”, which was done purely for purposes of transport. This is not a problem for most of the applications in practice as those are made into a plaster and it is relatively easy to fix capillary mats to a wall. However, it was found rather difficult to ensure the right position of the capillary mats during the casting into the concrete in this project, especially when the layer of concrete was only 30 mm thick. To solve this problem, a steel reinforcement net was inserted into a layer of high performance concrete to keep capillary mats in proper position in a concrete layer as can be seen in Figure 18. The first casting was however not successful since capillary mats started to come out and float on a top of the concrete. The reason for this was that capillary tubes contained air and also a density of polypropylene is smaller than density of concrete. For a second trial, the capillary mats were attached to a steel reinforcement by use of plastic strips at a distance of 20 cm. This solution was more expensive and time consuming as it was rather a tedious work to attach all the capillary tubes to an inserted reinforcement. Furthermore, a steel reinforcement is not normally part of a wall element and it was used purely for purposes of attachment of capillary mats. Producer of capillary tubes stated that capillary mats are a bit twisted always when coming from a production line since capillary tubes are stored in coils. In conclusion, a new ways to fix capillary mats in a proper position within a layer of high performance concrete need to be found and investigated. Current method does not allow production of designed solutions at reasonable cost and will most probably not attract potential producers.



Figure 18: Detail of steel reinforcement in concrete layer

5.3 Air handling unit

A decentralized air handling unit was placed under the prefabricated hollow core concrete deck at the area close to the technical room as shown in Figure 19. 2/3 of the air handling unit was situated in the plenum and 1/3 was situated in the test room. The supply and exhaust ducts were situated in the technical room

through which the unit was connected to the outside environment, see Figure 19 and Figure 20. The supply and exhaust ducts were insulated by 50 mm of thermal insulation. Installed air handling unit with uncovered lid is depicted in Figure 21. The fresh air was supplied from the air handling unit into the plenum through the opening with dimensions 0.8 m x 0.1 m situated on the front face of the air handling unit. Direction of the supply air can be seen in Figure 22. The plenum is a space between the suspended ceiling and concrete hollow core deck with a volume of 4.9 m³, see Figure 19 and Figure 22. A uniform air distribution was assumed in plenum as it created a chamber with equivalent static pressure drop between volume of the chamber and the room. An exhaust opening with dimensions of 0.15 m x 0.10 m was placed on a side of the air handling unit below suspended ceiling, see Figure 19 and Figure 22. The maximum capacity of the air handling unit was 550 m³/h.

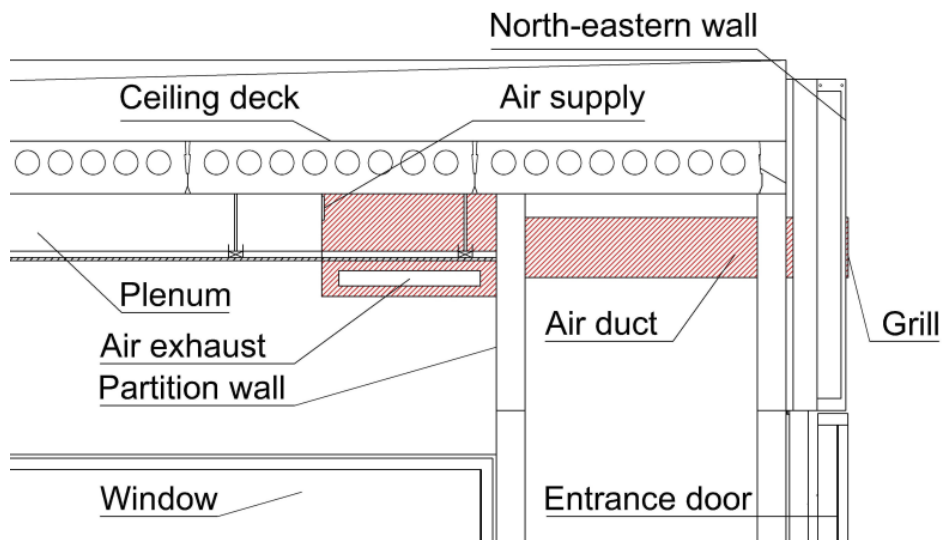


Figure 19: Vertical position of AHU and connecting ducts

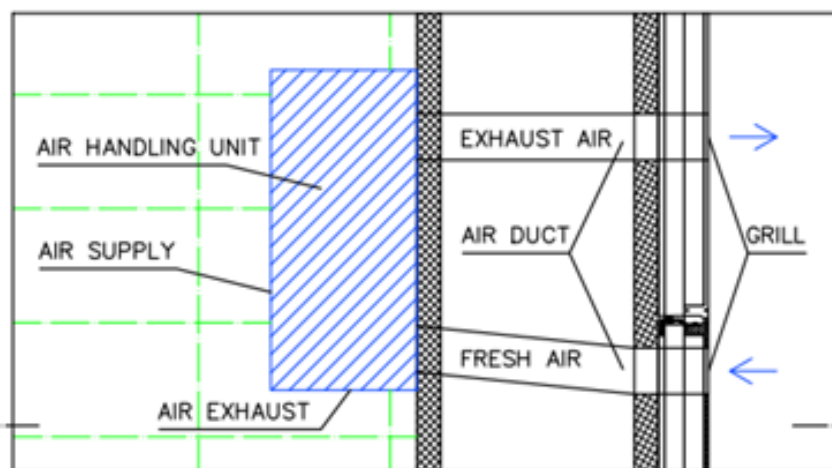


Figure 20: Horizontal position of AHU and connecting ducts

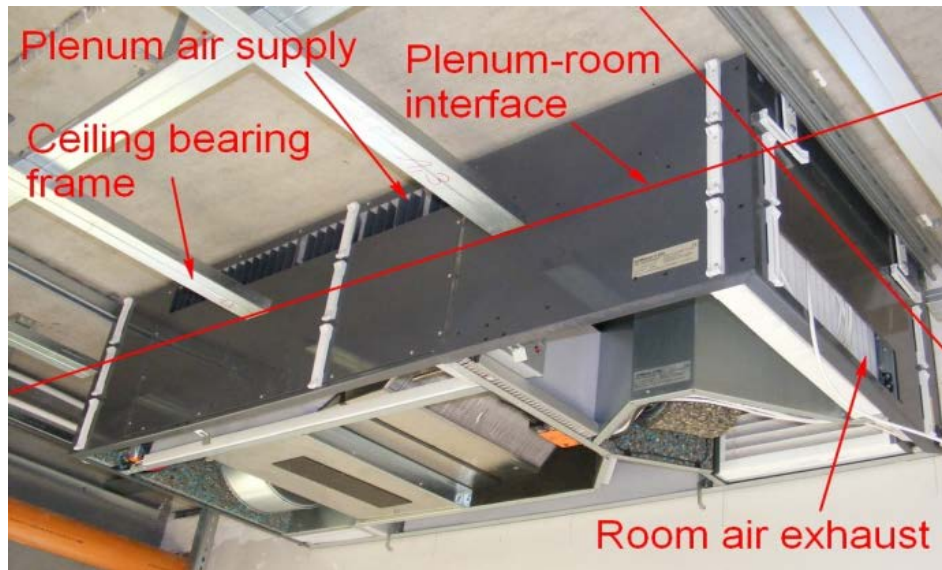


Figure 21: View on AHU without cover

5.4 Diffuse ceiling inlet

The diffuse ceiling inlet was created as suspended ceiling made of perforated gypsum boards with total perforated area of 15%. The diffuse ceiling inlet was constructed in a way to allow the whole area of suspended ceiling to act as a supply diffuser. Gypsum boards with dimensions of 0.9 m x 2.7 m were mounted onto the aluminum load bearing profiles, which can be seen in Figure 21. The connections of gypsum boards and any other penetrating objects were sealed together with use of silicone paste. Acoustic textile situated on top of the gypsum plates served for the purposes of creating pressure chamber from plenum and improving acoustic conditions of the room. The diffuse ceiling inlet was placed 0.25 m below the ceiling deck. The height of 0.25 m was chosen in order to separate the supply and exhaust opening situated on the air handling unit. The surface area of a diffuse ceiling inlet was decreased by obstructing air handling unit and resulted in area of 18.6 m². The diffuse ceiling inlet is depicted in Figure 22 and its construction in Figure 23.

The diffuse ceiling inlet construction is rather interesting solution as it serves number of different purposes. As it was originally designed for purposes of acoustic regulation, the whole area of suspended ceiling is used to dampen the noise created in the room. Noise is one of the main disrupting element in classrooms as found by relevant study [4]. Furthermore, the suspended ceiling often improve overall look of the room. The electrical, heating and other installations can be easily covered by suspended ceiling and at the same time being relatively easily accessible.

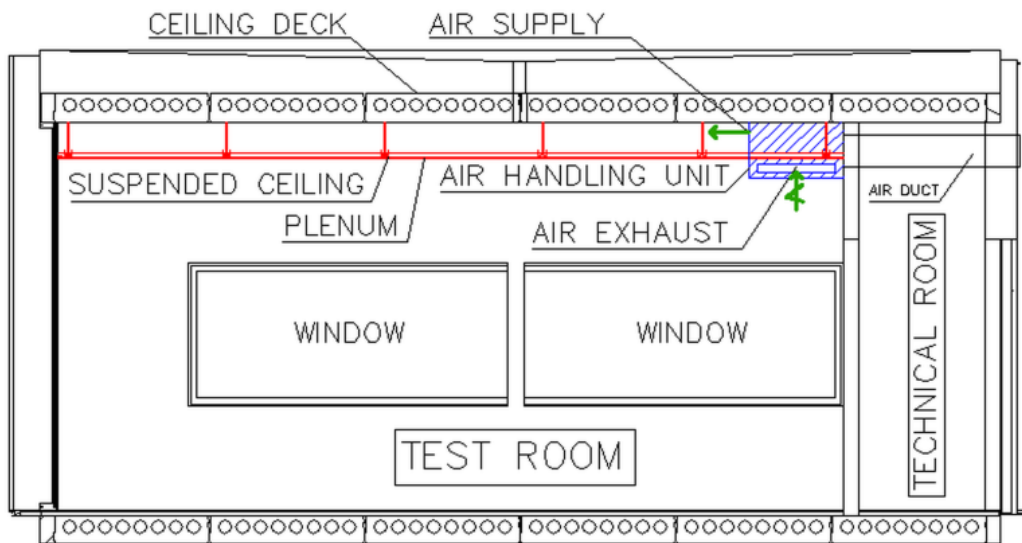


Figure 22: DCI construction and AHU position



Figure 23: Installation of suspended ceiling

6. Measurements

6.1 Measuring apparatus

The instruments used for measurements are described in the following sections together with procedure of their implementation and use.

6.1.1 Temperature measurements

A copper-constantan (T-type) wire soldered together was used to create thermocouples used to measure room air and surface temperatures. The third metal was introduced to the circuit during soldering process. According to producer of used acquisition/switch units, this has a little influence on precision of thermocouple measurements, provided that both ends of thermocouples are at similar temperature [55].

Thermocouple does not measure absolute temperature but electric potential (voltage difference) between measured point of interest and a reference point situated on data acquisition unit. Accuracy of T-type thermocouples for indoor measurements ranges between 0.7 °C to 1 °C involving a voltage to temperature conversion [56]. Two acquisition/switch units Agilent 34970A and Agilent 34972A were used to process the data from multiplexers [57]. Those units are able to directly convert electric potential generated by thermocouples to the temperatures. This can be done thanks to an in-built reference temperature compensation, so-called “cold-junction compensation”. Temperature on multiplexer board is measured by in-built thermistor. However, usually some inaccuracies arise as a result of this approach. The problem is that the reference temperature is measured just on one place situated on the used multiplexer board, contrary to connections of thermocouples, which are spread over the whole multiplexer board. The temperature difference across the whole multiplexer board can however be up to 1°C. This is an uncertainty brought additionally into the measurements. In order to improve the accuracy of our measurements, the reference temperature was not measured at each multiplexer card, but instead at a common cold junction reference point in a separate thermally insulated box. Closed insulated box was used to avoid influence of surrounding environment on measurements, see Figure 24.

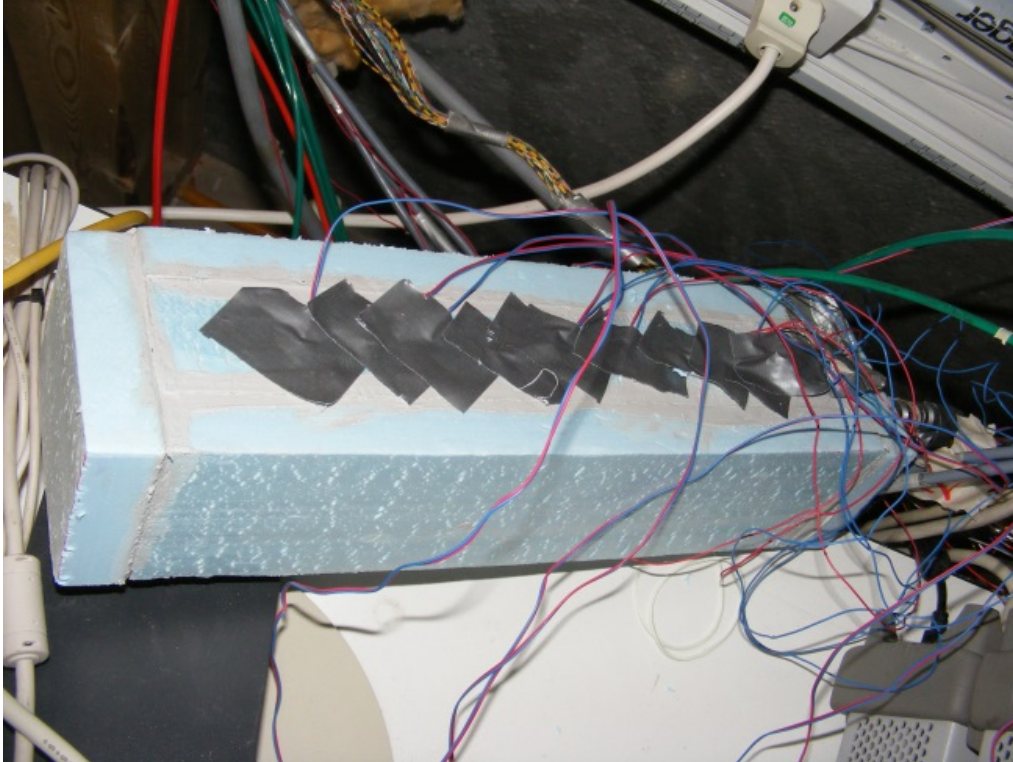


Figure 24: Insulated box for measurements of reference temperatures

Following connections have been made: One regular thermocouple type-T was connected directly to the channel on multiplexer board very close to the point where the thermistor measuring reference temperature was situated. This was done for each of four used multiplexers. Those four thermocouples were inserted into the external box to measure reference temperatures of used multiplexers. Additionally, the temperature in the insulated external box was checked with two pieces of platinum resistance thermometers with accuracy of 0.1 °C (PT100 sensors). Reference thermocouple with the smallest deviation from PT100 sensor's reading was used as our main reference temperature. The temperature difference between chosen thermocouple and PT100 sensor was 0.1 °C being acceptable for purposes of this project. All the measurements at points of interest within the test room and plenum were then made by connected T-type thermocouples and were related to the main reference temperature. The electric potentials from all thermocouples were measured and the resulting temperatures were calculated according to the Eq.(1), Eq.(2), Eq.(3) which express 3rd order power polynomial equation developed by Tomas Lund Madsen [56]. At known reference temperature t_{ref} and measured electric potential S , the algorithm allows to calculate the required temperature t directly.

$$T = T_{ref} + T_d \quad \text{Eq.(1)}$$

$$T_d = S(25,9 - 0,06 T_m + 0,00027 T_m^2 - 0,000001 T_m^3) \quad \text{Eq.(2)}$$

$$T_m = T_{ref} + 12,95 S \quad \text{Eq.(3)}$$

Where: S is measured electrical potential [mV], T_{ref} is measured reference temperature in insulated box [°C], T_m is auxiliary temperature value [°C], T is resulting temperature [°C].

Resulting set-up led to better accuracies during our investigations. Heller investigated accuracy of Lund Madsen’s algorithm and proved that absolute temperature deviation was maximum 0.27 K for room temperature range of 10 °C to 30 °C compared to frequently reported 1 K for direct connection of multiplexer [56]. The scheme of used connection of thermocouples is depicted in Figure 25.

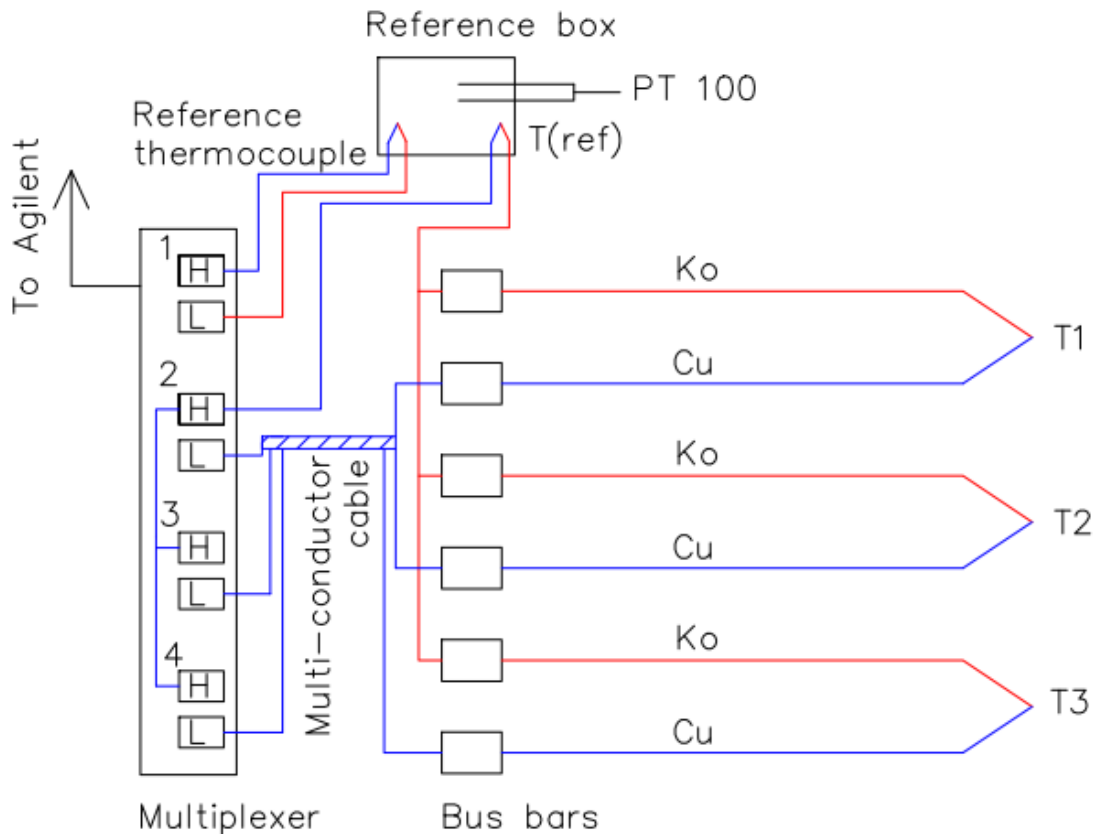


Figure 25: Schematic connection of thermocouples

Other measure was taken to reduce errors during our measurement. The thermocouples situated in test room and plenum were not led directly to the multiplexers, but instead those were wired the shortest possible way to bus bars where we connected them to copper multi-conductor cables leading to multiplexers, see Figure 26.

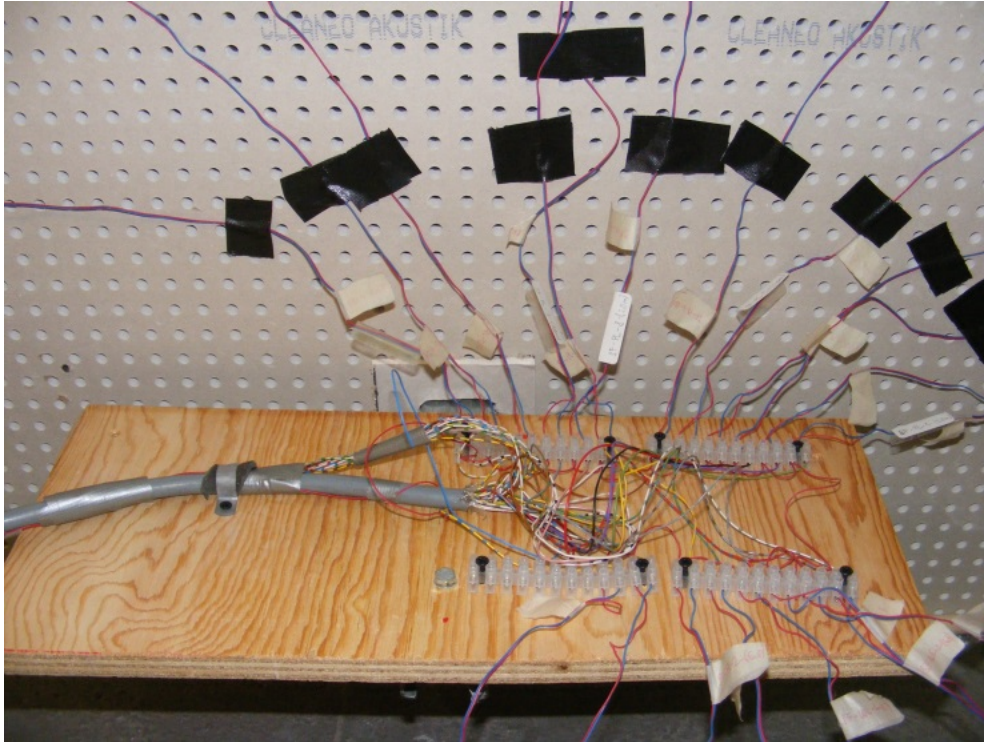


Figure 26: Connection of thermocouples to multi-conductor cable

A single constantan cable led from each bus bar alongside to the shielded multi-conductor cable to particular multiplexers creating a circuit for each connected thermocouple. In this way we were able to minimize the undesirable interferences from surrounding environment, such as noise in electromagnetic field. This installation was feasible due to the fact that Agilent works as switch unit, measuring a single channel at the time. This installation saved almost 500 m of rather expensive copper-constantan wire.

Altogether, 75 T-type thermocouples were installed in the room and four 20-channel multiplexers were used to connect all the used thermocouples. Fifteen T-type thermocouples were installed at different heights on three moveable, vertical stands situated within the occupied zone of room. Thermocouples were fixed at height levels 0.1 m; 0.6 m; 1.1 m; 1.7 m and 2.1 m respectively, in order to be able to see vertical temperature profile which is used as a factor of local thermal comfort evaluation in ISO 7730 [29]. Furthermore, 4 thermocouples were placed on floor and 2 thermocouples measured temperature of window's surface.

There were 36 thermocouples installed in the plenum in total; 3 horizontal planes with 12 pieces at each plane covering the area of plenum in 3 different height levels. Each plane had 4 rows of 3 thermocouples. In the top plane there were thermocouples measuring the surface temperature of the concrete hollow core ceiling deck, in the middle plane thermocouples measuring the air temperature in the plenum, and in the bottom plane thermocouples measuring the surface temperature of the porous suspended ceiling. Additional 12 thermocouples were placed on bottom side of porous suspended ceiling. Temperatures were measured continuously for the entire period of experiment and recorded once in a minute interval.

The precision of measurements could be influenced by differences of temperature between soldering point and thermocouple wire close to the soldered end. This is why each of thermocouple installed in the room

and plenum was coiled about 10 cm from soldering point to eliminate this co-called diffusion error which is otherwise difficult to spot [58]. Thermocouples measuring the air room and plenum temperatures were placed inside the 5 cm long aluminum cylinder working as protection against effect of radiation, see Figure 27. In this way the influence of radiation from surrounding surfaces could be eliminated to very high degree. Influence on results caused by radiation is most often error made during measurements of room air temperature [58].

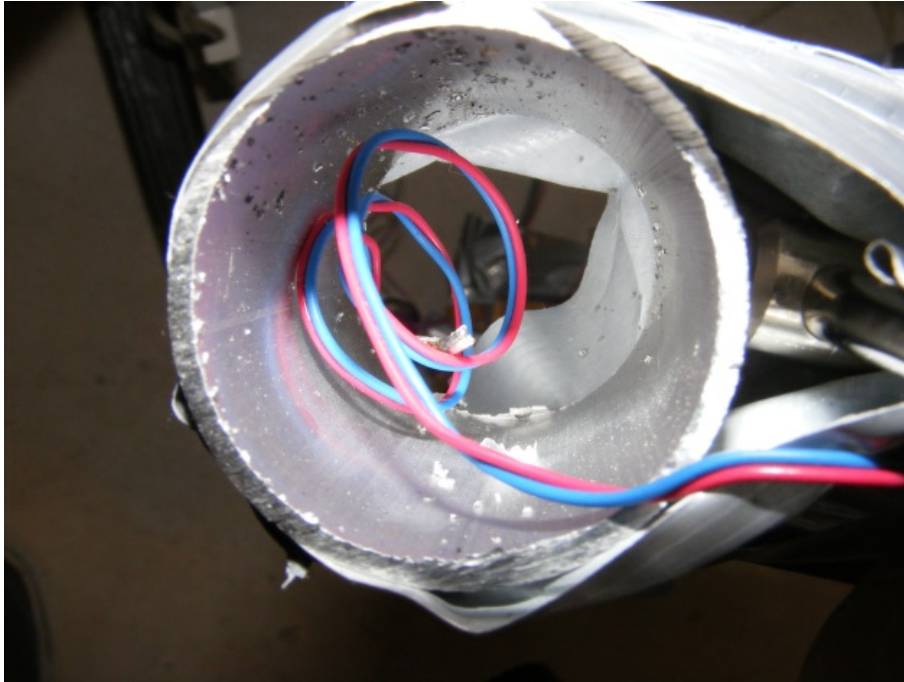


Figure 27: Aluminum cylinder used for shielding of thermocouples

Wall surface temperatures were measured with 12 thermocouples. The T-type thermocouple works in this solution as a contact thermometer. According to ISO 7726, the use of contact thermometer can lead to the measurement errors since contact thermometer can change the heat exchange between the measured surface and the environment, especially when properly shielded from environment [59]. The surface thermocouples were shielded against effects of thermal radiation by aluminum foil with dimensions of 5 cm x 5 cm. This is however needed in order to eliminate the direct influence of environment on measurement. In this project however, the measured surface has rather high thermal conductivity ($\lambda=2,6\text{W/mK}$) which eliminates mentioned error. The rule of thumb is that heat exchange between surface and sensor is much higher than heat exchange between sensor and environment. This was achieved by using special, thermally very conductive paste to attach the thermocouple to the measured surface in order to enhance the heat transfer and by using only small area of covering foil.

Furthermore, the air temperatures in the room were also measured on moveable stands by SensoAnemo5100SF transducers with accuracy of measurement of 0.2 °C [60].

Outside air temperature measurements were made by sets of HOBO Data loggers (model U12) with temperature accuracy $\pm 0.35\text{ K}$ [61].

6.1.2 Air velocity measurements

Air velocities in test room were measured by use of air velocity transducer SensoAnemo5100SF with accuracy of ± 0.02 m/s and $\pm 1\%$ of reading for velocities below 5 m/s [60]. Measurements were carried out in the occupied zone on positions of vertical stands at heights 0.1 m; 0.6 m; 1.1 m and 1.7 m respectively. Sufficient times were allowed for the air in the room to stabilize before any readings were taken.

6.1.3 Tracer-gas measurements

In order to find a pattern of ventilated air distribution in test room, the thorough investigations with use of tracer gas were performed. The units from producer Innova were used for those purposes [62]. The tracer gas was dosed and sampled by unit Brüel & Kjær Innova 1303 (multipoint sampler and doser), and its concentration was measured by use of Innova 1312 (photo acoustic multi gas monitor). Dosing and sampling tubes were firstly connected to special filters in order to prevent dust entering the sampler unit which could cause its malfunction and then were connected to the units. The dosing pipes with diameter of 3 mm were used. Experiments were carried out using Freon R134a ($C_2H_2F_4$) a tracer gas. Freon has advantage over other gases (such as CO_2) that it is usually not present in outside air (zero concentration), which can help to avoid any discrepancy when analyzing the results of the measurements. This feature makes the results of investigations more precise. The accuracy of dosing is $\pm 2\%$.

6.1.4 Pressure drop

The micromanometer FC0510 from Furness Control with the accuracy of 0.25% was used to measure the pressure drop between plenum and investigated room [63].

6.1.5 Thermo-graphic investigation

Thermo-graphic investigation with use of radiometric thermal camera *Hot-Find D* was carried out to investigate the proper functioning of the radiant systems [64]. Rather large temperature differences between walls with activated radiant systems and surrounding internal surfaces allowed us to uncover any problematic areas. Used thermo-graphic camera operates at temperature range from -20 °C to 250 °C with measuring accuracy ± 2 K and $\pm 2\%$ of reading.

6.2 Measurement and evaluation methods

6.2.1 Indoor climate

Predicted mean vote (PMV)

The PMV is based on thermal heat balance of occupant. The human body will always try to regulate any imbalance in heat losses and heat gains from (to) the body. PMV was established to allow evaluation of indoor climate based on mean value of votes of large group of people being exposed to the same environment. It is composed of 7 points scale (from -3 to +3). PMV value of zero represents thermally neutral feeling of occupant. In order to determine the PMV, the air temperature, mean radiant temperature, relative air velocity and humidity have to be known. Furthermore, the metabolic rate and thermal resistance of clothing have to be set. The PMV value can be calculated using equation stated in ISO 7730 or it can be directly read from Tables stated also in ISO 7730 [29].

Predicted percentage of dissatisfied (PPD)

Calculation of PPD is always based on PMV values. The PPD can be set from Eq.(4) or read from Figure 28.

$$PPD = 100 - 95xe^{-(0,033xPMV^4+0,2179xPMV^2)} \quad \text{Eq.(4)}$$

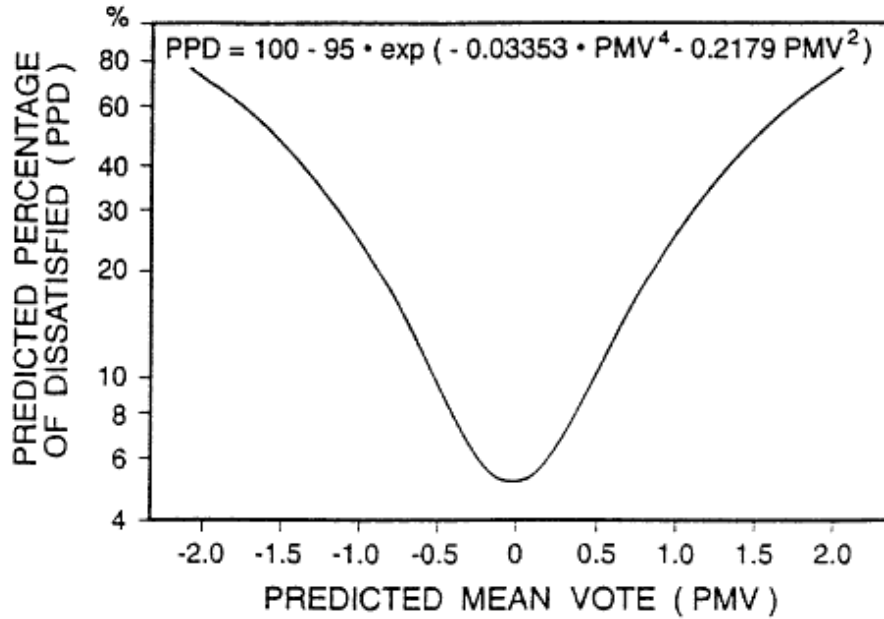


Figure 28: PPD based on PMV values [29]

6.2.2 Temperature measurements

Operative temperature

According to ISO 7726 operative temperature can be calculated according Eq.(5) as mean value of air temperature and radiant mean temperature [59]. This is however possible only if the velocity of air in occupied zone is less than 0.2 m/s and difference between air and mean radiant temperature is less than 4 K.

$$t_o = \frac{t_a + t_r}{2} \quad \text{Eq.(5)}$$

Where: t_o is room air temperature [$^{\circ}C$], t_a is room air temperature [$^{\circ}C$], and t_r is mean radiant temperature [$^{\circ}C$].

If mentioned conditions are not ensured then the average value of air temperature and mean radiant temperature need to be weighted by respective heat transfer coefficients h_c and h_r and Eq.(6) should be used to calculate operative temperature.

$$t_o = \frac{h_c t_a + h_r t_r}{h_c + h_r} \quad \text{Eq.(6)}$$

Where: t_a is room air temperature [$^{\circ}C$], t_r is mean radiant temperature [$^{\circ}C$], h_c is heat transfer coefficient by convection [$W/(m^2 \cdot K)$], and h_r is heat transfer coefficient by radiation [$W/(m^2 \cdot K)$].

Mean radiant temperature

Mean radiant temperature according to ISO 7726 represents "uniform temperature of an imaginary enclosure in which radiant heat transfer from the human body is equal to the radiant heat transfer in the actual non-uniform enclosure" [59]. Its measurement is of particular importance when using radiant

heating and cooling systems. It is calculated according to Eq.(7) by use of surface temperatures and angle factors. Angle factor is the value which represents relation of the surface to the person present in TR and its values can be found in ISO 7726 [59].

$$T_r^4 = T_1^4 F_{p-1} + T_2^4 F_{p-2} + T_N^4 F_{p-N} \quad \text{Eq.(7)}$$

Where: T_N is surface temperature of surface N [$^{\circ}\text{C}$], F_{p-N} is angle factor between person and surface N.

Vertical air temperature difference

The report CR 1752 suggests to measure the temperatures at heights 0.1 m and 1.1 m, which reflects the seated person [14]. American standard ASHRAE 55 suggests that temperatures should be measured at heights 0.1 m and 1.7 m representing standing person [65]. The difference of temperature should not exceed 3 K. The idea here is to investigate the temperature difference between head and ankles of occupant. In Figure 29 is shown the percentage of occupants likely to feel dissatisfied due to vertical air temperature difference in the room.

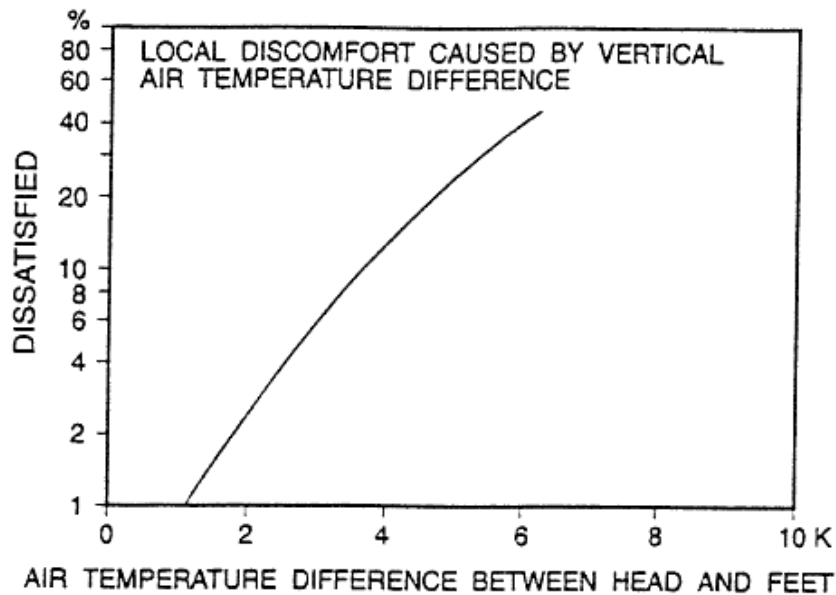


Figure 29: Discomfort caused by vertical air temperature difference [14]

Radiant temperature asymmetry

People could experience a discomfort if large differences in temperatures of surrounding surfaces in the room are present. According to ASHRAE 55 is the maximum acceptable radiant temperature asymmetry 5 K in vertical direction (floor to ceiling) and 10 K in horizontal direction (wall to wall) [65]. Relation of dissatisfaction of occupants and radiant temperature asymmetry is shown in Figure 30.

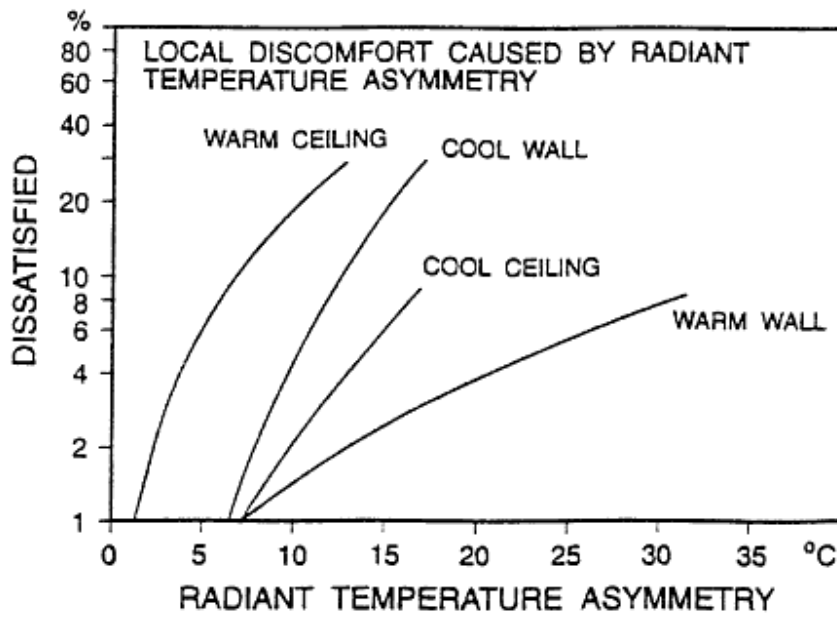


Figure 30: Discomfort caused by radiant asymmetry [14]

6.2.3 Velocity measurements

Draught feeling can be very annoying and therefore much attention should be paid to it. Draught is also most common cause of local discomfort. Draught rating index was used to investigate the critical areas in the room where the draught could bother occupants. Draught rating describes the magnitude of draught and is defined as a percentage of people predicted to be bothered by draught. The model applies for people at light, mainly sedentary activity with a thermal sensation for the whole body close to neutral and for the height of the neck level (1.1 m). For the abdomen and ankle level, the model could overestimate. Draught rating was calculated according to Eq.(8) and it is recommended by ISO 7730 to be kept below value of 15% [29].

$$DR = (34 - t_a)(v - 0,05)^{0,62}(0,37 * v * Tu + 3,14) \quad \text{Eq.(8)}$$

Where: DR is percentage of people dissatisfied due to draught [%], t_a is temperature of air at place of measurement [°C], v is mean air velocity at place of measurement [m/s] and T_u is turbulence intensity at place of measurement [%]. The turbulence intensity represents the magnitude of change of velocity at certain place and time in the space. Turbulent intensity is calculated by use of Eq.(9), Eq.(10) according to [59].

$$T_u = \frac{SD}{v_a} \times 100 \quad \text{Eq.(9)}$$

$$SD = \sqrt{\frac{1}{n-1} \sum_{i=1}^n (v_{ai} - v_a)^2} \quad \text{Eq.(10)}$$

Where: v_a is mean velocity [m/s], v_{ai} is velocity at the time "i" of the measuring period [m/s].

Concerning general velocities in occupied zone, those should not exceed 0.15 m/s in winter and 0.25 m/s in summer [66]. The values could be possibly adjusted according to the activity and clothing level of the occupants. The value also depends on the designed thermal comfort class [14].

6.2.4 Tracer-gas measurements

Ventilation effectiveness

Ventilation effectiveness gives us an idea about the removal of air-borne contaminant from the investigated space and also indicates the level of mixing in the test room. According to [14], “ventilation effectiveness is a function of location and characteristics of air terminal devices and of pollution sources”. An influence on ventilation effectiveness has also flow rate and temperature of supply air. Ventilation effectiveness can be calculated according to Eq.(11). It is based on the measured values of tracer gas concentrations in supply, exhaust and room air in the occupied zone.

$$\varepsilon_v = \frac{C_e - C_s}{C_i - C_s} \quad \text{Eq. (11)}$$

Where: ε_v is ventilation effectiveness [-]; C_e is pollution concentration in the exhaust air [PPM]; C_s is pollution concentration in supply air (background concentration) [PPM] and C_i is pollution concentration in the breathing zone [PPM].

Ventilation effectiveness is directly linked to the position of pollutant source in the room. So if positions of future contaminants are not known, the ventilation effectiveness should not be the only indicator of ventilation performance as it could be very misleading.

Local age of air

Age of air describes a time required for a supply air to reach a particular point in the occupied zone. The air can, however, reach the point through different paths. The mean value of ages of air path is therefore used, called Local mean age of the air [67].

Local mean age of the air can be calculated according to a step up method adapted from Han [67] according to Eq.(12)

$$\theta_p = \int_0^{\infty} \left(1 - \frac{c_p(t)}{c_p(\infty)} \right) dt \quad \text{Eq. (12)}$$

Where θ_p is local mean age of air [s] and c_p is measured concentration in point P in equilibrium [ppm].

7. Numerical simulations

The aim of development of a CFD model of the test room was to allow for deeper understanding of the diffuse ceiling inlet and wall radiant cooling system and to facilitate efficient and economical optimization of the design taking into account various parameters. The commercial fluid dynamics program Ansys Fluent 14.0 was used for numerical calculations [68]. Investigations included air temperatures and air velocities, as those are being regarded as most important variables allowing proper understanding and evaluation of indoor climate. Most importantly, room air temperatures and velocities were measured and can be therefore used to evaluate developed CFD model.

7.1 Model of the test room

The 3D model of investigated room was created in Design Modeler which is a drawing module in Ansys software, see Figure 31. The occupants were modeled as prismatic volume elements with surface area being equal to cylindrical dummies used for measurements. The window, tables, supply and exhaust devices were created as surface elements imprinted into the model body. Porous suspended ceiling was modeled as 5 cm thick in CFD, mainly to allow for proper generation of mesh (in reality, the thickness of porous suspended ceiling was 0.012 m).

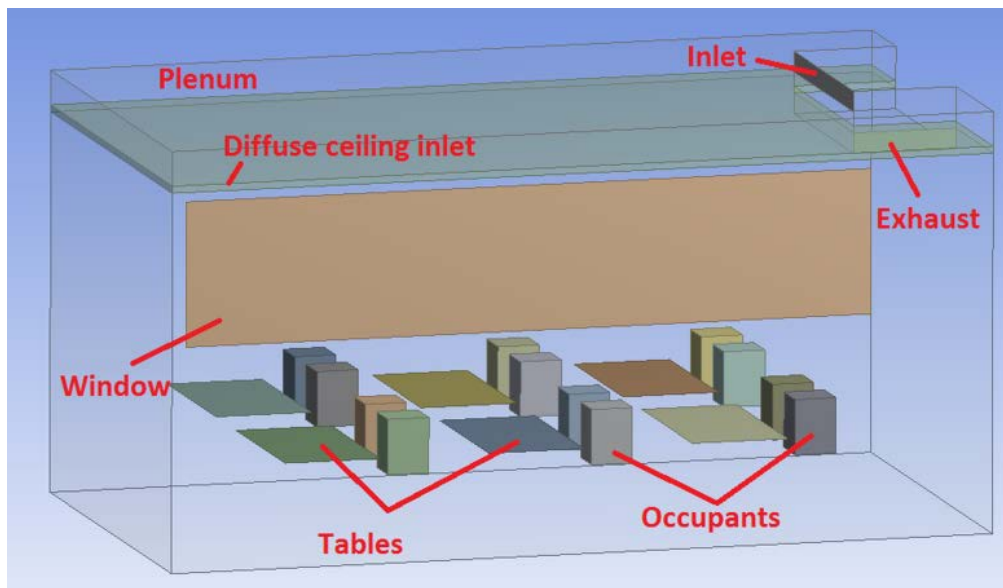


Figure 31: CFD model

7.2 Boundary conditions

Blocks representing the occupants had floor-plan dimensions of 0.25 m x 0.20 m and height 0.45 m. Occupants were placed on horizontal plates with floor-plan dimensions of 0.45 m x 0.40 m, representing the chair. The plate was situated at height of 0.55 m. Tables were modeled as horizontal plates with dimensions of 1.3 m x 0.7 m placed at height of 0.7 m. The heat generated by lighting fixtures was released into the volume close to porous suspended ceiling. Dimensions of supply opening were 0.8 m x 0.1 m. Boundary on exhaust element was defined as static pressure outlet of 0.0 Pa with dimensions of 0.45 m x 0.10 m.

7.3 Grid creation

The general guideline for sufficient amount of volume cells is given by Nielsen [69] (derived originally from German standard VDI 6019) in Eq. (13).

$$N=44.4 \times 10^3 V^{0.38} \quad \text{Eq.(13)}$$

Where: N is number of necessary grid cells and V is room volume ($59.4m^3$). The resulting number of required grid cells yields to 209 615.

The hexahedral grid was created by use of sweep method with final amount of grid cells of 4 354 482. The maximum skeweness of our model was 0.3 which is considered to be very good according to Nielsen [69]. Average value of skeweness was smaller than 0.00045. This is the foundation for the good CFD model.

The necessary amount of cells in the model also depends on position within the model. The areas with quick changes in velocity, temperature or pressure require more precise mesh with more cells to be able to properly model those high gradients. At least 5-10 grid points are needed in areas where some physical changes take place, for example close to the boundaries. For that reason the grid was refined in CFD model in areas close to the wall surfaces. The typical recommended grid distance in the space of ventilated rooms is 10cm for smaller rooms and 30 cm in bigger rooms [69]. Grid distance in developed CFD model was 2.5 cm, which is much more detailed then required. The main reason for this was to get precise CFD predictions around the occupants, which were the main source of movement in the room.

The independence of the grid was investigated by creating four grids with different cell counts. The investigations started with rather coarse grid with 645,432 cells, which is already three times more compare to the minimum requirement according to Nielsen [69]. Final mesh had 4,354,482 cells, see Table 1. The results for each case were taken after full convergence was achieved, meaning that the solution reached stable conditions and energy and mass were conserved. By comparing different variables at certain locations in models with different amount of grid cells, we can elaborate on grid independence. The deviations in results of calculated temperatures and velocities for horizontal plane at height 1.1 m were minor. Based on this finding the solution can be regarded as grid independent, which is the precondition of successful validation of CFD model.

Table 1: Study of grid independence

		Grid 1	Grid 2	Grid 3	Grid 4
Grid cells amount	[pcs]	645,432	1,030,544	1,964,820	4,354,482
Average air temperature at 1.1 m	[°C]	24.2	24.1	24.2	24.3
Average air temperature at exhaust	[°C]	24.5	24.6	24.6	24.6
Average velocity at 1.1 m	[m/s]	0.073	0.069	0.073	0.079
Heat flux imbalance	[W]	12.6	2.8	8.7	3.3
Heat flux imbalance	[%]	1.2	0.3	0.9	0.3

7.4 Turbulence modeling

When a diffuse ceiling inlet is used in ventilated room, the air is often moved due to natural convection, especially in close proximity to walls and heat sources. The Boussinesq model was used to account for buoyancy forces. Boussinesq model assumes that the density of fluid is the same throughout the test room, instead of being a function of the temperature. This simplification could be made in our model, since variations in temperature within the investigated domain were rather small. Temperature was then specified as average temperature in the calculated domain. The buoyant model was defined by gravity-acceleration vertical component with value of 9.81 m/s^2 .

7.4.1 Steady-state turbulence modeling

The steady-state approach to turbulent modeling was taken during numerical simulations in **Paper III** when wall radiant cooling system has been activated. The semi-empirical two equation k - ξ model was used to account for the effects of the turbulence. Two additional equations k and ξ were solved besides mass, energy and momentum equations (as described in section 7.1). RNG type of k - ξ model was used as it partly accounts for low Reynolds number effects when combined with optimal near wall treatment [70]. The k - ξ model works well in fully developed turbulent flows and is therefore suitable for free stream areas of domain but has its limitations in areas close to the wall regions and very often yields in a high wall shear stress and high heat transfer rates [71]. It is rather important for developed CFD model to solve properly the area close to the wall surfaces because two walls were used for radiant cooling system. As large gradients in momentum and temperature occur in area close to the surfaces, the k - ξ turbulent model needs to be combined with proper near wall treatment. That is a wall function in case of k - ξ turbulent model. Wall function represents the effect of the wall boundaries by bridging the viscosity affected layers (viscous sub-layer and buffer layer) in calculation and use semi-empirical functions to solve this area [72]. The scalable wall function was applied because it has advantage over other types of wall functions in that there is no limitation on the grid spacing close to the wall surface. The limiting value of 11.067 is used to ensure that the first grid point will always be in the logarithmic profile area [71].

7.4.2 Transient turbulence modeling

The transient approach was taken to model the turbulence in the room during numerical simulations in **Paper II**. The CFD calculations had difficulties to converge when steady-state turbulence modeling was applied. Large Eddy Simulation method was chosen to account for fluctuation of air in the room. Large Eddy Simulation is using an alternative to the wall function, which is the solution with low Reynolds number turbulence modeling. A fine grid needs to be used in vicinity of wall surface, so the first few nodes can be situated in laminar sub-layer. The grid was refined in developed CFD model in areas close to the wall surfaces in order to allow for proper modeling at this area.

7.5 Porous zone modeling

The pressure drop across a diffuse ceiling inlet was simulated by use of porous zone model in developed CFD model. The diffuse ceiling inlet was modelled in Fluent as fluid domain with added momentum loss equation. The inputs to the porous zone model were based on measured pressure drop across the suspended ceiling. The porosity was set as isotropic with value of 0.15, according to known open area of perforated gypsum plate given by the producer. The momentum loss was defined by viscous and inertial

resistance coefficients, being $1.306 \times 10^9 \text{ m}^{-2}$ and $1,185,000 \text{ m}^{-1}$, respectively. Those values were obtained from quadratic regression analysis of measured values of pressure drop and velocity expressed by Eq. (14)

$$\Delta p = 35554 \cdot v^2 + 1181.8 \cdot v \quad \text{Eq. (14)}$$

Where: Δp is measured pressure drop across the porous suspended ceiling and v is velocity of the air flowing through porous suspended ceiling.

7.6 Solver settings

As pressure-velocity coupling the scheme SIMPLE was used, as it is recommended for steady-state calculations [73] Since the flow in the test room and plenum is turbulent, the second order upwind schemes were used for momentum, turbulence and energy spatial discretization as recommended by Fluent manual [73]. The PRESTO! scheme was used for pressure being suitable for modeling of natural convection.

8. Methods of investigation used in research papers

Paper I

Full scale measurements and CFD simulations of a diffuse ceiling inlet for ventilation and cooling of densely occupied rooms

Measurements and theoretical calculations were used to study and document the performance of a diffuse ceiling inlet. The measurements were carried out in an outdoor full scale test facility prepared for the purposes of the project. Theoretical investigations were done using a CFD model of a test room developed in Ansys Fluent. The evaluation of indoor climate included factors such as air temperatures, air velocities, and ventilation effectiveness. A parametrical study with reduced supply area for a diffuse ceiling inlet was carried out using a validated CFD model.

Paper II

Study of thermal performance of capillary micro tubes integrated into the building sandwich element made of high performance concrete

The performance of a cooling/heating system based on thin plastic capillary tubes cast in an inner layer of a wall element made of high performance concrete was investigated numerically. Steady-state calculations were carried out in a two-dimensional program HEAT2 [74]. Parametrical variations included differences in spacing between the plastic capillary tubes, in the diameter of the plastic capillary tubes, in the thickness of high performance concrete, and in the temperature of the cooling and heating water. The focus was on the temperature and heat flux distribution on the surface of a high performance concrete element.

Paper III

Full scale measurements and CFD investigations of a wall radiant cooling system based on plastic capillary tubes in thin concrete walls

The indoor climate of a test room equipped with a wall radiant cooling system and a diffuse ceiling inlet was investigated in a steady-state situation. The study included measurements and numerical simulations. A full scale testing facility specifically built for the purpose of testing technical solution designs was used for the measurements. The output from the measurements was used to specify the boundary conditions in a CFD model and also for evaluations of its performance. The evaluated CFD model was used for thorough parametrical analysis.

Paper IV

Dynamic behavior of a radiant cooling system based on capillary tubes in walls made of high performance concrete

Paper IV investigated the dynamic effects of the test room with an inbuilt system of radiant cooling based on plastic capillary tubes. The investigations were done as measurements in a real full-scale house built outside and subject to constant changes in weather. This affected the measurements and provided the valuable information on the behaviour of designed systems under real operating conditions. The dynamic effects included the response to changes in a control system.

9. Summary of the research papers

9.1 Paper I

Paper I focused on the investigation of the indoor climate of a test room equipped with a diffuse ceiling inlet for ventilation. **Paper I** focused on the evaluation of **sub-hypothesis 1**.

9.1.1 Investigated setup

Two different scenarios were investigated. The first scenario had a flow rate of 350 m³/h corresponding to an air change rate of 6.6 h⁻¹ and a flow rate of 5.8 l/s·m² of floor area. The second scenario had a flow rate of 480 m³/h corresponding to an air change rate of 9.1 h⁻¹ and a flow rate of 8.2 l/s·m² of floor area. The internal heat load during the investigation was 1012 W, representing the sensible heat load of 12 occupants (each occupant 75 W) and used lighting (112 W).

The investigations in both the scenarios in **Paper I** simulated a classroom with a high density of occupants. The classroom was chosen since it was found that existing classrooms often experience a poor indoor climate, as described in section 1.1.2. The classroom with a high density of occupants was chosen in order to investigate an extreme situation which could be experienced in reality. The floor area was 1.64 m² per occupant, which is slightly less than recommended by EN 15251 for classrooms [51]. Figure 32 shows the layout of the room used in **Paper I** including the measuring points. The boundary conditions of the external wall surfaces were defined with external heat transfer coefficients of 0.33 W/(m²·K) for the roof, 0.36 W/(m²·K) for walls, 2.5 W/(m²·K) for the floor, and 0.8 W/(m²·K) for windows. The surrounding air temperatures for scenario 1 were 0.1 °C for the roof, walls and windows, and 24.2 °C for the floor, and for scenario 2 were 2.8 °C for the roof, walls and windows, and 22.9 °C for the floor. The inlet boundary was assigned a velocity magnitude of 1.22 m/s and an inlet air temperature of 21 °C for scenario 1, and a velocity magnitude of 1.67 m/s and an inlet air temperature of 21 °C for scenario 2.

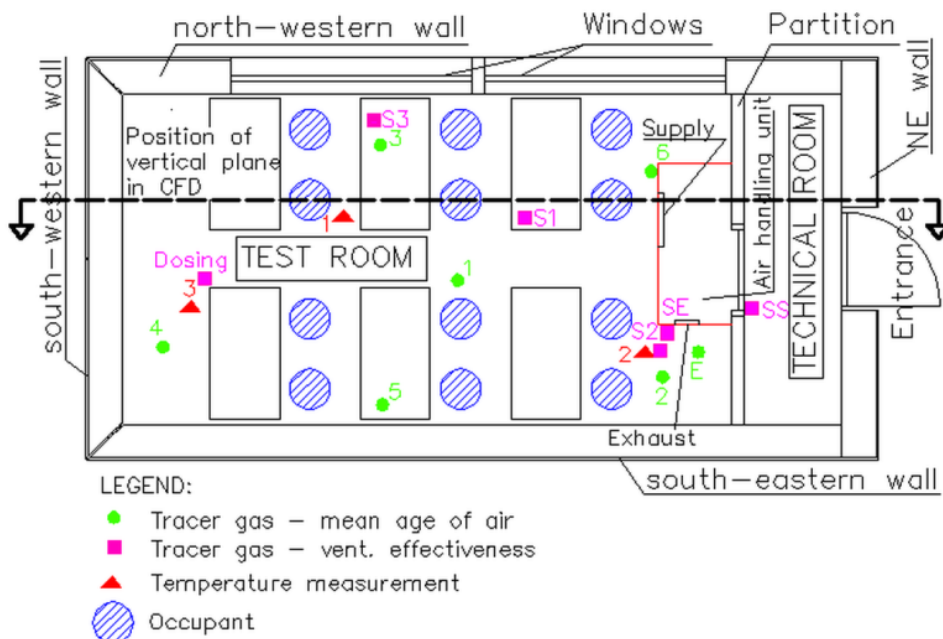


Figure 32: Layout and description of the room investigated in Paper I (Figure 2 in Paper I)

9.1.2 Results and discussion

The assessment of the indoor climate was carried out in the form of Predicted Percentage of Dissatisfied (PPD) values, and the results are presented in Table 2. The higher values for PPD in scenario 2 were a result of the higher ventilation flow rate. Scenario 1 was in category A and scenario 2 was in category B with regard to the PPD evaluation [51].

Table 2: PPD results of measured values (Table 2 in Paper I)

Height [m]	Scenario 1			Scenario 2		
	Stand 1	Stand 2 [%]	Stand 3	Stand 1	Stand 2 [%]	Stand 3
0.1	9.0	9.0	6.0	10.0	13.0	7.0
0.6	5.0	6.0	5.0	6.0	7.0	6.0
1.1	6.0	5.0	5.0	7.0	6.0	6.0
1.7	6.0	5.0	5.0	7.0	6.0	6.0

As can be seen from Figure 33, the temperature distribution is similar for measured and calculated scenarios in lower levels of the room up to the height of 0.6 m. The CFD model overestimated the temperatures at higher levels of the room, resulting in a higher vertical temperature difference than the measured results. This may have been caused by a stronger interaction of the supplied ventilated air with room air in the measured case resulting in better mixing, which was not captured by the CFD model. This may have been because of the way the porous zone model was defined in CFD (for a more detailed description, see in section 7.5). The lowest temperatures close to the floor can be explained by the colder supply air dropping down to the floor surface in combination with internal heat gains creating thermal plumes which move to the upper parts of the room due to buoyancy effects, as can be seen in Figure 34. The higher velocities close to the floor combined with lower temperatures could cause decreased comfort for occupants in the form of draught. Draught rating calculations were therefore made and the results can be seen in Table 3. The position of the longitudinal, vertical plane where results from CFD were taken is shown in Figure 32.

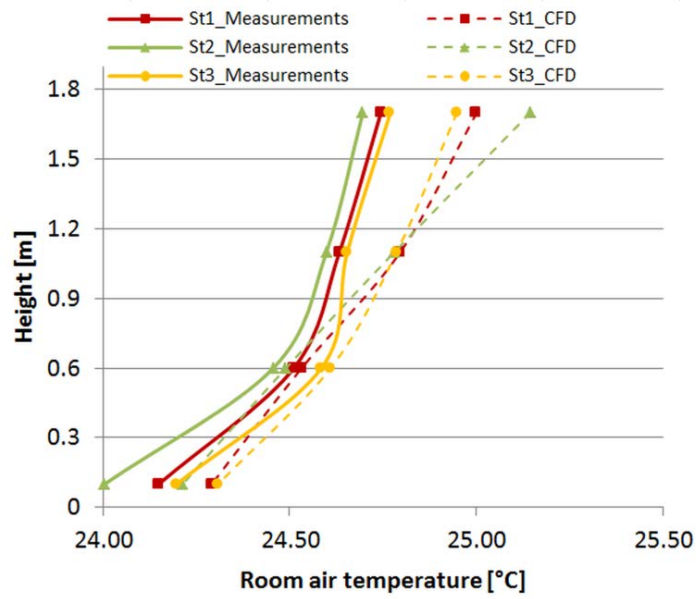


Figure 33: Measured and calculated temperatures on measuring stands for Scenario 1 (Figure 5 in Paper I)

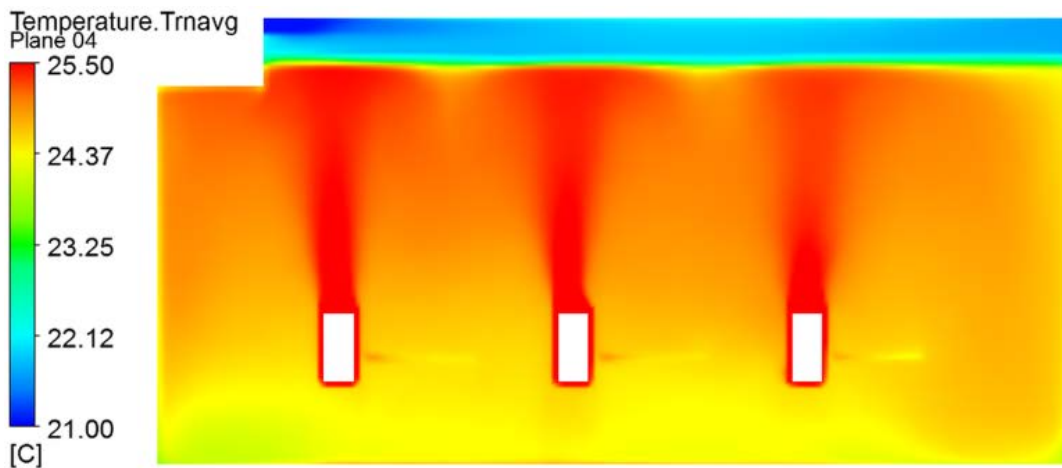


Figure 34: Thermal plumes in CFD calculations of scenario 1 (Figure 7 in Paper I)

Table 3: Draught rating results based on measurements (Table 3 in Paper I)

Height [m]	Scenario 1			Scenario 2		
	Stand 1	Stand 2 [%]	Stand 3	Stand 1	Stand 2 [%]	Stand 3
0.1	0.0	4.8	0.0	0.0	8.9	3.0
0.6	0.0	0.0	2.7	0.0	2.7	3.3
1.1	0.0	0.0	4.4	0.0	0.0	5.8
1.7	3.3	4.5	0.0	5.0	3.0	0.0

The results of the temperature distribution in the room shown in Figure 34 suggest that the air was distributed to the occupied area of the room predominantly in the part of the room furthest away from the air handling unit (upper right part of Figure 34). As no internal heat sources were present in this part of the room, no interactions of supplied and room air could occur that would allow the air to easily flow into the room. As only minor variations in air velocity and pressure were experienced in the diffuse ceiling inlet in the CFD model (see Figure 35), it is assumed that most of the re-distribution of the air happened in the room itself. In other words, nearly the same amount of supply air went through the diffuse ceiling inlet into the room over its whole area. The very small variations were caused by the fact that the inlet air entering the plenum from the air handling unit created higher pressure at the part of the plenum furthest away from the air handling unit. This increased pressure in this area resulted in slightly higher air velocities through the diffuse ceiling inlet. The theoretical average velocity in the porous zone is 0.005 m/s. The results in the room depicted in Figure 36 show higher velocities in the area of the room furthest from the air handling unit directed towards the floor. This further supports the hypothesis that more air was distributed into the room in this area. Figure 36 also shows that higher velocities at height levels close to the floor were experienced as a result of a cold down orientated flow. The occupant situated most to the right in Figure 36 could feel discomfort. The higher velocities were also experienced above the occupants, which could be expected because the occupants acted as internal heat sources resulting in thermal plums created due to buoyancy effects.

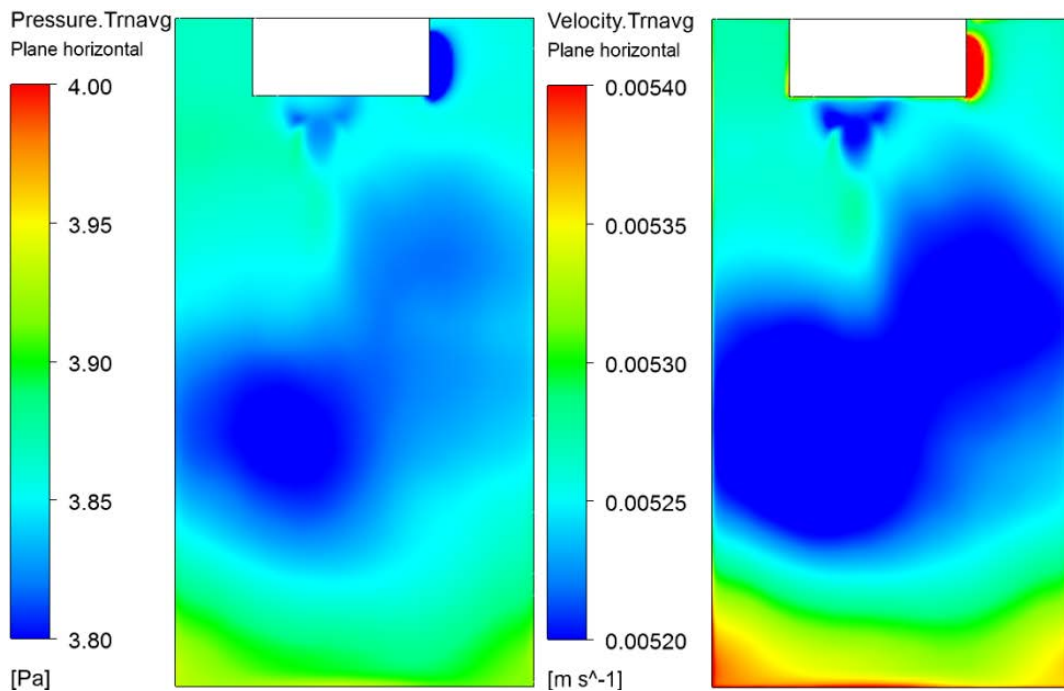


Figure 35: Velocity and pressure distribution in the diffuse ceiling inlet in CFD calculations

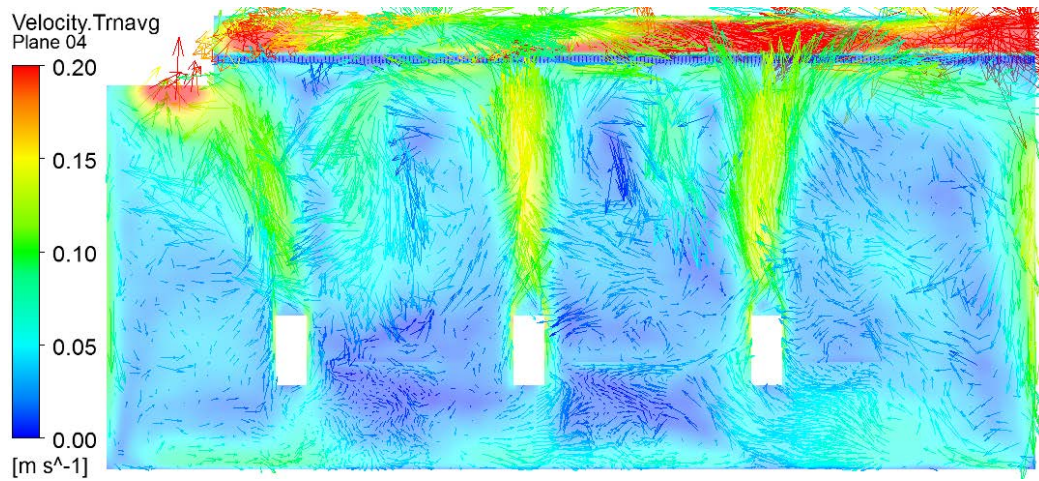


Figure 36: CFD velocity distribution in the room in Scenario 1 (Figure 8 in Paper I)

As can be seen in Figure 37, the velocities experienced were rather low throughout the room considering the rather high ventilation flow rates used during the investigation. The differences between measured and calculated values could be caused by the method used in CFD to interpret the diffuse ceiling inlet. This method ensured the same pressure drop across the diffuse ceiling inlet but did not ensure the same velocity (more details in section 7.5). The whole area of the diffuse ceiling inlet was used to supply the air to the room in CFD calculations, but only 15% of the diffuse ceiling inlet was used during measurements. The chosen method therefore resulted in lower velocities in the area below the DCI in the CFD model. This could potentially influence the overall flow pattern in the room. The larger vertical temperature difference in the calculated scenario, which can be seen in Figure 33, further supports the hypothesis about the lower level of mixing in the CFD model. It was very challenging to get some consistent patterns of velocity development in the room because large fluctuations occurred, mainly due to the buoyancy forces in the room as result of the presence of the large number of occupants representing heat gains in the room. To deal with these fluctuations in CFD calculations in a proper way, the Large Eddy Simulation transient turbulence model was used. Large Eddy Simulation took into account the fluctuations in the room by averaging the values in different time steps. This provided a more precise picture about the behaviour of the air in the room.

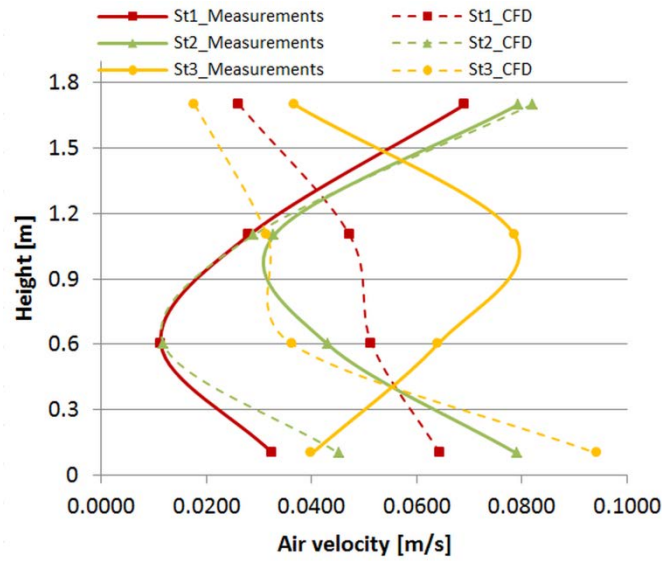


Figure 37: Measured and calculated velocities on measuring stands for Scenario 1 (Figure 9 in Paper I)

Tracer-gas measurements were used to obtain the ventilation effectiveness of the room. The averaged values of ventilation effectiveness were 0.81 for scenario 1 and 0.87 for scenario 2. The results of one hour of measurements are shown in Figure 38.

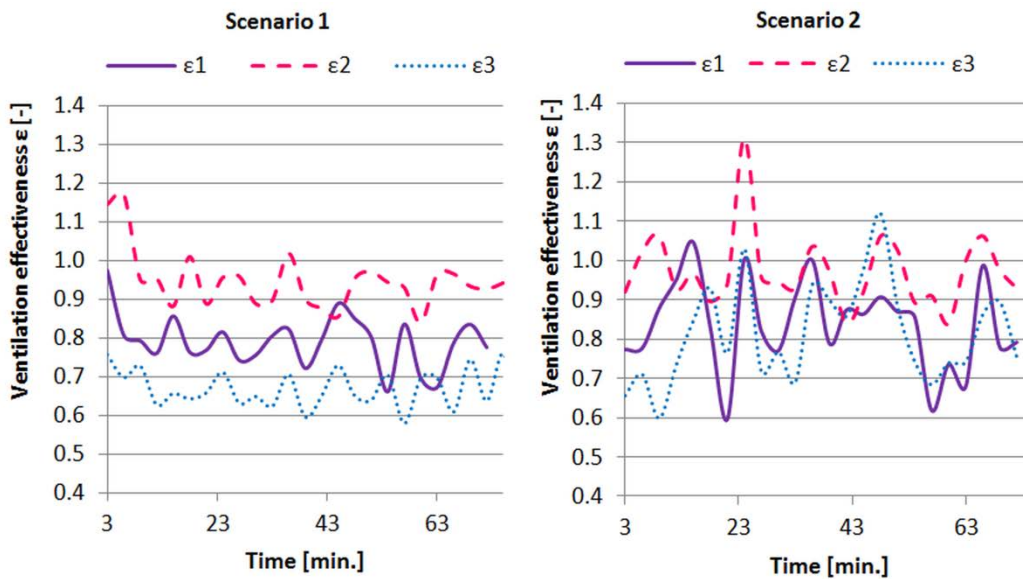


Figure 38: Ventilation effectiveness (Figure 4 in Paper I)

The results of local mean age-of-air investigations can be seen in Table 4. Based on the results of the local mean age-of-air analysis, it seems that exhaust orientation has influence on the flow pattern in the room. This is based on the fact that the local mean age-of-air values were higher at measured points 3 and 6 than at other measured points in the room. The position of the measured points is shown in Figure 32. The higher flow rate resulted in the lower values of the local mean age of air.

Table 4: Local mean age of air (Table 4 in Paper I)

Point	Local mean age of air (minutes)							Room mean age of air
	1	2	3	4	5	6	Exhaust	
Scenario 1	11.52	N/A	11.10	9.89	10.02	N/A	10.61	10.63
Scenario 2	6.37	6.16	7.90	7.42	6.31	10.95	7.56	7.52

The parametrical study included a scenario with the area of the diffuse ceiling inlet reduced to approximately 35% of its original size. The new supply area is shown in Figure 39 by three green rectangles with dimensions of 3.15 m x 0.70 m. The rest of the suspended ceiling area was assumed to be solid gypsum through which the air could not penetrate.

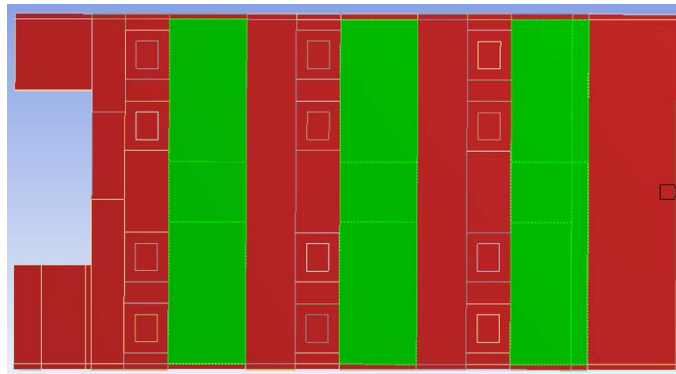


Figure 39: Reduced area of supply inlet (Figure 12 in Paper I)

As can be seen from Figure 40, the temperatures in the room were generally lower in the scenario with the reduced area of diffuse ceiling inlet. This can be explained by a different flow pattern in the room, which has considerable influence on the heat losses through the building façade. It can be seen from Figure 41, that air velocities in the room were higher in the scenario with the reduced area of the diffuse ceiling inlet. This resulted in the higher convective heat transfer coefficient of the room surfaces which led to the higher heat loss through the building façade, and temperatures in the room were lowered as a consequence. Shown in numbers, the heat loss through the room constructions of the original solution was 580 W and 641 W in the solution with the reduced area of the diffuse ceiling inlet. The vertical temperature difference is smaller in the solution with the reduced area of the diffuse ceiling inlet, implying that a better mixing was achieved. However, a different situation might be experienced in larger rooms where the ratio of room volume to the area of external wall is much higher. The influence of heat losses through the external walls would not be so high, which could result in a different temperature distribution in the room.

The above explanations are supported by the results of measurements from **Paper III** where the scenario with the reduced area of inlet was investigated with activated walls for cooling. In that case, the differences in results for room air temperature distribution between the original scenario and the scenario with a reduced area of supply inlet were minor. The reason was that the same temperature of cooled walls was maintained during investigations in both cases. More details can be found in section 9.3.2.

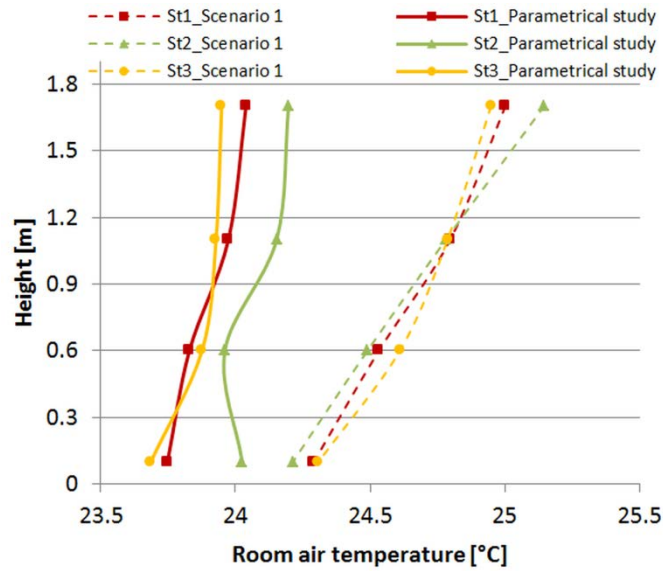


Figure 40: Temperature distribution in the solution with the reduced area of the diffuse ceiling inlet (Figure 13 in Paper I)

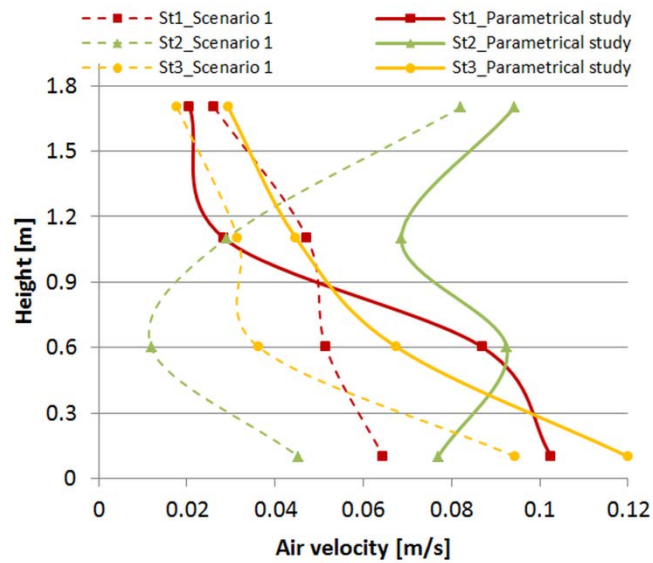


Figure 41: Velocity distribution in the solution with the reduced area of the diffuse ceiling inlet (Figure 14 in Paper I)

To validate an assumption about the airtightness of perforated gypsum board connections, thermo-graphic pictures were taken. The green line in Figure 42 shows the position where two perforated gypsum boards are connected. Air with a temperature of 21 °C was supplied, which was a lower temperature than that of the perforated gypsum boards. Figure 42 shows that less air was supplied at the position of the connection of the two perforated gypsum boards because some of the perforations were blocked in that area by the silicon paste used to seal the connection.

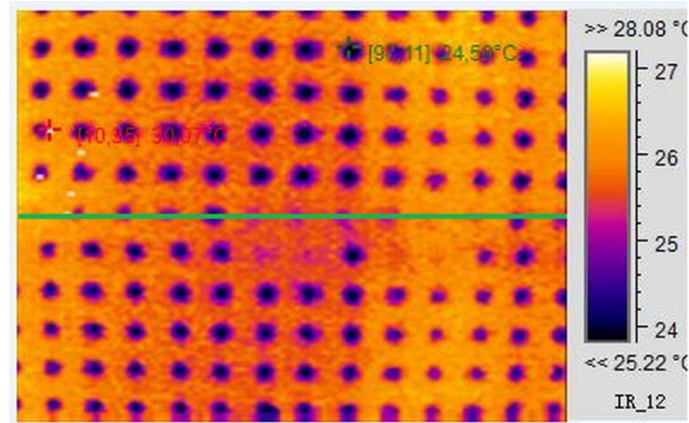


Figure 42: Airtightness of the connection of two perforated gypsum boards (Figure 11 in Paper I)

The pressure drop measured across the diffuse ceiling inlet was 7.2 Pa for Scenario 1 and 10.16 Pa for Scenario 2.

9.1.3 Conclusion

It has been shown that the diffuse ceiling inlet is an appropriate solution for ventilation in spaces with a high density of occupants for flow rates between $5.8 \text{ l/s}\cdot\text{m}^2$ and $8.2 \text{ l/s}\cdot\text{m}^2$ of floor area resulting in cooling by outside air between 23 W/m^2 and 32 W/m^2 . Only slightly higher air velocities were experienced in the lower parts of the test room, so the designed system is a draught-free solution. The average ventilation effectiveness was 84%, corresponding to mixing ventilation. The results show that **sub-hypothesis 1** is true for the scenarios investigated. The results from investigations in **Paper I** were used as the starting point for investigations in **Paper III**.

9.2 Paper II

Paper II studied the thermal performance of the plastic capillary tubes cast in the layer of high performance concrete. **Paper II** focused on the evaluation of **sub-hypothesis 2**.

9.2.1 Investigated setup

The section of the investigated high performance concrete element is depicted in Figure 43. The element was composed of a 20 mm outer layer of high performance concrete, 250 mm of thermal insulation, and a 30 mm inner layer of high performance concrete containing the plastic capillary tubes. The plastic capillary tubes were located in the middle of the layer of high performance concrete during this investigation. The plastic capillary tube investigated in **Paper II** had an outer diameter of 3.5 mm and a wall thickness of 0.75 mm, resulting in an inner diameter of 2 mm. These dimensions were different from the dimensions of the plastic capillary tubes actually cast in the layer of high performance concrete in the wall elements used in the full scale test building and used in further investigations in **Papers III** and **IV**. Further description of the plastic capillary tubes used there can be found in section 5.2.

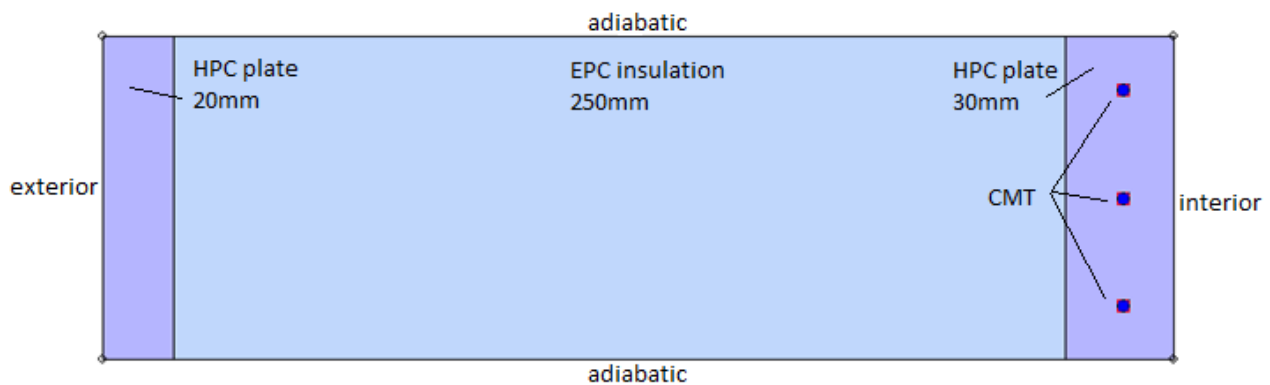


Figure 43: Section of the high performance concrete element built in the program HEAT2 (Figure 1 in Paper II)

The circular shape of the plastic capillary tube was modelled as a rectangular shape due to the limitations of the program HEAT2, which works only with a rectangular grid [74]. However, the producer of the program offered appropriate equations suited for recalculation from circular to rectangular shape. More details on the calculation procedure can be found in the appended **Paper II**.

The parametrical study included investigation of variation in the spacing between the plastic capillary tubes of 30 mm, 50 mm, 70 mm, and 100 mm, variation in the thickness of the high performance concrete's inner layer of 30 mm and 50 mm, variation in the diameter of the plastic capillary tube of 3.5 mm and 4.5 mm, and variation in the working fluid temperature of 21 °C, 22 °C, and 24 °C for the heating scenario and 18 °C, 21 °C, and 22 °C for the cooling scenario. The temperatures were chosen based on the fact that designed systems for heating and cooling should work with temperatures of heating and cooling water similar to the air temperatures in the room.

9.2.2 Results and discussion

The temperatures were evenly distributed over the surface of the inner layer of the high performance concrete wall element even with increased spacing of the plastic capillary tubes, as can be seen in Figure 44

and in Table 5. This finding is the main precondition for creating an element which will contribute to a uniform thermal environment in the room and will maximize the potential of natural sources of energy.

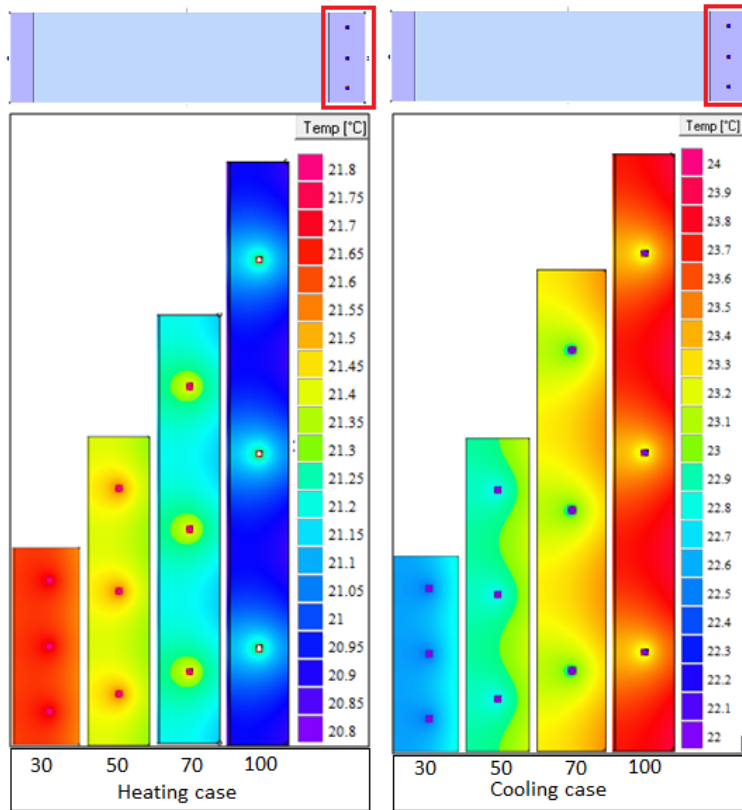


Figure 44: Temperature distribution in the inner layer of the high performance concrete element (Figure 4 in Paper II)

Table 5: Differences in Kelvin between the maximum and minimum temperatures over the inner surface of the high performance concrete wall element (Table 2 in Paper II)

Max. Temperature differences over the surface of HPC wall						
Distance of CMT	Heating				Cooling	
	21 °C	22 °C	24 °C	18 °C	21 °C	22 °C
Mm						
30	0.006	0.010	0.018	0.031	0.020	0.016
50	0.024	0.042	0.076	0.136	0.085	0.067
70	0.055	0.060	0.173	0.310	0.216	0.152
100	0.110	0.125	0.347	0.622	0.385	0.306

As the required power output of heating and cooling systems depends on a particular installation, the aim of this study was to investigate how different configurations of plastic capillary tubes behave under different operating conditions.

Figure 45 shows the results of the heat flux on the inner surface of the high performance concrete wall element for each the investigated scenarios. The temperature of heating and cooling water has the biggest

influence on the experienced power output from the wall element. The heat removed from the room can be increased by 60% when the temperature of cooling water decreases 3 K.

However, the idea in this project was to use water at a similar temperature to the room air temperature. Therefore further investigations focused on various other ways of increasing the power output from the wall without changes in the temperature of the water. One way to increase the power output is to decrease the spacing between the plastic capillary tubes. The increase in the power output was about 50% when the spacing was decreased from 100 mm to 30 mm. Another way is to increase the diameter of the plastic capillary tubes. This resulted in a considerable increase in power output, see Figure 45.

The influence of the thickness of the high performance concrete layer of the wall element on the power output was also investigated, because there can be situations where the designed 30 mm will not be sufficient. From Figure 45 it can be seen that an increase in the thickness of the high performance concrete layer from 30 mm to 50 mm has a rather small influence on the power output. This is due to the rather high thermal conductivity of the high performance concrete used, resulting in a mild increase in the thermal resistance of the high performance concrete layer. This is a positive finding, which means that the thickness of the inner layer of the high performance concrete wall element should not be a limiting factor in the design of the solution presented.

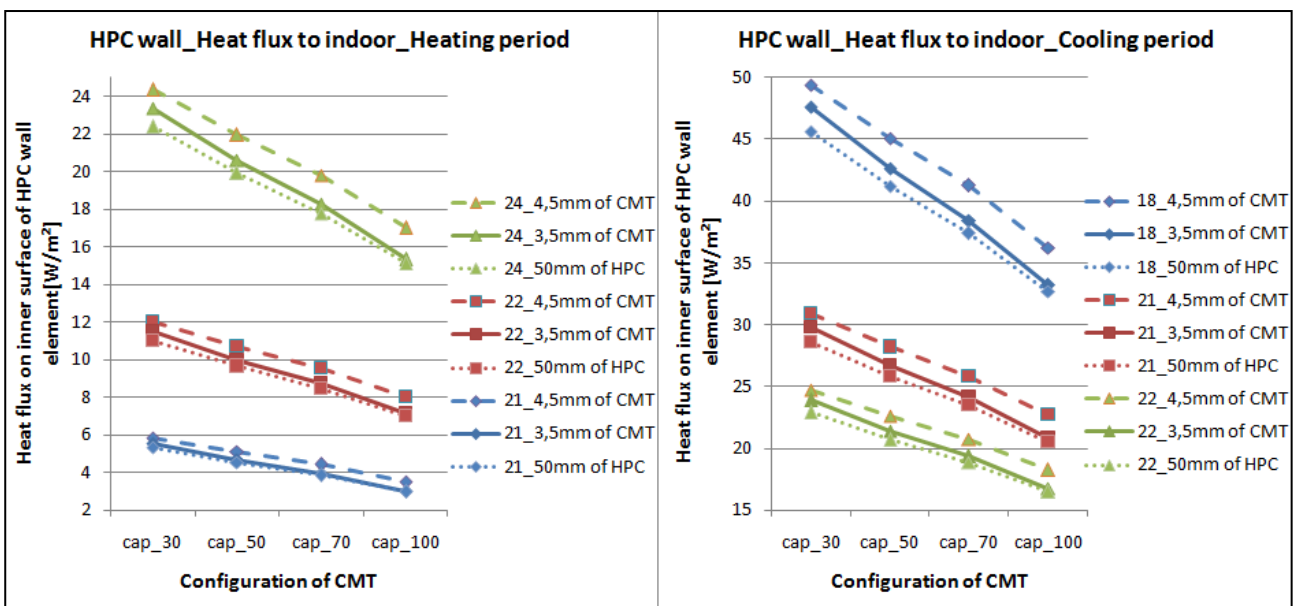


Figure 45: Heat flux of the high performance concrete element towards an indoor environment for various scenarios (Figure 6 in Paper II)

The limiting factor for the cooling could be the dew point temperature of the room air, which limits the surface temperature of the cooled walls. The ISO 7730 standard recommends maintaining the humidity level in the room between 30% and 70% [29]. The acceptable indoor operative temperature according to ISO 7730 is 26 °C (for environmental class B) [29]. From the measurements described in section 9.4, it can be seen that the operative temperature is 1 – 1.5 K lower than the room air temperature, depending on the position of the measurement in the room. Therefore the maximum acceptable room air temperature was assumed to be 27 °C for further analysis in this paper. The dew point for air at 27 °C, assuming the middle value in the recommended range for humidity of 50%, is 16 °C. The minimum surface temperature of the

scenario with spacing of 30 mm and a capillary tube diameter of 3.5 mm was found to be 20.6 °C, which means that condensation would not be present. The resulting values from this scenario for cooling, recalculated to the floor area of the test room used for the investigations in this thesis (described in section 5.1), were 59.6 W/m², 37.6 W/m², and 29.5 W/m² for cooling water temperatures of 18 °C, 21 °C, and 22 °C respectively. It was found during measurements and CFD calculations in Paper III that the indoor air temperature was 24.5 °C – 25 °C when a cooling power of 29 W/m² was used and 22 °C – 23 °C when a cooling power of 59 W/m² was used. The value 29 W/m² can therefore be assumed as a suitable and sufficient amount of cooling power for the scenarios investigated in the test room to maintain a comfortable indoor climate without draughts. Based on these findings, it can be concluded that **sub-hypothesis 2** is true for the cooling mode.

The targeted value for heat flux to the indoor environment for the heating scenario was set to 10 W/(m²·K). This value was chosen as reference so that the results would be comparable with other radiant heating systems, for example with one of the most commonly used radiant heating systems composed of thick plastic (cross-linked polyethylene) pipes cast in the floor construction. The value of 10 W/(m²·K) is the usual design value for the required power of floor heating for passive houses. The required energy output of the system depends on the type of building and the location it is built in. The variables influencing the design are the heat loss of the building (including transmission and ventilation heat loss), comfort issues (temperature of the surface, draft, etc.), the surface area available for installation of the RHCS, and the required reaction time of the system. Different scenarios were therefore investigated to assess the performance of the system under different circumstances. The resulting values of the scenario with spacing of 30 mm and a capillary tube diameter of 3.5 mm for heating, recalculated to the floor area of the test room used for the investigations in this thesis (described in section 5.1), were 28.8 W/m², 14.8 W/m², and 6.9 W/m² for heating water temperatures of 24 °C, 22 °C, and 21 °C respectively. The heating was not needed in the test room because the heat gains (between 51.5 W/m² and 77.8 W/m² of floor area in the test room) were higher than those actually needed for heating. However, the results for heating would be applicable for any other type of building and are therefore relevant as part of the study. It can be concluded that **sub-hypothesis 2** is true for the heating mode.

Increased energy losses to the outside environment were experienced during the investigations as a result of changes in the temperature of the inner layer of high performance concrete: increases in the case of heating mode and decreases in the case of cooling mode. The configurations with integrated plastic capillary tubes were compared with the situation without any tubes in the inner layer of the high performance concrete. Figure 46 shows the increase of the heat flux to the outside environment for various configurations in heating mode. The heat loss increased substantially with increased heating water temperature and the increase is about 20% for a heating water temperature of 24 °C. This finding further supports our initial aim of using heating and cooling water with a temperature very close to the room air temperature. However, this also means that large areas should be available in a building for the application of such a solution. Thorough discussions in the early stages of a project are therefore necessary between all the parties involved in the design of a building. The resulting value for heat loss is rather high and could possibly influence the overall heat balance of the building to a considerable degree. This finding could mean limitations in the use of radiant systems for heating and cooling in buildings in general. The next step in the investigation was to find out how big the influence of increased heat loss from the high performance concrete wall element is on the overall heat losses from the building. The energy performance calculations were carried out using the tool called IDA ICE for dynamic calculations of buildings [75]. The overall heat loss increase was found to be 2.6% for the case under investigation.

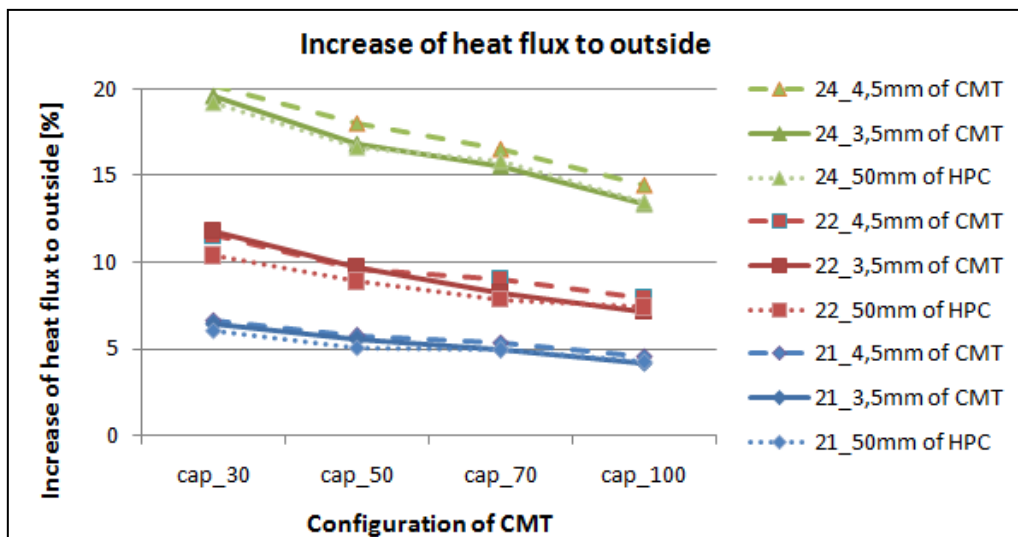


Figure 46: Increase of heat flux to the outside environment as result of the use of CPTs in the high performance concrete inner layer (Figure 9 in Paper II)

9.2.3 Conclusion

The temperature was evenly distributed over the whole surface of the cooled walls, even with bigger spacing of the plastic capillary tubes, such as 100 mm. The investigations in **Paper II** showed that the temperature of the cooling water has the biggest influence on the power output experienced from the wall components. The heat removed from the room can be increased by 60% when the temperature of cooling water decreases from 22 °C to 18 °C (4 K). The increase in the power output was about 50% when the spacing of plastic capillary tubes was decreased from 100 mm to 30 mm. Changing the spacing between the plastic capillary tubes is the most feasible option for power increase if the solution is to remain economically attractive and if a low temperature difference between cooling water and room air is to be maintained. Increasing diameter of the plastic capillary tubes would mean greater complications for a manufacturer. These statements are based on information obtained from the manufacturer of the plastic capillary tubes used in this project. The increased heat loss to the outside environment is rather small proportionally to the overall heat losses of the building. However, it must be taken into account during the design of a building. The investigations in **Paper II** showed that **sub-hypothesis 2** is true for the scenarios investigated.

9.3 Paper III

Paper III investigated the temperature and velocity distribution in the room when two walls were activated for cooling. **Paper III** focused on the evaluation of **sub-hypothesis 3**.

9.3.1 Investigated setup

The internal heat gains during the experiment were 1327 W. The cooling power delivered was 1112 W using cooling water with a mean temperature of 16.3 °C. Measured data were mainly used to evaluate the validity of the developed CFD model (described in more detail in section 7). The CFD model was used for further parametrical studies with various room setups and configurations of the diffuse ceiling inlet and wall radiant cooling systems. Boundary conditions for the external wall surfaces were defined with external heat transfer coefficients of 0.18 W/(m²·K) for the roof, 0.19 W/(m²·K) for walls, 2.47 W/(m²·K) for the floor, and 1.26 W/(m²·K) for windows, and surrounding air temperatures of 8.5 °C for the roof, walls and windows, and 19.8 °C for the floor. The inlet boundary was assigned with a velocity magnitude of 1.44 m/s and a temperature of 26.6 °C.

The layout of the test room and a description of the measuring points are shown in Figure 47. Two walls were used for cooling purposes and are shown by blue lines.

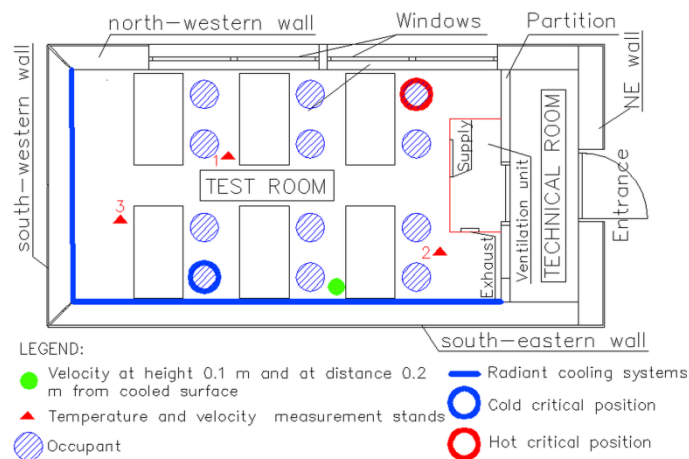


Figure 47: Layout and description of the test room in Papers III and IV (Figure 4 in Paper III)

The two critical positions shown in Figure 47 by blue and red circles were used to assess the operative temperature in the test room. It could be expected that the temperature of the radiant cooling system would have a rather significant influence on the operative temperature in the room. Occupants situated in different critical positions could feel different levels of thermal comfort. The position close to the two cooled walls is shown by the blue circle. The occupant could feel too cold in this area. The position in the opposite corner of the room is shown by the red circle. Theoretically, the occupant situated in this area could feel too hot because it is situated rather far from the cooled surfaces and can be also influenced by solar radiation from the window (although this was not the case in **Paper III** because solar radiation was not present during the measurements).

Ventilation flow rate

A constant ventilation flow rate of 415 m³/h was used during investigations in **Paper III** and **Paper IV**, corresponding to an air change rate of 7.8 h⁻¹ and a flow rate of 6.9 l/s·m² of floor area. This air flow rate is

between class B and class A according to the relevant standard [51]. The use of only one ventilation flow rate was chosen based on the fact that the main focus in these two papers was on the radiant systems, and the range of the papers would be too broad and therefore more difficult to analyse if different ventilation flow rates were used. Ventilation during the investigations in **Paper III** and **Paper IV** was used purely for the purpose of fresh air delivery in accordance with the relevant standards, since the temperature of the supply air was too high to cool the room.

Flow rate of water in the cooling loop

A constant water flow rate of 0.125 l/sec was maintained in the cooling loop of the radiant cooling system for all the experiments carried out as part of this thesis. The flow rate was the highest that the water pumps installed could handle. It was high enough to ensure that the surface temperature of the cooled walls was evenly distributed over the whole surface. This is important for achieving overall uniformity of thermal comfort in the room. The pressure drop of the radiant system with plastic capillary tubes with this water flow rate of 0.125 l/s was 0.03 bar.

9.3.2 Results and discussion

Measured temperature development

Measurement of temperatures in the room was carried out for a period of 72 hours and is shown in Figure 48. Such a long period of measurements allowed us to select a time period which would be closest to a steady-state situation. The selected time period was assumed to be in a quasi-steady-state situation because the temperatures in the room did not change markedly and were therefore considered to be constant. The same applied to the outside temperature. An absolute steady-state situation could not be achieved in the facility used in this project due to the constantly changing outside environment. Furthermore, some of the features, such as the sky temperature and solar radiation on the outer surfaces of the building were not measured. The quasi-steady-state situation is therefore the most precise period of time which could be used for the validation of the developed CFD model.

The measured values of the temperatures and velocities were averaged values taken from the period between hours 68 and 71. This was one of the three quasi-steady-state periods experienced during whole time span of the measurements. This period was between 4 a.m. and 7 a.m. The temperatures and velocities on the moveable stands in the room were measured during this period.

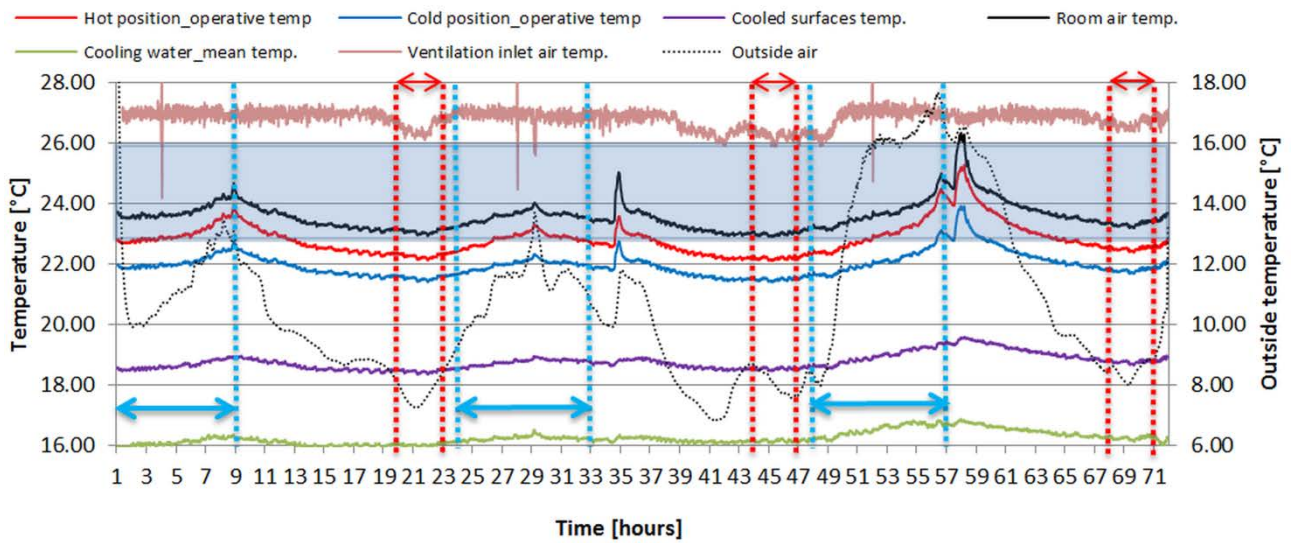


Figure 48: Temperature development from measurement (Figure 6 in Paper III)

Operative temperatures were close to 23 °C and 22 °C for hot and cold critical points respectively (critical positions are described in section 9.3.1 and are shown in Figure 47) and by the red and blue lines in Figure 48. It is clear that the operative temperatures were significantly influenced by the temperatures of the cooled surfaces. This resulted in environment category classes B and C, respectively [51]. The temperature of the cooled surfaces was 18.5 °C most of the measurement period.

Evaluation of the developed CFD model

The measured and calculated temperatures of room air on moveable stands are compared in Figure 49. The rather small variations in measured and calculated values suggest that the developed CFD model (described in section 7) gave reliable predictions. The CFD model was assumed to have been validated at this point with regard to the air room temperatures.

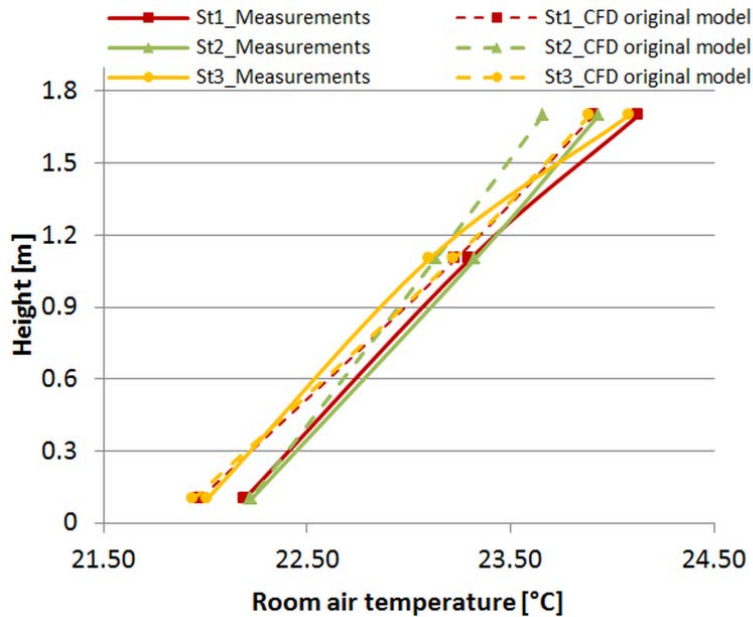


Figure 49: Measured and CFD predicted temperature distribution in the test room (Figure 7 in Paper III)

The air velocities in the room were not so predictable because the flow of the air in a room is a complex phenomenon dependent on many different factors, such as the turbulence level in the room, the shape of the room, the source of convective air jets, and the presence of obstacles in the room. CFD predictions of the air velocities in mechanically ventilated rooms are rather difficult as is well-known from previous studies. The calculated results obtained were mainly used to predict potential areas of the room where a draught might possibly be created as a result of high velocities, rather than for direct comparison with the measured values. As can be seen from Figure 50, the CFD model slightly underestimated the velocities in the room. However, the calculated vertical velocity profile predictions followed the measured development of the velocities, which means that the general behaviour and flow pattern within the test room was predicted and captured well by CFD calculations. Based on these findings, the developed CFD model was assumed to have been validated and suitable for further investigations of velocities in mechanically ventilated rooms. This CFD model will be referred to as the “original model”. Velocities close to the floor surface were generally higher than in the rest of the room. This can be explained by the effects of buoyancy forces resulting from the internal heat sources combined with the cold vertical walls.

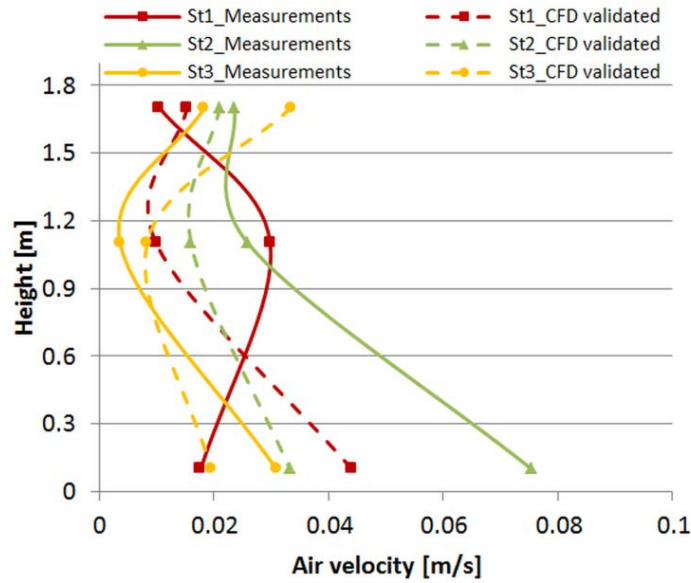


Figure 50: Measured and CFD velocity magnitude distribution in the test room (Figure 8 in Paper III)

Parametrical study: Reduced area of the diffuse ceiling inlet

The original CFD model was further studied in the scenario with the area of the supply inlet reduced to 35% of its original area. The reduced area of supply inlet is shown by the green colour in Figure 51. The temperature of the cooled surfaces was 18.5 °C.

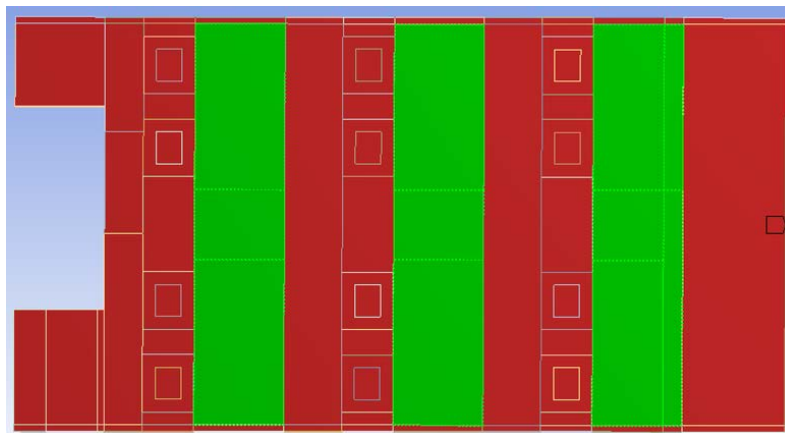


Figure 51: Position of reduced area of supply inlet (Figure 10 in Paper III)

The resulting temperature and velocity developments in the room were very similar to the results of the original model except for the situation at stand 2, where larger differences in temperature were experienced, see Figure 52. The specific reason for this behaviour was not found. Disruption in this area of the room can be also seen in the velocity distribution depicted in Figure 53.

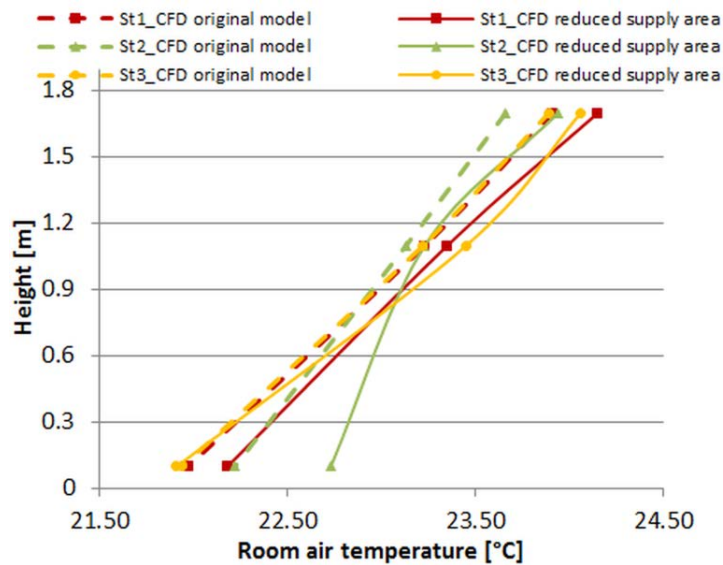


Figure 52: Temperature distribution in the scenario with reduced supply area (Figure 11 in Paper III)

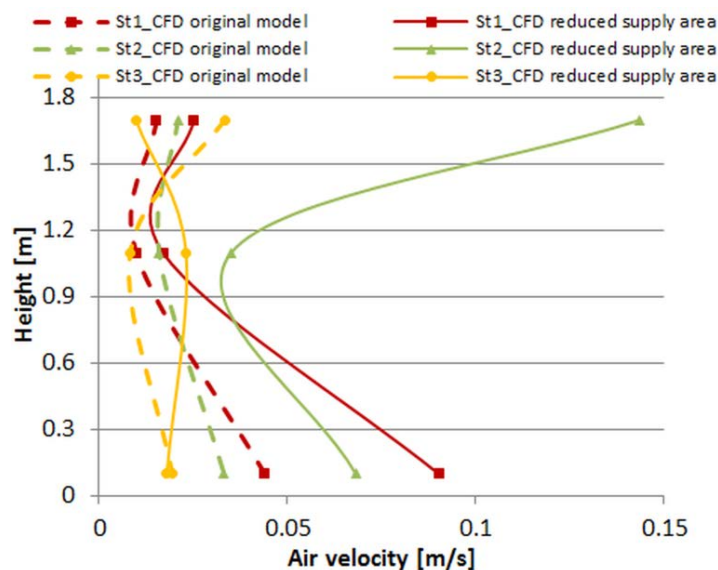


Figure 53: Velocity distribution in the scenario with reduced supply area (Figure 12 in Paper III)

Even when the area of the supply inlet was substantially reduced, the effect on the temperature and velocity development in the room was minor. This is an important finding because it could be anticipated that the ceiling area available for the purposes of ventilation will be more limited in most future applications in real buildings (due to lighting fixtures, etc.).

Parametrical study: Variation in the temperature of the cooled surfaces

In order to see the effect of surface temperature of the cooled walls on temperature and velocity distribution in the room, two additional scenarios with cooled wall temperatures of 14 °C and 21.5 °C were numerically investigated in CFD in addition to the scenario with the original model with the temperature at

18.5 °C. The vertical temperature difference was higher in the scenario with the temperature at 14 °C, as can be seen in Figure 54. This could be explained by a higher velocity of colder air close to the cooled walls as found in the CFD calculations. The velocities at a height of 0.1 m and a distance of 0.01 m from the south-eastern wall were 0.05 m/s, 0.04 m/s, and 0.03 m/s for cooled wall temperatures of 14 °C, 18.5 °C, and 21.5 °C respectively.

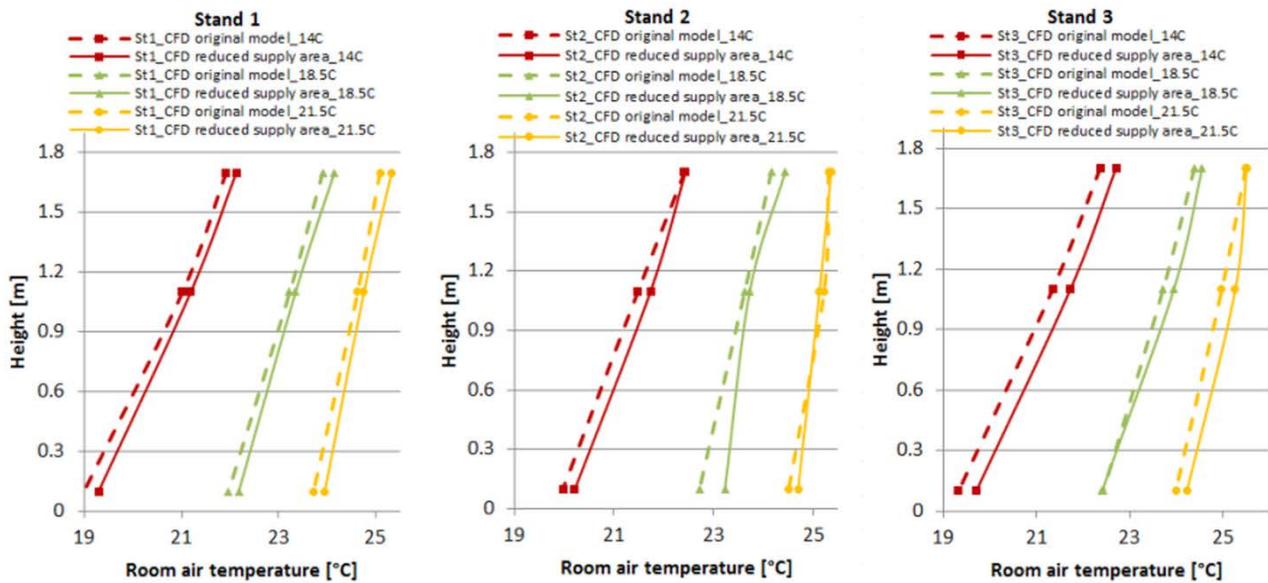


Figure 54: Comparison of temperature distribution between the original scenario and the scenario with reduced supply area for various wall temperatures (Figure 13 in Paper III)

The results of the velocity distribution for the scenarios with different cooled wall temperatures are shown in Figure 55. Higher velocities were experienced on stand 2 close to the floor in the scenario with the cooled wall temperature of 21.5 °C. This was experienced in both the original scenario and the scenario with the reduced area of supply inlet, and it was caused by a stronger flow pattern created in the corner of the room, as can be seen in Figure 56. This flow pattern was probably created by a combination of the cold surface of the south-eastern wall and the general flow pattern in the test room. A similar flow pattern was also observed when the temperature of the cooled walls was 14 °C, but was not observed when the temperature of the cooled walls was 18.5 °C. Regardless of this phenomenon, draughts were not created in the room in any of the investigated scenarios (see Table 3 and Table 4 in Paper III).

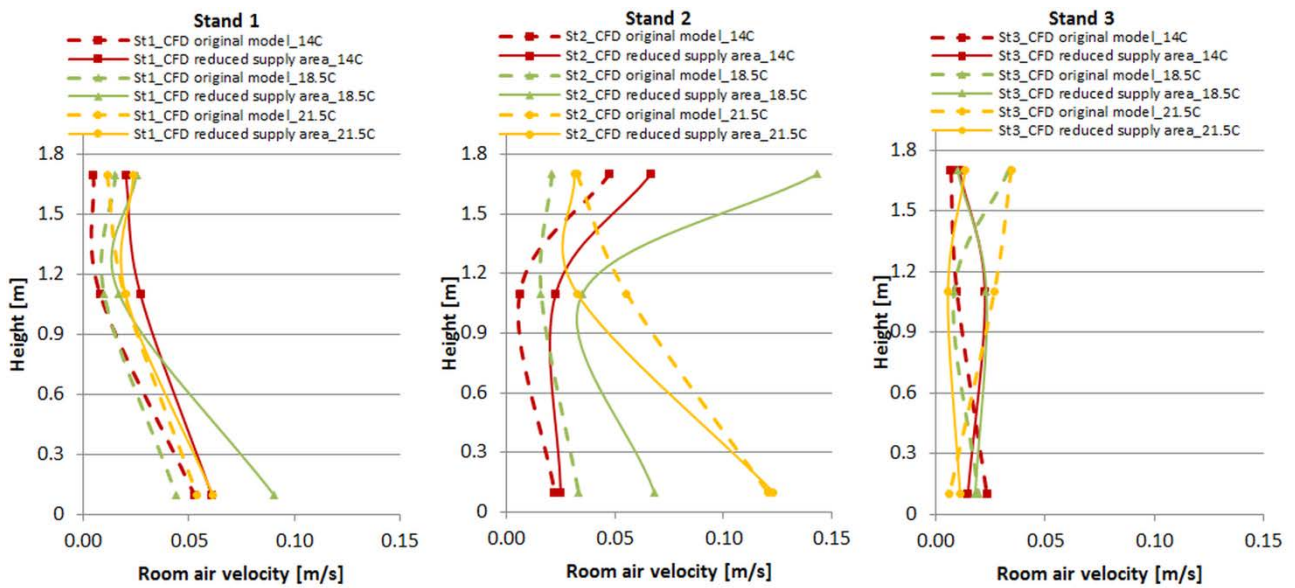


Figure 55: Comparison of velocity magnitude distribution between the original scenario and the scenario with the reduced supply area for various wall temperatures (Figure 14 in Paper III)

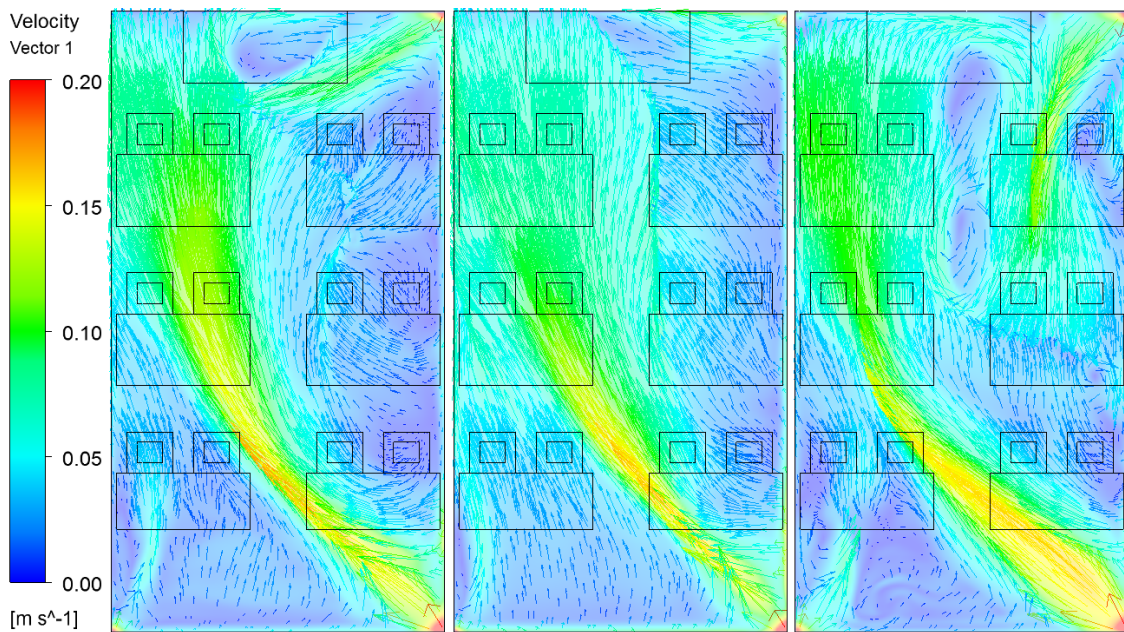


Figure 56: Velocities for the validated scenarios at height 0.1 m with cooled wall temperatures of 14°C, 18.5°C and 21.5°C (Figure 15 in Paper III)

Parametrical study: Variation in the heat gains

To see the effect of internal heat loads on temperature and velocity distribution in the room, two scenarios were investigated. The first with increased internal heat gain (2654 W) and the second with reduced internal heat gain (664 W). The results showed that increased internal heat loads mean higher velocities in the room, mainly in areas close to the floor surface (Figure 57). These findings could mean that air flow patterns in the room were governed to certain degree by buoyancy forces. This idea is further supported by

the smaller vertical temperature difference in the scenario with the lower internal heat gain, because the movement in the room is limited, see Figure 58.

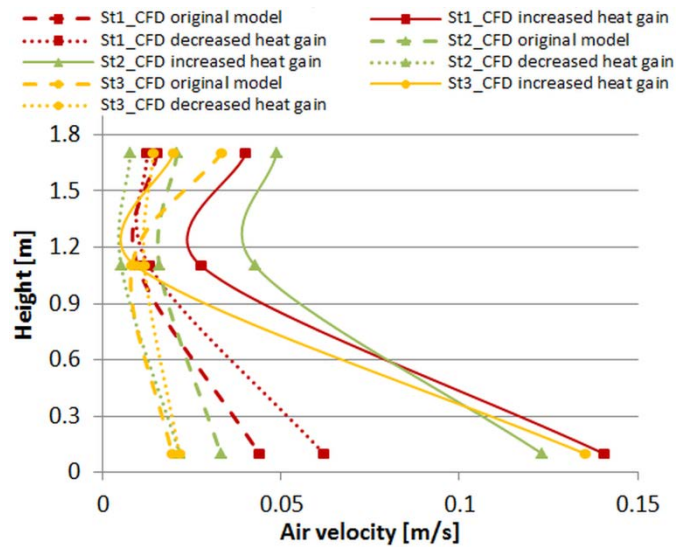


Figure 57: Velocity distribution in the scenarios with increased and decreased heat load (Figure 17 in Paper III)

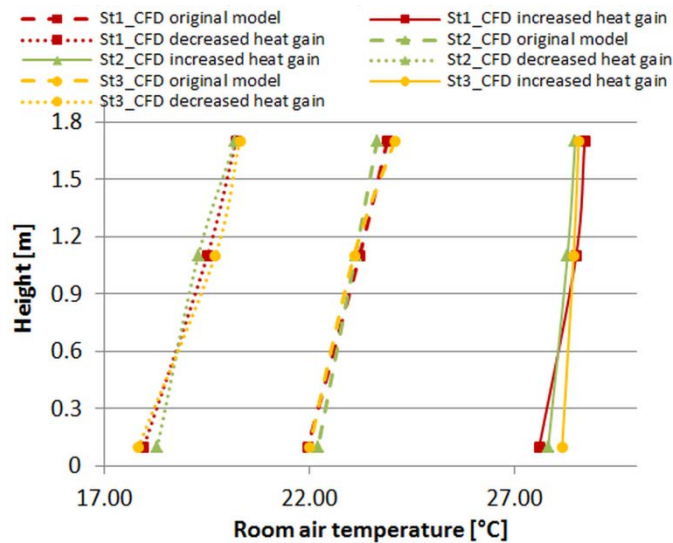


Figure 58: Temperature distribution in the scenarios with increased and decreased heat load (Figure 16 in Paper III)

The effects of variations in internal heat gains on draught ratings can be seen in Table 5 in **Paper III**.

Parametrical study: Variation in the number of walls used for cooling

The aim of this part of our investigation was to find out how the indoor climate in the test room is influenced by supplying all the cooling power to just one surface instead of two as in the original scenario. In practice, it could very often be that only one wall surface is available and can be activated for cooling purposes. Two additional scenarios were therefore investigated. In the first scenario, only the south-eastern wall was activated, and in the second scenario only the south-western wall was activated for cooling. The cooling power delivered in each scenario was the same as in the original scenario where both walls were activated for cooling.

The resulting surface temperature was 17.8 °C for the south-eastern wall and 12.3 °C for the south-western wall. Figure 59 shows the temperature distribution in the room for the different scenarios. The temperature distribution was similar for all the scenarios at stands 2 and 3. A slightly lower temperature and higher velocity was experienced at the lower part of stand 1 for the scenario with the south-western wall activated for cooling. Because stand 3 was situated closest to the south-western wall, air velocity at a height of 0.1 m was increased, as shown in Figure 60. These findings were the result of the flow pattern created in the room when the south-western wall was activated for cooling, as can be seen in Figure 61, which shows the flow pattern in the room at a height of 0.1 m. It is interesting to see that air flow increased along the sides of the room parallel to the longer walls in the scenario with the south-western wall activated for cooling. This could create discomfort for occupants sitting in the front part of the room close to the walls.

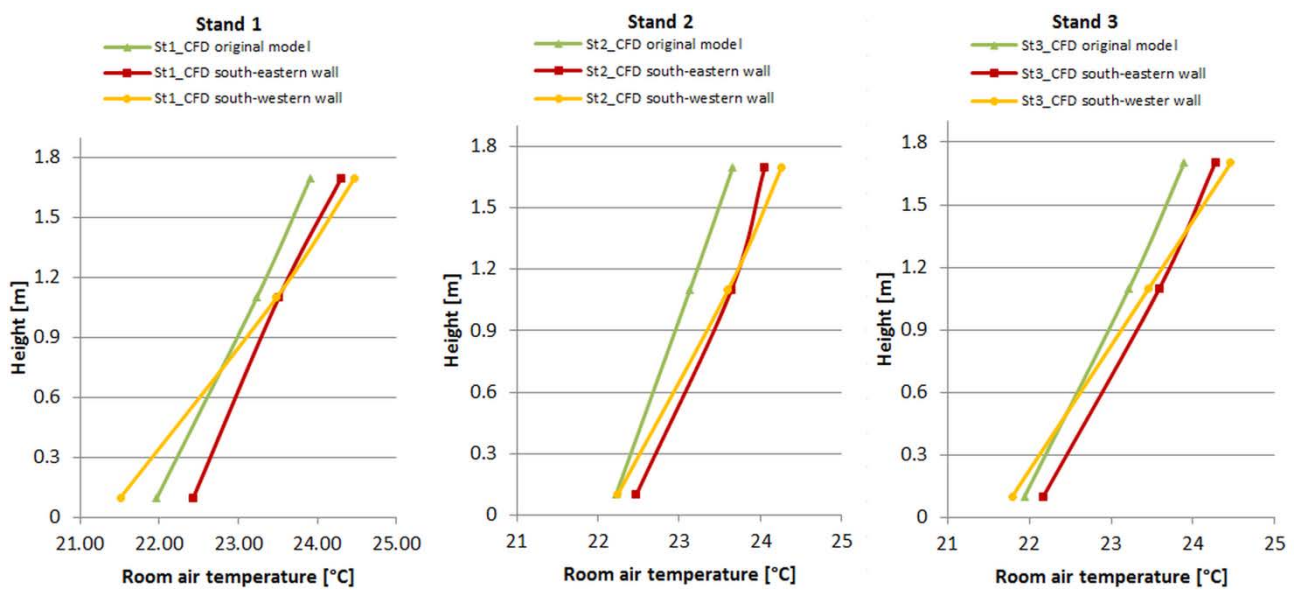


Figure 59: Temperature distribution for scenarios with different surfaces activated for cooling (Figure 18 in Paper III)

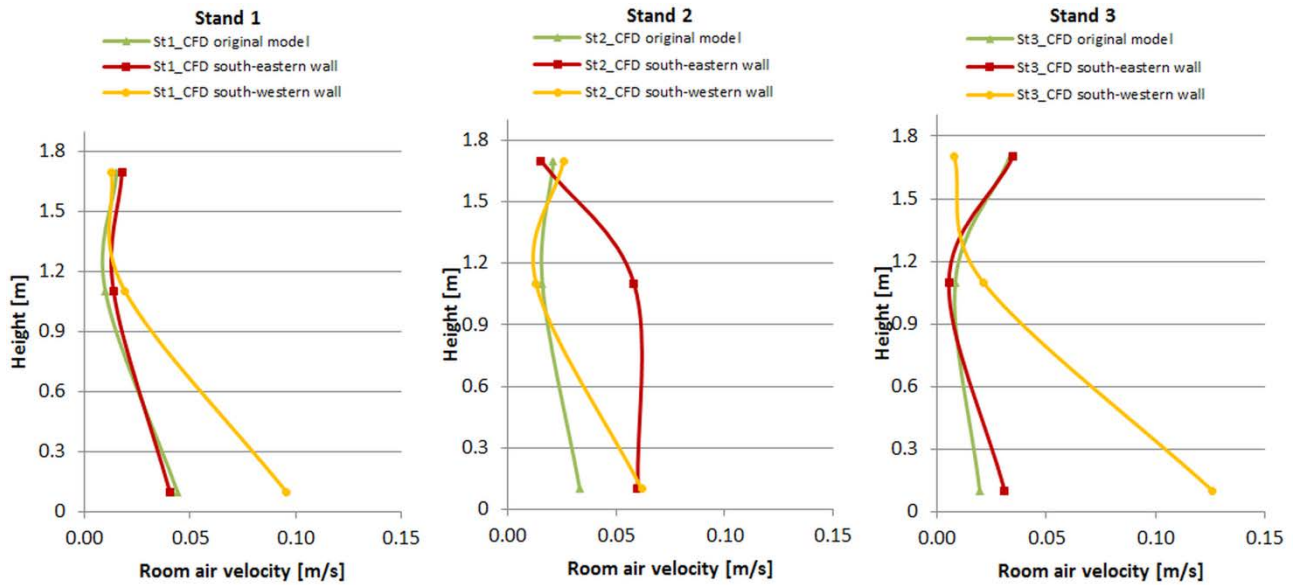


Figure 60: Velocity distribution for scenarios with different surfaces activated for cooling (Figure 19 in Paper III)

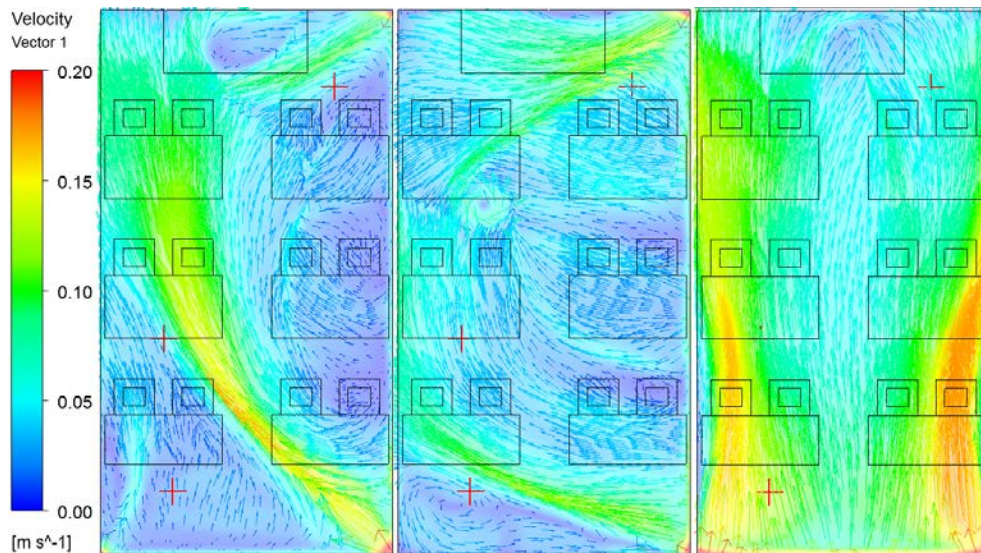


Figure 61: Velocity distribution at a height of 0.1m for three scenarios: original model (left); south-eastern wall (middle); south-western wall (right), (Figure 20 in Paper III)

It can be seen from Figure 62 that the lowest temperatures were experienced in the scenario with the south-western wall activated for cooling. The highest temperatures were found in the scenario with the south-eastern wall activated for cooling. Since the velocities at a height of 0.1 m were also lowest in this scenario, it could be concluded that the scenario with the south-eastern wall activated for cooling is the optimal solution with regard to comfort for occupants.

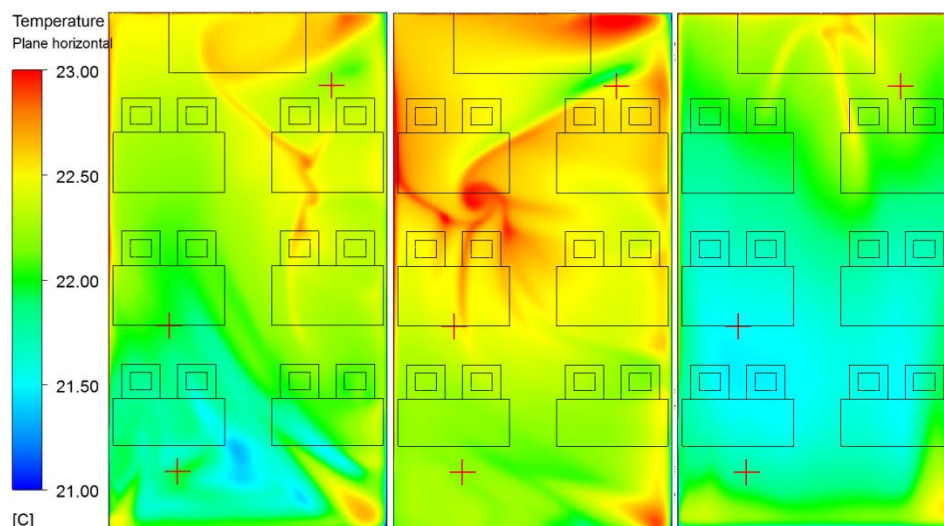


Figure 62: Temperature distribution at height 0.1m for three scenarios: original model (left); south-eastern wall (middle); south-western wall (right)

9.3.3 Complementary CFD investigation of air flow in the test room using tracer-gas methods (not included in Paper III)

The aim of this investigation was to obtain more detailed information about the air distribution in the test room and to further evaluate the findings from the research papers with regard to the air distribution in the test room. The investigation was carried out on the original scenario from **Paper III** with both cooling walls activated. Freon ($C_2H_2F_4$) was used as a tracer gas added to the inlet air in a concentration of 5 PPM. The results of the Freon distribution in horizontal planes are shown in Table 6 and Table 7. The results were calculated for time steps of 1, 2, 3, 4, 5, 6.5, 8, and 10 minutes from the start of the ventilation system. The time steps are shown on the left-hand side of Table 6 and Table 7 in seconds. The concentration of Freon in the test room at the beginning of the investigation was 0 PPM. The results were captured in a horizontal plane at heights of 0.1 m, 1.1 m, 1.7 m, and 2.5 m. The first three heights were in the occupied zone and the last one was 0.15 m below the diffuse ceiling inlet. The results were also investigated in a horizontal plane situated in plenum at a height of 2.75 m. It is clear that the Freon was well mixed in the plenum. Already after 1 minute from the start of the calculation, the Freon is distributed from the plenum into the test room at a height of 2.5 m in areas where there are no interactions between the incoming air and the thermal plumes resulting from heat sources situated in the test room. These areas include positions between occupants and at both ends of the test room. This is clearly shown in Table 8. (The position of vertical plane for the results in Table 8 is shown in Figure 32). The further distribution of the Freon can be seen after 2 minutes from the start of the calculation mainly in the areas of the test room close to the wall surfaces and in the area of the test room furthest from the air handling unit. This is especially true at heights close to the floor surface. Some of the Freon was moved down towards the floor, where it was spread over the floor surface while the rest interacted with the thermal plumes from occupants.

Table 6: Freon distribution in horizontal planes for the first 4 minutes after the start of the ventilation system

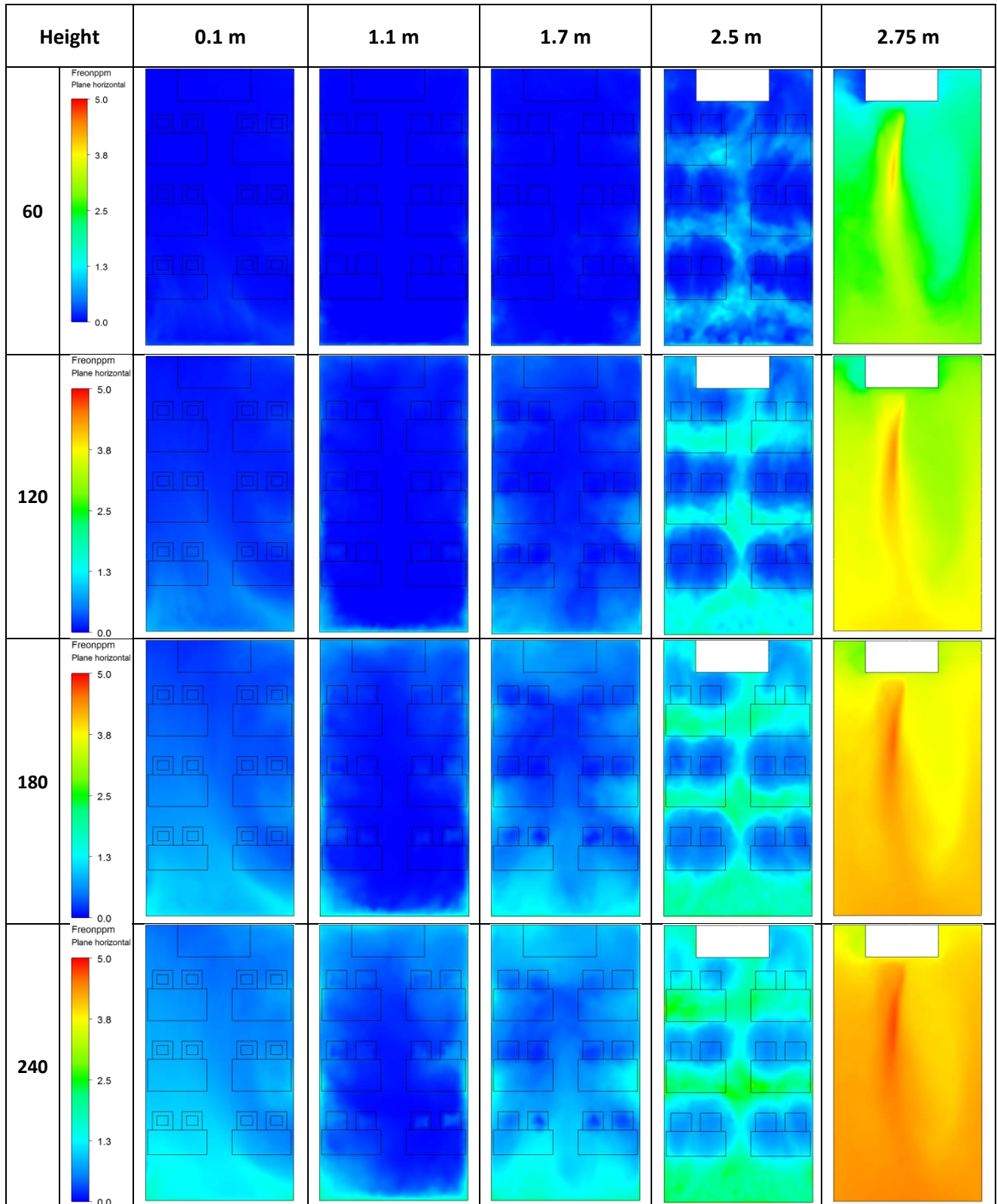


Table 7: Freon distribution in horizontal planes between 4 and 10 minutes after the start of the ventilation system

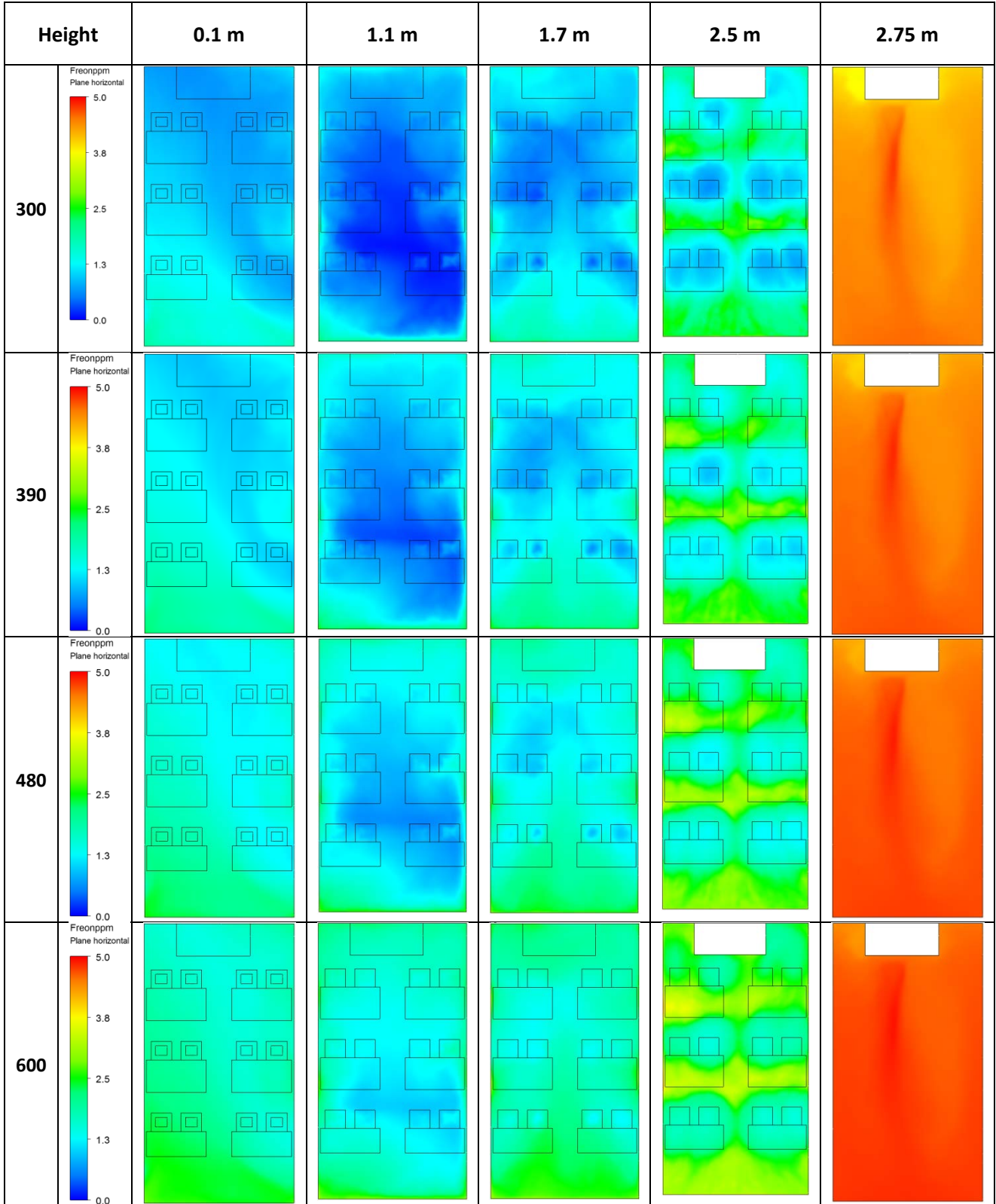
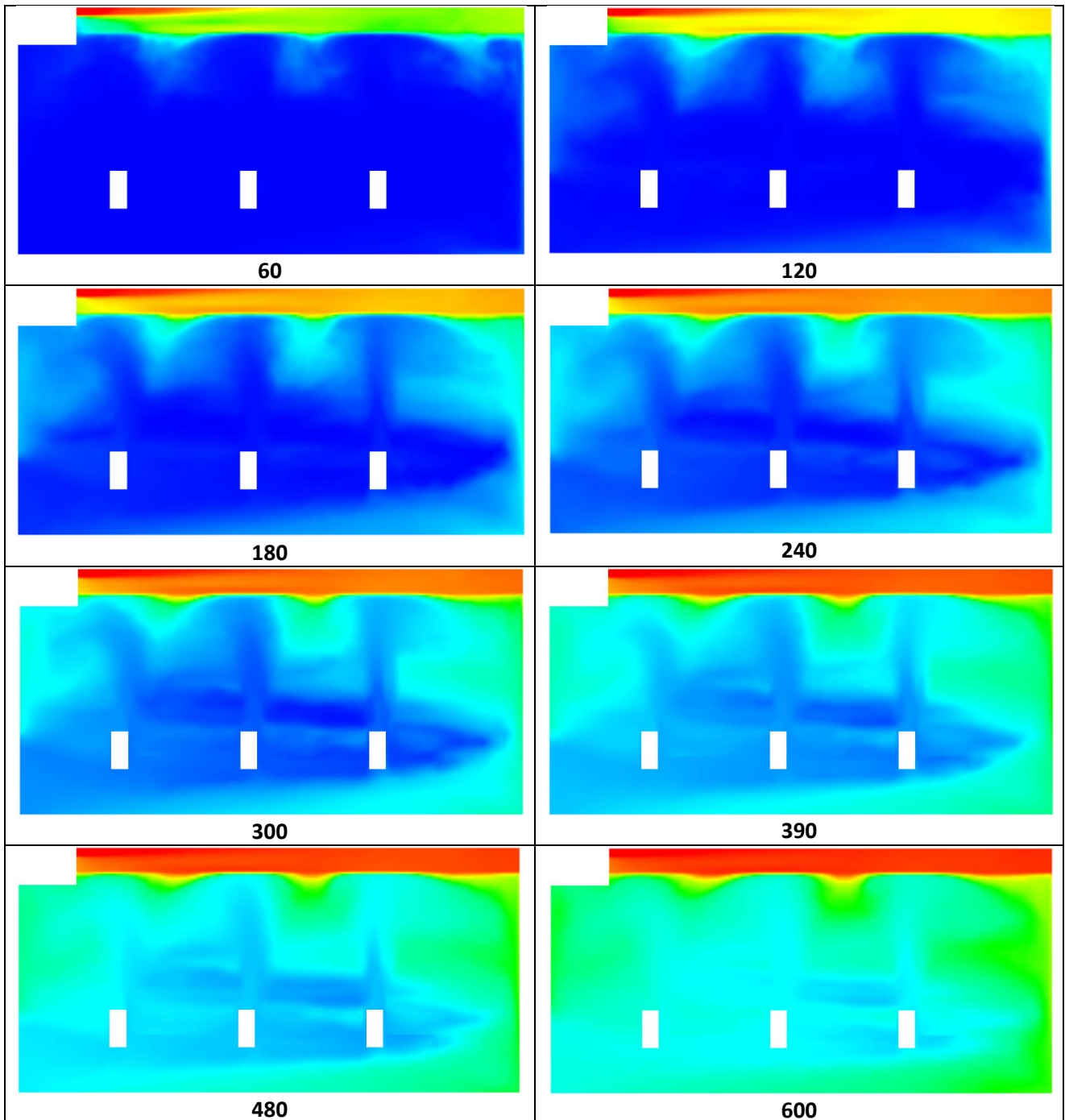


Table 8: Freon distribution in the vertical plane for the whole period of calculation (numbers below pictures are time steps in seconds)



9.3.4 Conclusions

A wall radiant cooling system made of plastic capillary tubes integrated into a thin layer of interior walls made of high performance concrete provided draught-free radiant cooling and created a comfortable indoor climate. Higher air velocities were observed in areas close to the floor, which can be attributed to high internal heat gains in combination with the low temperature of cooled walls. The air distribution in the

room was to a large degree governed by buoyancy forces. The influence of the wall radiant cooling system on the operative temperature was up to 2 K in the areas close to the cooled surfaces. The decreased temperatures of the cooled surfaces had a mild influence on the vertical temperature difference in the room with a maximum value of 2 K. Using a decreased area of diffuse ceiling inlet did not pose any restrictions on the temperature and velocity distribution in the room. When all the cooling power was supplied to just one wall, higher velocities were observed in the lower parts of the room, and the temperatures were a bit lower. These investigations showed that **sub-hypothesis 3** is true for the scenarios investigated.

9.4 Paper IV

Paper IV investigated the dynamic behaviour of the wall radiant cooling system and its influence on the overall temperature and velocity distribution in the test room. **Paper IV** focused on the evaluation of **sub-hypothesis 4**.

9.4.1 Investigated setup

The layout of the test room and its equipment is depicted in Figure 47. The two blue lines represent the two walls used for cooling.

The same values were used for the ventilation flow rate and water flow rate in the cooling loop as in investigations carried out in **Paper III**, see section 9.3.1 for a detailed description.

9.4.2 Results and discussion

Dynamic behaviour of the test room during pre-cooling period

This specific scenario was investigated in order to find out the ability of the installed wall radiant cooling system in terms of cooling a highly overheated room. The results may allow engineers to properly design a control system to enable a building to work with good energy efficiency and to make sure that rooms are always preconditioned to the required state before occupancy.

The test room was overheated to 32 °C over the course of a few days. This could be understood as simulating the situation at the beginning of the week after a weekend with very hot weather in an unconditioned room with high solar heat gains. It is desirable to know the behaviour of the installed wall radiant cooling system in such a situation. The cooling of the room from 32 °C to 26 °C took approximately 3.5 hours, as can be seen from Figure 63 (the blue field shows the acceptable range). The operative temperature of 26 °C was chosen as a limiting temperature since it represents the upper comfort range for indoor environment in class B, which was chosen for the investigations [29]. The supply temperature of cooling water was maintained at 15 °C (± 0.5 K). Figure 63 shows that the temperature of the cooled surfaces was influenced immediately by the cooling system when it was activated. The operative temperature in the room was affected after a short delay of about 15 minutes. This was a good sign indicating that the solution used for cooling was well-designed with respect to the dynamics of the system. This can be attributed to the small thermal mass of the rather slim layer of concrete (30 mm) in the wall and the overall design of the installed wall radiant cooling system described in more detail in section 5.2.

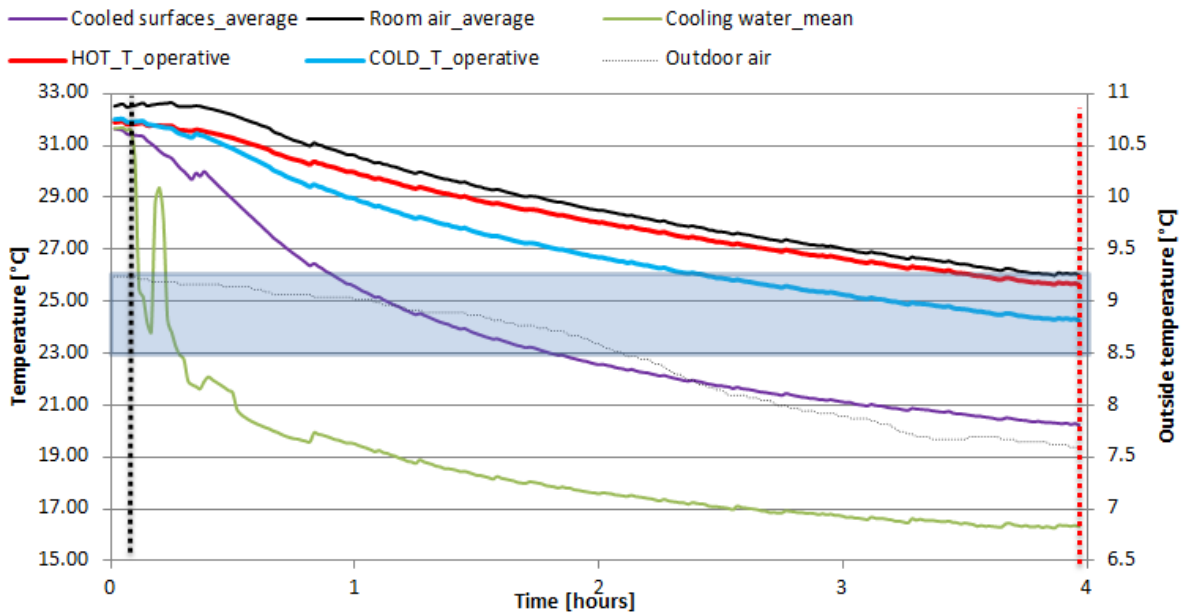


Figure 63: Cooling of the room before the presence of occupants (Figure 8 in Paper IV)

Dynamic behaviour of the test room during the occupied hours

The room air and surface temperatures were maintained at around 26 °C as a starting situation for the investigation of the development of the indoor climate when people entered the room, and the wall radiant cooling system was started. Three scenarios were investigated to examine the dynamic behaviour of the room when different boundary conditions were applied, see Table 9.

Table 9: Investigated scenarios (Table 1 in Paper IV)

Scenario	Internal heat gains [W]	Temperature of cooling water [°C]	Weather
1	1530	15.5	Overcast
2	1530	18.5	Overcast
3	1530	21.5	Overcast

The room air temperature increased at the beginning of the experiment as a result of the internal heat gains from occupancy. However, after approximately 30 minutes, the room air temperature started to decrease. The operative temperatures started to decrease after 20 minutes as a result of the influence of the cooled surfaces, which already had a temperature about 24.5 °C. The temperature of the cooled surfaces was decreased from 26 °C to 20 °C in the first 4 hours. Stabilization of the temperatures was observed after 4 hours when the operative temperatures within the room were between 23.5 °C and 24.5 °C. The rise in temperatures at a later stage of the measurements is attributed to the increased outside air temperature, as can be seen in Figure 64. In Figure 64, Figure 65, and Figure 66, time is shown in logarithmic scale in order to expand the most relevant part of the measurements right after the start of the cooling.

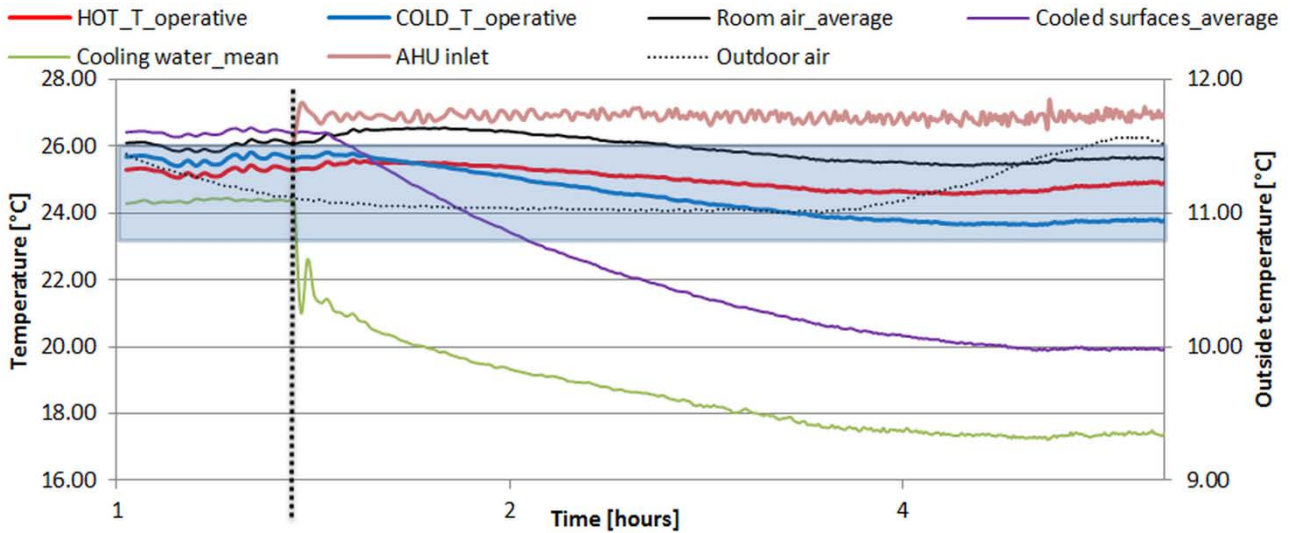


Figure 64: Temperature development in Scenario 1 (Figure 9 in Paper IV)

In scenario 2, the temperature of the cooled surfaces was decreased from 26 °C to 21.5 °C after 4 hours of experiment when the situation in the room became fairly stable, as can be seen in Figure 65. The room air temperature was around 26 °C for most of the time. The operative temperatures at the critical points were maintained between 24 °C and 25 °C at that time as a result of the use of the radiant cooling system to achieve class B of standard EN15251 with regard to the temperature in the room [29]. The cooling loop was supplied with water at a temperature of 18.2 °C when stabilized. It is an interesting finding that the operative temperatures were very similar to those measured in scenario 1, even though the temperature of the cooling water was about 3 K higher. The small increase in the temperatures within the room after 4 hours of measurements can be connected with the increase of the outside air temperature shown in Figure 65 by the dotted line.

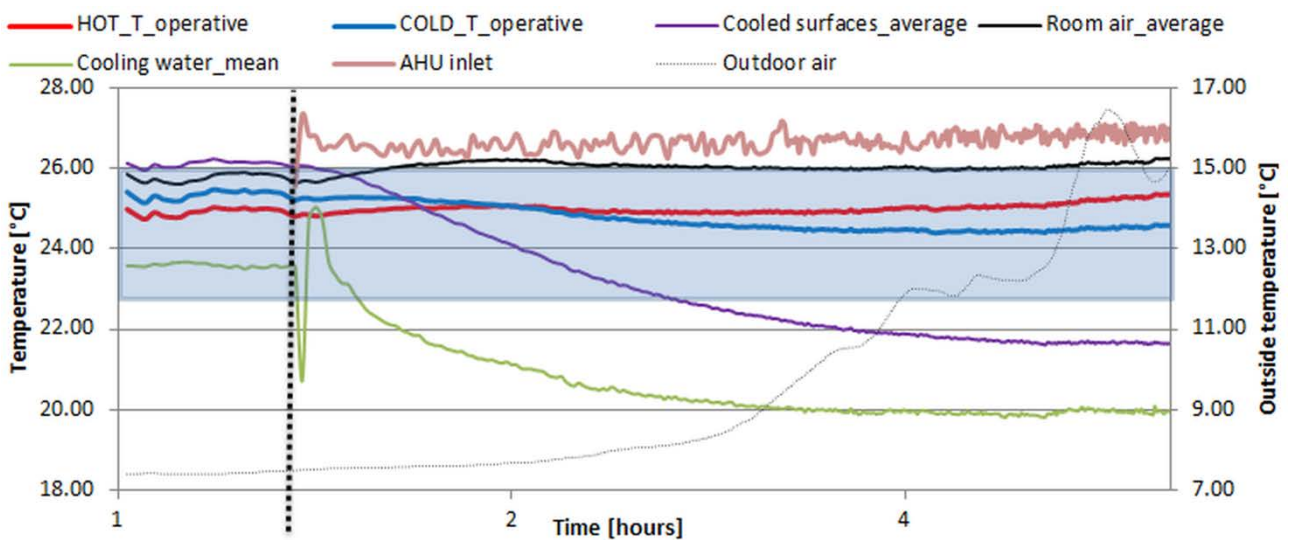


Figure 65: Temperature development in Scenario 2 (Figure 10 in Paper IV)

The results for scenario 3 are shown in Figure 66. It can be seen that the room air temperature was maintained above 26 °C for most of the duration of the experiment, which is in environmental category C

[51]. However, the operative temperatures at the critical positions were maintained around 25 °C, which is in environmental category B, even though the temperature of the cooling water was about 21.5 °C.

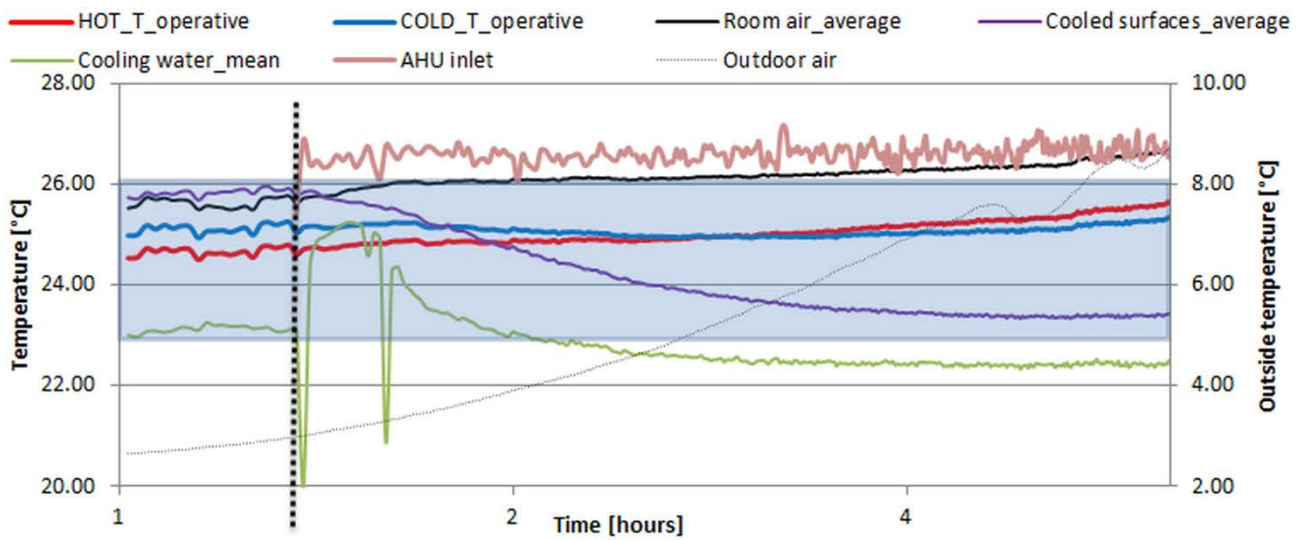


Figure 66: Temperature development in Scenario 3 (Figure 11 in Paper IV)

Air velocities close to the cooled walls were investigated in **Paper III** since there was a potential for the creation of a draught. The position of the measuring point was at a distance of 0.2 m from the south-eastern wall and at a height 0.1 m, representing the height of occupants' ankles, and this is shown by the green dot in Figure 47. This part of the body is usually very sensitive, especially in summer when people wear light clothes and shoes and cooling is activated [14]. The distance of 0.2 m was assumed to be appropriate since the occupants were placed in close proximity of the south-eastern wall, see Figure 47. The results of the velocities are shown in Figure 67 together with the temperatures of the room air and the cooled surface. Higher velocities were experienced for lower cooling water temperatures. Velocities fluctuated around 0.11 m/s in scenario 1, around 0.1 m/s in scenario 2 and around 0.07 m/s in scenario 3. In none of the investigated scenarios did the velocities reach the threshold for maximum velocity in the room of 0.19 m/s for summer conditions [29].

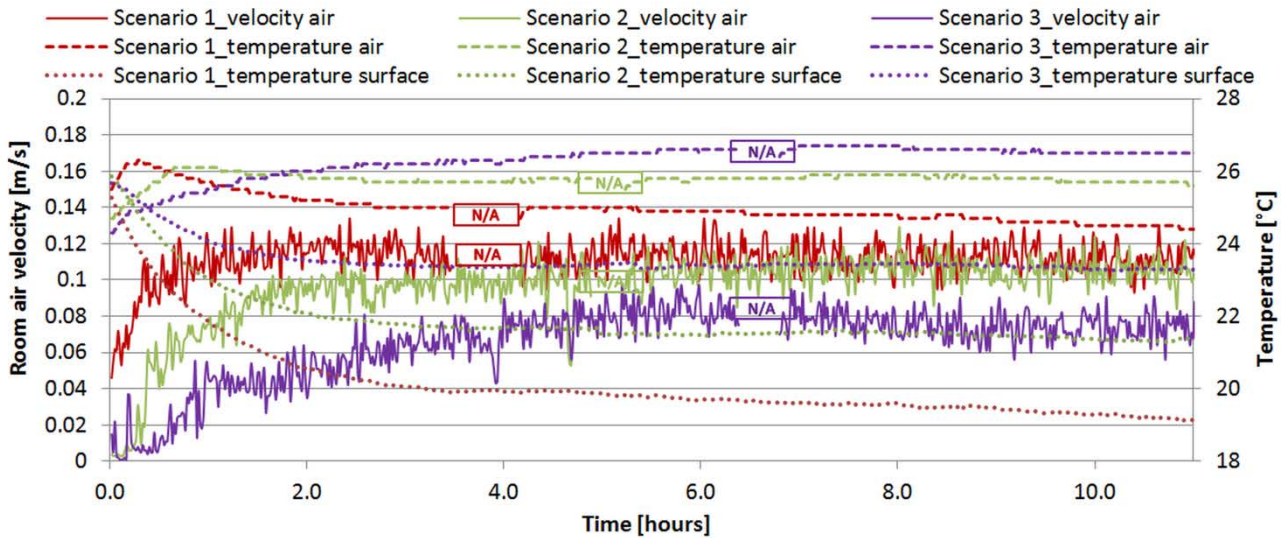


Figure 67: Velocity development at a distance of 0.2 m and a height of 0.1 m (Figure 12 in Paper IV)

The draught rating values were highest for scenario 1 because the high room air velocities were combined with low room air temperatures, see Figure 68. The draught rating reached a maximum value of about 9%, which is well below the recommended limit of 15% [29].

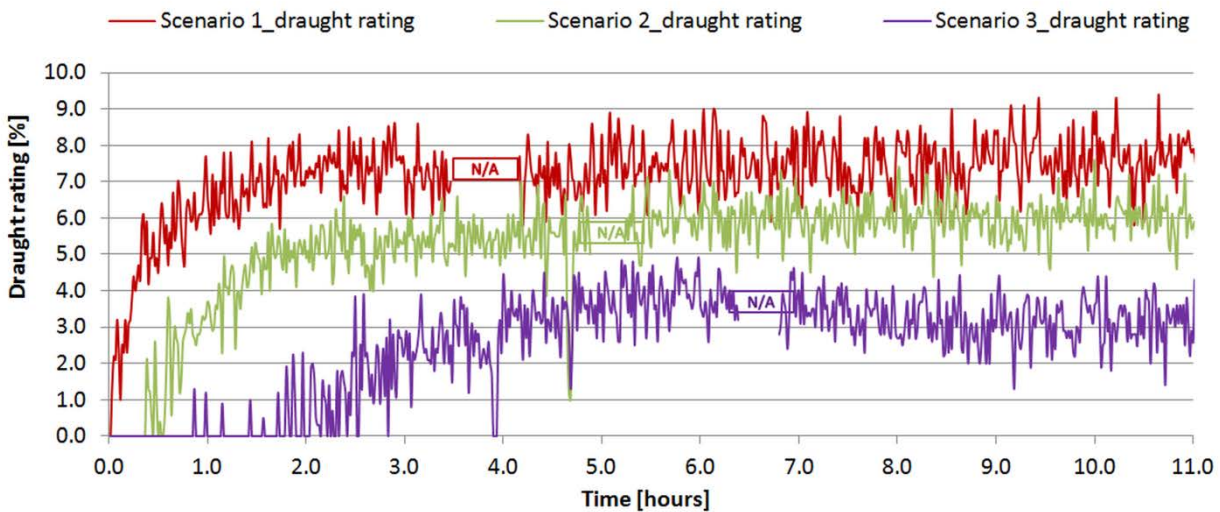


Figure 68: Draught rating results for all the scenarios at a distance of 0.2 m and a height of 0.1 m (Figure 13 in Paper IV)

The proper heat distribution over the wall element was checked during the measurements, since there were concerns about possible temperature differences occurring over the surface of the wall. The reason for this was that the plastic capillary tubes integrated in the wall run vertically in parallel to each other, and connections for both supply and return manifold pipes were made in the upper part of the wall element, see Figure 16. This could potentially result in differences in the surface temperature along the height of the wall element, especially when a small velocity of circulated water is used. The results of our measurements with a water flow rate of 0.125 l/s, however, showed that the temperature was evenly distributed over the whole surface area of the wall. This was checked by making temperature measurements on the surface of the cooled walls and by using a thermo-graphic camera.

The thermo-graphic investigation showed that one vertical strip on the south-western wall was not functioning properly and did not cool the room, see Figure 69. One possible explanation for this is clogging of the small plastic capillary tubes with impurities present in the circulating water because no special filtration system was used during the experiments. Another reason could be blockage with plastic material created during the production of the capillary tubes during manufacture. The proper functioning of the capillary mats was not assessed prior to the casting in the layer of high performance concrete.

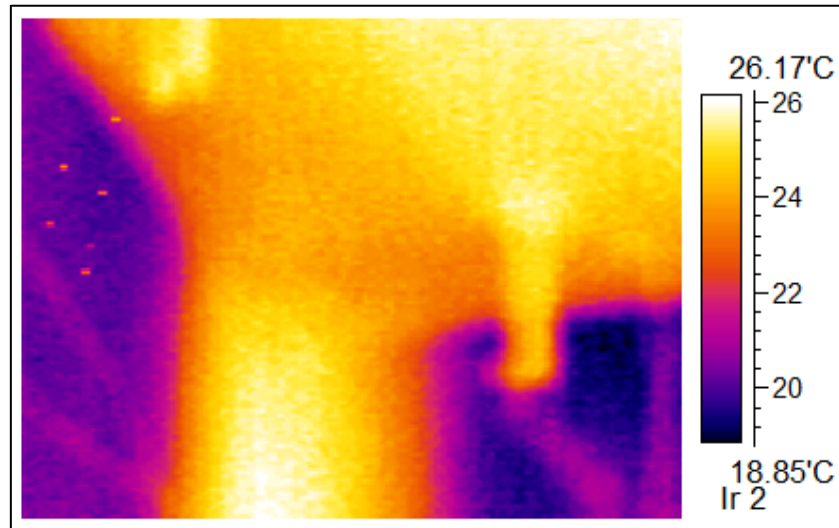


Figure 69: The un-cooled part of the south-western wall (Figure 17 in Paper IV)

9.4.3 Complementary investigations (not included in Paper IV)

Comparison with the dynamics of thick piping in a thick layer of concrete

The aim of this part of the investigation was to compare the designed radiant system using small plastic capillary tubes cast in a thin layer of high performance concrete with the conventional radiant system using thick piping made of cross-linked polyethylene cast in a thick concrete construction. Two numerical models were created in the program HEAT 2 for this purpose [74]. Transient simulations were performed in order to find out the behaviour of the wall element when the system for radiant cooling was activated. The aim was to numerically investigate the three scenarios presented in section 9.4.2. Both cooling walls (the south-eastern wall and the south-western wall) were assumed to be activated for cooling purposes. The evolution of the mean temperature of cooling water from measurements was used as input for the temperature development of the cooling water in the numerical models, which should make them more realistic. The differences in the temperature of cooling water between measured and calculated values in the solution with capillary tubes were between 0.1 °C and 1.1 °C, with a mean value of 0.5 °C. This precision was considered to be sufficient because it is not very important in this case considering that the main aim was to investigate the differences in the dynamic responses of the two different systems. The same inputs were used for the solution with thick piping.

Due to the limitations of the simulation software, the following simplifications were made:

a) The room air temperature was constant for the whole period of calculation. The air temperature in the room did not change dramatically over the course of the measurements, as can be seen in the previous section. This simplification was therefore assumed to make little difference to the temperature distribution in the wall element.

b) The boundary conditions were kept constant on the external side of the wall element. Changes here make even less difference to the temperature development on the internal side of the wall element.

The thick piping made of cross-linked polyethylene that was used had an outer diameter of 16 mm with a wall thickness of 1.5 mm. The spacing between the pipes was 150 mm, which was assumed to be the average value used in building practice. The layer of concrete in which the pipes were cast was 100 mm thick and the pipes were situated in the middle of the concrete layer. A period from 8 a.m. to 5 p.m. was investigated, and the cooling system was activated for all of this period except from 12 a.m. to 1 p.m. when it was assumed that all the occupants would leave for lunch.

The results of the temperature distribution for both scenarios are shown in Figure 70. It can be seen that the system with the thick piping did not reach a quasi-steady-state, which means that the full cooling potential of the element was not reached. The system with capillary tubes was close to quasi-steady-state after 4 hours of running the cooling system, and the surface temperatures were 20.1 °C, 22.0 °C, and 23.6 °C for scenarios 1, 2, and 3 respectively. The corresponding temperatures in the solution with thick piping were 23.5 °C, 24.3 °C, and 24.9 °C after 4 hours. The surface temperature difference between two systems increased when the cooling water temperature was decreased. Higher temperature differences were also experienced in the early stages of the experiment, because the reaction of the system using thick piping was much slower than the system using capillary tubes. The advantage of the system with capillary tubes in fast reaction to changes in a control system is obvious.

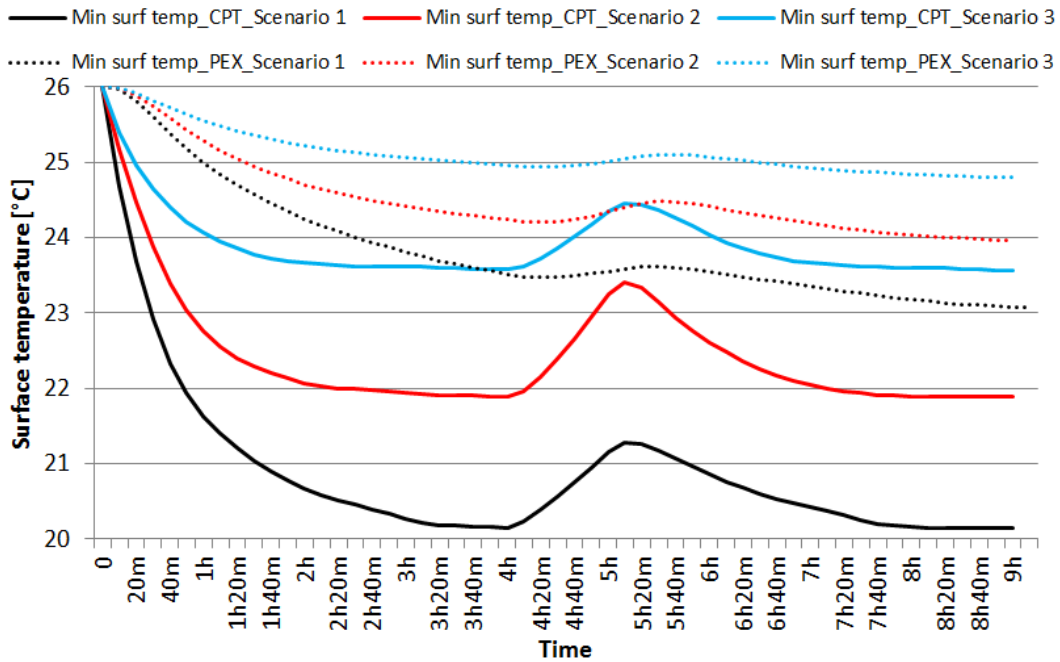


Figure 70: Comparison of surface temperatures for the scenarios with capillary tubes and with thick tubing

The difference is even more profound when the heat fluxes of the two systems are compared, as can be seen in Figure 71. The surface heat flux in the system with capillary tubes was 6 times, 4 times, 3 times, and 2 times higher than in the system with the thick piping 1 hour, 2 hours, 3 hours, and 4 hours after the start of the experiment respectively. In other words, the system with capillary tubes was able to deliver from 2 to 6 times as much cooling energy as the system with the thick piping. It should be stressed that these differences were obtained for the same temperature of cooling water in both cases.

To discuss and evaluate the comparative dynamic performance of the two systems, the term “4 hours cooling capacity” is introduced. The “4 hours cooling capacity” is defined as the cooling capacity available after 4 hours from the start of the experiment. The reason for this is that after 4 hours the cooling was stopped for 1 hour. The aim is to use the value of the continuous development of cooling capacity for dynamic evaluation. The system with capillary tubes reached 50% of its “4 hours cooling capacity” already half an hour after the start of the experiment, while the system with the thick piping reached only 8.5% of its “4 hours cooling capacity” at the same time.

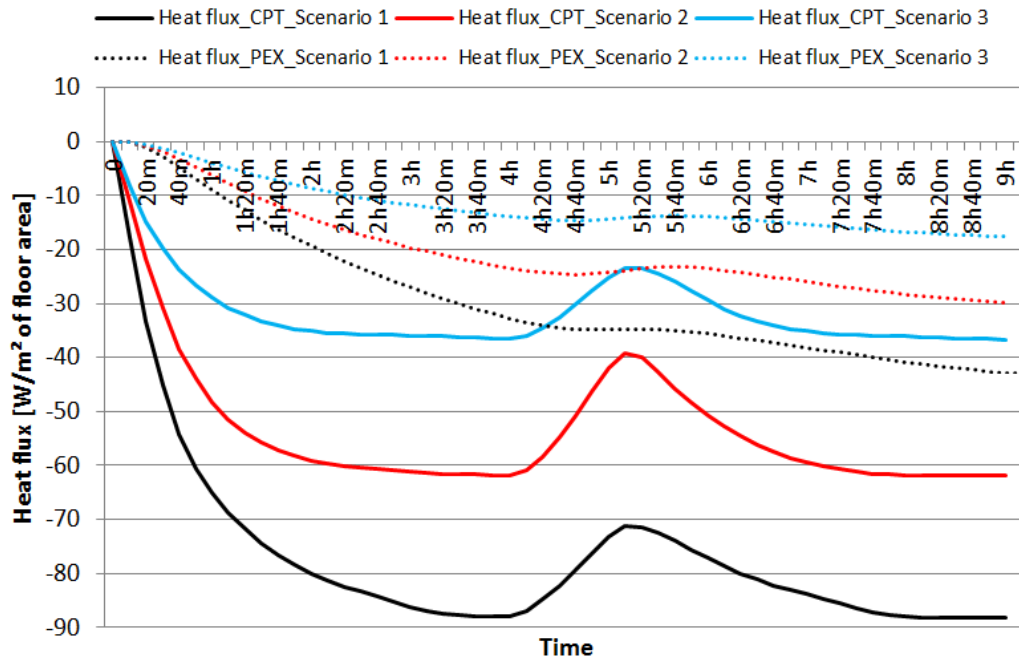


Figure 71: Comparison of surface heat fluxes for scenarios with capillary tubes and thick tubing

Dew point temperature investigation

This part of the investigation focused on the dew point temperature of the room air, which limits the surface temperature of a radiant cooling system. The performance of the system with the plastic capillary tubes was compared with the system with the thick tubes on the basis of the results of transient calculations done in program HEAT 2. The need for transient calculations was due to the slow reaction of the system with the thick tubes, as found in the previous section. The occupancy hours in the test room were taken into account and were set to between 8 a.m. and 12 a.m. and 1 p.m. and 5 p.m. (the same settings as in the previous section). There is one hour between those two periods where the cooling system was turned off (lunch time). The temperature of the test room was 26 °C before the experiment started, which is the same as the situation used during the measurements in **Paper IV**, and the reasoning behind this choice is described in section 9.4.2.

The temperature of the cooling water was constant for all of the following experiments. No measured data were available for the evolution of cooling water temperature for the investigated supply temperature values of the cooling water. Three scenarios were calculated with cooling water temperatures of 10 °C, 15 °C, and 18 °C.

The standard recommends that the humidity is maintained between 30% and 70% [29]. The acceptable indoor operative temperature according to the standard is 26 °C. From the measurements, we can see that the operative temperature is about 1 – 1.5 K below the room air temperature, depending on the position of the measurement in the test room. For further analysis it was therefore assumed that the maximum acceptable room air temperature in the space equipped with the designed solution for radiant cooling was 27 °C. The dew point for air with a temperature of 27 °C and a humidity of 50% (a middle value in the recommended range) is 16 °C. The surface temperature of the cooled surfaces should not fall below the dew point temperature. In the event that the required cooling load is greater and a dehumidification is

available as part of the air handling unit, the surface temperature could go down to 8 °C, which is the dew point for humidity of 30% with an air temperature of 27 °C. Figure 72 shows that the surface temperature of cooled walls of 15.4 °C is already too low for cooling water with a temperature of 10 °C.

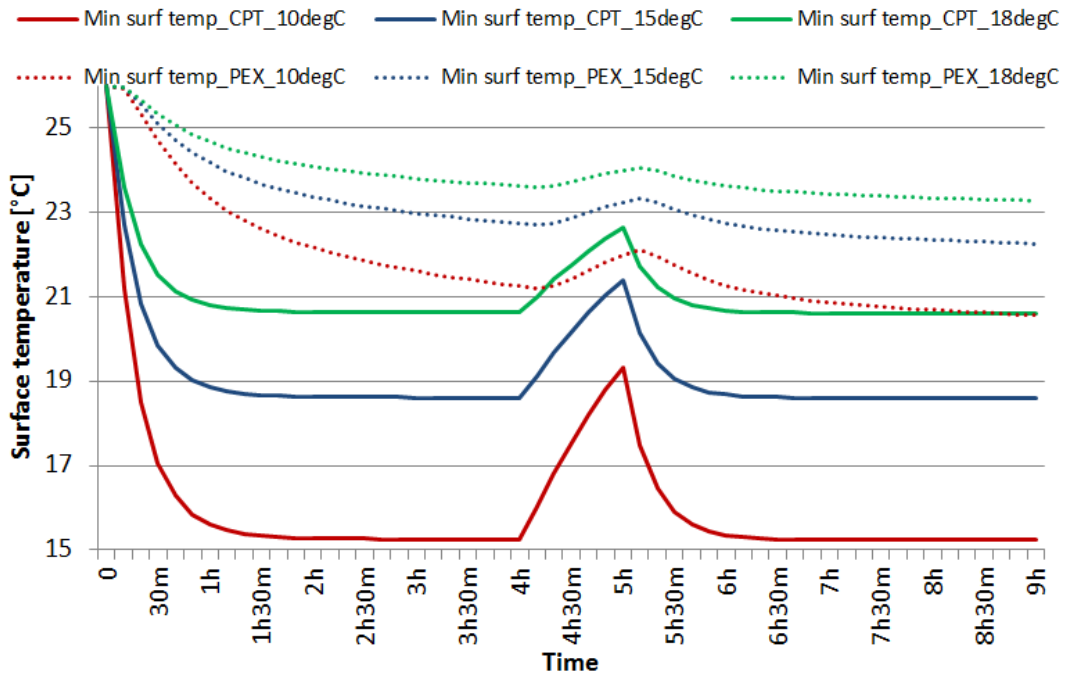


Figure 72: Surface temperatures for different temperatures of cooling water

The maximum cooling load limited by the dew point temperature of the room air (16 °C) was 140 W/m² with the use of cooling water with a temperature of 12 °C. The resulting lowest surface temperature was 16.6 °C. The heat flux development is shown in Figure 73. The results are relevant for the situation when both cooling walls (the south-eastern wall and the south-western wall) were activated.

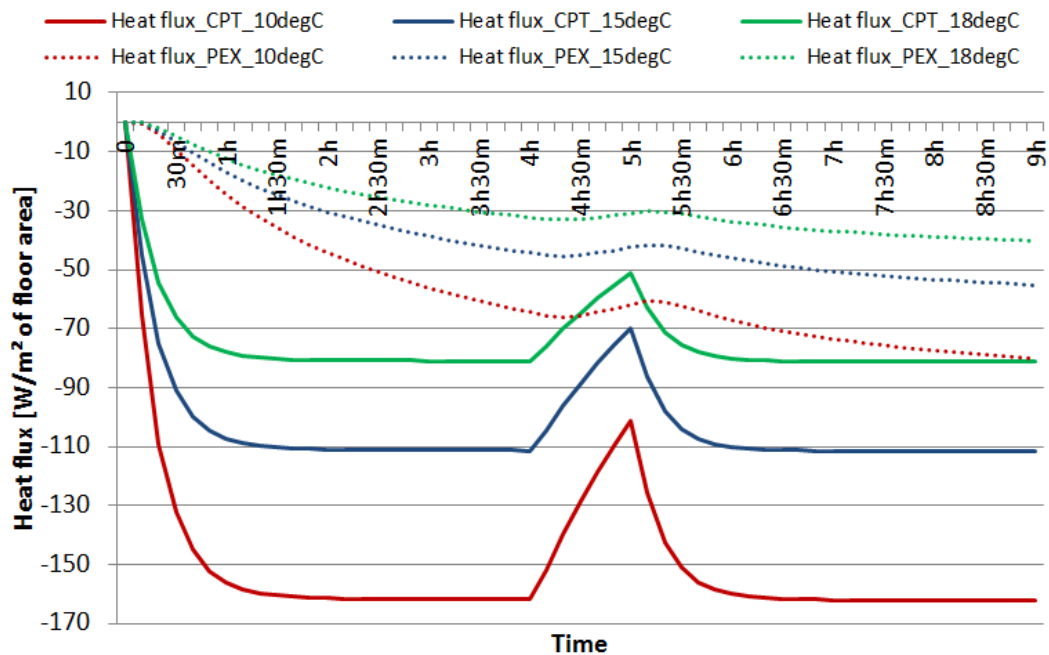


Figure 73: Surface heat fluxes for different temperatures of cooling water

9.4.4 Conclusions

It can be concluded that the designed solution of the wall radiant cooling system does not greatly benefit from substantial lowering of the cooling water temperature in the scenarios investigated. This is an interesting finding, especially in connection with the use of renewable sources of energy such as ground and sea water. These can be utilized to a much greater degree when higher temperatures of cooling water are used. The designed solution can be therefore considered as environmentally friendly. Such installations may greatly support the development of the highly sustainable buildings of the future.

Higher velocities were experienced for lower cooling water temperatures. However, they did not reach the threshold for the maximum velocity in the room of 0.19 m/s for summer conditions in any of the scenarios investigated. Draughts were not created in the room.

The investigations showed that **sub-hypothesis 4** is true, especially in comparison with the common solution made of thick tubing integrated into a thick layer of concrete.

Further investigations need to be done with regard to the clogging of the system. The installation of proper filtering is recommended to avoid any complications with the system in practice.

10. Practical use of radiant cooling systems

The experimental measurements were carried out in a relatively small room which did not represent the real size classroom. Furthermore, mainly due to the delays during construction phase, the investigations concerning cooling scenario have been carried out during the autumn months. This means that experienced outside temperatures were not very realistic (this concerns mainly transmission losses as the supply temperature was adjusted during the experiment- heated up to simulate summer outside temperatures).

It is therefore relevant to carry out further investigations which would give us better understanding about performance of designed radiant cooling system in more realistic conditions. The dynamic calculations were carried out for those purposes and are presented in the following text.

10.1 Software tool

The dynamic calculations were carried out in software IDA ICE, which is commercially available tool for investigations of dynamic behavior of buildings [75].

10.1.1 Limitations

The IDA ICE software does not offer radiant cooling system integrated into the wall structures. The approach taken towards solving this issue was the use of floor and ceiling areas instead of wall areas.

In IDA ICE is the construction in which the cooling object is inserted divided into two parts- a layer above and a layer below. This cooling object (heat exchanger model) corresponds to the piping layer. It is assumed to be very thin and infinitely conductive layer of material, so all the 2D effects can be disregarded [76]. The required input from the user is total heat transfer coefficient (H-value) including convection between water and tube wall, heat conduction through tube wall material and co-called “fin efficiency” corresponding to the distance between the tubes. The modelling method corresponds to the resistance method presented in standard EN 15377-1 [77].

10.2 Validation of the model in IDA ICE

The idea behind the first model was to see if the resulting values in IDA ICE will correlate with the results from the experimental measurements and CFD investigations. The main concern was about the applicability of radiant cooling systems in the floor and ceiling surfaces instead of in the wall surfaces. This first investigated model of the test room created in IDA ICE had exactly the same dimensions as the model investigated in CFD, respectively the same dimensions as the real tested room, 7m x 3.25m including the technical room. The floor plan can be seen on Figure 74 and model of the room created in IDA ICE on Figure 75. More detailed description of the investigated room can be found in section 5.

The internal heat gains during the experiment were 1327 W, implemented in IDA ICE as heat gains from equipment and lights. This was more precise way to do it, compared to the heat load from occupants as the heat gains during the experimental measurements were provided by light bulbs, therefore no latent loads were provided. The cooling power delivered to the radiant cooling was 1112 W using the cooling water with a mean water temperature of 16.3 °C. Boundary conditions for the external wall surfaces were defined

with external heat transfer coefficients of $0.18 \text{ W}/(\text{m}^2\cdot\text{K})$ for roof, $0.19 \text{ W}/(\text{m}^2\cdot\text{K})$ for walls, $2.47 \text{ W}/(\text{m}^2\cdot\text{K})$ for floor, and $1.26 \text{ W}/(\text{m}^2\cdot\text{K})$ for windows. The surrounding air temperature was $8.5 \text{ }^\circ\text{C}$ for the roof, walls and windows and $19.8 \text{ }^\circ\text{C}$ for the floor. The inlet boundary was assigned with a velocity magnitude of 1.44 m/s and a temperature of $26.6 \text{ }^\circ\text{C}$. To sum up, the same boundary conditions as for CFD investigations were applied for investigations in IDA ICE, see section 9.3.

The cooling area of walls was 27.8 m^2 . The same area, equally divided between floor and ceiling, was used in IDA ICE model. This resulted in radiant cooling element with size of $5 \times 2.3 \text{ m}$ (13.9 m^2) in floor and in ceiling. The main focus was on investigation of the transferred energy from radiant cooling as defined in IDA ICE in comparison to the amount of energy transferred to the room in the CFD model and the experimental measurements. The first calculations resulted in overestimated energy transferred to the room. It was decided to decrease the area of the radiant cooling installed in the ceiling as this had higher convective heat transfer coefficient and therefore more energy was supplied from ceiling compare to the floor. An iterative process was used until the fit between the results of heat flux in CFD and IDA ICE models was reached as presented in Table 10. The resulted are of radiant cooling element implemented in ceiling was reduced to 70% of its original size.

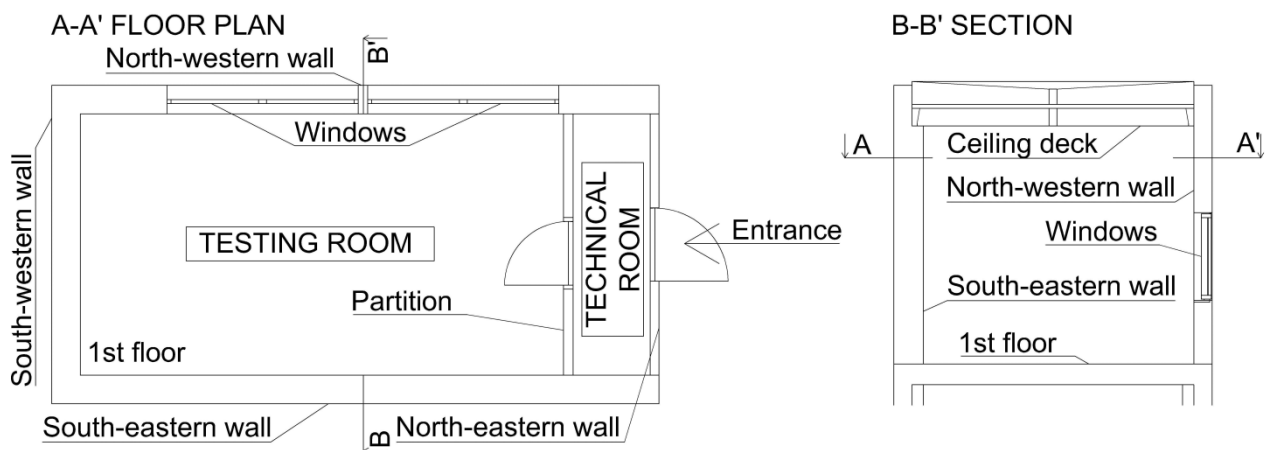


Figure 74: Floor plan and section cut of original test room

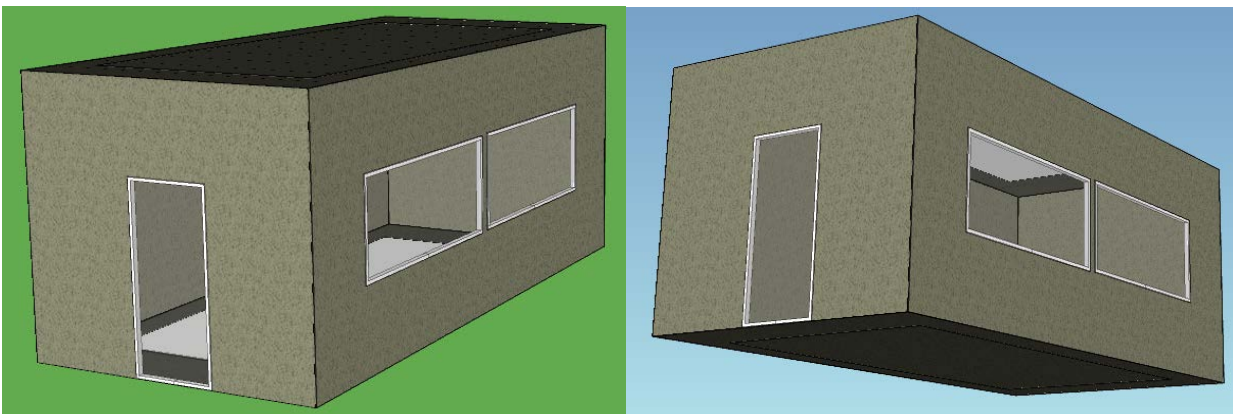


Figure 75: Original size room modeled in IDA ICE

In Table 10, it can be seen that the resulting values of operative temperature and also temperature of cooled surfaces in IDA ICE model are higher compared to the results from the measurements and CFD calculations. More precisely, the operative temperature is 0.3 K higher. The heat flux from the cooled walls is however nearly the same as during the measurements. The experienced differences are within the magnitude which can be regarded as acceptable for further investigations. The radiant cooling systems approximated to the real concept of radiant cooling integrated in the wall is assumed to be sufficient for further parametrical study and investigation of performance of proposed solution in real conditions.

Table 10: Comparison of results from IDA ICE with results from Measurements and CFD

	Top	Tsurf	Tcool. water	Heat flux
	[°C]	[°C]	[°C]	[W]
Measurements	22.5	18.8	16.3	1112
CFD	22.5	18.5	X	X
IDA ICE	22.8	19.25	16.3	1120

10.3 Setting up realistic model

The surrounding rooms were included in the IDA ICE model in order to get more realistic situation concerning the heat losses by transmission. Additional rooms were attached to the investigated room from both sides. Furthermore, the corridor was attached to all rooms. No windows were used in the corridor. The model is depicted on Figure 76. The heat loads were now modelled as occupants. This means that it was now accounted also for the latent loads (80 W/occupant- sensible and 25 W/occupant- latent). Additionally, the U-values of the constructions used corresponded to the very low energy buildings (U-wall 0.12 W/m²K, U-roof 0.12 W/m²K, U-floor 0.12 W/m²K, U-glazing 0.6 W/m²K). The floor area used for one occupant was 1.64m². Concerning the occupancy, I assumed that 100% people were present as the main purpose of this part of work was to show the limits of the designed system, therefore investigated with full possible occupancy. Some investigations were however done with various occupancies to show the effect of heat load on overheating in the room and overall performance of the radiant cooling system. The ventilation flow rate was 35 m³/h per occupant.

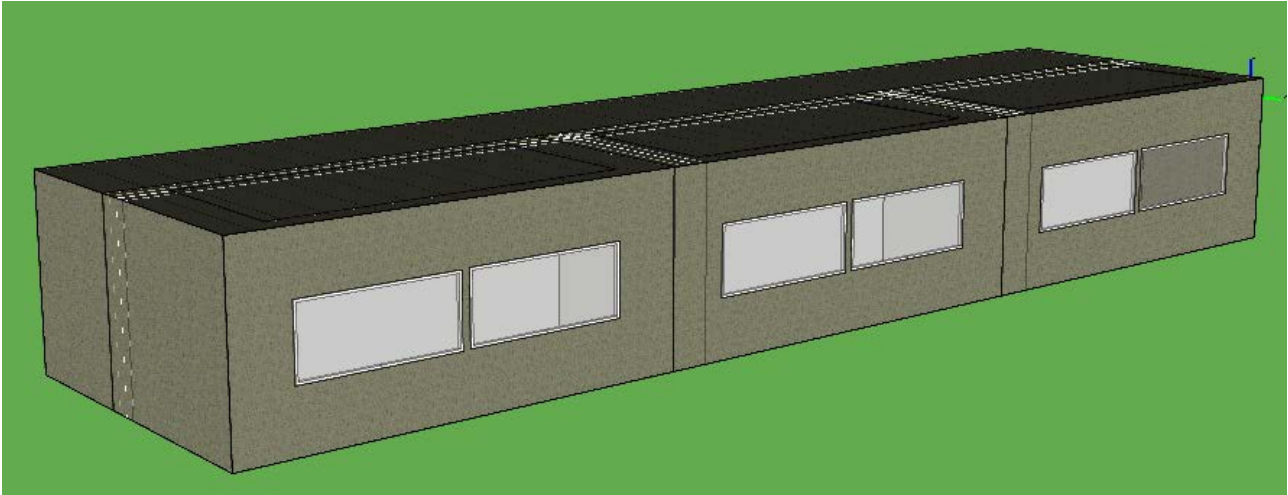


Figure 76: The 3D model created in IDA ICE

The investigations were carried out for four different locations representing different climate conditions. Firstly was the building situated in Denmark (Copenhagen), then in Austria (Vienna) representing the mild European climate (with more solar radiation than in Denmark). The third location was France (Nice), representing warmer climate with rather high temperatures but relatively low humidity. Last location was Thailand (Bangkok) representing very hot and also humid climate. The humidity can play a large role in usability of designed radiant cooling system as its performance can be limited by condensation.

The amount of accepted hours with internal temperature above 26°C is 108 hours from occupied hours per year, as defined in the standard EN 15251 [51]. It should be mentioned that no means of shading were used during the investigations- neither active shading, nor shading from surrounding buildings.

10.4 Parameter investigation on realistic model

10.4.1 Wall to floor ratio

The idea in this part of the investigation was to evaluate the influence of the size of the room on the wall cooling performance. The ratio of the walls (available for the cooling) to the floor area decreases with the size of the room when the height of the room is kept constant. This means that the benefit (or influence) of the wall cooling is getting smaller in larger rooms. The corresponding wall to floor ratio was investigated in four scenarios with different floor areas as presented in Table 11. The classrooms are relatively large rooms and therefore the floor area was increased. The heat loads and ventilation flow rates were used proportional to the floor area (based 1.64 m²/occupant).

However it should be also mentioned that in reality the height of the room increases with the floor area of the room. Occupants would simply not feel good when the same height is used for larger rooms. This has something to do with people's perception of the space. Furthermore, it is more difficult to get enough daylight into the deep rooms when using small heights of the rooms and proper amount of daylight is very important in classrooms. Therefore, in order to get more realistic idea about the performance of the wall radiant cooling system also in rooms with increased height, additional four scenarios were investigated and can be seen in Table 11. The corresponding wall to floor ratios are depicted on Figure 77. It can be seen

that the wall to floor ratio decreases with larger floor areas also when the height of the room is increased. This decrease is however not so dramatic compare to situation when constant height is used.

Table 11: Dimensions of different scenarios of investigated rooms

Room name	Dimensions of the room			
	length	weith	constant height	variable height
orig.size	7	3.3	2.9	2.9
2x size	9	5	2.9	3.3
3x size	10.5	6.5	2.9	3.7
5x size	13	8.9	2.9	4.1

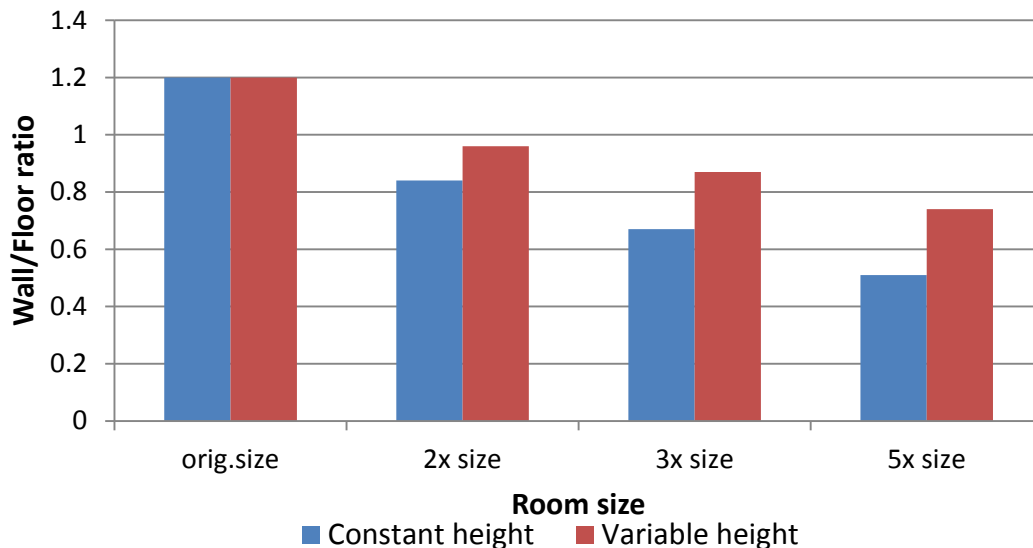


Figure 77: Wall to floor ratios for different scenarios of investigated rooms

The investigations have been carried out for the Danish climate, building located in Copenhagen and the windows were situated to the south. The temperature of the cooling water was 15°C.

Figure 78 shows the resulting overheating hours in the room. The four different room areas with the same height of 2.9 m are presented. It can be seen that the general trend is an increase in overheating hours with increase in floor area of the room. The overheating hours in original size room at operative temperature 26°C and 27°C are however higher than in rooms with larger areas. This can be explained by the effect of the sun. The effect of the direct solar radiation is smaller in larger rooms as the operative temperature was calculated as average for 9 people at different position in the investigated room (described in more details in following part) and direct solar radiation probably did not reach so often so large number of occupants.

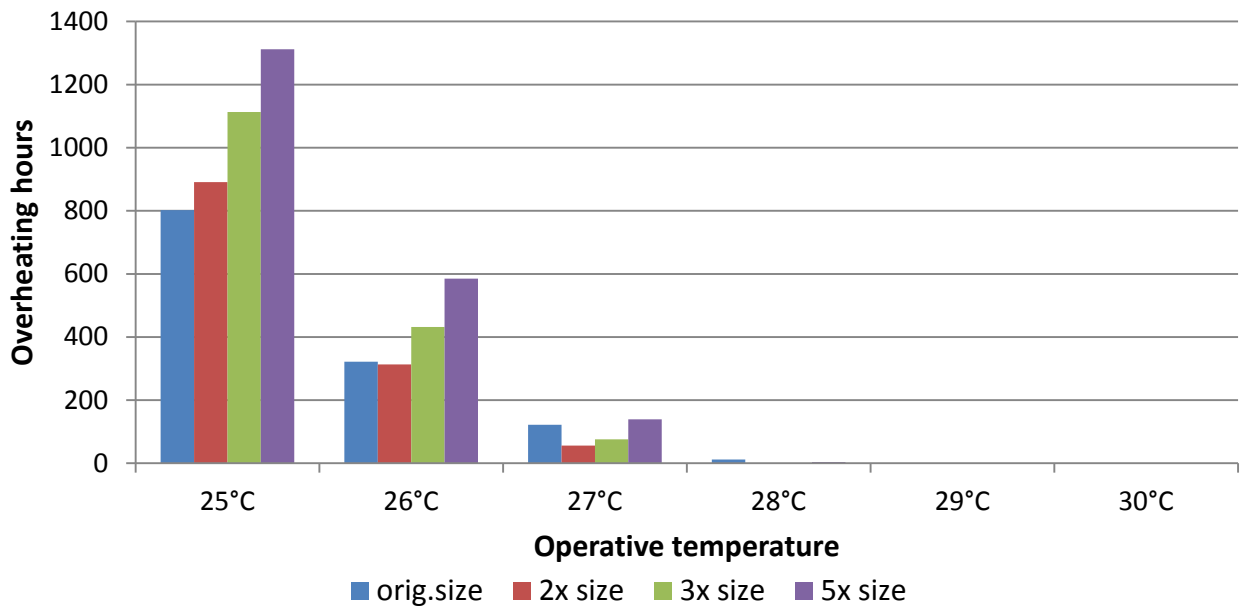


Figure 78: Overheating hours for four investigated floor areas with constant height of the rooms

Figure 79 shows the situation when the height of the rooms was increased with increased floor area. The resulting overheating hours varied only mildly compare to the case with constant room height.

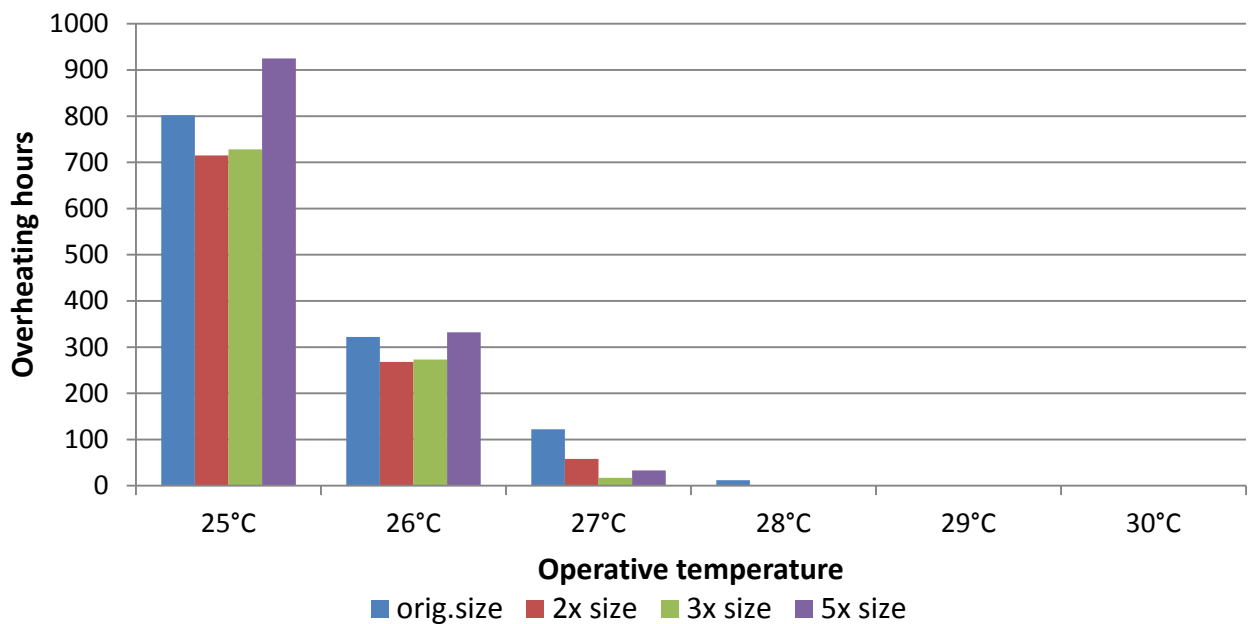


Figure 79: Overheating hours for four investigated floor areas with changing height of the rooms

From Figure 80 it can be observed that the room with five times larger floor area results in nearly two times more overheating hours at operative temperature of 26°C when the constant height of the room is kept.

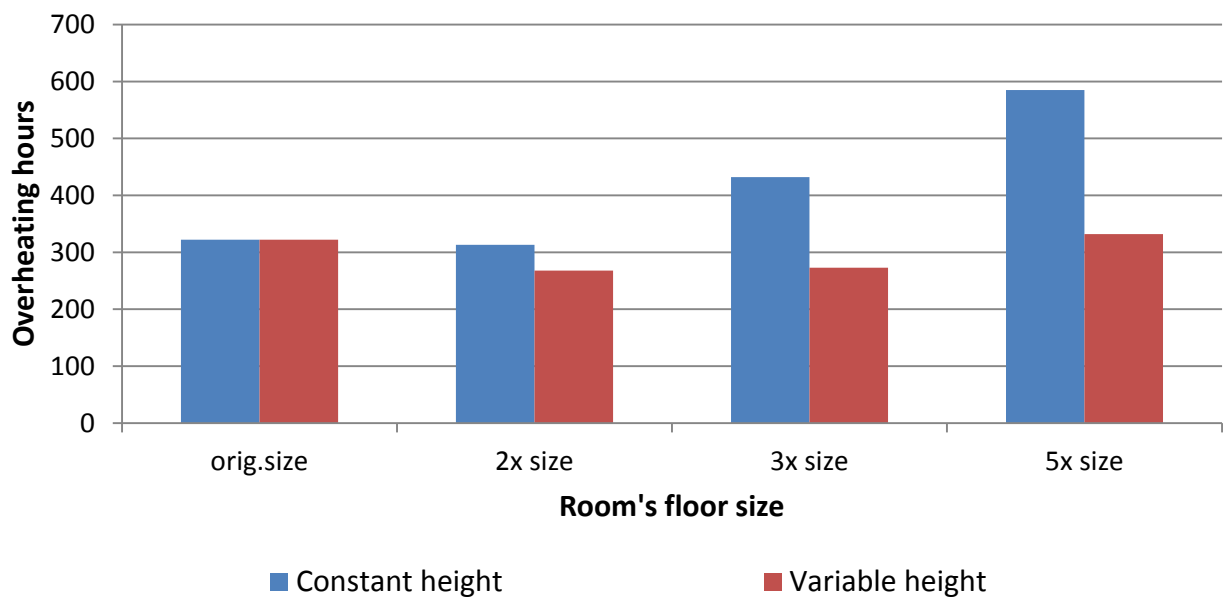


Figure 80: Comparison of overheating hours for scenarios with constant and changing height at operative temperature of 26°C

It can be concluded that the height of the room is important factor when considering the use of the wall radiant cooling systems. With the further growing area of the room the increase in height is usually smaller and the designer should keep this in mind when considering the use of wall radiant cooling systems.

10.4.2 Effect of condensation on operation of radiant cooling

The IDA ICE does not provide the control system which would take into account the creation of the condensate on the cooled surfaces. This is however very important as the condensation can be a strong factor which limit the power output of radiant cooling systems. For that reason, the controller which considered the condensation on the surfaces had to be created. The function for the lower limit for dew point temperature was implemented together with the higher limit for operative temperature in investigated room. It should be noted that the setting of the radiant cooling controller is working with direct value of the dew point temperature to limit the condensation. In other words, the controller is set in the way to let the temperature of the cooling surface go down to the level of the dew point. It was done in this way in order to see the absolute limit of designed radiant system before the condensation occurs. In practice it would be however advisable to set the limit for the temperature of cooled surfaces a bit above the temperature of the dew point. The maximum relative humidity could be set for example to 90%, so there is still certain buffer and solution is designed "on the safe side". This seems to be necessary in case of radiant systems as the threshold for dew point temperature was sometimes reached during investigations. The reason for this behavior could be connected with the rather slow reaction of the radiant systems to the control impulses, being a natural feature of radiant systems. It is problematic especially for hot and humid climates where the moisture content in the air changes rapidly. To investigate the performance of such controller in reality and compare it with performance in IDA ICE could be an interesting topic for further research.

The two scenarios with different settings of controller were investigated. In the first scenario was the condensation on surfaces ignored. The proportional controller controlling the operative temperature in the room was used. In second scenario, the limitation on the output of cooling power from the cooled surfaces was used. The radiant cooling system is designed with unlimited flow rate available for cooling water. This can be done when investigating capillary tubes in high performance concrete as it was shown that the temperature was evenly distributed over the whole cooled surface. This was found during measurements and also calculations [49]. Even when unlimited flow rate is available, IDA ICE automatically adjusts the flow in order to reach the power needed. This was set on purpose unrealistically high so the heat flux is controlled based on the real heat transfer to the room (limited only by operative and dew point temperature). Energy output from radiant system is then governed by situation in the room (convection and radiation coefficients) for selected boundary conditions (temperature of cooling water and H-value). The temperature of cooling water was therefore the only control parameter influencing further the performance of the radiant cooling system. The settings of radiant system in IDA ICE are shown in Figure 81.

Floor heating and cooling (temperature control)	
	Cooling Heating
Design power	200 200 W/m ²
dT(water) at design power	0.1 0.1 °C
Controller	HCCtrlMacro1
Sensor	Surface temperature
Coil massflow	
<input type="radio"/> Given by supply massflows (no separate circulation pump)	
<input checked="" type="radio"/> Constant flow, giving at most a coil temp. difference 0.1 °C	
Location in slab	
Depth under surface	0.01 m
Heat transfer coefficient	
H-water-pipe-fin*	23 W/(m ² ·K)

Figure 81: Settings of radiant cooling system in IDA ICE

In order to get the average operative temperature in the room, nine occupants were inserted in the space as shown on Figure 82. The operative temperature was then calculated as average to all of those. The heat load from occupants was however assigned based on occupant density criterion (1.64 m² per occupant). The investigations have been carried out for south orientation and temperature of cooling water of 15°C was used.

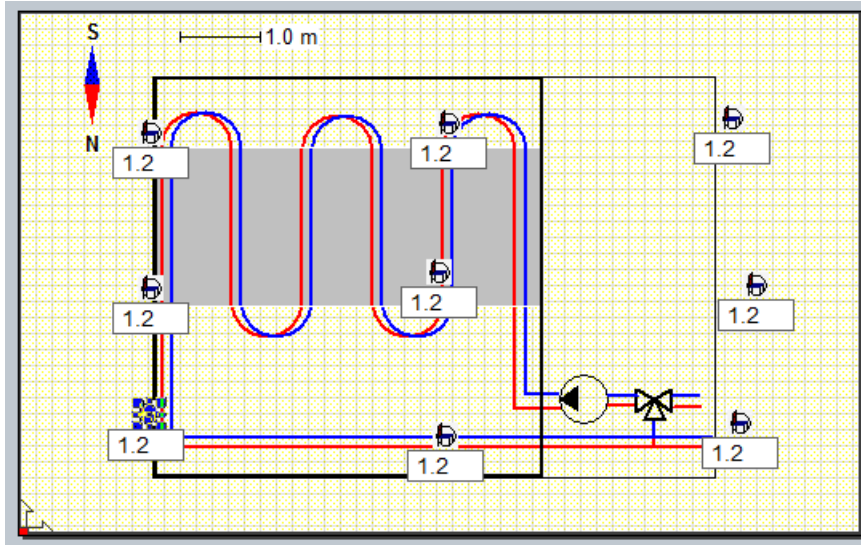


Figure 82: Positions for measurements of operative temperature in the investigated room

The effect of condensation on overheating hours can be seen on Figure 83. The condensation on surfaces has shown to be an important limiting factor for wall radiant cooling systems. This is especially true for the humid climates such as for example Thailand as can be seen in Table 12. Table 13 gives also percentage differences for both used methods.

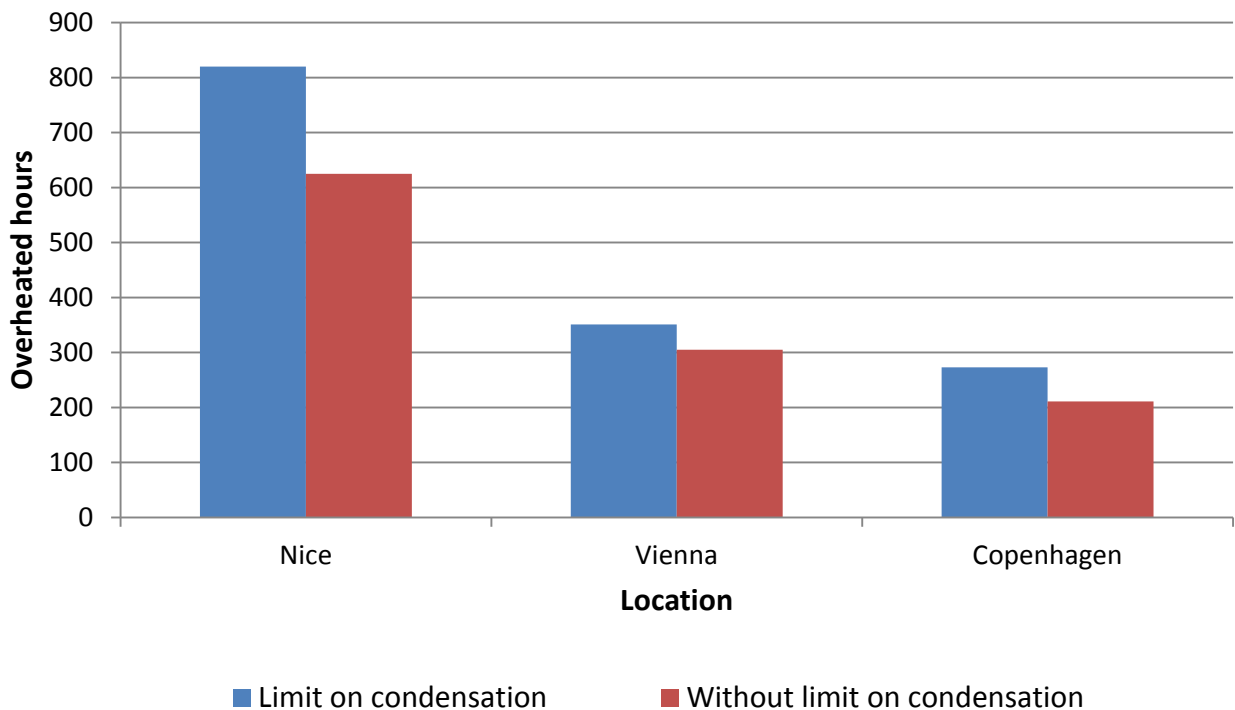


Figure 83: Effect of implementation of limit on condensation in the control system of radiant cooling on overheating (limiting operative temperature is 26°C)

Table 12: Effect of implementation of limit on condensation in the control system of radiant cooling on overheating (values with limitations are in red color)

		Overheating					
		Number of hours with Troom air being > than					
		25°C	26°C	27°C	28°C	29°C	30°C
Thailand	Bangkok	3284	3247	3074	2775	2037	860
France	Nice	1596	820	289	103	14	0
Austria	Vienna	857	351	74	3	0	0
Denmark	Copenhagen	728	273	17	0	0	0
Thailand	Bangkok	3282	3143	2351	1058	218	6
France	Nice	1507	625	99	0	0	0
Austria	Vienna	809	305	74	3	0	0
Denmark	Copenhagen	638	211	15	0	0	0

Table 13: Effect of implementation of limit on condensation in the control system of radiant cooling on overheating (values with limitations are in red color)

		Overheating					
		Number of hours with Troom air being > than					
		25°C	26°C	27°C	28°C	29°C	30°C
Bangkok Lim		3284	3247	3074	2775	2037	860
Bangkok		3282	3143	2351	1058	218	6
% increase with Lim		0	3	31	162	834	14233
Nice Lim		1596	820	289	103	14	0
Nice		1507	625	99	1	1	0
% increase with Lim		6	31	192	10200	1300	0
Vienna Lim		857	351	74	3	0	0
Vienna		809	305	74	3	0	0
% increase with Lim		6	15	0	0	0	0
Copenhagen Lim		728	273	17	0	0	0
Copenhagen		638	211	15	0	0	0
% increase with Lim		14	29	13	0	0	0

In conclusion, the effect of limitation on condensation in control system is substantial for resulting overheating. This is especially true for hot and humid climates like Thailand where the radiant cooling system needs a support of air handling unit in pre-cooling and mainly dehumidifying of the supply air.

10.4.3 Sun radiation influence

The investigations were carried out on the room model “3x size” with the height of 3.7m (see Table 11). This floor area was chosen as it is believed it represents the regular classroom well. No solar shading was implemented during the investigations in order to see purely the differences in overheating caused by change in orientation. The results of performed calculations are presented in Table 14.

Table 14: Differences in overheating between south and north orientation for different locations

			Overheating					
			Number of hours with Troom air being > than					
Orientation	Country	City	25°C	26°C	27°C	28°C	29°C	30°C
South	Thailand	Bangkok	3284	3247	3074	2775	2037	860
	France	Nice	1596	820	289	103	14	0
	Austria	Vienna	857	351	74	3	0	0
	Denmark	Copenhagen	728	273	17	0	0	0
North	Thailand	Bangkok	3222	3078	2873	2497	1726	696
	France	Nice	756	236	131	23	0	0
	Austria	Vienna	426	53	2	0	0	0
	Denmark	Copenhagen	237	0	0	0	0	0

Figure 84 shows the overheating hours for different orientation for limiting operative temperature 26°C stressing the dramatic increase in overheating hours for south orientation.

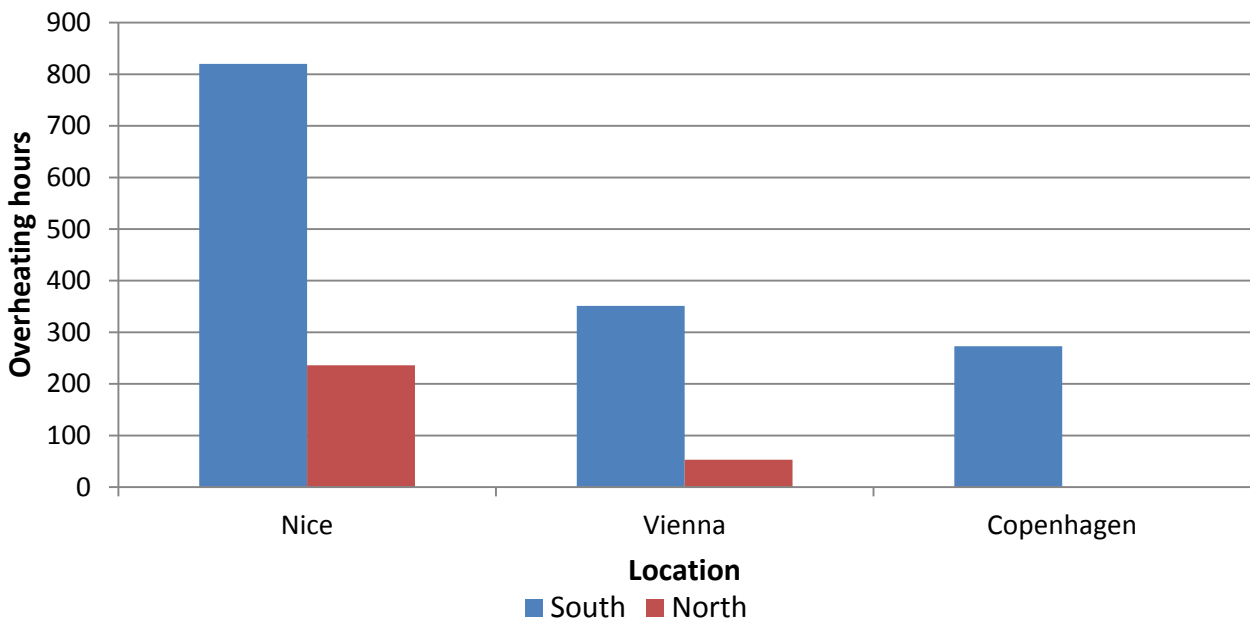


Figure 84: Comparison of overheating hours for south and north orientation (limiting operative temp was 26°C)

It can be concluded that the sun radiation can have a high influence on overheating in the space. The proper solar shading should be always implemented, no matter what type of cooling system is installed. It should be however kept in mind that enough daylight should still get to the room, which is particularly important in case of classrooms.

10.4.4 Temperature of supply water

Based only on physics behind a heat transfer one would assume that with further lowering of temperature of cooling water also the number of overheating hours will be lowered. The radiative and convective heat transfer coefficients stay the same and therefore the amount of energy transferred from the wall is only dependent on the difference between temperature of surface (governed mainly by temperature of cooling water), temperature of other surfaces in the room and room air temperature. However, as already shown, the creation of condensate on the wall surface is an important limiting factor. This is the reason why rather small decrease in overheating hours when temperature of cooling water was decreased from 15°C to 10°C can be seen on Figure 85. In order to validate this assumption, the additional calculations with no limit on condensation were done for climate in France and different temperatures of cooling water. The results of the comparison between two different control used can be seen on Figure 86. It can be concluded that the small decrease in overheating hours for smaller temperatures of cooling water in Figure 85 was caused by control limited by condensation. The further results with control including the limitation on condensation are in Table 15.

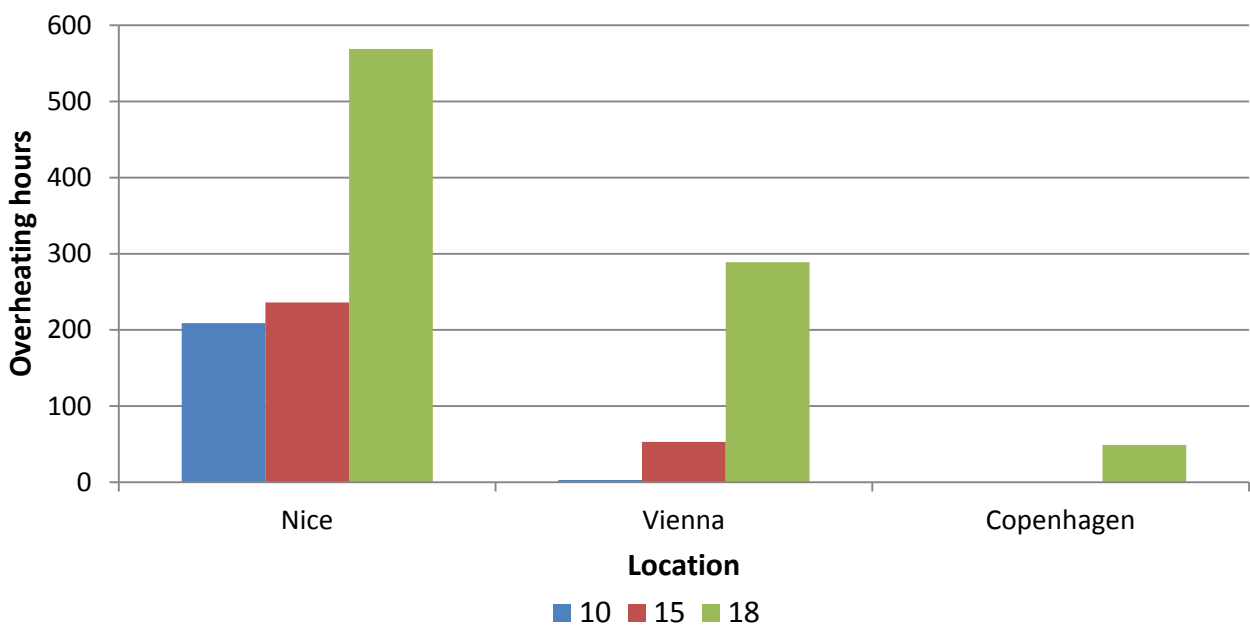


Figure 85: Overheating depending on temperature of cooling water (limit temperature was 26°C)

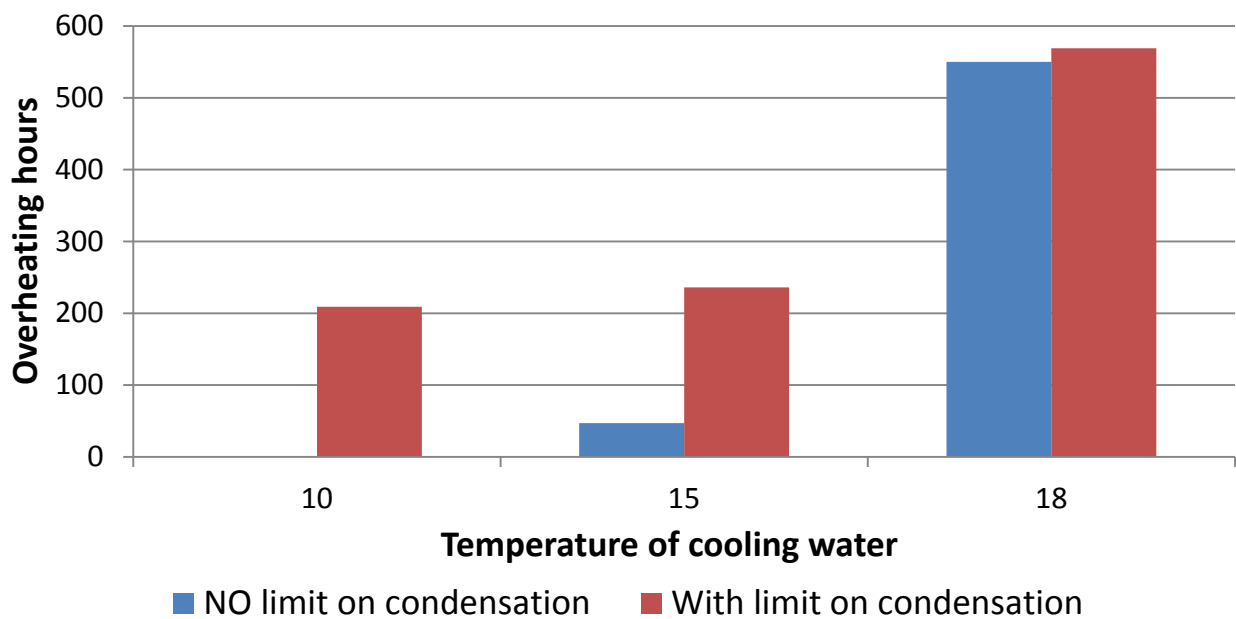


Figure 86: The validation of limiting effect of condensation control

Table 15: Overheating depending on temperature of cooling water supplied to radiant cooling system

			Overheating					
			Number of hours with Troom air being > than					
Tcool water	Country	City	25°C	26°C	27°C	28°C	29°C	30°C
10	Thailand	Bangkok	3100	2948	2759	2420	1666	659
	France	Nice	656	209	118	18	0	0
	Austria	Vienna	275	3	0	0	0	0
	Denmark	Copenhagen	224	0	0	0	0	0
15	Thailand	Bangkok	3222	3078	2873	2497	1726	696
	France	Nice	756	236	131	23	0	0
	Austria	Vienna	426	53	2	0	0	0
	Denmark	Copenhagen	237	0	0	0	0	0
18	Thailand	Bangkok	3285	3247	3066	2689	1851	770
	France	Nice	1482	569	181	25	0	0
	Austria	Vienna	1000	289	65	2	0	0
	Denmark	Copenhagen	598	49	0	0	0	0

In conclusion, in order to allow for increase of power delivery by radiant cooling systems when lower temperature of supply water is used, the additional dehumidification of supply air would be required to effectively use the potential this low temperature of water has. It could very well be, that such a low temperature is not however needed for radiant cooling systems when the supply air would be already precooled in air handling unit.

10.4.5 Heat flux from the cooling surface

In one of journal papers I investigated the heat flux from the cooled walls [49]. It was found that for supply water temperature 18°C and operative temperature 26°C the resulting heat flux was 47 W/m². On Figure 87 are shown results from investigations in IDA for the same boundary conditions. The bars on Figure 87 show the temperature of cooled surface and the number of corresponding heat flux from cooled surfaces. Naturally, with decreasing temperature of cooled surface the heat flux increases. The reason why there are so large differences between various locations (climates) is not known as the same boundary conditions were applied (temperature of supply water, thickness of structure etc.).

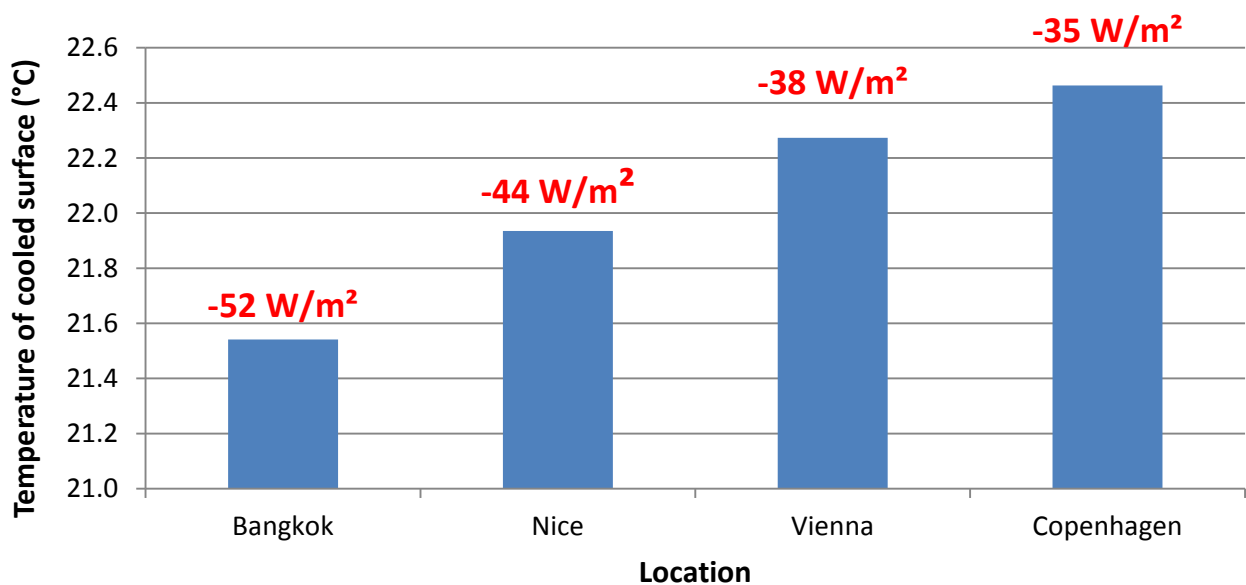


Figure 87: Heat flux and temperature of cooled surfaces for various locations at operative temperature 26°C and temperature of cooling water 18°C

10.4.6 Heat loads variations

Figure 88 and Table 16 present the results of the calculations with various occupancy of the investigated room. The number of overheating hours decreases with lower heat gains and increases with higher heat gains. This resulting trend corresponds to what could be naturally expected. However what is interesting here is how large influence has the factor of heat loads on the resulting overheating.

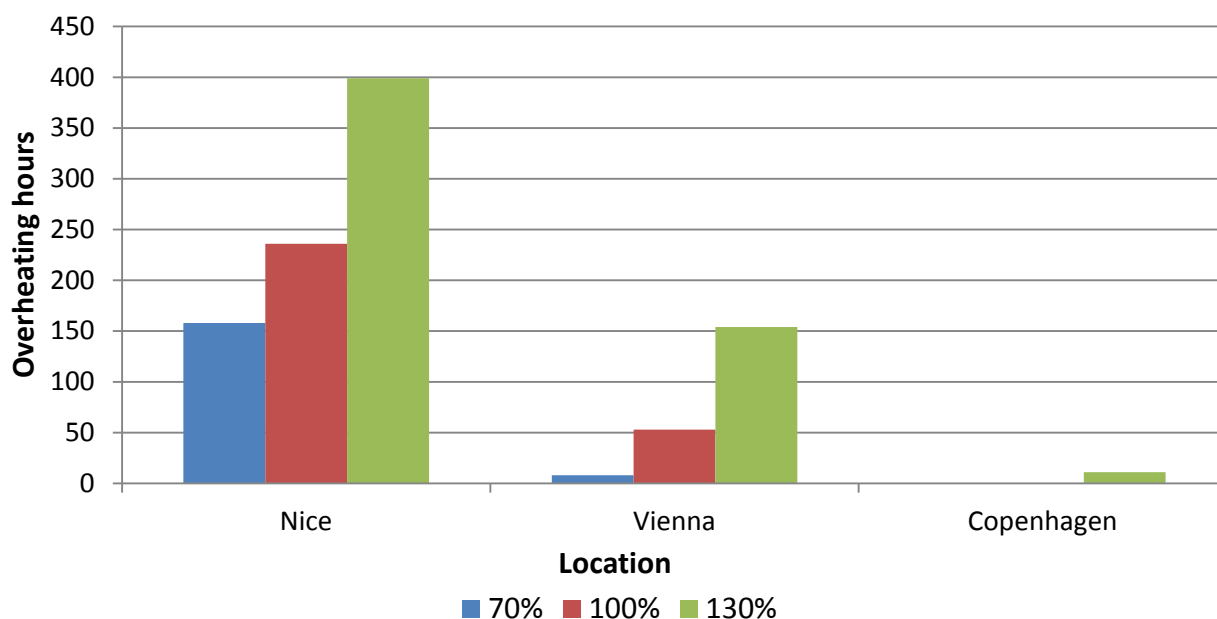


Figure 88: Overheating hours for different heat loads (limiting operative temperature 26°C)

The results in Figure 88 suggest that designed solution can work below the threshold for overheating hours only in Denmark for increased heat loads. In case of Vienna, some additional precooling in air handling unit would be required in case we want strictly keep the limit for overheating. For French climate, dehumidification (precooling) in the air handling unit would be required for all the heat loads.

Table 16: Overheating hours for different heat loads

Occupant load	Location	City	Overheating					
			Number of hours with Troom air being > than					
			25°C	26°C	27°C	28°C	29°C	30°C
70%	Thailand	Bangkok	3163	2956	2678	2102	1134	291
	France	Nice	536	158	40	0	0	0
	Austria	Vienna	290	8	0	0	0	0
	Denmark	Copenhagen	179	0	0	0	0	0
100%	Thailand	Bangkok	3222	3078	2873	2497	1726	696
	France	Nice	756	236	131	23	0	0
	Austria	Vienna	426	53	2	0	0	0
	Denmark	Copenhagen	237	0	0	0	0	0
130%	Thailand	Bangkok	3277	3186	3005	2731	2210	1231
	France	Nice	1186	399	203	85	2	0
	Austria	Vienna	785	154	19	0	0	0
	Denmark	Copenhagen	415	11	0	0	0	0

11. Discussion on hypotheses

This section discusses the most relevant findings of the thesis. The discussion is divided into different parts in accordance with the topic and focus. All the sub-hypotheses, listed in section 1.2.2, are covered in this discussion.

Diffuse ceiling used for ventilation and cooling (sub-hypothesis 1)

“A diffuse ceiling inlet for ventilation of classrooms with a high density of occupants can work without local discomfort when supplying large amounts of fresh air, and give a good indoor climate.”

It has been shown that a diffuse ceiling inlet used for the ventilation and cooling of classrooms with a high density of occupants could deliver large amounts of fresh air without creating any local discomfort in the form of draught. The use of supply air with a temperature of 21 °C resulted in a cooling potential of 23 W/m² for a flow rate of 5.8 l/s·m² of floor area. The average air temperature in the test room was 24.5 °C. A cooling power of 32 W/m² for a flow rate of 8.0 l/s·m² of floor area resulted in an average room air temperature of 24 °C. The temperature of 21 °C was chosen because it represents the outside air temperature in Denmark during most of the period when cooling is required. However, there are days when the temperature of outside air is higher and cooling by ventilation is not sufficient to maintain comfortable temperatures inside a room. Radiant cooling systems can then be activated and can remove most of the sensible heat gains from the room. Slightly higher air velocities were experienced in the lower parts of the room, but the designed system is a draught-free solution. The average ventilation effectiveness was 84%, corresponding to mixing ventilation. The diffuse ceiling inlet can be considered as a well-performing alternative to the traditional means of mechanical ventilation in spaces with a high density of occupants. The draught rating in the test room increased from 4.8% to 8.9% when the flow rate was increased from 5.8 l/s·m² to 8.0 l/s·m² of floor area. The draught rating is in environmental category B for both cases [29]. The use of transient equations to model the turbulence in the room with CFD is recommended because more precise results can be obtained.

Cooling capacity of radiant systems with plastic capillary tubes (sub-hypothesis 2)

“Radiant heating and cooling systems based on plastic capillary tubes installed in a thin layer of high performance concrete can provide sufficient power to heat or cool the space using a low temperature difference between heating or cooling water and room air, and therefore allow the use of natural sources of energy, such as ground water and sea water for cooling and solar heat for heating.”

The results show that radiant heating and cooling systems based on plastic capillary tubes integrated into a thin layer of high performance concrete can provide the energy needed for cooling between 29 W/m² and 59 W/m² of floor area with cooling water temperatures between 22 °C and 18 °C. The indoor air temperature was 24.5 °C – 25 °C when a cooling power of 29 W/m² was used and 22 °C – 23 °C when a cooling power of 59 W/m² was used. The value 29 W/m² can therefore be assumed as a suitable and sufficient amount of cooling power for scenarios investigated in the test room with a ratio of cooling walls to floor area of 1.2. This means that cooling water with a temperature of 21 °C can be used for sufficient cooling. That is favourable for the use of renewable sources of cooling water, such as ground water and sea water. However, the investigated test room does not represent the real classroom, because it is assumed that real classrooms would be bigger. A classroom with dimensions of 12.1 m x 6.5 m giving a floor area of 78.7 m² is used for further comparisons in this thesis (the length and width of the test room were doubled

in this case). In order to get approximately the same value of cooling power of 29 W/m^2 for such big room, cooling water with a temperature of $18.5 \text{ }^\circ\text{C}$ would need to be used. This is still considered to be a rather high temperature for cooling purposes. Furthermore, the bigger room used for comparison has the same height of 2.65 m as the original test room. In a real case, however, the height of a classroom would probably be greater to allow for better daylight, ventilation and general comfort of occupants. This means that the presented comparison with the bigger room is a critical case because the ratio of wall to floor area would be higher in real conditions. A limiting factor of radiant cooling systems can be the dew point temperature of the cooling surfaces. Condensation of water vapour happens when the dew point temperature is reached, which creates a favourable environment for fungus growth and can cause damage to building constructions among other things. This means that it is absolutely necessary to avoid the condensation of water on the surfaces used for radiant cooling as well as on any other surfaces. The dew point surface temperature for room air with a temperature of $27 \text{ }^\circ\text{C}$ and a humidity level of 50% (a middle value in the recommended range [29]) is $16 \text{ }^\circ\text{C}$. The maximum cooling load limited by this dew point temperature of $16 \text{ }^\circ\text{C}$ was 140 W/m^2 using cooling water with a temperature of $12 \text{ }^\circ\text{C}$. The resulting lowest surface temperature was $16.6 \text{ }^\circ\text{C}$. The heat flux value of 140 W/m^2 is nearly 5 times the cooling power required for the scenarios investigated in the test room in this thesis. It can therefore be concluded that the designed solution for radiant wall cooling using plastic capillary tubes integrated in high performance concrete has sufficient reserves with regard to cooling power potential. This means that this cooling system can also successfully cool down spaces with especially high cooling loads.

The cooling ability of the system proved suitable for classrooms with a high density of occupants. Further limitations could be set by thermal radiant asymmetry – in other words, the differences in temperature of different surfaces in the room. According to ISO 7730, the temperature of a cooled wall can be up to 10 K lower than surrounding surfaces [29]. The temperature of the surrounding surfaces in the test room was about $25 \text{ }^\circ\text{C}$ and the dew point temperature of the cooled surfaces was $16 \text{ }^\circ\text{C}$. This limit for radiant asymmetry cannot therefore be exceeded, since the dew point would be reached sooner and condensation would be present.

With regard to the heating ability of the system, power output between 7 W/m^2 and 29 W/m^2 of floor area was achieved with heating water temperatures between $21 \text{ }^\circ\text{C}$ and $24 \text{ }^\circ\text{C}$. However, heating would not be needed because heat gains between 51.5 W/m^2 and 77.8 W/m^2 of floor area were present in the test room in the scenarios investigated. These heat gains were higher than the actual need for heating. A need for heating in classrooms can be anticipated early in the morning before occupancy. On the other hand, after some time with occupants in the room, cooling can be necessary. If the same radiant system is to work as a cooling system as well as a heating system, it must be able to react rather quickly. The dynamic behaviour of the designed system is discussed later in this section.

Indoor environment in test room cooled by radiant wall system (sub-hypothesis 3)

“A wall radiant cooling system combined with a diffuse ceiling inlet for ventilation can provide a comfortable indoor climate in classrooms with a high density of occupants and does not cause any discomfort in the form of draught.”

The wall radiant cooling system combined with a diffuse ceiling inlet for ventilation provided a comfortable indoor climate in the test room with a high density of occupants (0.6 occupants per m² of floor area) and did not cause any discomfort in the form of draught. The highest draught rating value of 5.1% was experienced in an area close to the floor and is within environmental class A according to ISO 7730 [29]. The low difference in temperature between the cooling water and the room air of 4 K was sufficient to maintain a comfortable indoor climate. The vertical temperature difference in the test room was 2 K, but was increased when the surface temperature of the cooled walls was lowered from 18.5 °C to 14 °C. This was the result of the downward directed flow close to the cooled walls, which caused colder air to be distributed to areas close to the floor. However, a scenario with 14 °C would need dehumidification of the supply air because the dew point temperature is 16 °C when we assume a relative humidity of 50% in the room air. Higher air velocities were observed in areas close to the floor, which can be attributed to the high internal heat gains in combination with the low temperature of cooled walls. The air distribution in the room was governed by buoyancy forces to a large degree. The influence of the wall radiant cooling system on the operative temperature was 2 K in the areas close to cooled surfaces and 1 K in areas furthest from the cooling surfaces. The influence of the wall radiant cooling system on the operative temperature would be less in bigger classrooms. This could potentially create large differences in the comfort of occupants in different places in the room. The activation of ceiling and/or floor surfaces for cooling would seem to be a better approach with regard to the view factors of occupants towards cooling surfaces. Decreasing the temperatures of cooled surfaces had a mild influence on the vertical temperature difference in the room, with a maximum value of 2 K.

When all the cooling power was supplied to only one wall, higher velocities and lower temperatures were observed in the lower parts of the room. However, the decrease in temperature was only in the magnitude of 0.3 K. The calculated tracer-gas investigations showed that the supply air is distributed in the test room mainly to the areas close to the wall surfaces and to the area of the test room furthest from the air handling unit. This is especially true at heights close to the floor surface. Some of the Freon moved down towards the floor where it spread over the floor surface, while the rest interacted with the thermal plumes from occupants. The tracer-gas investigations further confirm that the air movement in the test room was governed by buoyancy forces to a considerable degree. This means that the position of heat sources in the room has considerable influence on the overall indoor climate development.

Dynamic behaviour of radiant cooling system (sub-hypothesis 4)

“The dynamic response of a wall radiant cooling system based on plastic capillary tubes installed in a thin layer of high performance concrete is fast enough to provide cooling capacity faster than the cooling load is developed, so that the operative temperature in the room remains in a comfortable range.”

As shown earlier, a cooling power of 29 W/m² is sufficient to keep the room at a temperature of 24.5 °C – 25 °C. With a cooling water temperature of 15.5 °C, this required cooling power was reached after 15 minutes with the system using capillary tubes and after 3 hours and 20 minutes with the system using thick tubing. With a cooling water temperature of 18.5 °C, the required cooling power was not even achieved in 4 hours with the system using thick piping, while the system with capillary tubes reached the required value for cooling in 25 minutes. It can be concluded that the system using thick piping cannot be used for dynamic cooling of the room. This corresponds with a similar finding reported by Weitzmann that stated

that providing a fast cooling capacity can become a problem using thick concrete structures and uncomfortable temperatures can occur in the room as a result [48].

The system with capillary tubes reached 50% of its “4 hours cooling capacity” after just half an hour from the start of experiment, while the system with the thick piping reached only 8.5% of its “4 hours cooling capacity” at the same time. The surface heat flux in the solution with capillary tubes was 6 times, 4 times, 3 times, and 2 times greater than in the solution with the thick piping after 1 hour, 2 hours, 3 hours, and 4 hours from the start of the experiment, respectively. In other words, the system with capillary tubes was able to deliver 2 – 6 times the cooling energy of the system with the thick piping. It should be stressed that these differences were obtained with the same cooling water temperature in both cases.

An interesting finding was that the operative temperatures were very similar in the test room even when the cooling water temperature was increased by 3 K. We can conclude that the designed solution of wall radiant cooling did not greatly benefit from further lowering in the temperature of cooling water in the scenarios investigated. A comfortable indoor environment was achieved with a supply cooling water temperature only 4 K lower than the average operative temperature in the room. This finding means that the designed solution is suitable for making use of natural sources of cooling water such as ground water or sea water.

The effect of reduced area of supply inlet (general)

A scenario with the area of supply inlet reduced to 35% of its original area was investigated in **Paper II** and **Paper III**. Different results were obtained in each paper. Temperatures in the test room were lower as a result of heat losses to the outside environment in **Paper II**. However, the effect of the reduced area of supply inlet on the temperature and velocity development in the test room was minor in **Paper III** when the wall radiant cooling system was activated. The surface temperature of the cooled walls was the same for the original CFD model as for the scenario with the reduced supply area of inlet, and the heat loss through the cooled walls to the outside environment was therefore the same. This explains the different results obtained in **Paper II** and **Paper III**.

These are rather important findings, because the ceiling area available for the purpose of ventilation can be limited in most applications in real buildings. Chodor and Taradajko found a lower cooling capacity when the area of supply diffuser was reduced [33], whereas an increased cooling capacity was experienced in the research for this thesis. The reasons for this difference may include the different number and position of heat gains, the different shape of the room, and different material used for the diffuse ceiling inlet.

Velocities of air in the test room (general)

Air velocities were rather low throughout the whole space of the room. The results showed that increased internal heat gains resulted in higher velocities in the room, especially in areas close to the floor surface. This was found also by investigations carried out in an office room by Nielsen and Jakubowska [9]. This suggests that to a certain degree the air flow patterns in the room were governed by buoyancy forces. Stronger flow patterns were created at the corner of the room in the scenario in which two walls were activated for cooling as a result of the collision of the two downward directed cold flow patterns. A correlation was found between the flow rate and the draught rating, which was higher for higher flow rates, especially in areas close to the floor. This finding differs from those of Nielsen and Jakubowska [9]. Velocities and flow patterns can be somewhat different in a bigger room if the height of the room is

increased. It is assumed that this can influence the velocities in the room considerably. However, it is difficult to predict, since the position of heat gains might be different and the effect of radiant cooling installed in walls might be minimized. Further investigation in this area is required.

CFD model (sub-hypothesis 5)

“CFD can predict indoor environment with acceptable precision and therefore can be used in engineering practice to make the design process more efficient, especially in the first stages of a project and product development.”

The CFD model overestimated the temperatures in the higher levels of the room, giving higher vertical temperature differences than in the measured results. It is assumed that this difference was caused by stronger interaction of supplied air with room air in the case of the measurements, which resulted in better mixing of the air in the room. This strong interaction of supplied and room air was not captured by the CFD model due to the limitations in definition of the porous zone used to represent the diffuse ceiling inlet.

The air velocities in the room were often not predicted in the CFD model with high precision due to the fact that the flow of air in a room is a complex phenomenon and is dependent on factors such as the turbulence level in the room. The CFD results for air velocities were mainly used to predict potential areas of the room where draught might possibly be created as a result of high air velocities, rather than for direct comparison with the measured values. It was concluded that precision of the CFD model was sufficient for the purposes of this research. Two different turbulence models were applied during CFD investigations in the different research papers presented in this thesis. The transient turbulent model (Large Eddy Simulation) was considered to be the most precise, and that was also our experience during calculations in **Paper II**, when compared to calculations using steady-state turbulence models. The CFD calculations in **Paper III** started using the transient turbulent model, but the results of these calculations did not give us good predictions when the wall radiant cooling systems were activated. Consequently, a steady-state turbulent model was used for further investigations in **Paper III**, where the better agreement between CFD model and measured data was obtained using the $k-\xi$, steady-state turbulent model. Heat transfer from surfaces to the room is governed by the use of analytical (wall) functions. The $k-\xi$ and Large Eddy Simulation models have different approaches to how to solve the situation in proximity of surfaces and use different wall functions. This could possibly be the reason behind the differences in the results using various turbulence models. The CFD tool has been used to model heat transfer problems only occasionally. Some professionals in the field of CFD assume that as little as 1% of all CFD simulations carried out in industrial practice have been for heat transfer analysis [71]. This further supports the feeling that more investigation is needed in this area.

The experience of CFD calculations carried out in the research for this thesis resulted in doubts about the applicability and usability of CFD as a tool for the “everyday” design of indoor climate in engineering practice. The selection of the proper settings for a CFD model can be very challenging when no results from measurements are available to be used for validation of the CFD model created. Authors of a similar study dealing with the use of CFD for the investigation of indoor environment concluded that CFD simulations should be compared with measurements because the results will be different with the use of different turbulence models for each specific design [78]. The authors of another study agree and add that understanding the various turbulence models is important [79]. The authors further stated that k-ε turbulent models give good agreement with measurements only at some distance from the surfaces. The results in this thesis, however, showed good agreement with measurements when using k-ε turbulence models with the proper wall function to model areas close to the wall surfaces. The calculated scenario in this thesis included the activation of surfaces for cooling, which might possibly result in different behaviour from previous studies. It seems to be relevant to focus on the proper understanding, application, and development of wall functions and an overall approach to the modelling of a situation close to surfaces in a room because this seems to have a substantial effect on the results and therefore on the design and optimization of the indoor climate in buildings. Sufficient experience with CFD modelling seems to be one of the main prerequisites for the successful prediction of the behaviour of the indoor environment. The use of CFD seems to be optimal during the product development of new solutions for building components and systems such as the diffuse ceiling inlet, especially in the early phases of the process. This goes hand in hand with the idea of designing buildings with building components presented in section 4. CFD can be then used for the development and optimization of building components, and general guidelines might then be sufficient for the design of the building itself.

Practical challenges during production (sub-hypothesis 6)

“Radiant systems in the form of plastic capillary tubes can be cast in a layer of high performance concrete that is only 30 mm thick without the casting process itself significantly affecting the project financially.”

Practical challenges were encountered during the casting of the capillary mats in the layer of the high performance concrete. It was found to be rather difficult to ensure that the capillary mats were in the right position during the casting. The solution used to ensure the proper positioning of capillary mats within the layer of concrete was expensive and time consuming. In conclusion, a new way to fix the capillary mats in the proper position within the layer of high performance concrete needs to be developed. The current method does not allow production of the designed solutions at reasonable cost and will most probably not attract potential producers.

Practical application of gained knowledge (sub-hypothesis 7)

“The theoretical and measured findings from this work can be generalized in the way to be sufficient for the use as assessment of the radiant cooling systems in practice”

The thorough investigation concerning the different parameter variations influencing the design of the radiant cooling was carried out in the thesis in order to reflect on its practicality. It has been shown that the size of the room together with the height of the room have a strong influence on performance of the proposed system concerning the indoor climate. An activation of additional areas which could be used for cooling purposes can be necessary in large rooms with a low height. It has been also found that the proposed system can be very often limited by creation of condensation on the cooling surfaces. This is mainly a concern for very humid climates. The special type of control system which takes into account the

limit for condensation should always be used together with radiant cooling systems. In very humid climates (such as Bangkok), the use of radiant cooling system alone is not even possible, the pre-cooling in a central ventilation unit is necessary.

12. Conclusions on hypotheses

Sub-hypothesis 1

“A diffuse ceiling inlet for ventilation of classrooms with a high density of occupants can work without local discomfort when supplying large amounts of fresh air, and give a good indoor climate.”

Sub-hypothesis 1 is true. The results show that a diffuse ceiling inlet used for ventilation and cooling of classrooms with a high density of occupants was able to deliver large amounts of fresh air without creating any local discomfort in the form of draught. The resulting cooling potential was between 23 W/m² and 32 W/m² of floor area depending on the ventilation flow rate.

Sub-hypothesis 2

“Radiant heating and cooling systems based on plastic capillary tubes installed in a thin layer of high performance concrete can provide sufficient power to heat or cool the space using a low temperature difference between heating or cooling water and room air, and therefore allow the use of natural sources of energy, such as ground water and sea water for cooling and solar heat for heating.”

Sub-hypothesis 2 is true. The results show that radiant heating and cooling systems based on plastic capillary tubes integrated into a thin layer of high performance concrete can provide the energy needed for cooling between 29 W/m² and 59 W/m² of floor area for cooling water temperatures between 22 °C and 18 °C, resulting in indoor air temperatures between 25 °C and 22 °C.

Sub-hypothesis 3

“A wall radiant cooling system combined with a diffuse ceiling inlet for ventilation can provide a comfortable indoor climate in classrooms with a high density of occupants and does not cause any discomfort in the form of draught.”

Sub-hypothesis 3 is true. The results show that the wall radiant cooling system combined with a diffuse ceiling inlet for ventilation provided a comfortable indoor climate in a test room with a high density of occupants (0.6 occupants per m² of floor area) and did not cause any discomfort in the form of draught.

Sub-hypothesis 4

“The dynamic response of a wall radiant cooling system based on plastic capillary tubes installed in a thin layer of high performance concrete is fast enough to provide cooling capacity faster than the cooling load is developed, so that the operative temperature in the room remains in a comfortable range.”

Sub-hypothesis 4 is true. The dynamic behaviour of the installed radiant cooling system provided sufficient power (29 W/m²) to cool the space in the relatively short time of 15 minutes without causing any discomfort for occupants because the cooling capacity is developed faster than the cooling load and fast enough to keep the operative temperatures in a comfortable range of 24.5 °C – 25 °C.

Sub-hypothesis 5

“CFD can predict indoor environment with acceptable precision and therefore can be used in engineering practice to make the design process more efficient, especially in the first stages of a project and product development.”

Sub-hypothesis 5 is partially true, since the results in the research papers show an acceptable correlation between measured and calculated values. It was concluded that the precision of the developed CFD model was sufficient for the purposes of this thesis. However, the correct settings of the CFD model in order to obtain good correlations with the results of measurements took an enormous amount of time. This was mainly with regard to the turbulence model and wall function settings. Everyday use of CFD in engineering practice as a reliable tool for indoor environment optimization is therefore questionable. The appropriate use of CFD tools for the design and optimization of the indoor environment of buildings needs to be further studied with a rather critical attitude.

Sub-hypothesis 6

“Radiant systems in the form of plastic capillary tubes can be cast in a layer of high performance concrete that is only 30 mm thick without the casting process itself significantly affecting the project financially.”

Sub-hypothesis 6 turned out to be false. New ways of fixing the capillary mats in the proper position in the layer of high performance concrete need to be developed. The current method does not allow production of the designed solutions at a reasonable cost and will probably not attract potential producers.

Sub-hypothesis 7

“The theoretical and measured findings from this work can be generalized in the way to be sufficient for the use as assessment of the radiant cooling systems in practice”

Sub-hypothesis 7 is true. The investigations concerning practical use of radiant cooling have uncovered the influence of different, relevant parameters on the performance of the proposed system. It has turned out that the most critical parameter limiting the design of the radiant cooling is creation of the condensate on the cooled surfaces, therefore mainly concerning very humid climates.

Main conclusion

Wall radiant cooling systems based on plastic capillary tubes integrated into a thin layer of high performance concrete combined with a diffuse ceiling inlet can provide sufficient cooling and heating power in classrooms with high internal heat gains by using cooling (heating) water with a low temperature difference between the cooling (heating) water and room air without creating any local discomfort when supplying large amounts of fresh air.

13. Recommendations for further work

It would be advisable to focus on validation of CFD models. It is recommended that CFD studies are carried out systematically and outcomes are compared and critically assessed. Results from those studies and gained experiences could be used to create a kind of database with various CFD studies dealing with design and optimization of indoor environment. The impact of different settings on the results should be presented and clearly explained. The used CFD models should preferably differ in size and shape of the room, in principle of ventilation system used, and in density of occupants. All of the mentioned variables can influence the results into the large degree. Furthermore, the application of different turbulent models is crucial in order to understand the behaviour of different models. The position of CFD in engineering practice as mean of design tool for buildings can be improved by systematically investigated and documented results of concrete applications of CFD models.

It is recommended to carry out further measurements in the test building used in this thesis with the same measuring setup for different flow rates. The results would be relevant for further validation of conclusions made in this thesis. Investigations in **Paper III** and **Paper IV** were done only with use of one ventilation flow rate due to the time constrains.

It is recommended to investigate the developed solution for wall radiant cooling in laboratory conditions which could give us more precise results. More focus could be then on investigations of modes of heat transfer when wall radiant system for cooling is combined with a diffuse ceiling inlet. In this way the potential for precooling of incoming air could be assessed.

Future investigations of a diffuse ceiling inlet and radiant cooling systems could also include special construction of perforated suspended ceiling with integrated radiant cooling system. It is anticipated that such an installation would have high cooling potential due to the optimal position of radiant system for cooling and also due to the increased convective heat transfer coefficient resulting from movement of supply air over the area of suspended ceiling.

Bibliography

- [1] B. W. Olesen, »Indoor Environment- Health- Comfort and Productivity,« International Center for Indoor Environment and Energy, Technical University of Denmark.
- [2] J. Sundell, »On the History of Indoor Air Quality and Health,« *Indoor Air*, årg. 14, pp. 51-58, 2004.
- [3] P. Wargocki og D. P. Wyon, »Providing Better Thermal and Air Quality Conditions in School Classrooms Would Be Cost-effective,« *Building and Environment*, årg. 59, pp. 581-589, 2013.
- [4] M. e. a. Turunen, »Indoor Environmental Quality in School Buildings, and the Health and Wellbeing of Students,« *Int. J. Hyg. Environ. Health*, 2014.
- [5] P. Wargocki, D. P. Wyon, J. Sundell, G. Clausen og O. P. Fanger, »The Effects of Outdoor Air Supply Rate in an Office on Perceived Air Quality, Sick Building Syndrome (SBS) Symptoms and Productivity,« *Indoor Air*, nr. ISSN 0905-6947, pp. 222-236, 2000.
- [6] BP, »Energy Outlook 2030,« January 2013. [Online]. Available: http://www.bp.com/content/dam/bp/pdf/statistical-review/EnergyOutlook2030/BP_Energy_Outlook_2030_Booklet_2013.pdf. [Senest hentet eller vist den 1 July 2014].
- [7] EIA, State Energy Consumption Database, »Building Energy Data Book,« U.S. Department of Energy, [Online]. Available: http://buildingsdatabook.eren.doe.gov/docs/xls_pdf/1.1.3.pdf. [Senest hentet eller vist den 1 July 2014].
- [8] EPDB, »Energy Performance of Building Directive,« European Union, [Online]. Available: http://europa.eu/legislation_summaries/other/l27042_en.htm. [Senest hentet eller vist den 1 July 2014].
- [9] P. V. Nielsen og E. Jakubowska, »The Performance of Diffuse Ceiling Inlet and Other Room Air Distribution Systems«.
- [10] J. L. Jensen, »Experimental and numerical analysis of the cooling potential with diffuse ceiling ventilation,« Technical University of Denmark, 2012.
- [11] S. Svendsen, Development of energy-efficient products in the building component industry, BYG DTU U-034, ISSN 1396-4046, Educational Note, 2002.
- [12] J. A. Leech, W. C. Nelson, R. T. Burnett, S. Aaron og M. E. Raizenne, »Its about time: A comparison of Canadian and American time-activity patterns,« *Journal of Exposure Analysis and Environmental Epidemiology*, årg. 12, pp. 427-432, 2002.

- [13] J. C.-C. Derek, »Work Performance, Productivity and Indoor Air,« årg. SJWEH Suppl (4), pp. 69-78, 2008.
- [14] CR1752, »Ventilation for Buildings- Design Criteria for the Indoor Environment,« CEN report, 1998.
- [15] T. Salthammer, »Critical evaluation of approaches in setting indoor air quality guidelines and reference values,« *Chemosphere*, årg. 82, pp. 1507-1517, 2011.
- [16] D. S. Robertson, »Health Effects of Increase in concentration of Carbon Dioxide in the Atmosphere,« *Current Science*, årg. 90, nr. 12, 2006.
- [17] EPA, »Indoor Air Facts No.4 (revised), Sick Building Syndrome,« Environmental Protection Agency, Research and Development, 1991.
- [18] H. Levin, »Sick Building Syndrome: Review and Exploration of Causation Hypotheses and Control Methods,« i *Proceedings of the ASHRAE/SOEH Conference IAQ*, San Diego, California, April 17-20 1989.
- [19] WHO, »Indoor Air Pollutants: Exposure and Health Effects,« World Health Organization, 1983.
- [20] O. A. Seppanen, W. J. Fisk og M. J. Mendell, »Association of Ventilation Rates and CO₂ Concentrations with Health and Other Responses in Commercial and Institutional Buildings,« *Indoor Air*, årg. 9, nr. ISSN 0905-6947, pp. 226-252, 1999.
- [21] D. P. Wyon, »The effects of indoor air quality on performance and productivity,« *Indoor Air*, årg. 14 (Suppl.7), pp. 92-101, 2004.
- [22] O. Seppanen, W. J. Fisk og Q. H. Lei, »Ventilation and Performance in Office Work,« *Indoor Air Journal*, årg. 18, pp. 28-36, 2006.
- [23] ANSI/ASHRAE Standard 62-2001, »Ventilation for Acceptable Indoor Air Quality,« Atlanta,GA, 2003.
- [24] D. S. Robertson, »The Rise in the Atmospheric Concentration of Carbon Dioxide and the Effects on Human Health,« *Med. Hypotheses*, årg. 56, pp. 513-518, 2001.
- [25] D. G. Shendell, W. J. Fisk, M. G. Apte og D. Faulkner, »Associations Between Classroom CO₂ Concentrations and Student Attendance in Washington and Idaho,« *Indoor Air*, nr. LBNL-54413, 2004.
- [26] Danish Society of Engineers, »The IDA Climate Plan 2050,« Main Report, 2009.
- [27] P. Lombard, L. Ortiz og J. Poutch, »A review on buildings consumption information,« *Energy and Buildings*, nr. 40, pp. 394-398, 2008.
- [28] P. V. Nielsen, »Analysis and Design of Room Air Distribution Systems,« *HVAC Research Journal*, årg. 13, nr. 6, pp. 987-997, 2012.

- [29] EN ISO 7730:2005, »Ergonomics of the Thermal Environment: Analytical Determination and Interpretation of Thermal Comfort Using Calculation of the PMV and PPD Indices and Local Thermal Comfort Criteria,« International Organization for Standardization, Geneva, 2005.
- [30] Lindab A/S, »Lindab Catalogue,« [Online]. Available: http://itsolution.lindab.com/lindabwebproductsdoc/pdf/documentation/comfort/lindab/technical/theory_air.pdf. [Senest hentet eller vist den 1 July 2014].
- [31] C. A. Hviid og S. Svendsen, »Experimental study of perforated suspended ceilings as diffuse ventilation air inlets,« *Energy and Buildings Journal*, årg. 56, pp. 160-168, 2013.
- [32] C. A. Hviid og S. Terkildsen, »Experimental Study of Diffuse Ceiling Ventilation in a Classroom,« Technical University of Denmark.
- [33] A. D. Chodor og P. Taradajko, »Experimental and Numerical Analysis of Diffuse Ceiling Ventilation,« Aalborg University, 2013.
- [34] L. Jacobsen, »Air Motion and Thermal Environment in Pig Housing Facilities with Diffuse Inlet,« Aalborg University Department of Civil Engineering, 2006.
- [35] Y. Honglu, »Experimental and Numerical Analysis of Diffuse Ceiling Ventilation,« Department of Civil Engineering, Technical University of Denmark, 2011.
- [36] P. Jacobs, E. C. van Oeffelen og B. Knoll, »Diffuse Ceiling Ventilation, a New Concept for Healthy and Productive Classrooms,« TNO Built Environment and Geosciences, Delft, 2008.
- [37] B. W. Olesen, R. Bean og W. K. Kwang, »History of Radiant Heating and Cooling Systems- part 1,« *ASHRAE Journal*, 2010.
- [38] B. W. Olesen, »Radiant Floor Heating in Theory and Practice,« *Ashrae Journal*, 2002.
- [39] B. W. Olesen, R. Bean og W. Kwang, »History of Radiant Heating and Cooling Systems- part 2,« *ASHRAE Journal*, 2010.
- [40] P. Simmonds, S. Reuss og W. Gaw, »Using Radiant Cooled Floors to Condition Large Spaces and Maintain Comfort Conditions,« *Ashrae Journal*, 2000.
- [41] S. A. Mumma, »Ceiling Panel Cooling Systems,« *Ashrae Journal*, 2001.
- [42] J. Dieckmann, »Radiant Ceiling Cooling,« *Ashrae Journal*, 2004.
- [43] P. Weitzmann, E. Pittarello og B. W. Olesen, »The cooling capacity of the Thermo Active Building System combined with acoustic ceiling«.
- [44] J. Dieckmann , K. McKenney og J. Brodrick, »Radiant Floor Cooling in Practice,« *Ashrae Journal*, 2009.

- [45] H. Karlsson, »Self-Regulating Floor Heating Systems in Low Energy Buildings,« i *Building Physics Nordic Symposium*, 2008.
- [46] B. W. Olesen, »Radiant Floor Cooling Systems,« *Ashrae Journal*, 2008.
- [47] L. Fang, G. Clausen og P. O. Fanger, »Impact of Temperature and Humidity on the Perception of Indoor Air Quality,« *Indoor Air*, nr. 8(2), pp. 80-90.
- [48] P. Weitzmann, »Modelling Building Integrated Heating and Cooling Systems,« Technical University of Denmark, 2004.
- [49] T. Mikeska og S. Svendsen, »Study of Thermal Performance of Capillary Micro Tubes Integrated into the Building Sandwich Element Made of High Performance Concrete,« *Applied Thermal Engineering*, nr. 52, pp. 576-584, 2013.
- [50] S. A. Mumma, »Designing Dedicated Outdoor Air Systems,« *Ashrae Journal*, 2001.
- [51] EN 15251:2007, »Indoor Environmental Input Parameters for Design and Assessment of Buildings Addressing Indoor Air Quality, Thermal Environment, Lighting and Acoustics,« European Committee for Standardization, 2007.
- [52] N. Cross, *Engineering Design Methods Strategies for Product Design*, UK: Third Edition, The Open University, Milton Keynes, 2000.
- [53] »Connovate A/S,« [Online]. Available: www.connovate.dk. [Senest hentet eller vist den 1 July 2014].
- [54] The Danish National Advanced Technology Foundation, »Connovate- optimized building system using High Performance Concrete,« Technology Institute of Denmark, 2010.
- [55] HP, »HP 34970A Data Acquisition/Switch Unit,« 1997.
- [56] A. Heller, »Large-Scale Solar Heating- Evaluation, Modelling and Designing,« Technical University of Denmark, 2000.
- [57] Agilent, »Data Acquisition/Switch Unit Product Datasheet,« 1 July 2014. [Online]. Available: <http://www.amplicon.com/data/34972a.pdf>.
- [58] Agilent Technologies, »Agilent 34970A Data Acquisition/Switch Unit User's Guide,« 2003.
- [59] EN ISO 7726, »Ergonomics of the Thermal Environment- Instruments for Measuring Physical Quantities,« International Organization for Standardization , Geneva, 1998.
- [60] Sensor-electronic, »AirDistSys 5000 product datasheet,« [Online]. Available: http://www.sensor-electronic.pl/pdf/KAT_AirDistSys5000.pdf. [Senest hentet eller vist den 1 July 2014].

- [61] Onset, »HOBO Data Loggers Product Datasheet,« [Online]. Available: <http://www.onsetcomp.com/products/data-loggers/u12-012>. [Senest hentet eller vist den 1 July 2014].
- [62] Innova, »Innova 1303 and Innova 1312 Product Datasheets,« Lumasense Technologies, [Online]. Available: <http://www.lumasenseinc.com/EN/products/gas-monitoring-instruments/>. [Senest hentet eller vist den 1 July 2014].
- [63] Furness Control, »Micromanometer,« [Online]. Available: file:///C:/Users/tommi/Downloads/68475_FCO510.pdf. [Senest hentet eller vist den 1 July 2014].
- [64] SDS-Infrared, »Hot-Find D,« [Online]. Available: http://www.emtamericas.com/pdf/Satir_Hotfind.pdf. [Senest hentet eller vist den 1 July 2014].
- [65] ANSI/ASHRAE 55, »Thermal Environmental Conditions for Human Occupancy,« An American National Standard, 1992.
- [66] H. Skistad, E. Mundt, P. Nielsen, K. Hagstrom og J. Railio, Displacement ventilation in non-industrial premises, REHVA guidebook no.1, 2002.
- [67] H. Han, »Ventilation Effectiveness Measurements Using Tracer Gas Technique«.
- [68] Ansys Fluent, »Product Datasheet,« [Online]. Available: <http://ansys.com/Products/Simulation+Technology/Fluid+Dynamics/Fluid+Dynamics+Products/ANSYS+Fluent> . [Senest hentet eller vist den 1 July 2014].
- [69] P. V. Nielsen, F. Allard, H. Awbi , L. Davidson og A. Schalin, Computational Fluid Dynamics in Ventilation Design, REHVA Guidebook no.10, 2007, p. 48.
- [70] Ansys 14.5, »Fluent Theory Guide 4.3.2«.
- [71] W. Vieser, T. Esch og F. Menter, »Heat Transfer Predictions Using Advanced Two-equation Turbulence Models,« Ansys, CFX Validatin Report.
- [72] Ansys 14.0, Fluent Theory Guide 4.13.
- [73] Ansys 14.0, »Fluent User's Guide 28.2.3, 28.3.1.1, 28.8.2.1«.
- [74] T. Blomberg, »Heat 2. A PC Program for Heat Transfer in Two Dimensions- Manual with brief Theory and Examples,« Lund-Gothenburg, 2000.
- [75] IDA ICE, »<http://www.equa-solutions.co.uk/de/software/idaice>,« [Online]. Available: <http://www.equa-solutions.co.uk/de/software/idaice>. [Senest hentet eller vist den 1 July 2014].
- [76] I. ICE, »IDA User Manual, Version 4.5,« EQUA Simulation , Februar 2013.

- [77] EN15377-1, »Heating systems in buildings-Design of embedded water based surface heating and cooling systems- Part 1: Determination of the design heating and cooling capacity,« 2008.
- [78] J. Le Dreau, P. Heiselberg og P. V. Nielsen, »Simulation with different turbulence models in an Annex 20 benchmark test using Star-CCM+,« Aalborg University, 2012.
- [79] L. Rong og P. V. Nielsen, »Simulation with different turbulence models in an annex 20 room benchmark test using Ansys CFX 11.0,« 2008.
- [80] R. J. Shaughnessy, U. Haverinen-Shaughnessy, A. Nevalainen og D. Moschandreas, »A preliminary study on the association between ventilation rates in classrooms and student performance,« *Indoor Air*, årg. 16, pp. 465-468, 2006.
- [81] ASTM, »Standard Guide for Using Indoor Carbon Dioxide Concentrations to Evaluate Indoor Air Quality and Ventilation,« American Society for Testing Materials, West Conshohocken (CA), 1998.
- [82] O. P. Fanger, »What is IAQ?,« *Indoor Air*, årg. 16, pp. 328-334, 2006.
- [83] Y. A. Cengel, Heat Transfer: A Practical Approach, 2nd edition red., McGraw-Hill, 2003, pp. 562, chapter 6, 9 and 11.
- [84] J. Babiak, B. W. Olesen og D. Petras , Low Temperature Heating and High Temperature Cooling, Guidebook no 7 red., Rehva, 2007.
- [85] D. Laussmann og D. Helm , »Air Change Measurements Using Tracer Gases,« Robert Koch Institute, Germany.
- [86] E. Bjørn, »R&D department in Airmaster A/S,« [Online]. Available: www.airmaster.dk. [Senest hentet eller vist den 1 July 2014].
- [87] Keyinstrument Series FR4000. [Online]. Available: www.keyinstruments.com. [Senest hentet eller vist den 1 July 2014].
- [88] J. Cook , D. Nuccitelli, S. A. Green, M. Richardson, B. Winkler, R. Painting, R. Way, P. Jacobs og A. Skuce, »Quantifying the consensus on anthropogenic global warming in the scientific literature,« *Environmental Research Letters*, årg. 8, 2013.
- [89] H. K. Versteeg og W. Malalasekera, An Introduction to Computational Fluid Dynamics, The Finite Volume Method, England: Longman Scientific and Technical, 1995.
- [90] T. Mikeska og J. Fan, »Full Scale Measurements and CFD Simulations of Diffuse Ceiling Inlet for Ventilation and Cooling of Densely Occupied Rooms,« *Energy and Buildings*, 2014.
- [91] EPDB, »Energy Performance of Building Directive,« European Union, [Online]. Available: http://europa.eu/legislation_summaries/energy/energy_efficiency/en0021_en.htm. [Senest hentet

eller vist den 1 July 2014].

[92] »Advanced projects 2010, application form,« Technology Institute of Denmark, 2010.

[93] EN ISO 13786, »Thermal performance of building components- Dynamic thermal characteristics- Calculation methods,« ISO, Brussels, 2007.

List of Figures

Figure 1: CO ₂ as an indicator of human bioeffluents [14]	8
Figure 2: Mixing ventilation principle [30]	14
Figure 3: Displacement ventilation principle.....	14
Figure 4: Objective tree method	25
Figure 5: Product attributes vs engineering characteristics.....	26
Figure 6: Ceiling cooling element made of high performance concrete.....	27
Figure 7: Creation of space for plenum between the exposed ribs	27
Figure 8: A diffuse ceiling inlet as building component made of high performance concrete	28
Figure 9: Diffuse wall inlet	28
Figure 10: Test House after its construction	29
Figure 11: Drawing of sandwich wall element made of high performance concrete	30
Figure 12: Design of Test House	30
Figure 13: Photo and layout with positions of lighting fixtures	31
Figure 14: Drainage pipe situated below suspended ceiling.....	31
Figure 15: Casting of CPTs in the HPC wall element.....	32
Figure 16: Capillary mat made of plastic capillary tube	33
Figure 17: Connection of capillary mats with manifold pipes	33
Figure 18: Detail of steel reinforcement in concrete layer	34
Figure 19: Vertical position of AHU and connecting ducts.....	35
Figure 20: Horizontal position of AHU and connecting ducts	35
Figure 21: View on AHU without cover	36
Figure 22: DCI construction and AHU position.....	37
Figure 23: Installation of suspended ceiling.....	37
Figure 24: Insulated box for measurements of reference temperatures	40
Figure 25: Schematic connection of thermocouples.....	41
Figure 26: Connection of thermocouples to multi-conductor cable.....	42
Figure 27: Aluminum cylinder used for shielding of thermocouples	43
Figure 28: PPD based on PMV values [29].....	45
Figure 29: Discomfort caused by vertical air temperature difference [14].....	46
Figure 30: Discomfort caused by radiant asymmetry [14]	47
Figure 31: CFD model	49
Figure 32: Layout and description of the room investigated in Paper I (Figure 2 in Paper I)	55
Figure 33: Measured and calculated temperatures on measuring stands for Scenario 1 (Figure 5 in Paper I)	57
Figure 34: Thermal plumes in CFD calculations of scenario 1 (Figure 7 in Paper I)	57
Figure 35: Velocity and pressure distribution in the diffuse ceiling inlet in CFD calculations	58
Figure 36: CFD velocity distribution in the room in Scenario 1 (Figure 8 in Paper I)	59
Figure 37: Measured and calculated velocities on measuring stands for Scenario 1 (Figure 9 in Paper I).....	60
Figure 38: Ventilation effectiveness (Figure 4 in Paper I)	60
Figure 39: Reduced area of supply inlet (Figure 12 in Paper I)	61

Figure 40: Temperature distribution in the solution with the reduced area of the diffuse ceiling inlet (Figure 13 in Paper I).....	62
Figure 41: Velocity distribution in the solution with the reduced area of the diffuse ceiling inlet (Figure 14 in Paper I)	62
Figure 42: Airtightness of the connection of two perforated gypsum boards (Figure 11 in Paper I)	63
Figure 43: Section of the high performance concrete element built in the program HEAT2 (Figure 1 in Paper II).....	64
Figure 44: Temperature distribution in the inner layer of the high performance concrete element (Figure 4 in Paper II).....	65
Figure 45: Heat flux of the high performance concrete element towards an indoor environment for various scenarios (Figure 6 in Paper II)	66
Figure 46: Increase of heat flux to the outside environment as result of the use of CPTs in the high performance concrete inner layer (Figure 9 in Paper II)	68
Figure 47: Layout and description of the test room in Papers III and IV (Figure 4 in Paper III)	70
Figure 48: Temperature development from measurement (Figure 6 in Paper III)	72
Figure 49: Measured and CFD predicted temperature distribution in the test room (Figure 7 in Paper III)..	73
Figure 50: Measured and CFD velocity magnitude distribution in the test room (Figure 8 in Paper III)	74
Figure 51: Position of reduced area of supply inlet (Figure 10 in Paper III)	74
Figure 52: Temperature distribution in the scenario with reduced supply area (Figure 11 in Paper III).....	75
Figure 53: Velocity distribution in the scenario with reduced supply area (Figure 12 in Paper III)	75
Figure 54: Comparison of temperature distribution between the original scenario and the scenario with reduced supply area for various wall temperatures (Figure 13 in Paper III).....	76
Figure 55: Comparison of velocity magnitude distribution between the original scenario and the scenario with the reduced supply area for various wall temperatures (Figure 14 in Paper III)	77
Figure 56: Velocities for the validated scenarios at height 0.1 m with cooled wall temperatures of 14°C, 18.5°C and 21.5°C (Figure 15 in Paper III)	77
Figure 57: Velocity distribution in the scenarios with increased and decreased heat load (Figure 17 in Paper III).....	78
Figure 58: Temperature distribution in the scenarios with increased and decreased heat load (Figure 16 in Paper III)	78
Figure 59: Temperature distribution for scenarios with different surfaces activated for cooling (Figure 18 in Paper III)	79
Figure 60: Velocity distribution for scenarios with different surfaces activated for cooling (Figure 19 in Paper III).....	80
Figure 61: Velocity distribution at a height of 0.1m for three scenarios: original model (left); south-eastern wall (middle); south-western wall (right), (Figure 20 in Paper III)	80
Figure 62: Temperature distribution at height 0.1m for three scenarios: original model (left); south-eastern wall (middle); south-western wall (right).....	81
Figure 63: Cooling of the room before the presence of occupants (Figure 8 in Paper IV).....	87
Figure 64: Temperature development in Scenario 1 (Figure 9 in Paper IV).....	88
Figure 65: Temperature development in Scenario 2 (Figure 10 in Paper IV).....	88
Figure 66: Temperature development in Scenario 3 (Figure 11 in Paper IV).....	89
Figure 67: Velocity development at a distance of 0.2 m and a height of 0.1 m (Figure 12 in Paper IV).....	90

Figure 68: Draught rating results for all the scenarios at a distance of 0.2 m and a height of 0.1 m (Figure 13 in Paper IV)	90
Figure 69: The un-cooled part of the south-western wall (Figure 17 in Paper IV)	91
Figure 70: Comparison of surface temperatures for the scenarios with capillary tubes and with thick tubing	93
Figure 71: Comparison of surface heat fluxes for scenarios with capillary tubes and thick tubing.....	94
Figure 72: Surface temperatures for different temperatures of cooling water.....	95
Figure 73: Surface heat fluxes for different temperatures of cooling water	96
Figure 74: Floor plan and section cut of original test room	98
Figure 75: Original size room modeled in IDA ICE	98
Figure 76: The 3D model created in IDA ICE.....	100
Figure 77: Wall to floor ratios for different scenarios of investigated rooms.....	101
Figure 78: Overheating hours for four investigated floor areas with constant height of the rooms	102
Figure 79: Overheating hours for four investigated floor areas with changing height of the rooms	102
Figure 80: Comparison of overheating hours for scenarios with constant and changing height at operative temperature of 26°C.....	103
Figure 81: Settings of radiant cooling system in IDA ICE	104
Figure 82: Positions for measurements of operative temperature in the investigated room.....	105
Figure 83: Effect of implementation of limit on condensation in the control system of radiant cooling on overheating (limiting operative temperature is 26°C)	105
Figure 84: Comparison of overheating hours for south and north orientation (limiting operative temp was 26°C)	107
Figure 85: Overheating depending on temperature of cooling water (limit temperature was 26°C)	108
Figure 86: The validation of limiting effect of condensation control	109
Figure 87: Heat flux and temperature of cooled surfaces for various locations at operative temperature 26°C and temperature of cooling water 18°C	110
Figure 88: Overheating hours for different heat loads (limiting operative temperature 26°C).....	111

List of Tables

Table 1: Study of grid independence.....	50
Table 2: PPD results of measured values (Table 2 in Paper I)	56
Table 3: Draught rating results based on measurements (Table 3 in Paper I)	57
Table 4: Local mean age of air (Table 4 in Paper I).....	61
Table 5: Differences in Kelvin between the maximum and minimum temperatures over the inner surface of the high performance concrete wall element (Table 2 in Paper II)	65
Table 6: Freon distribution in horizontal planes for the first 4 minutes after the start of the ventilation system.....	82
Table 7: Freon distribution in horizontal planes between 4 and 10 minutes after the start of the ventilation system.....	83
Table 8: Freon distribution in the vertical plane for the whole period of calculation (numbers below pictures are time steps in seconds)	84
Table 9: Investigated scenarios (Table 1 in Paper IV).....	87
Table 10: Comparison of results from IDA ICE with results from Measurements and CFD	99
Table 11: Dimensions of different scenarios of investigated rooms.....	101
Table 12: Effect of implementation of limit on condensation in the control system of radiant cooling on overheating (values with limitations are in red color)	106
Table 13: Effect of implementation of limit on condensation in the control system of radiant cooling on overheating (values with limitations are in red color)	106
Table 14: Differences in overheating between south and north orientation for different locations.....	107
Table 15: Overheating depending on temperature of cooling water supplied to radiant cooling system....	109
Table 16: Overheating hours for different heat loads.....	111

Part II

Appended papers

Paper I

**Full Scale Measurements and CFD Simulations of Diffuse Ceiling Inlet for
Ventilation and Cooling of Densely Occupied Rooms**

Mikeska T., Jianhua F.

Accepted for publication in Energy and Buildings (2015)

Full Scale Measurements and CFD Simulations of Diffuse Ceiling Inlet for Ventilation and Cooling of Densely Occupied Rooms

Tomas Mikeska, Jianhua Fan*

Department of Civil Engineering, Technical University of Denmark, Brovej, Building 118, DK-2800 Kgs. Lyngby, Denmark

Abstract

Spaces with high occupant densities result in high heat gains and need for relatively high air change rate. By means of traditional mechanical ventilation diffusers it becomes a challenge to supply large amounts of fresh air into the space without creating a local discomfort for occupants. One solution to this problem is use of a diffuse ceiling inlet supplying a fresh air into the room through a large area of perforated ceiling.

The aim of this paper was to report the research conducted on diffuse ceiling inlet installed in the full scale test outdoor facility. The diffuse ceiling inlet based on gypsum boards with airtight connections was created utilizing the full potential of diffuse layer without undesirable crack flow reported by other authors. The measured values were used to validate the detailed Large Eddy Simulation model of test room created in CFD software with aim to evaluate an indoor comfort numerically.

Results of our investigations have shown that diffuse ceiling inlet is a suitable solution for the spaces with high density occupancy. The results have shown that transient calculations using Large Eddy Simulation models can predict well temperatures and velocity magnitude of air flow in the room.

**Corresponding author: Tel.: +4527338619, E-mail: tommi@byg.dtu.dk*

Keywords

Diffuse ceiling inlet

Large Eddy Simulation

Computational Fluid Dynamics

Indoor climate

Classroom

Nomenclature

CFD Computational Fluid Dynamics

EU European Union

PMV Predicted mean vote

PPD Predicted percentage of dissatisfied

USA United States of America

1. Introduction

The use of mechanical ventilation in buildings occupied by humans is getting more importance nowadays, since it is no longer possible to meet energy requirements with use of natural ventilation. The energy use in new buildings must be reduced in all countries within EU to the level of nearly zero energy building [1]. The requirements of EU are understandable, taking into account that about 40 % of overall consumption of energy within EU is in building sector [1]. Similar situation is in the USA. On worldwide scale, the fraction of energy used for buildings is about 24 % [2]. The use of mechanical ventilation with a heat recovery can save up to 90 % of energy, otherwise used for ventilation of buildings. Such savings are unrealistic with use of natural ventilation.

Due to the wrong choice of ventilation system and poor overall design, schools have generally very poor indoor climate [3]. Similar findings were obtained from investigations in buildings with different purposes which were poorly ventilated, such as offices, call centers etc. [4]. Wyon in his experiment found that poor indoor climate can result in decrease of performance up to 9 % [5]. Wargocki and Wyon observed increased performance among students when outdoor air supply was increased from 4 l/s-person to 10 l/s-person [6]. Authors also claim that the performance of children in schools can be increased by up to 30 % compared to the situation in average educational institution.

Traditional mixing and displacement inlet diffusers are usually used for most of the installations in buildings occupied by humans. However, there are situations where traditional types of diffusers are not able to deliver required amount of conditioned air in comfortable ways, are not able to remove large heat gains and are not able to comply with relevant standards concerning indoor climate. Spaces difficult to ventilate with traditional types of diffusers include educational rooms, meeting rooms, conference centers, theaters etc. Diffuse ceiling inlet seems to be a better alternative to traditional diffusers for mentioned spaces.

Diffuse ceiling inlet ventilation is characterized by activation of large area of ceiling as an inlet device. The fresh air is supplied into the space at very low velocity. The large air volumes can be supplied to the space without having a risk of creating any draughts. In principle, the fresh outside air is supplied into the space between the ceiling slab and perforated suspended ceiling, so-called plenum, where it gets uniformly distributed. Then the air comes into the room through perforated gypsum boards. The over-pressure is kept in the plenum thanks to a sound absorbing material (an acoustic textile) being installed on top of the perforated gypsum boards. This solution creates a pressure chamber, allowing the supply air to be distributed equally through the whole area of the perforated suspended ceiling. This

results in a whole surface acting as a supply air terminal device. Perforated suspended ceiling can be created from different types of materials (other than gypsum). As an example, Hviid used aluminum tiles in one work [7] and shredded spruce wood mixed with wool and cement in other study [8].

Diffuse ceiling inlet is nowadays mainly known in livestock industry where it was previously used as a supply diffuser in agricultural buildings [7, 9]. Some of the applications were also done in public buildings, mainly during renovation of classrooms [10]. Other example of installation of diffuse ceiling inlet is administrative building for headquarter of large company [11]. Some previous investigations have been done in real buildings. Hviid studied performance of diffuse ceiling inlet in classroom [8]. He found that good level of mixing was reached in the room. The uniform temperature and airflow distribution was experienced, without any risk of draught. Jensen studied the cooling benefits of diffuse ceiling inlet. Reduced hours of overheating in the room were reported [10]. Other investigations took place in experimental facilities. Nielsen focused in his study on performance of diffusive ceiling ventilation in office space with two manikins and basic office equipment [12]. The results have shown that diffuse ceiling inlet was able to handle higher thermal loads and higher flow rates compare to five other ventilation systems. Hviid in his experiment realized that suspension construction had great influence on the air flow to the room [7]. He found out that more air was coming from the plenum to the room through the attachment of perforated tiles with suspension construction, instead of going directly through the perforation of the tiles.

To the best knowledge of authors, no work has been so far done on diffuse ceiling inlet based on acoustic ceiling gypsum boards with absolutely airtight connections distributing the supply air equally over the whole area of suspended ceiling. The aim of this paper is to report the research conducted on diffuse ceiling inlet based on acoustic ceiling gypsum boards with airtight connections, hence utilize the full potential of diffuse layer without undesirable crack flow reported by Hviid [7]. Such a solution creates a basis for validation of a CFD model using a porous zone to simulate the diffuse ceiling inlet. The thorough CFD calculations are done with use of Large Eddy Simulation equations in order to reliably model the effect of turbulence fluctuations on the air flow in the room. The reduced area of supply diffuser is investigated with aim to improve the mixing of supply air with room air and also to improve air distribution in the room. Diffuse ceiling inlet cools the room down by use of outside air without creating any draught problems and with use of relatively small amount of energy to run the fans as pressure drop over the suspended ceiling is rather

small. A densely occupied classroom situated in the real test building equipped with de-centralized ventilation unit is investigated.

2. Materials and methods

2.1 Experimental measurements

The following chapters describe the materials and methods which have been used during our investigation.

2.1.1 Full scale testing facility

The experimental part of this research was carried out in the full scale test building, which was built from sandwich elements made of high performance concrete. It is two storeys building, where upper floor was used for purposes of this paper. The outer layer of high performance concrete had 20 mm, inner layer of high performance concrete had 30 mm and thermal insulation was 300 mm thick. The planar inside dimensions of the test room were 6.05 m x 3.25 m, resulting in an area of 19.66 m², (Figure 1). The height of the test room after installation of suspended ceiling was 2.65 m. Two windows with three-layer glass and dimensions 2.50 m x 1.10 m were installed in the north-western facade. The resulting area of windows was 5.50 m². The partition wall separated the room from an entrance space which also served as a small technical room (Figure 1). Its purpose was purely to divide the two spaces in terms of air flow. The partition wall was made of wood and gypsum boards. Floor and ceiling decks were made of hollow core concrete elements with a thickness of 0.2 m.

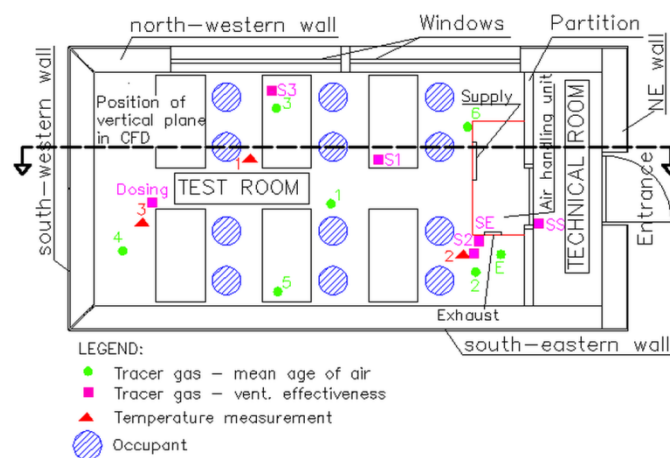


Figure 1: Layout of test room and positions of measuring points

2.1.2 Diffuse ceiling inlet construction

Diffuse ceiling inlet was created from perforated gypsum boards with dimensions 0.9 m x 2.7 m and total perforated area of 15.5 %. Connections between boards and slots around any penetrating objects were sealed by silicone paste. The plenum was built 0.28 m high in order to separate the inlet and exhaust of the air handling unit by the perforated suspended ceiling construction. Resulting height of the room after installation of perforated suspended ceiling was 2.65 m. The surface area of perforated suspended ceiling is decreased by obstructing ventilation unit resulting in an area of 18.6 m². The volume of the investigated room (excluding plenum) was then 52.9 m³.

2.1.3 Air handling unit

The decentralized air handling unit was installed under the concrete ceiling deck being partially situated in the plenum and partly in the room (Figure 2). The fresh air was supplied from the air handling unit into the plenum through the grill with dimensions of 0.8 m x 0.1 m situated on the front face of the unit, 0.05 m below the ceiling deck, oriented into the plenum. An uniform air distribution in the plenum was assumed, creating a chamber with equivalent static pressure drop. The exhaust opening with dimensions of 0.15 m x 0.1 m was placed on a side of the unit and situated just below the perforated suspended ceiling in the room.

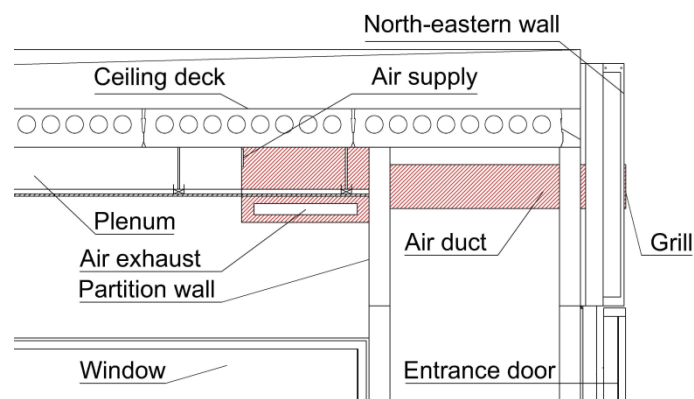


Figure 2: Position of air handling unit

2.1.4 Other appliances installed in the room

Four lighting units with fluorescent tubes with power of 28 W/unit were installed, situated 0.2 m below the perforated suspended ceiling. The room was further equipped with 12 class room tables with dimensions of 1.2 m x 0.7 m and 12 chairs. The occupants were simulated by manikins created from steel buckets and painted to black color so the generated heat is emitted from the body of manikin. The manikins had cylindrical shape with diameter of 0.35 m and height of 0.45 m and were placed at chairs.

2.1.5 Investigated scenarios

Our setup simulated a densely occupied classroom. Twelve manikins were seated in pairs behind the tables in three rows (Figure 1). The heat was generated by 75 W bulbs inside each manikin, which is an equivalent to a sensible heat production of a sedentary person. The assumption was that occupants have activity level of 1.0 met (seated, quiet) and clothing insulation equal to 0.8 clo (spring period). Latent heat gains generated by human respiration were neglected.

Two different scenarios were investigated with balanced supply and exhaust airflows of: 1) 350 m³/h and 2) 480 m³/h, corresponding to the air change rate 6.6 h⁻¹ and 9.1 h⁻¹ respectively. The flow measurement was done by principle of a multi-port averaging pitot tube and resulting accuracy of flow measurements was $\pm 10\%$ [13]. Chosen airflows complied with class B and A, respectively, required by a standard for classrooms [14]. The temperatures of outside air were 0.1 °C and 2.6 °C for Scenario 1 and 2 respectively. The temperatures of air in the room situated below the test room were 24.2 °C and 22.9 °C for Scenario 1 and 2 respectively.

2.1.6 Indoor climate evaluation

Indoor climate is most often evaluated by air quality and thermal comfort. Thermal comfort criteria were assessed by means of Predicted Mean Vote (PMV) and Predicted Percentage of Dissatisfied (PPD) [15]. Furthermore, airflow behavior and ventilation effectiveness were assessed by means of tracer-gas measurements.

2.1.7 Temperature measurements

The T-type thermocouples were used to measure temperatures of air in the room and plenum and also of all surfaces. Temperatures were measured continuously for the entire period of experiment and recorded in a minute interval.

12 pieces of T-type thermocouples were installed at different heights on three moveable stands situated within the occupied zone of the room, see Figure 1. Thermocouples were situated in aluminum cylinders in order to be shielded against the effects of thermal radiation. Thermocouples were fixed at height levels of 0.1 m, 0.6 m, 1.1 m and 1.7 m, respectively, in order to be able to evaluate the vertical temperature profile, which was used as an indicator of local thermal comfort evaluation, as shown in [15]. The difference between heights 0.1 m and 1.7 m should not exceed 3 K. Additional 12 thermocouples were installed to measure the surface temperatures of walls, 12 thermocouples were placed on the bottom side of the perforated suspended ceiling, 4 thermocouples were placed on the floor and 2 measured temperature of window surface. A total of 36 thermocouples were installed in the plenum. The precision of measurements with installed thermocouples was 0.3 K [16]. The outside temperature was measured by use of HOBO loggers with precision of 0.35 K [17].

2.1.8 Air velocity measurements

Air velocities in the room were measured by use of air velocity transducers SensoAnemo5100SF [18]. Accuracy of used equipment was 1 % for velocities below 5 m/s. Measurements were carried out in the occupied zone on positions of the vertical stands at heights 0.1 m, 0.6 m, 1.1 m and 1.7 m respectively. The measurements were taken after the room was stabilized. Draught rating index was used to describe the magnitude of draught and is defined as a percentage of people predicted to be bothered by draft. Draught rating is most common cause of local discomfort and it is recommended by ISO7730 to be kept below 15 % [15]. Draught rating was calculated according to Eq. (1).

$$DR = (34 - t_a) \cdot (v - 0.05)^{0.62} (0.37 \cdot v \cdot T_u + 3.14) [\%] \quad \text{Eq. (1)}$$

Where: t_a is temperature of air at place of measurement [$^{\circ}C$], v is mean air velocity at place of measurement [m/s], T_u is turbulence intensity at place of measurement [%].

Concerning general velocities in occupied zone, those should not exceed 0.16 m/s in winter and 0.19 m/s in summer period (for class B) [15]. The values could be possibly adjusted according to the activity and clothing level of the occupants.

2.1.9 Tracer-gas measurements

In order to find a pattern of air distribution in the room, the thorough investigations with use of tracer gas were performed. The multi-gas analyzers Innova [19] were used for those purposes. The tracer gas was dosed and sampled

by a multipoint sampler and doser unit Innova 1303, and its concentration was measured by use of a photo acoustic multi gas monitor Innova 1312. Freon R134a ($C_2H_2F_4$) was used as a tracer gas. The accuracy of dosage amount was $\pm 2\%$.

Ventilation effectiveness (ε_v) was calculated, in order to evaluate a level of air mixing in the room. The tracer gas concentrations were measured in supply duct (S), exhaust duct (SE) and three different positions within the occupied zone (S1, S2, S3), at height of 1.1 m, see Figure 1. Freon was dosed in the room in distance of 2.5 m from closest sampling point. Eq. (2) was used to calculate the ventilation effectiveness for each investigated point in the room. Overall room ventilation effectiveness was then calculated as an average of the three measured points.

$$\varepsilon_v = \frac{C_e - C_s}{C_i - C_s} [\%] \quad \text{Eq. (2)}$$

Where: C_e is pollution concentration in the exhaust air [PPM]; C_s is pollution concentration of the supplied air (background concentration) [PPM]; and C_i is pollution concentration in the breathing zone [PPM].

Additionally, the Local Mean Age of air describing a time required for a supply air to reach a particular point in the occupied zone was measured. This was done in order to compare the performance of ventilation system in different positions of the room. Freon was supplied at a constant rate to the air handling unit where it was dispersed by the fan and supplied into the plenum and then to the room. Freon concentrations were measured at 6 points at height level of 1.1 m in the occupied zone (see Figure 1). Local Mean Age of air was obtained by integrating the area above concentration curve divided by steady state concentration, according to the step up method adapted from Han [20], see Eq. (3).

$$\theta_p = \int_0^{\infty} \left(1 - \frac{c_p(t)}{c_p(\infty)} \right) dt [s] \quad \text{Eq. (3)}$$

Where: c_p is measured concentration in point P in equilibrium [ppm].

2.2 Numerical calculations

The 3-dimensional numerical model was created in a Computational Fluid Dynamics (CFD) software tool in order to allow for further investigations of diffuse ceiling inlet performance, see Figure 3. The commercial CFD program Ansys Fluent 14.0 was used for numerical calculations [21].

2.2.1 The grid creation

The hexahedral grid with 4,354,482 cells was created. The maximum skeweness of the model was 0.3 which is considered to be very good according to Nielsen [22]. Average value of skeweness was smaller than 0.00045, and therefore the main precondition for having a successful correlation with experimental measurements was reached. The mesh was refined in areas close to the surfaces where rapid change in velocity or temperature can occur. The independence of the grid on results of CFD calculations was investigated by creating four grids with different cell counts and the results are shown in Table 1. The results of calculated temperatures and velocities for horizontal plane at height 1.1 m show only minor deviations. The calculated solutions are therefore grid independent.

Table 1: Grid independence investigations

		Grid 1	Grid 2	Grid 3	Grid 4
Grid cells amount	[pcs]	645,432	1,030,544	1,964,820	4,354,482
Average air temperature at 1.1 m	[°C]	24.2	24.1	24.2	24.3
Average air temperature at exhaust	[°C]	24.5	24.6	24.6	24.6
Average velocity at 1.1 m	[m/s]	0.073	0.069	0.073	0.079
Heat flux imbalance	[W]	12.6	2.8	8.7	3.3
Heat flux imbalance	[%]	1.2	0.3	0.9	0.3

2.2.2 Boundary conditions

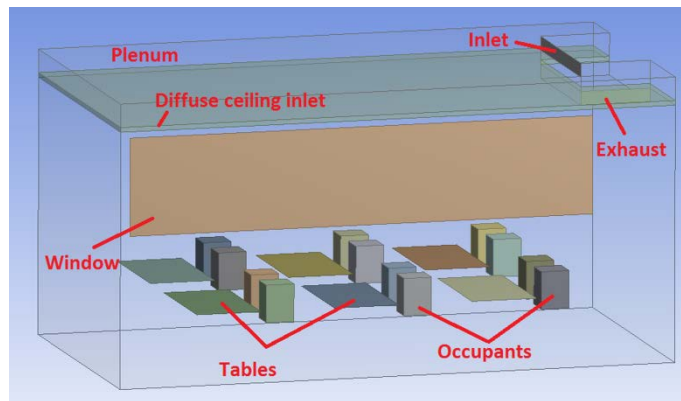


Figure 3: CFD model of the investigated room

The boundary conditions were used to define the situation from experimental setup in CFD. The inlet element situated on air handling unit was assigned with a uniform and constant velocity and temperature of the inlet air (see Table 5).

Dimensions of inlet opening from air handling unit to plenum were 0.8 m x 0.1 m. Boundary on exhaust element was defined as static pressure outlet with dimensions of 0.45 m x 0.10 m. Occupants were modeled as blocks with floor-plan dimensions of 0.25 m x 0.20 m and height of 0.45 m, (see Figure 3). Occupants were placed on horizontal plates with floor-plan dimensions of 0.45 m x 0.40 m, representing the chairs. The plates were situated at a height of 0.55 m. The tables were modeled as horizontal plates with dimensions of 1.3 m x 0.7 m placed at a height of 0.7 m. The heat generated by lighting fixtures was released into the volume close to porous suspended ceiling. The surfaces boundary conditions were assigned with an external heat transfer coefficient (0.33 W/(m²·K) for roof, 0.36 W/(m²·K) for wall, 2.50 W/(m²·K) for floor and 0.8 W/(m²·K) for window).

2.2.3 Porous zone model

Porous zone model was used in CFD calculations to simulate the pressure drop across the porous suspended ceiling. The inputs were determined based on measured pressure drop. The porous suspended ceiling was modelled in Fluent as fluid domain with added momentum loss equation. The porosity was set as isotropic with a value of 15 %, according to known open area of perforated gypsum plate. The momentum loss was defined by viscous and inertial resistance coefficients, being 1.306x10⁹ m⁻² and 1,185,000 m⁻¹, respectively. Those values were obtained from quadratic regression analysis of measured values of pressure drop and velocity expressed by Eq. (4)

$$\Delta p = 35554 \cdot v^2 + 1181.8 \cdot v \quad \text{Eq. (4)}$$

Where: Δp is measured pressure drop across the porous suspended ceiling and v is velocity of the air flowing through porous suspended ceiling.

2.2.4 Turbulence modeling

The air in the room ventilated by use of diffuse ceiling inlet could often move due to natural convection, especially in close proximity to walls and heat sources. The Boussinesq model was used to calculate natural convection caused by buoyancy forces [21]. The buoyant model was defined by gravity-acceleration vertical component of 9.81 m/s². The transient approach was applied for our calculations with use of the Large Eddy Simulation method to model the turbulence effects. It was found that steady-state calculations investigating ventilation in the room had difficulties to converge and results of such calculations were not satisfactory to validate the CFD model. Some authors also stated

that Large Eddy Simulation model gives more accurate results than models using steady-state approach, for investigations of air flow in the room [21].

3. Results analysis and discussion

3.1 Indoor climate

Table 2 shows results of PPD calculations. The highest values were obtained at heights close to the floor, as a result of combination of low temperatures and high velocities in this area. The average values of PPD were 6.0 % and 7.3 % for air change rate of 6.6 h⁻¹ and 9.1 h⁻¹ respectively. Scenario 1 was in category A and Scenario 2 was in category B concerning the PPD evaluation [14]. Even though that Scenario 1 was in category B and Scenario 2 in category A concerning the air change rates. The higher air change rates very often result in higher velocities in the room. Those are often accompanied with lower indoor temperatures since more heat is removed from the room.

Table 2: PPD results based on measurements

Height [m]	Scenario 1			Scenario 2		
	Stand 1	Stand 2	Stand 3	Stand 1	Stand 2	Stand 3
0.1	9.0	9.0	6.0	10.0	13.0	7.0
0.6	5.0	6.0	5.0	6.0	7.0	6.0
1.1	6.0	5.0	5.0	7.0	6.0	6.0
1.7	6.0	5.0	5.0	7.0	6.0	6.0

3.2 Draught rating

Table 3: Draught rating results based on measurements

Height [m]	Scenario 1			Scenario 2		
	Stand 1	Stand 2	Stand 3	Stand 1	Stand 2	Stand 3
0.1	0.0	4.8	0.0	0.0	8.9	3.0
0.6	0.0	0.0	2.7	0.0	2.7	3.3
1.1	0.0	0.0	4.4	0.0	0.0	5.8
1.7	3.3	4.5	0.0	5.0	3.0	0.0

As already mentioned in section 3.1, higher flow rates can contribute to decreased comfort of occupants. This is suggested also by draught rating results shown in Table 3. The draught ratings for different stand points in the room

were kept rather low. The main reasons were generally low velocities of the air within the room. Highest draught rating value was 8.9 % and average value was 1.6 % and 2.6 % for air change rates 6.6 h^{-1} and 9.1 h^{-1} respectively. Both scenarios were in indoor environmental category A concerning draught rating [14].

3.3 Tracer-gas measurement

The ventilation effectiveness was calculated for a period of one hour, based on the tracer-gas measurements. The results for both investigated scenarios are depicted on Figure 4. The averaged values for ventilation effectiveness were 0.81 and 0.87 for Scenario 1 and 2 respectively.

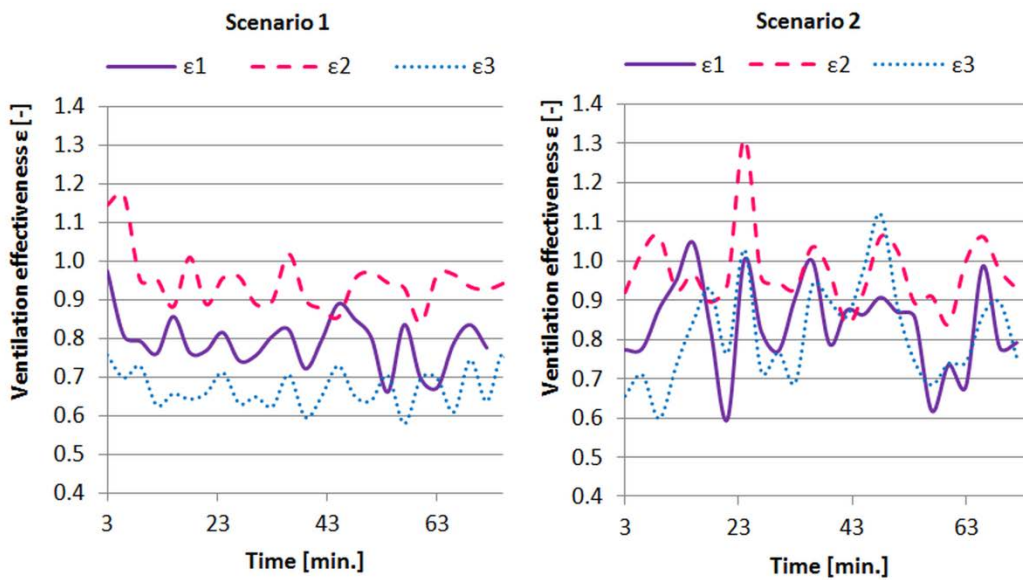


Figure 4: Ventilation effectiveness

The Local Mean Age of air analysis suggests that exhaust orientation influenced the airflow patterns, assuming that fresh air distribution from the porous suspended ceiling was uniform. The Local Mean Age of air at points 3 and 6 was higher than other points which can be attributed to the position of exhaust (see Figure 1). The results of all investigated points are shown in Table 4.

Table 4: Local Mean Age of air results

Point	Local mean age of air (minutes)							Room mean age of air
	1	2	3	4	5	6	Exhaust	
Scenario 1	11.52	N/A	11.10	9.89	10.02	N/A	10.61	10.63
Scenario 2	6.37	6.16	7.90	7.42	6.31	10.95	7.56	7.52

3.4 Temperatures

The results of temperature measurements were taken for periods when the indoor temperature conditions were stabilized. The measured temperatures of the inlet air (from air handling unit to plenum) were 21.0 °C and 20.9 °C for air change rates 6.6 h⁻¹ and 9.1 h⁻¹ respectively. The measured and calculated exhaust air temperatures are shown in Table 5. The resulting cooling loads were 23 W/m² and 30 W/m² for Scenario 1 and 2 respectively.

Table 5: Temperatures of inlet and exhaust openings

		Scenario 1	Scenario 2
Inlet	[°C]	21.0	20.9
Exhaust measured	[°C]	24.7	24.3
Exhaust calculated	[°C]	25.0	23.6

When looking at the temperature development of the three investigated points (the locations of temperature measurement points are shown in Figure 1), one could notice that the highest temperatures were experienced at higher positions of sensors as can be seen on Figure 5. The most rapid change in temperature was found between height 0.1 m and 0.6 m. Lower temperatures below the level of 0.6 m can be explained by supplying colder air into the room which is dropping down and spreading across the floor. This phenomenon was evaluated by use of draught rating values, since people are most sensitive to high velocities at height of ankles (see Table 3). On the contrary, smaller temperature increase was experienced between heights 0.9 m and 1.7 m. This can be explained by interaction of heated room air with colder supply air entering the room through the perforated suspended ceiling. As it can be seen from Figure 5, the results from numerical calculations gave slightly higher values of room air temperatures for Scenario 1. Different situation was however for Scenario 2, depicted on Figure 6. In this scenario, the calculated temperatures were lower than measured values, see Table 6 for difference. The explanation for this situation could be the fact that fresh air was supplied to the room with higher velocity, therefore causing better mixing of the supply air and room air. The smaller vertical temperature difference in Scenario 2 compare to Scenario 1, for measured and also calculated values, further supports this assumption, see Table 7. Furthermore, the higher ventilation effectiveness for Scenario 2 found by tracer-gas measurements means that the air in the room is replaced faster with the supply air (which has lower temperature) and therefore resulting in lower temperatures in the room, (see section 3.3).

Table 6: Air room temperature difference between measured and CFD values

ΔT [K]

	Min.	Max.	Average
Scenario 1	0.02	0.44	0.16
Scenario 2	0.16	0.83	0.61

Table 7: Vertical temperature differences

Vertical temperature difference [K]			
Scenario 1		Scenario 2	
Measured	CFD	Measured	CFD
0.62	0.76	0.43	0.37

The difference between measured and calculated temperatures could also be attributed to uncertainty in determining heat transfer coefficients of building facades. The test room was placed outdoor and therefore its thermal behavior was subject to variations of the outdoor environment. The external part of the heat transfer coefficient is influenced by wind conditions and sky temperature - neither of those values was taken into account during experiment. The internal part of the heat transfer coefficient of building facades was influenced by the flow pattern in the room in proximity to the wall surfaces. This can also influence the heat loss through the constructions. As there was a large temperature difference between the indoor air and the outside environment (23 – 25 K), slight variation of heat transfer coefficient of building facades would result in a noticeable disagreement in temperature prediction of the indoor air.

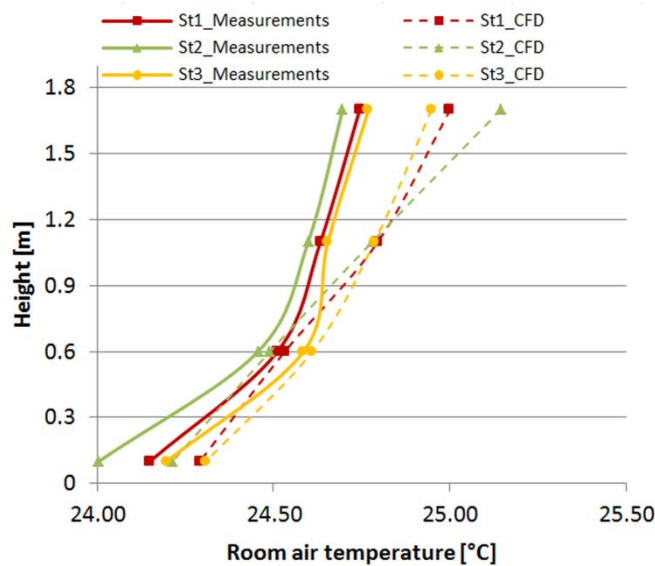


Figure 5: Measured and calculated temperatures in investigated points for Scenario 1

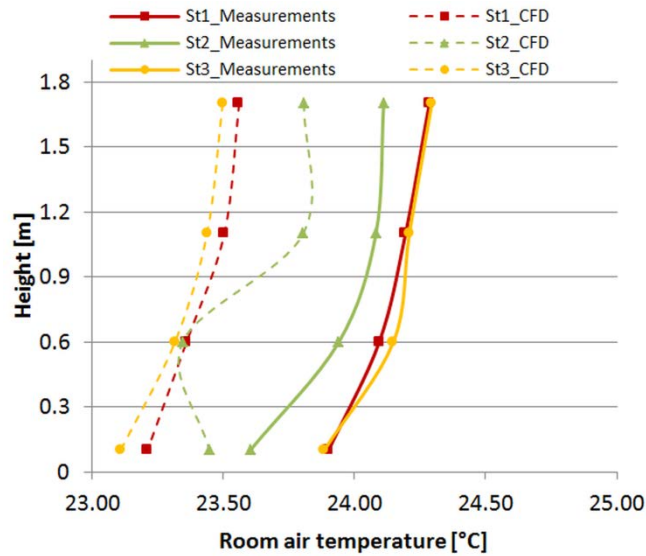


Figure 6: Measured and calculated temperatures in investigated points for Scenario 2

Figure 7 shows the result of the room air temperature distribution of Scenario 1 from CFD calculations (the position of longitudinal, vertical plane where results are taken is shown on Figure 1). The thermal plumes were created above the occupants being the heat sources. Those thermal plumes were rising up to the ceiling and could possibly restrict the air flow at areas above the occupants. Situation in Figure 7 suggests that the supply air was entering the room mainly in areas between the occupants and in the area of the room further away from the air handling unit. The higher amount of supplied air at the end of the room can be explained by lack of heat sources in this area. Furthermore, the inlet air was supplied from air handling unit into the plenum with certain momentum which could cause a higher pressure gradient in the area of plenum further away from the air handling unit, resulting in larger amounts of fresh air entering the room in that area.

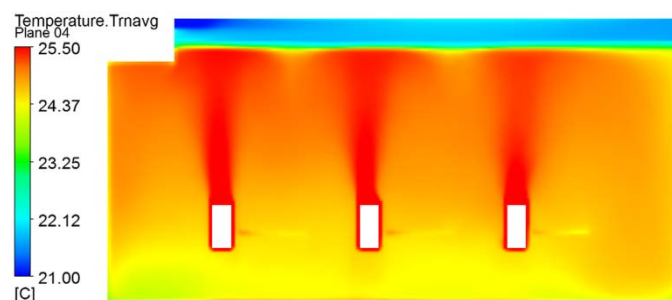


Figure 7: Temperature distribution of Scenario 1 from CFD

3.5 Velocities

Figure 8 shows the velocities in the room and plenum from CFD calculations. Higher air velocities in the room were experienced in area situated further away from the air handling unit. This can also be problematic area concerning the thermal comfort since the cold air is falling down resulting in higher velocity close to the floor surface. The results of air velocity measurements and calculations for two different scenarios are depicted on Figures 9-10. The locations of velocity measurement points are shown in Figure 1. The showed values were calculated as average of 10 minutes measurements taken every 10 seconds. The velocities were generally low throughout the room, considering rather high ventilation flow rates used during our investigations. There were differences between measured and calculated velocities, mostly in areas close to the floor. The possible cause for those differences was the lower level of mixing in CFD calculations compared to measurements, which can be explained by approximate interpretation of perforated suspended ceiling in the CFD model (as explained in section 2.2.3). The porous zone ensured that proper pressure drop was applied for air flowing from the plenum to the room, however it did not ensure the same air velocity just below the porous suspended ceiling. Since the whole area of suspended ceiling was used as supply area in CFD, while the supply area was only 15 % of the suspended ceiling area in measurements. This approximation inevitably results in lower air velocity just below the porous suspended ceiling in CFD calculations. Also larger vertical temperature difference depicted on Figure 5 supports the opinion about lower level of mixing in CFD calculations. The air movement around and above the occupants was increased dramatically as a result of generated heat, as can be seen on Figure 8. It was very challenging to get some consistent patterns concerning velocity development in the room when large fluctuations occurred. This is the reason why we used transient calculations which took into account the fluctuation of the air flow by averaging the values in different time steps. In conclusion, the CFD models are considered to be reliable.

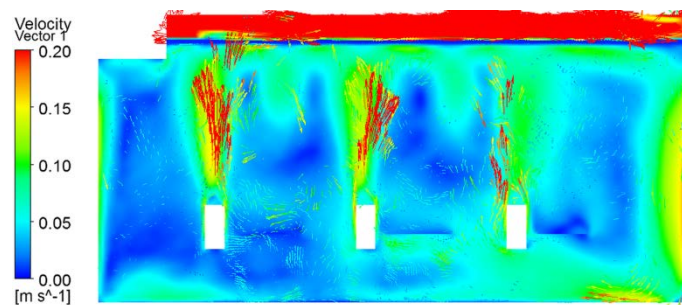


Figure 8: Velocity distribution of Scenario 1 from CFD

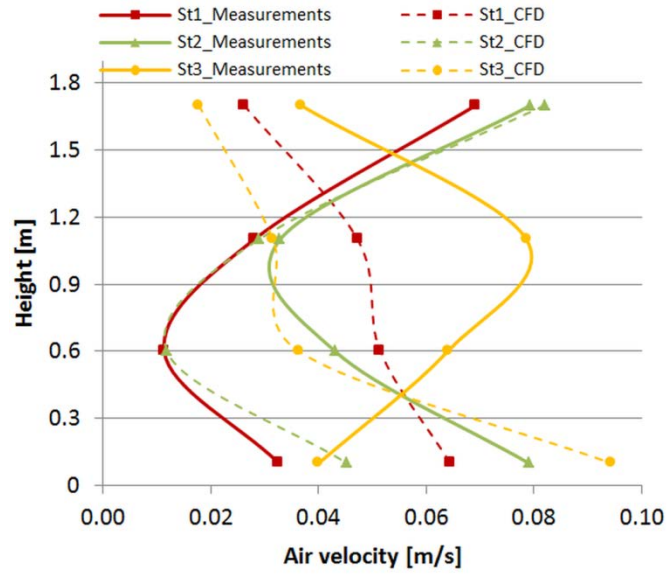


Figure 9: Measured and calculated velocities in investigated points for Scenario 1

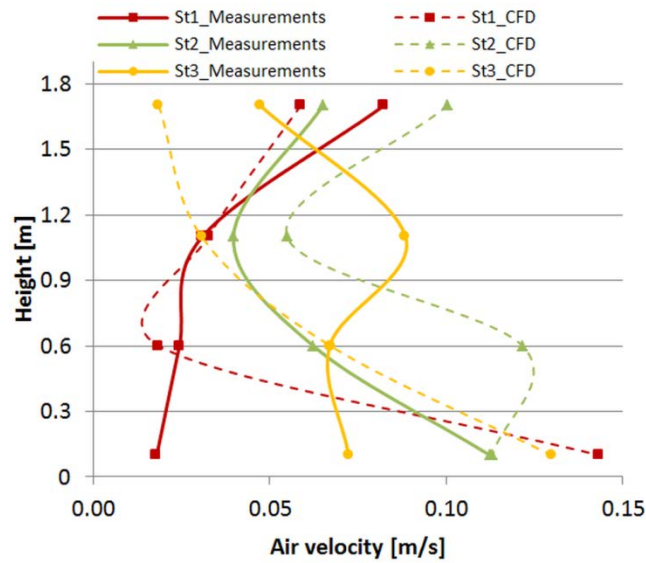


Figure 10: Measured and calculated velocities in investigated points for Scenario 2

3.6 Airtightness of gypsum connections and pressure drop across diffuse ceiling inlet

Figure 11 shows the picture taken by thermo-graphic camera [23] during our investigations to validate the assumption that the connections between gypsum boards were air tight. The green line on the Figure 11 shows place of connection of the two neighboring gypsum plates. Increased air flow was not experienced in that area. On the

contrary, the air flow was decreased as a result of application of silicone paste in and around connections of gypsum boards. The measured pressure drop across the diffuse ceiling inlet was 7.2 Pa for Scenario 1 and 10.16 Pa for Scenario 2.

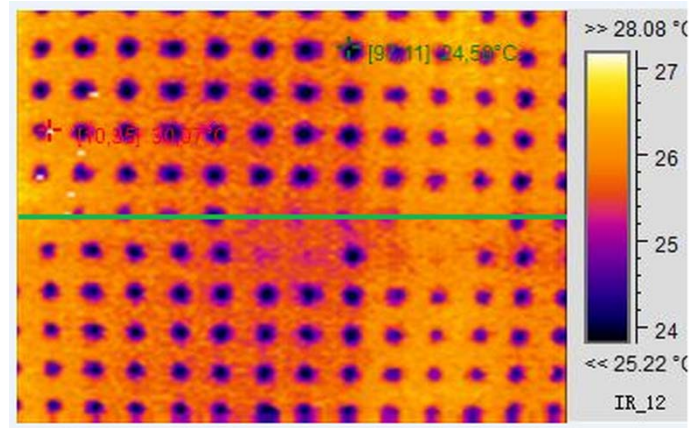


Figure 11: Thermo-graphic picture of gypsum connection

3.7 Parametrical study results

In order to investigate the influence of different suspended ceiling setup on indoor climate, the scenario with reduced ceiling inlet area was studied in CFD, see Figure 12. It consisted of three rectangles (green color) situated at positions above the tables. Each supply rectangle had dimensions of 3.15 m x 0.70 m, resulting in overall area of 6.60 m² (compare to original supply area of 18.60 m²). The rest of the area of suspended ceiling was assumed to be solid, so the air could not penetrate through it.



Figure 12: Parametrical study-reduced area of supply opening

As it can be seen from Figure 13, the temperatures in the case of reduced supply area of suspended ceiling were generally low. This can be explained by different flow pattern in the room compare to the situation where the whole

area of suspended ceiling was activated as a supply diffuser. The flow pattern has an influence on velocity and temperature development in the room and also on the heat loss through the building facades. As can be seen on Figure 14, the velocities were higher in the case with reduced supply area. This resulted in higher convective heat transfer coefficient of the room surfaces, leading to higher heat losses and resulting in lower temperatures in the room. The heat loss through the room surfaces was 641 W in alternative with reduced supply area, whereas it was 580 W in case with whole area of suspended ceiling activated as a supply diffuser. The heat loss by ventilation was 371 W for the case of reduced supply area and 432 W for the case of whole area of suspended ceiling activated as a supply diffuser. On Figure 13 it can be seen that vertical temperature difference was smaller in the case of reduced supply area of suspended ceiling, which further lowers the ventilation heat loss, since exhaust opening was situated in proximity of suspended ceiling. It also means that the air is better mixed in the case of reduced supply area of suspended ceiling.

The validated CFD model can be used in further parametrical studies with focus on investigation of indoor climate in different scenarios with various boundary conditions.

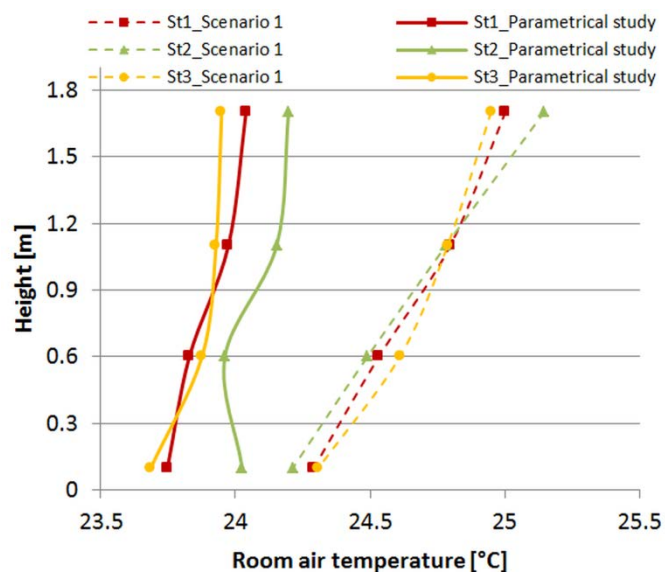


Figure 13: Comparison of temperatures from two different CFD calculations

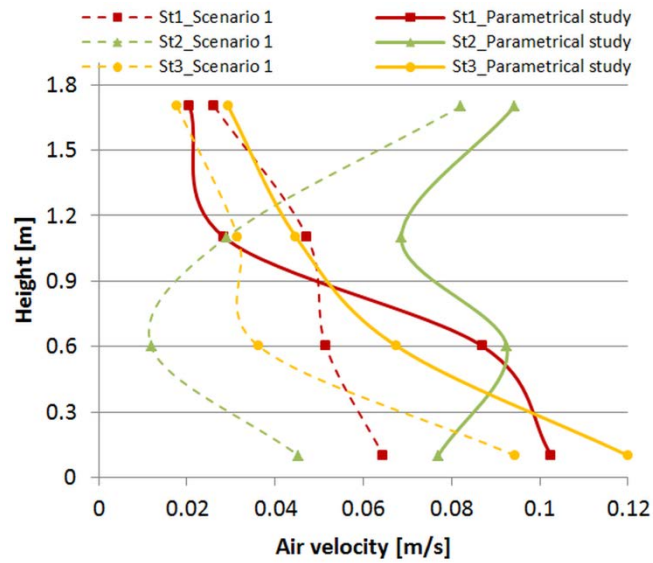


Figure 14: Comparison of velocities from two different CFD calculations

4. Conclusion

Experimental and numerical investigations were carried out in real test room placed in an outdoor environment. Results of our investigations have shown that diffuse ceiling inlet is a suitable solution for the spaces with high density occupancy. The diffuse ceiling inlet can therefore be considered as well performing alternative to the traditional means of mechanical ventilation for air change rate of $6.6 \text{ h}^{-1} - 9.1 \text{ h}^{-1}$. The room was cooled by outside air by $23 - 30 \text{ W/m}^2$ without draught problem due to high speed of air and low temperature. The velocities of air in the room were reasonably low throughout the whole investigated space. The special attention should be paid to areas close to the floor, where highest velocities were experienced in measured and also calculated results. The tracer-gas investigations have shown that the air in the room is mixed with average ventilation effectiveness of 84 %. The authors recommend the use of transient equations for CFD investigations of air flow in the room.

Acknowledgement

This research came to existence thanks to kind sponsorship of companies Airmaster[®], Knauf Danoline[®], and Connovate A/S. We were able to do thorough numerical investigations thanks to the high performance computing platform kindly provided by Beijing Computing Center.

References

- [1] EPDB, Energy Performance of Building Directive, European Union, http://europa.eu/legislation_summaries/other/l27042_en.htm
- [2] LOMBARD, P., L., ORTIZ, J., POUTCH, A review on buildings consumption information, *Energy and Buildings* 40 (2008). pp. 394–398.
- [3] Shaughnessy, R. J., Haverinen-Shaughnessy U., Nevalainen A., Moschandreas D., 2006. A preliminary study on the association between ventilation rates in classrooms and student performance. *Indoor Air*, 16, 465–468.
- [4] Seppanen O.A., Fisk W.J., Mendell M.J., Association of Ventilation Rates and CO₂ Concentrations with Health and Other Responses in Commercial and Institutional Buildings, *Indoor Air* 1999;9:226-252; ISSN 0905-6947
- [5] Wyon, D. P., 2004. The effects of indoor air quality on performance and productivity. *Indoor Air*, 14 (Suppl. 7), 92–101.
- [6] Wargocki, P., Wyon, D. P., 2013. Providing better thermal and air quality conditions in school classrooms would be cost-effective. *Building and Environment*, 59, 581-589.
- [7] Hviid^{a,b} Ch. A., Svendsen^b S., Experimental and numerical analysis of perforated suspended ceilings as diffuse ventilation air inlets, *Energy and Buildings* 56(2013) 160-168
- [8] Hviid Ch.A., Terkildsen S., Experimental study of diffuse ceiling ventilation in a classroom, Technical University of Denmark, *Corresponding author: sterk@byg.dtu.dk*
- [9] Jacobsen L., Air Motion and Thermal Environment in Pig Housing Facilities with Diffuse Inlet, Aalborg University Department of Civil Engineering Architectural Engineering, December 2006, Phd thesis
- [10] Jensen, J. L., *Experimental and numerical analysis of the cooling potential with diffuse ceiling ventilation*. Thesis (MSc). Technical University of Denmark, 2012
- [11] Yang H., Experimental and numerical analysis of diffuse ceiling ventilation, M.Sc. thesis, Department of Civil Engineering, Technical University of Denmark, (2011)
- [12] Nielsen¹ P.V., Jakubowska² E., The Performance of Diffuse Ceiling Inlet and other Room Air Distribution Systems, Corresponding email: pvn@civil.aau.dk

- [13] Information provided by Erik Bjørn, Ph.D, who is R&D Manager in company Airmaster A/S producing ventilation unit, www.airmaster.dk
- [14] European Committee for Standardization, 2007. EN 15251:2007. Indoor environmental input parameters for design and assessment of buildings addressing indoor air quality, thermal environment, lighting and acoustics.
- [15] International Organization for Standardization, 2005. EN ISO 7730:2005. Ergonomics of the thermal environment: Analytical determination and interpretation of thermal comfort using calculation of the PMV and PPD indices and local thermal comfort criteria.
- [16] Heller, A., 2000. Large-Scale Solar Heating – Evaluation, Modelling and Designing. Thesis (PhD). Technical University of Denmark.
- [17] <http://www.onsetcomp.com/products/data-loggers/u12-012>
- [18] http://www.sensor-electronic.pl/pdf/KAT_AirDistSys5000.pdf [Last accessed: 19th April 2014].
- [19] <http://www.lumasenseinc.com/> [Last accessed: 19th April 2014].
- [20] Han H., Ventilation Effectiveness Measurements Using Tracer Gas Technique, Fluid Dynamics, Computational Modeling and Applications, 2012, Dr. L. Hector Juarez (Ed.), ISBN: 978-953-51-0052-2, InTech.
- [21] <http://ansys.com/Products/Simulation+Technology/Fluid+Dynamics/Fluid+Dynamics+Products/ANSYS+Fluent> [Last accessed: 19th April 2014].
- [22] Nielsen P., Allard F., Awbi H., Davidson L., Schalin A., Computational Fluid Dynamics in Ventilation Design, Rehva Guidebook no.10, 2007, page 48
- [23] SDS-Infrared®. *Hot-Find D*. [Online.] Available from: http://www.emtamericas.com/pdf/Satir_Hotfind.pdf [Last accessed: 19th April 2014].

Paper II

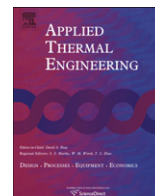
Study of thermal performance of capillary micro tubes integrated into the building sandwich element made of high performance concrete

Mikeska T., Svendsen S.

Published in Applied Thermal Engineering (2013)

Contents lists available at [SciVerse ScienceDirect](http://www.sciencedirect.com)

Applied Thermal Engineering

journal homepage: www.elsevier.com/locate/apthermeng

Study of thermal performance of capillary micro tubes integrated into the building sandwich element made of high performance concrete



Tomas Mikeska*, Svend Svendsen

Department of Civil Engineering, Technical University of Denmark, Brovej, Building 118, DK-2800 Kgs. Lyngby, Denmark

HIGHLIGHTS

- ▶ A temperature distribution around the integrated tubes was studied.
- ▶ Different thickness of concrete plate and distance of the pipes investigated.
- ▶ Capillary micro tubes can supply sufficient amount of energy for heating (cooling).
- ▶ Temperature on the inner surface of the HPC element is evenly distributed.

ARTICLE INFO

Article history:

Received 1 August 2012

Accepted 15 December 2012

Available online 8 January 2013

Keywords:

Capillary micro tube

Radiant surface heating and cooling systems

High performance concrete

Thermal performance

ABSTRACT

The thermal performance of radiant heating and cooling systems (RHCS) composed of capillary micro tubes (CMT) integrated into the inner plate of sandwich elements made of high performance concrete (HPC) was investigated in the article. Temperature distribution in HPC elements around integrated CMT was studied. Thermal heat flux on the inner surface of HPC element, and the increase of heat losses to the outside environment were carefully investigated. Calculations were carried out for different temperatures of the circulating fluid, different spacing between CMT and different thicknesses of the inner HPC layer covering the CMT. This paper shows that CMT integrated into the thin plate of sandwich element made of HPC can supply the energy needed for heating (cooling) and at the same time create the comfortable and healthy environment for the occupants. This solution is very suitable for heating and cooling purposes of future low energy buildings. The investigations were conceived as a low temperature concept, where the difference between the temperature of circulating fluid and air in the room was kept in range of 1–4 °C.

© 2013 Elsevier Ltd. All rights reserved.

1. Introduction

Energy use in the building sector must be reduced in most European countries to approximately 20 kWh/m²/year by the year 2020 [1]. Buildings with low energy use can be built by use of highly insulated building envelopes, high performance windows, high performance heating and cooling systems, and ventilation systems with heat recovery. This applies to residential, commercial and also industrial buildings. The highly insulated sandwich panels of high performance concrete (HPC) offer good thermal insulation with a minimum of thickness of walls as the concrete plates are only 2–5 cm thick. New concepts of integrated heating and cooling systems need to be developed to allow a full prefabrication of HPC

elements and provide the required indoor environment in an optimal way. New concept of radiant heating and cooling systems (RHCS) could be based on capillary micro tubes (CMT) cast in the inner concrete plate of HPC element.

The authors believe that low quality heat sources such as solar heat, waste heat and geothermal heat can supply energy to future buildings in a safe, sustainable, and environmentally-friendly way. The secure supply of energy is an important issue. The production and distribution of most of the world's energy are controlled by a small group of people nowadays. Scarcity of energy can have serious repercussions for mankind, and can lead to conflict when demand exceeds supply. Therefore, it is in the interest of all countries in the world to investigate the proper use of alternative, sustainable energy sources. As one of the largest global consumers of energy, efficient energy use is a serious concern for the building sector.

Several RHCS, integrating pipes, ducts or electric cables in different building constructions, are available [2,3]. This article deals

* Corresponding author. Tel.: +45 27338619.

E-mail address: tommi@byg.dtu.dk (T. Mikeska).

Nomenclature	
c	specific heat capacity [J/kg K]
C	volumetric specific heat capacity [MJ/K m ³]
d	outer diameter of the pipe [m]
d_i	thickness of the pipe wall [m]
D	size of approximated square in HEAT2 [m]
g	gravitational acceleration [m/s ²]
G_r	Grashof number [–]
h	convective heat transfer coefficient [W/m ² K]
h_{surf}	convective heat transfer coefficient from fluid to surface of CMT [W/m ² K]
h_{wall}	convective heat transfer coefficient for the wall [W/m ² K]
L_c	characteristic length of geometry [m]
N_{Nu}	Nusselt number [–]
r	outer radius of the pipe [W/m ² K]
R_c	total thermal resistance of CMT calculated in HEAT2 [m ² K/W]
R_{in}	total thermal resistance for surface facing inside [m ² K/W]
R_{pipe}	total thermal resistance of the wall of the CMT [m ² K/W]
R_{surf}	total thermal resistance between fluid and inner surface of CMT [m ² K/W]
R_{out}	total thermal resistance for surface facing outside [m ² K/W]
T_{air}	temperature of air [°C]
β	coefficient of volume expansion [1/K]
λ_{water}	thermal conductivity of water at 22 °C [W/m K]
λ_i	thermal conductivity of pipe wall material [W/m K]
λ	average thermal conductivity of fluid and air [W/m K]
ρ	density of the material [kg/m ³]
ν	kinematic viscosity of the fluid [m ² /s]

with water based RHCS using thin tubes (diameter of 2–4 mm) to hold the heating or cooling fluid.

RHCS can operate with low temperature differences between the fluid circulating in the pipe and air in the room. Systems running with low temperature differences can regulate the power output from RHCS, a kind of passive control system. This passive control takes place without the installation of an additional controlling system, which means that self regulation is independent of the equipment used for active control system. When there is a small decrease in room temperature, there is a corresponding decrease of the heat transfer from the surface to the room. Conversely, when there is an increase in room temperature, the corresponding heat flux increases as well.

When using RHCS in buildings, the comfort of the occupants can be achieved at a lower room temperature compared to the use of convective systems (in the case of heating). This means that energy can be saved on heat losses for ventilation and on transmission losses. Similarly, the cooling can operate with higher air temperature in the room, resulting in lower energy consumption.

The uniform thermal environment is established in the designed space when using RHCS due to the radiant heat exchange between the activated surface and surrounding surfaces in the room. As a result, there is improved comfort for occupants. When properly designed, the RHCS do not cause any draughts and do not produce any noise, which is often the case when using air-convective systems. RHCS can also add to the aesthetic value of buildings as they do not disrupt the designed space and therefore increase the architectural value of the building construction.

The heat loss of the building element using RHCS could be higher than the element without integrated RHCS, since the inner surface of an HPC element has a higher temperature during activation. The increased heat loss could be a limiting factor for design of RHCS, so it needs to be carefully investigated.

To date, there has been little research into the use of very thin tubes in RHCS. As far as heat transfer is concerned, the systems utilizing CMT could behave differently compared to systems using pipes with a bigger diameter. The overall thermal performance of RHCS technology using CMT needs to be investigated.

2. Background

When RHCS are used in a building, different modes of heat transfer occur. Among the main heat transfer principles is the radiation. The radiant surface does not directly heat the air in the room, rather it heats the surrounding surfaces and solid objects in

the room which then indirectly heat up the air in the room [4]. In the case of floor heating, the radiant portion could vary between 60 and 80% of the overall heat transfer coefficient, depending on the temperature difference between the floor surface and the air in the room [5]. While the radiation is the main heat transfer mechanism in RHCS, the heat convection and conduction are also present. The heat convection coefficient is not easy to define since there are many variables influencing this value [4]. The heat conduction takes place only on a very limited area between the surface and the thermal boundary layer [4].

The heating and cooling capacity of the RHCS depends on many aspects, such as the total heat transfer coefficient between the surface of the investigated element and the air in the room, the emissivity of different surfaces in the room, the view angle between the surfaces and the occupant, and the spacing between the tubes. Furthermore, the thermal resistance between the fluid circulating in the pipe and the surface of the investigated element influences the heating and cooling capacity of RHCS. This resistance depends on the flow type of the fluid circulating in the pipe and on roughness of the inner surface of the pipe. The presence of forced convection in the room strongly influences the heating and cooling capacity of RHCS.

3. Materials and methods

3.1. Model of the HPC element

A small section of the HPC element was chosen for investigation in the program HEAT2 [6]. The element was composed of two plates of HPC with the insulation material placed in between. Fig. 1 shows the investigated section of the HPC element. The dimensions of the HPC element were as follows (from exterior to interior): HPC layer – 20 mm, polystyrene insulation – 250 mm, HPC layer – 30 mm. The CMT were placed in the middle of the inner HPC plate, as can be seen from Fig. 1, showing the slice of a vertical wall. The properties of the materials used in the investigations are given in Table 1.

3.2. Capillary micro tubes

The CMT are assembled into the capillary mats, see Fig. 2. The capillary mats are composed of two main manifold pipes and the CMT itself. The investigated CMT are circular shape with an outer diameter of 3.5 mm, an inner diameter of 2 mm, resulting in a wall thickness of 0.75 mm. The CMT run in parallel and with a small distance between each tube, which creates evenly distributed

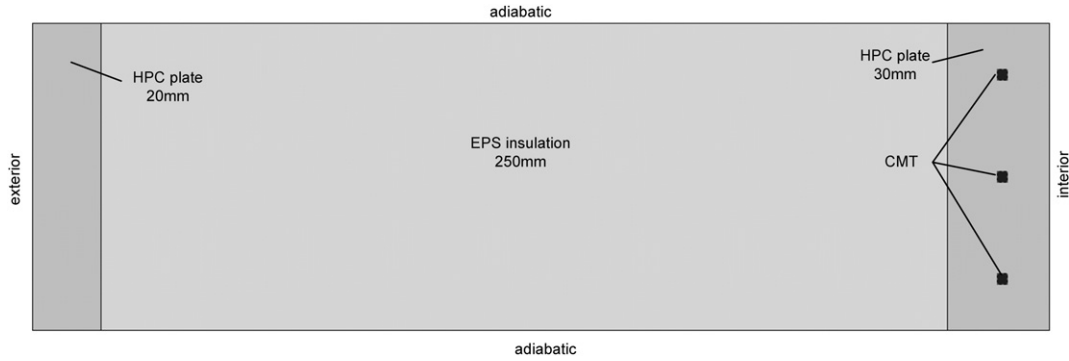


Fig. 1. Section of HPC vertical wall element built in program HEAT2.

temperature in the HPC element. The mat with CMT is a way of implementing RHCS into the surfaces where only a thin layer of construction is available, which is the case with the HPC elements. Because of the relatively small size of the CMT, construction can be activated much quicker compared to RHCS using pipes with the bigger diameter. The solution is very suitable for a construction made of the HPC since the thickness of the concrete layer where the pipes are to be installed is only 30 mm. Therefore it would not be even possible to install RHCS with bigger diameter pipes, for example pipes made of cross-linked polyethylene (PEX), which have usually outer diameter of 11–18 mm.

3.3. Calculations

HEAT2 is a program designed to perform two-dimensional steady-state and transient heat transfer calculations. The program uses the method of explicit finite differences to solve the heat conduction equations. The investigated objects can be modeled only in rectangular mesh defined by the user [6].

3.3.1. Modeling of the circular pipe in the program

The program HEAT2 uses a rectangular grid, therefore only rectangular objects can be accurately modeled. However, the different shapes can be approximated to rectangular shape (see Fig. 3). Therefore, the modeled CMT were approximated to a square by the use of Eq. (1) [6]. This equation approximates the circular pipe with a square having the same area as the circular pipe.

$$D = \sqrt{\pi r} \sim 1.77r \quad (1)$$

The r -value [m] is an outer radius of the pipe. The D -value [m] is the size of the approximated square side that is to be used in program HEAT2.

The size of the approximated square side was calculated to be 3.1 mm for an outer diameter of the CMT of 3.5 mm. The outer diameter of the CMT was used because the total resistance of the pipe was assigned to the side of the approximated square. This means that the thermal behavior of the CMT's material was taken into account in the calculations. The total thermal resistance of the

CMT was calculated according to Eq. (2) and assigned to the surface of the approximated square side.

$$R_c = \frac{2D \ln\left(\frac{r}{r-d_i}\right)}{\pi \lambda_i} \quad (2)$$

The approximation of the circular pipe to the square is shown in Fig. 3 including the values used in Eq. (2).

Eq. (2) takes originally into account only the resistance of the wall of the pipe (R_{pipe}). This paper attempts to also include in this equation the resistance between the fluid and surface of the tube wall (R_{surf}).

To find the value of the R_{surf} , the dimensionless number for convective heat transfer coefficient N_u was used [4]. Eq. (3) was used for obtaining the convective heat transfer coefficient from the fluid to the inner surface of the CMT, assuming fully developed laminar flow.

$$N_u = \frac{h_{\text{surf}} d}{\lambda_{\text{water}}} = 3.66 \quad (3)$$

The d -value is diameter of the pipe [m].

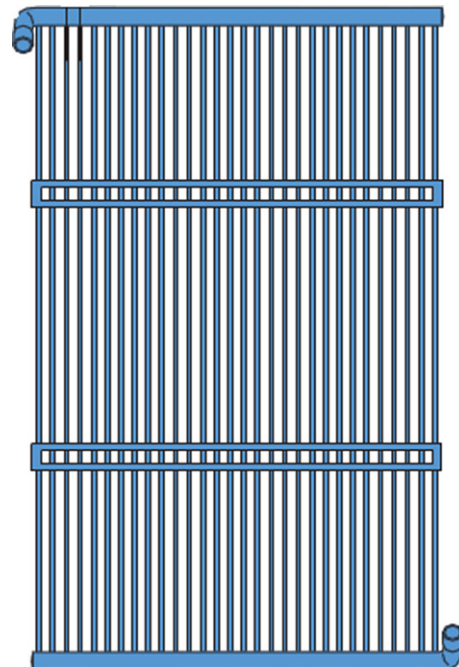


Fig. 2. CMT mat.

Table 1
Properties of materials used in HPC element.

Material	λ [W/m K]	c [J/kg K]	ρ [kg/m ³]	C [MJ/K m ³]
High performance concrete	1.9	1020	2320	2.3664
EPS_expanded polystyrene	0.035	1270	35	0.04445
Water	0.6	4182	998	4174
PP_polypropylene	0.15	1800	930	1674

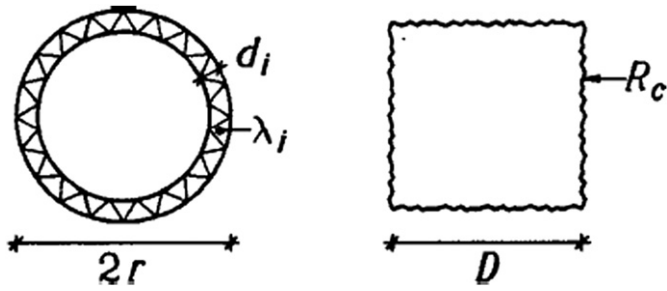


Fig. 3. Approximation of the circular pipe and assigned total heat resistance of the pipe.

The calculations were done with water as the circulating fluid working at a temperature of 22 °C and corresponding thermal conductivity of 0.602 W/m K. The resulting value of heat transfer coefficient from fluid to the surface of the pipe (h_{surf}) was 630 W/m² K. This yielded value of R_{surf} and by adding it to the value of R_{pipe} , the resulting resistance of the CMT was found. As a next step, the new thermal conductivity coefficient (λ_i) was calculated, which was used in Eq. (2) to get proper total thermal resistance coefficient (R_c), used for calculations in HEAT2. The resulting R_c of the CMT was calculated to be 0.0021 m² K/W. This number was then used as the internal resistance of the approximated square side in HEAT2 program.

3.3.2. Energy input assigned to the CMT

The energy input to the CMT was assigned as a heat source with constant temperature of the fluid. The heat flow from the CMT depended on its total heat transfer resistance. Properly assigned properties of the water together with the precise value of the total heat resistance coefficient were presumptions for correct results of further calculations.

3.4. Boundary conditions

The boundary conditions assigned in the HEAT2 program can be seen in Fig. 1. The boundaries on the bottom and the top side were assigned as adiabatic in order to avoid any influence of the resting part of the construction on the calculations. The adiabatic condition ensured that no heat flow would go through those boundaries in any direction. The boundary at the interior side was specified with an air temperature, $T_{\text{in-heating}} = 20$ °C and $T_{\text{in-cooling}} = 26$ °C, and total heat transfer resistance, R_{in} . The value of 0.13 W/m² K for R_{in} is taken by engineers as a reference number for general calculations of heat losses through the vertical wall construction. In this work, however, the objective was to get a more detailed value since it can substantially influence the results of the heat flux on the inner surface. In this total heat transfer coefficient, all three mechanisms of heat transfer, which are radiation, convection and conduction are included. In the case of internal surfaces, the radiation has a dominant influence. According to standard, the value of 5.5 W/m² K is appropriate to use for a radiant heat transfer coefficient as a fixed value in the range of room air temperature between 15 and 30 °C [7]. To get the convective part of the heat transfer coefficient is more complicated. This is because convective heat transfer is influenced by many variables, such as temperature of the air in the room and of the surface, velocity of the air, roughness of the surface etc. [4]. Most of the values for convective heat transfer coefficient stated in the literature were obtained from experimental investigations. However, the results of those investigations differ substantially. Many authors developed the empirical equations for a calculation of convective heat transfer coefficient as a result of their investigations [8–14]. One of the most relevant works was

carried out by Awbi and Hatton [8]. The Nusselt number in this paper was calculated according to Eq. (4), taken from authors Awbi and Hatton [8]. The Grashof number obtained by use of Eq. (5) was calculated using the temperature of the surface of the wall, $T_{\text{surf}} = 22$ °C, and the temperature of the air, $T_{\text{air}} = 20$ °C. As characteristic length, L_c , the height of the room was used, which was assumed to be 2.6 m.

$$Nu = 0.289Gr^{0.293} \quad (4)$$

$$Gr = \frac{g\beta(T_{\text{surf}} - T_{\text{air}})L_c^3}{\nu^2} \quad (5)$$

The convective heat transfer coefficient of the wall was then calculated from Eq. (6) using the non-dimensional Nusselt number.

$$Nu = \frac{h_{\text{wall}}L_c}{\lambda} \quad (6)$$

The resulting value of Nu was 202. This yielded h_{wall} of 1.95 W/m² K. The total heat transfer coefficient was 7.45 W/m² K. The resistance of the inner surface of the wall was then 0.134 m² K/W.

The assumption in this project was that the floor would be used for heating purposes and ceiling for cooling purposes. This means that the R_{in} value was set to the same level for both surfaces [7].

$$Nu = 0.269Gr^{0.308} \quad (7)$$

The convective heat transfer coefficient for floor (ceiling) was then calculated from Eq. (7), taken from authors Awbi and Hatton [8]. The resulting value of Nu for floor heating (ceiling cooling) was 262. This yielded $h_{\text{floor/ceiling}}$ of 2.54 W/m² K. The total heat transfer coefficient of floor (ceiling) was 8.04 W/m² K. The resulting value of R_{in} for the floor (ceiling) construction was 0.124 W/m² K.

The boundary condition for the outdoor environment was set to the value of the outdoor air temperature, $T_{\text{out-heating}} = 0$ °C and $T_{\text{out-cooling}} = 20$ °C, and total heat transfer resistance for surfaces facing outside, $R_{\text{out}} = 0.04$ W/m² K. Wind has a strong influence on the heat transfer coefficient for the surfaces facing to the outside environment. In this case of heat transfer coefficient, the convection mechanism becomes dominant. The radiant heat transfer mechanism is influenced by the sky temperature and temperature of enclosure.

3.5. Variables

The targeted value for heat flux to indoor environment was set to 10 W/m² K. This value was chosen as a reference so we could compare the system to other radiant heating systems. For example, one of the most often used radiant heating systems is composed of plastic PEX pipes (cross-linked polyethylene) cast into the floor construction. The value of 10 W/m² K is the usual design value for the required power of floor heating in passive houses. The required energy output of the system depends on the type of building and its location. The variables influencing the design of RHCS are heat loss of the building (including heat loss through constructions and ventilation heat loss), comfort issues (temperature of the surface, draught etc.), surface area available for installation of the RHCS and required reaction time of the system. Therefore the different scenarios were investigated in order to assess the performance of the system under different circumstances.

Four different configurations of the CMT mats were prepared for the investigations. The differences were in distance between the CMT embedded in the HPC layer, which were set to 30, 50, 70 and 100 mm.

Other variables during the investigations were the diameter of the CMT (increased from 3.5 to 4.5 mm) and thickness of the inner HPC layer. The originally investigated 30 mm thick layer was increased to the 50 mm in some calculations.

3.6. Sensitivity analysis of thermal conductivity

The exact thermal conductivity of HPC was not known during the investigation. Compared to regular concrete, special additional compounds were inserted into the HPC to improve its performance. Therefore it could be assumed that the thermal properties would differ to a certain degree from regular concrete. In order to find out how the change in λ -value has influenced overall thermal performance of the element made of HPC, sensitivity analyses were carried out.

According to the standard, the thermal conductivity of regular concrete is around 1.9 W/m K [15]. This value was set according to the density of the concrete. The measured value for density of HPC is 2350 kg/m³. The λ -value sensitivity analyses were carried out for different configurations of the CMT. The λ -values used for investigations were set to 1.3; 1.6; 1.9; 2.2 and 2.5 W/m K. The idea was to create a range of λ -values around the assumed average value of 1.9 W/m K to see how the results of the heat flux calculations change for different λ -values.

4. Results and analysis

4.1. Temperature distribution on inner surface of the HPC wall element

The distribution of the temperature in the inner plate of the HPC wall element can be seen in Fig. 4. The four different configurations of CMT are presented with the distance of CMT of 30, 50, 70 and 100 mm. The presented results were obtained from the HEAT2 software after steady-state conditions were reached. On the left side

of Fig. 4, the results for the heating case and on the right side for the cooling case are shown. The temperature scale in Fig. 4 was set the same for all the configurations of the CMT so that comparisons can be made. The CMT with an outer diameter of 3.5 mm were investigated.

Table 2 shows the differences between maximum and minimum temperature on the inner surface over the whole area of the HPC wall element.

The results showed that the distribution of the heat in the inner plate of the HPC element is sufficient to keep the temperature evenly distributed over the whole inner surface of the HPC element. This could be caused by rather small distances between the CMT and by rather high thermal conductivity of HPC.

4.2. Heat flux distribution on inner surface of the HPC element

4.2.1. HPC wall element

Fig. 5 shows the heat flux distribution in the inner plate of the HPC wall element for four different configurations of the CMT. Just as in the temperature profile the heat flux on the inner surface is very uniform over the whole activated area of the HPC wall element. The heating case is shown on the left side of Fig. 5 and the cooling case on the right side.

The different variations of CMT were prepared for purposes of further investigations. The first variation was the increase of outer diameter of the CMT to 4.5 mm. The second variation was the increase of thickness of the inner plate of the HPC wall element to 50 mm. The results of the investigation can be seen on Figs. 6 and 7, which show how different variations of CMT influence the heat flux on inner surface of HPC wall for different configurations of the CMT, for heating and cooling periods respectively.

4.2.2. HPC floor/ceiling element

Investigations were also made for the floor element used for heating mode and ceiling element used for cooling mode. The investigations were done on elements with the same dimensions and

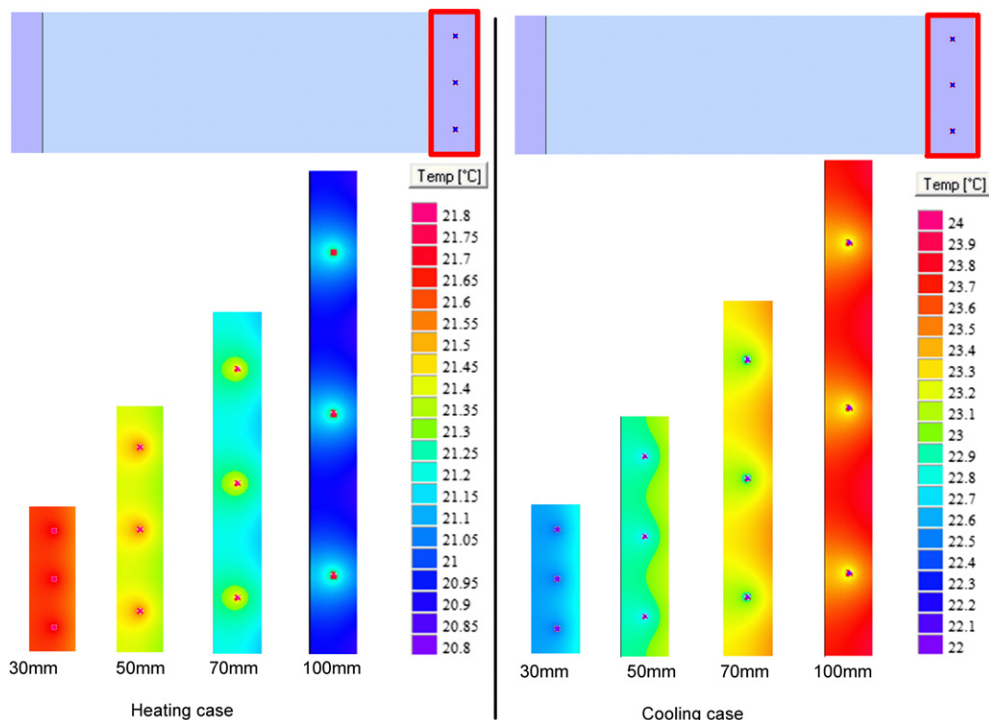


Fig. 4. Temperature distribution in the inner plate of the HPC wall element for heating and cooling cases.

Table 2

Differences between maximum and minimum temperature over inner surface of HPC element.

Max. temperature difference over the surface of HPC wall element [°C]						
Distance of CMT [mm]	Heating [°C]			Cooling [°C]		
	21	22	24	18	21	22
30	0.006	0.01	0.018	0.031	0.02	0.016
50	0.024	0.042	0.076	0.136	0.085	0.067
70	0.055	0.06	0.173	0.31	0.216	0.152
100	0.11	0.125	0.347	0.622	0.385	0.306

composition as in the case of the wall elements. However, different convective heat transfer coefficients were assigned to those constructions. The variations used during calculations were the same as in the case of the wall elements (see Section 4.2.1). The results can be seen in Figs. 8 and 9.

4.3. Heat flux distribution to outer surface of the HPC wall element

The increase of heat transfer to the outer part of the wall element can be expected with the growing temperature of the inner surface. As a result, the heat loss of the HPC element with integrated CMT is higher compared to the HPC element without any integrated CMT. Figs. 10 and 11 show the heat flux of the HPC element to the outside environment for the heating and cooling cases, respectively. Increase of heat flux in comparison to the situation when no RHCS is activated can be seen in Fig. 12.

4.4. Sensitivity analysis of thermal conductivity

From Table 3 it can be seen that the results of the heat flux differ with the changing thermal conductivity of HPC. How much the λ -

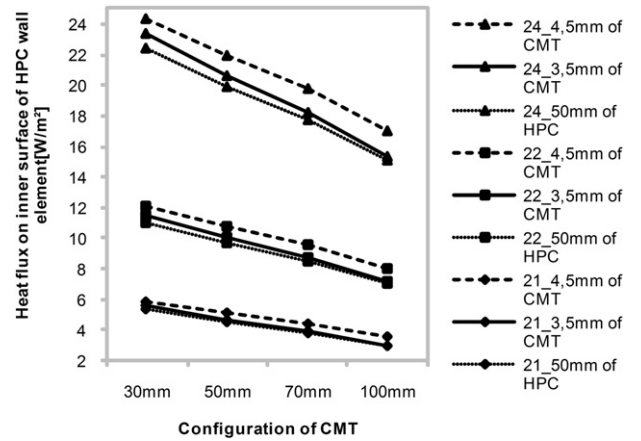


Fig. 6. Heat flux to indoor environment from HPC wall element for different variations – heating case.

value influences the results depends on the configuration of the CMT in the HPC plate. There is a relation between distance of the CMT in the HPC plate and heat flux on the surface. The influence of λ -value gets more important with the increase of distance between CMT. For a visual presentation of the relationship, see Fig. 13.

5. Discussion

The aim of the research was to investigate how RHCS with various configurations of CMT behave under different operational conditions. In this way, the variables with strongest influence on the performance can be identified. These findings can be used for the future design of the RHCS using CMT integrated into the

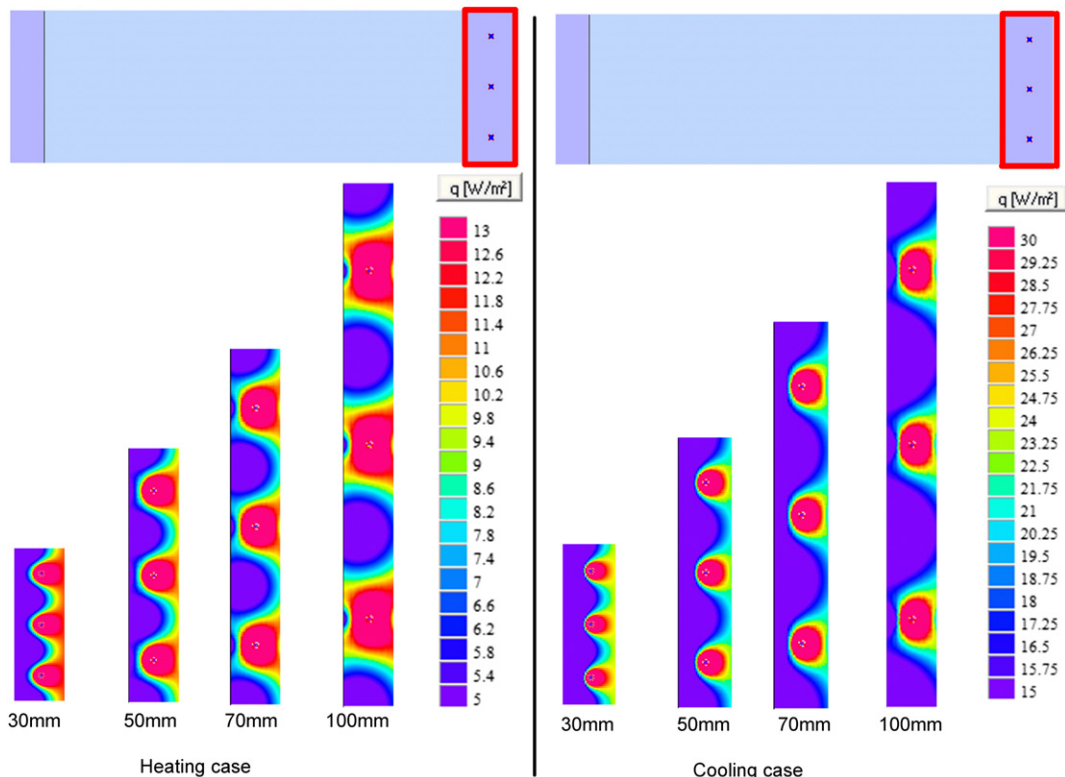


Fig. 5. Heat flux distribution in the inner plate of HPC wall element for heating and cooling cases.

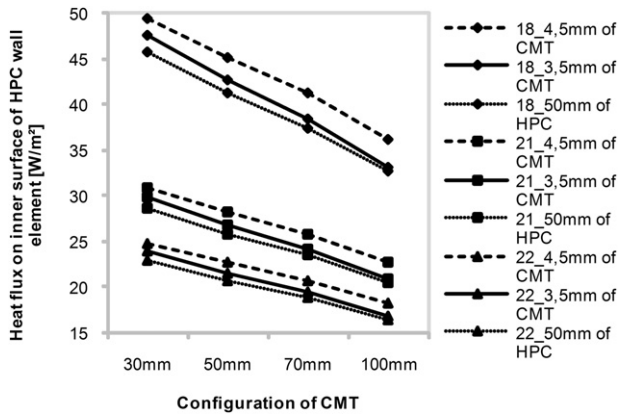


Fig. 7. Heat flux to indoor environment from HPC wall element for different variations – cooling case.

elements of building constructions. The suitability of this solution for use in very low energy buildings can be discussed.

5.1. Temperature distribution in the HPC element

The results of the investigations showed that the temperature on the inner surface of the HPC element was evenly distributed. This was an important finding since occupants feel less comfortable when exposed to large differences in surface temperature. An evenly distributed temperature is the main precondition for creating a comfortable indoor climate.

5.2. Heat flux distribution in the HPC element

The heat flux from the HPC element depends mainly on the temperature of the circulating fluid as can be seen from Figs. 6 and 7. The heat flux during the heating period can be doubled by increasing the temperature of circulating fluid by only about 2 °C. Similarly during the cooling period the heat removed from the room can be increased to 60% by decreasing the temperature of circulating fluid by about 3 °C. The main idea behind this project is however to keep the temperature difference between the

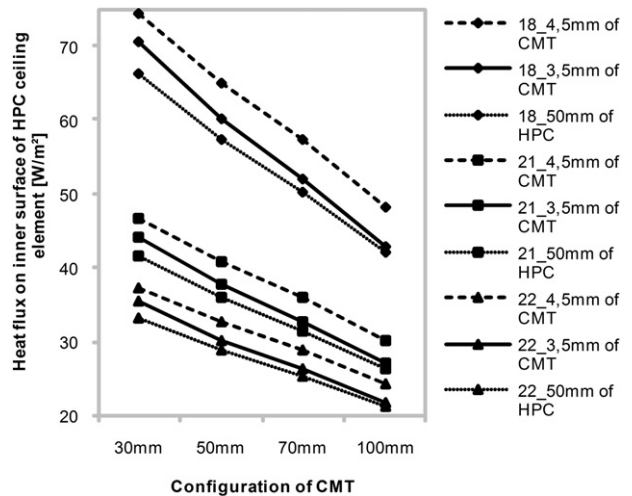


Fig. 9. Heat flux to indoor environment from HPC ceiling element for different variations – cooling case.

circulating fluid and air in the room as low as possible. Therefore the focus should be on different ways of increasing the heat flux from the HPC elements. Alternative solutions include smaller spacing between the CMT and increasing the diameter of the CMT. The spacing and diameter of CMT have a significant effect on the heat flux from the HPC element. However, the effect is far lower than a change in temperature. A change in distance between CMT seems to be a more suitable and feasible option of how to influence the heat flux. However, a bigger diameter of CMT can be beneficial regarding the clogging of the system with impurities. Both of those solutions, compared to a change in temperature of the circulating fluid, include the changes in the settings of production lines for CMT and therefore must be considered and investigated in the early stages of the project. The values of the heat flux are generally higher for floor heating and ceiling cooling in comparison to the wall element. This is caused by higher convective heat transfer coefficient.

The heat flux decrease with increasing thickness of the HPC layer is shown in Fig. 6. This is caused by increased thermal resistance between CMT and the inner surface of HPC element. The differences are however rather small and should not particularly influence the design of RHCS integrating the CMT. Therefore it can

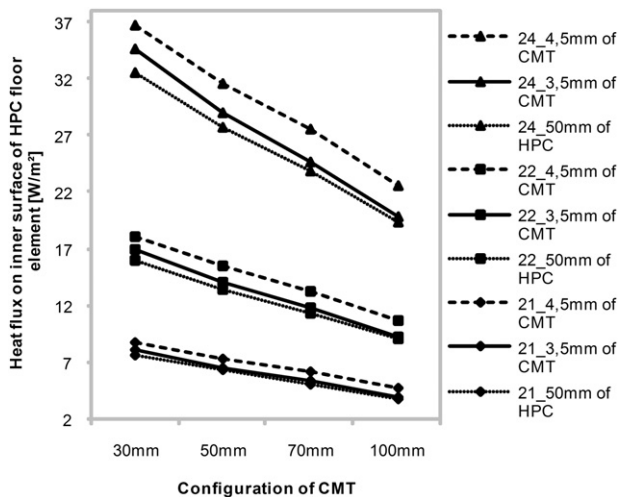


Fig. 8. Heat flux to indoor environment from HPC floor element for different variations – heating case.

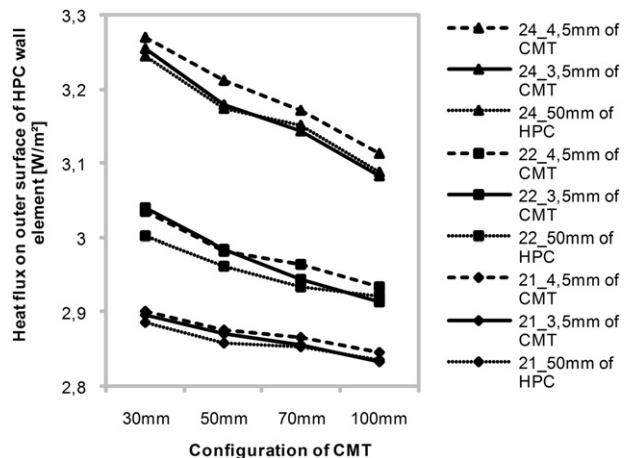


Fig. 10. Heat flux to outdoor environment from HPC wall element for different variations – heating case.

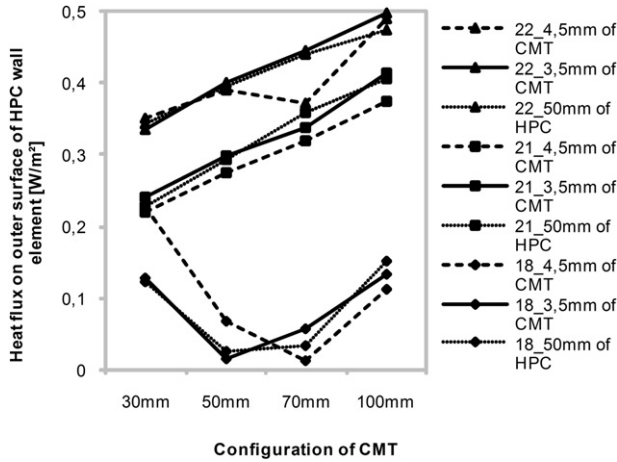


Fig. 11. Heat flux to outdoor environment from HPC wall element for different variations – cooling case.

be assumed that the thickness of the HPC layer is not going to be a limiting factor during the design of RHCS in the HPC elements.

5.3. Heat flux distribution to outer surface of the HPC wall element

All the configurations with the CMT are compared to the situation when no CMT are implemented. The reason for this was to measure the increased heat loss to the outside environment. The finding is that the result is quite substantial. In Fig. 12, the resulting increase in percentage is shown. The difference in heat loss between configuration with no heating tubes and configuration with a heat flux of 10 W/m² K (on the inner surface of HPC element) is about 10%. Just as with the heat flux to the interior, the heat flux to the exterior environment increases with increasing temperature of the circulating fluid in the CMT. The increase of the heat loss can go up by 20% for a temperature of circulating fluid of 24 °C. This is a rather high number and must be taken into account during the design of the element and a whole building. On the other hand, the heat loss through the wall elements is just a fraction of the overall heat losses of the building. Other heat losses include heat losses of roof, floor and window elements and also heat losses from ventilation system. Even though an increase of the heat loss by 20% can seem rather high, in the overall evaluation of the energy performance of the whole building the effect is actually rather small.

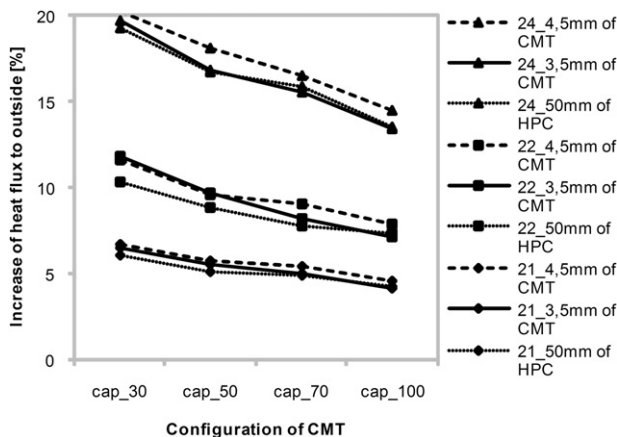


Fig. 12. Difference in heat flux to outer part of the HPC wall element expressed in percentage.

Table 3

Heat flux on inner surface of the investigated HPC wall element for different values of thermal conductivity of HPC.

λ -Value sensitivity analyses [W/m ²]						
Configuration	Pipe spacing mm	λ -Value (W/m K)				
		1.3	1.6	1.9	2.2	2.5
HPC 30 mm plate	30	11.3	11.5	11.7	11.8	11.9
HPC 30 mm plate	50	9.8	10.0	10.2	10.3	10.4
HPC 30 mm plate	70	8.5	8.8	9.0	9.1	9.2
HPC 30 mm plate	100	6.9	7.2	7.4	7.6	7.7

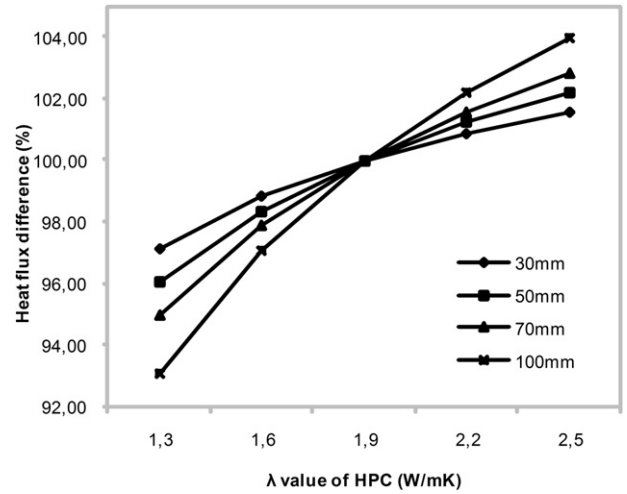


Fig. 13. Percentage differences in heat flux on inner surface of HPC element for different values of λ .

To investigate overall energy performance of the building, the dynamic calculations were carried out in the program IDA ICE [16]. The increase in heat demand was found to be 2.6% for the investigated case. This could be assumed as mild increase. When considering the use of the RHCS integrated in the building elements, one must consider if the small increase in heat demand can be sacrificed for improved indoor climate of the investigated building and advantages coming from usage of low temperature sources of energy.

5.4. Sensitivity analysis of thermal conductivity

As far as the investigation of influence of thermal conductivity of the HPC on the heat flux is concerned, the outcome of the comparison is that a decrease in λ -value of 15% causes the decrease in heat flux on interior side of HPC element by about 1–3%, depending on the actual configuration of the CMT. Similarly when the λ -value is increased by about 15%, the increase in the heat flux is about 2%. The change in heat flux is relatively small in comparison to the change in λ -value. Therefore its deviation is not a cause for concern.

6. Conclusion

The temperature and heat flux distribution from capillary micro tubes through the element made of high performance concrete has been investigated in the paper. Different configurations of the capillary micro tubes were investigated, concerning thickness and distance of the pipes. It can be concluded that a sufficient amount of energy can be supplied to the space in a comfortable and economic way, by means of radiant heating and cooling systems utilizing

capillary micro tubes. Designed heating and cooling systems are very suitable for low temperature concepts and create therefore precondition for use of renewable energy sources for heating and cooling purposes in the buildings.

Conflict of interest

There is no actual or potential conflict of interest including any financial, personal or other relationships with other people or organizations.

References

- [1] EPDB, Energy Performance of Building Directive, European Union. http://europa.eu/legislation_summaries/other/127042_en.htm.
- [2] www.uponor.com, 2012.
- [3] www.fenixgroup.cz, 2012.
- [4] Yunus A. Çengel, Heat Transfer: A Practical Approach, second ed., McGraw-Hill, 2003, ISBN 0072458933 (Chapter 11), p. 562, (Chapters 6 and 9).
- [5] P. Weitzmann, Modelling Building Integrated Heating and Cooling Systems, PhD thesis, Rapport BYG·DTU R-091, 2004, ISSN 1601-2917, ISBN 87-7877-155-2, p. 20.
- [6] T. Blomberg, Heat 2. A PC Program for Heat Transfer in Three Dimensions – Manual with Brief Theory and Examples, Lund-Gothenburg Group for Computational Building Physics, 2000, p. 9, http://www.buildingphysics.com/manuals/HEAT2_5.pdf, p. 113.
- [7] ISO/DIS 11855-2, International Standard, November 2010, p. 6.
- [8] H.B. Awbi, A. Hatton, Natural convection from heated room surfaces, UK, Energy and Buildings 30 (1999) 233–244.
- [9] Hazim B. Awbi, Calculation of convective heat transfer coefficients of room surfaces for natural convection, Energy and Buildings 28 (1998) 219–227.
- [10] E. Dascalaki, M. Santamouris, C.A. Balaras, D.N. Asimakopoulos, Natural convection heat transfer coefficients from vertical and horizontal surfaces for building applications, Energy and Buildings 20 (1994) 243–249.
- [11] L. Peetersa, I. Beausoleil-Morrisonb, A. Novoselacc, Internal convective heat transfer modeling: critical review and discussion of experimentally derived correlations, Energy and Buildings 43 (2011) 2227–2239.
- [12] Abdul-Jabbar N. Khalifa, Natural convective heat transfer coefficient – a review I. Isolated vertical and horizontal surfaces, Energy Conversion and Management 42 (2001) 491–504.
- [13] Petter Wallenten, Convective heat transfer coefficients in a full-scale room with and without furniture, Building and Environment 36 (2001) 743–751.
- [14] Francesco Causone, Stefano P. Corgnati, Marco Filippi, Bjarne W. Olesen, Experimental evaluation of heat transfer coefficients between radiant ceiling and room, Energy and Buildings 41 (2009) 622–628.
- [15] DS418, Calculation of Heat Loss from Buildings, Dansk Standard- Fonden Dansk Standard, 2011.
- [16] www.equa-solutions.co.uk, 2012.

Paper III

Full Scale Measurements and CFD Investigations of a Wall Radiant Cooling System Based on Plastic Capillary Tubes in Thin Concrete Walls

Mikeska T., Jianhua F., Svendsen S.

Accepted with major revision Energy and Buildings (2014)

Full Scale Measurements and CFD Investigations of a Wall Radiant Cooling System Based on Plastic Capillary Tubes in Thin Concrete Walls

Tomas Mikeska, Jianhua Fan, Svend Svendsen*

Department of Civil Engineering, Technical University of Denmark, Brovej, Building 118 DK-2800 Kgs. Lyngby, Denmark

Abstract

Densely occupied spaces such as classrooms can very often have problems with overheating. It can be difficult to cool such spaces by means of a ventilation system without creating draughts and causing discomfort for occupants. The use of a radiant cooling system is a suitable option for spaces with high occupant density. Radiant systems can remove most sensible heat loads resulting in a relatively small requirement for supply air for ventilation.

This paper reports on experimental and numerical investigations of a water-based radiant cooling system that uses plastic capillary tubes cast in a thin layer of high performance concrete to carry a cooling medium. A CFD model of a test room with the radiant cooling system was created. The measured temperatures and air velocities in the test room were used to validate the CFD model, which was then used for parametrical analysis.

The results show that a radiant cooling system based on plastic capillary tubes integrated in a thin layer of high performance concrete can provide energy for cooling between 29 W/m² and 59 W/m² of floor area with cooling water temperatures between 21.5 °C and 18.5 °C, which results in room air temperatures between 25 °C and 22 °C.

*Corresponding author: Tel.: +4527338619, E-mail: tommi@byg.dtu.dk

1. Introduction

A highly insulated sandwich wall element made of high performance concrete is an interesting option for the façades of future low-energy buildings. Its main benefit lies in the use of a concrete with high strength in which a smaller amount of concrete material is used than in traditional concrete elements. The resulting product has a rather thin layer for the load-bearing part of a wall, which leaves more space for thermal insulation. Such a wall element has better thermal performance characteristics than conventional products. The low weight of the element is also beneficial because savings can be made on transport and manipulation on a building site. Elements made of high performance concrete are also rather environmentally friendly, because the low amount of concrete material used also means low CO₂ emissions during their production.

Modern low-energy buildings need to provide good thermal performance and a good indoor environment. This is especially true for educational buildings. However, classrooms very often experience poor indoor climate, as found in various studies [1], [2], [3]. The limited supply air flow and the inability of ventilation systems to handle the high internal heat gains from high-density occupation result in the overheating and overall discomfort associated with “sick building syndrome” [4], [5], [6]. The cooling of densely occupied rooms using a ventilation system can also become challenging because draughts can be created due to the supply of large amounts of cold air. Furthermore, the cooling ability of a ventilation system decreases during the summer because the outdoor air is warmer. An interesting alternative to cooling with outside air is to use cold water from natural sources such as ground or sea water. The best way to make good use of the cooling potential of natural water sources is to use a system which can operate with water temperatures close to room air temperature. Use of renewable sources of energy improves the sustainability of a building and reduces its environmental impact. A radiant cooling system integrated in the inner surfaces of building structures is one promising approach. It can provide a comfortable indoor climate and at the same time improve the aesthetics and architectural value of the building because most of the technical installations are hidden in the building construction. Radiant cooling systems can handle most of the sensible heat gains, and the ventilation system need only be designed to provide the necessary air flow rates for air quality based on relevant standards [7]. Such air flow rates are usually sufficient to remove latent heat loads generated from occupants [8].

Radiant systems are optimal for small temperature differences because large surface areas are usually activated. Radiant systems can have high cooling capacity while maintaining a draught-free indoor environment, which makes them a suitable for spaces with a high density of occupants such as classrooms. Limitations to the cooling capacity could include the acceptable temperature of the cooled surfaces, vertical air temperature, radiant asymmetry, or a dew-point temperature [9]. An increase of comfort in an occupied space is very often experienced when radiant heating and cooling systems are installed because they produce virtually no noise, which is very often the case for fully convective systems [9].

Occupant comfort can be achieved with higher room air temperatures when radiant systems are used for cooling purposes instead of air cooling systems. This is experienced due to a radiant heat exchange which has great impact on the operative temperature and therefore on occupant perception of the thermal environment in a room. A more uniform thermal environment is also achieved because a radiant surface will greatly influence the temperatures of surrounding surfaces in a room, including for example the diffuse ceiling inlet which was used as a supply diffuser for the ventilation system in the research for this paper. The incoming air is then partly pre-cooled and energy otherwise needed to precondition incoming air can be saved. The diffuse ceiling inlet is a concept where the whole area of a suspended ceiling is used as a supply diffuser. Large amounts of air can be therefore supplied into a room with rather small velocities, which decreases the risk of draught. Jacobs *et al.* have carried out investigations with mechanical ventilation equipped with a diffuse ceiling inlet installed in an existing educational building. Two different types of perforated ceiling were investigated and compared with the results of a supply diffuser situated on a façade area. The results showed that the diffuse ceiling ventilation provided an indoor climate with good air quality and thermal comfort without any draught [10]. Hviid *et al.* have investigated the performance of diffuse ceiling inlets installed in an office room and a classroom. Uniform air flow and temperature distribution were experienced without the creation of any draught. Various types of material were tested as the diffuse ceiling inlet [11], [12]. A diffuse ceiling inlet with air tight connections of perforated gypsum boards has been studied by Mikeska [13], resulting in an even supply of fresh air over the whole area of a suspended ceiling.

There have been a few studies dealing with applications of a radiant cooling integrated as part of a building construction. One of them includes a floor cooling installation situated in the highly glassed buildings of Bangkok airport where the floor is exposed to direct solar radiation. Simmonds *et al.* describes the development and

performance of the radiant cooled floor combined with displacement ventilation [14]. The authors concluded that the designed system created a comfortable indoor climate with high thermal stratification. Most other applications of a radiant cooling involve ceiling radiant cooling panels installed in a suspended ceiling [15], [16].

This paper reports on the combined effect of wall radiant cooling and a diffuse ceiling inlet used for ventilation. The water-based radiant cooling system uses thin tubes to carry a cooling medium. The small plastic capillary tubes were cast in the inner layer of a wall element made of high performance concrete. The radiant cooling system described in this paper was designed and produced as an integrated solution and the resulting product is a fully prefabricated wall element with the radiant cooling system ready to provide the required cooling. Our literature review did not reveal any application of plastic capillary tubes cast in a layer of high performance concrete and used for radiant cooling. A simplified CFD model of a room with the radiant cooling system was developed and evaluated by results from measurements. The CFD model was then used for parametrical analysis to investigate various scenarios. This gave us a broader perspective and valuable information on the possibility of using the wall radiant cooling system combined with a diffuse ceiling inlet.

2. Methods of investigation

The performance of the designed and installed wall radiant cooling system and the diffuse ceiling inlet for ventilation was studied under a steady-state situation. The main focus was on an evaluation of the indoor climate in the test room. The investigations were divided into two parts. The experimental measurements were carried out in the full scale test building specifically built for the purpose of testing of prototype technical solutions. The numerical calculations were carried out in the CFD software Ansys Fluent based on a simplified CFD model of the test room with the radiant cooling system. The results from measurements were used partly as boundary conditions for the numerical calculations and partly to assess the usability of the CFD model for further parametrical analysis.

3. Test room and measurements

3.1 Test room

A two-floor, full scale house was built to allow the experimental analysis of the radiant cooling system installed in a test room ventilated using a diffuse ceiling inlet as air terminal device. The walls were built with sandwich elements

consisting of two layers of high performance concrete with thermal insulation in the middle. The internal dimensions of the test room were 6.05 m x 3.25 m giving a floor area 19.66 m². The height of the test room was 2.65 m. Two windows with dimensions of 2.5 m x 1.1 m were installed in the north-western wall giving an overall window area of 5.5 m². The floor and ceiling decks were made of hollow core concrete elements with a thickness of 0.2 m.

3.1.1 Diffuse ceiling inlet

The whole area of a suspended ceiling was made of perforated gypsum boards to create the diffuse ceiling inlet, see Figure 1. The perforations were made with a diameter of 8 mm. The perforated area was 15.5% of the total area of the suspended ceiling. The ventilation unit installed reduced the area of the suspended ceiling to 18.6 m². The test room volume was 52.9 m³.



Figure 1: Diffuse ceiling inlet construction and connection of capillary mats to manifold pipes

3.1.2 Ventilation unit

The suspended ceiling was installed 0.25 m below the ceiling in order to separate the supply and exhaust openings of the ventilation unit, see Figure 2. The supply opening with dimensions 0.8 m x 0.1 m was situated 0.05 m below the ceiling deck. The exhaust opening with dimensions of 0.15 m x 0.1 m was on the side of the ventilation unit and situated just below the perforated suspended ceiling in the test room, see Figure 2.

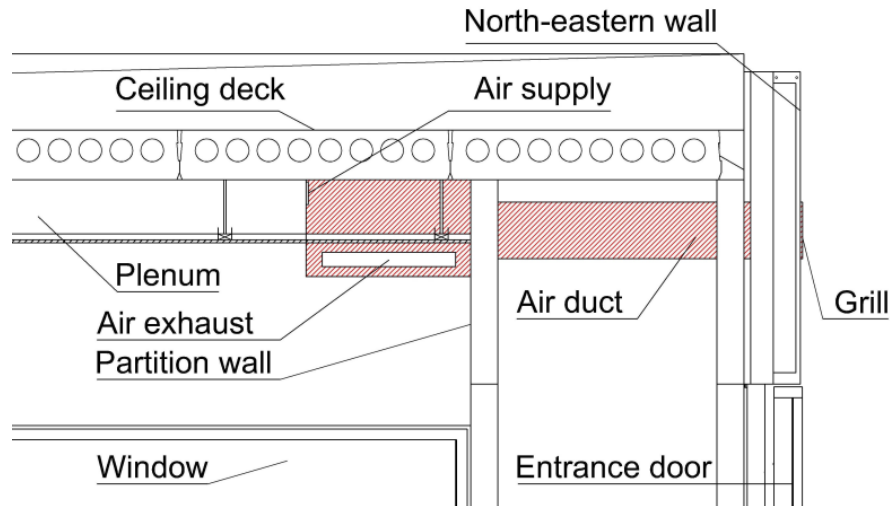


Figure 2: Ventilation unit

3.1.3 Radiant cooling system

The radiant cooling system was based on capillary mats made of polypropylene plastic capillary tubes cast in the inner layer of high performance concrete in the wall sandwich elements. The installation of the radiant systems and casting of the concrete are depicted in Figure 3. Two walls were used for the radiant cooling and are shown by the blue lines in Figure 4. The walls were constructed with sandwich elements made of high performance concrete. The inner layer of concrete was 30 mm thick, the outer layer of concrete was 20 mm thick, and the thermal insulation in the middle was 300 mm thick. The special feature of the radiant system installed is the small dimensions of the plastic capillary tubes. The outer diameter of the capillary tubes was only 4.3 mm and their wall thickness was 0.8 mm giving an inner diameter of 2.7 mm. Such a small dimension allowed the radiant cooling system to be integrated into a layer of high performance concrete only 30 mm thick. The plastic capillary tubes were connected to supply and return plastic tubes with a diameter of 12 mm, creating so-called capillary mats with dimensions of 2.7 m x 1.0 m. Altogether, there were 10 capillary mats providing a total radiant area of 27 m² and containing 4.32 l of cooling water installed in the two walls used for cooling. The capillary mats were connected to the polypropylene manifold pipes by flexible hoses with an outer diameter of 10 mm. The manifold pipes had an outside diameter of 20 mm and were used to run cooling water from the technical room into the plenum, see Figure 1.



Figure 3: Casting of radiant cooling made of capillary mats

3.1.4 Investigated scenario

The investigated scenario represented a densely occupied classroom ventilated by using a diffuse ceiling inlet and conditioned by using a radiant wall cooling system. The 12 occupants were modeled by using metal buckets with light bulbs mounted inside representing heat gains. The overall internal heat gain during the experiment was 1327 W, which was about 110 W per occupant. This included heat gains from the occupants and from equipment such as computers. The positions of the occupants, the furniture and the ventilation unit are shown in Figure 4. The mean temperature of the cooling water was 16.3 °C and the delivered cooling power was measured to be 1112 W.

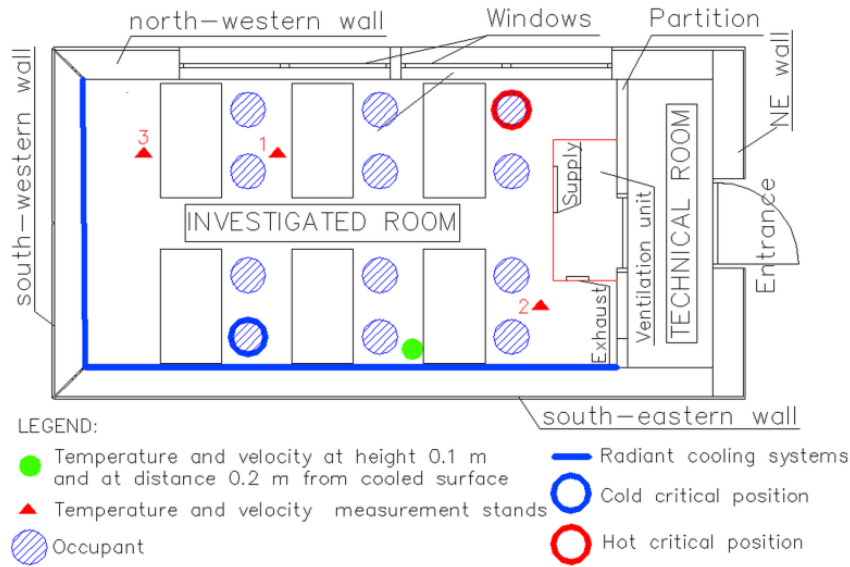


Figure 4: Floor plan of test room and description of investigated points

The temperature development was continuously measured in the test room for a period of 72 hours. The main purpose of a rather long period of measurement was to obtain measured values of temperature and velocities in the period which came closest to a steady-state situation (a quasi-steady state). These measured values were then used for the comparisons with the results of the CFD calculations. Based on this comparison, the CFD model could be validated and used for further parametrical studies.

3.1.5 Temperature measurements

Temperatures within the test room were measured by using T-type thermocouples. The acquisition units Agilent 34970A were used to process the readings. To improve the accuracy of the measurements, a reference temperature was measured at a common cold junction reference point situated outside of the Agilent's multiplexer cards. The reason for this was that the temperature difference across the whole multiplexer card can be up to 1 °C [17], which would bring an unnecessary error into the measurements. The reference temperature was measured using a thermocouple connected directly to the multiplexer card close to the position of the device measuring the temperature of the board. The precision of the thermocouple used to measure the reference temperature was further checked by using PT100 sensors connected to a separate measuring unit. The points of interest were then measured by the thermocouples as a voltage difference and recalculated to temperatures. The precision of such a measuring setup should be about 0.3 °C [17].

Fifteen thermocouples on the three vertical stands measured room air temperatures at heights of 0.1 m, 0.6 m, 1.1 m, 1.7 m and 2.1 m as shown in Figure 4. The temperatures were measured in 1 minute intervals. Aluminum cylinders were used to shield the thermocouples against the effects of a thermal radiation. Twelve thermocouples were used to measure the wall surface temperatures. These thermocouples were attached to the walls by using a thermally conductive paste which enhanced the heat transfer between the wall surface and the thermocouples. Aluminum tape was used in this case to shield the thermocouples against thermal radiation effects. Furthermore, two thermocouples were used to measure the surface temperature of the window, four thermocouples measured the temperature of the floor surface, and twelve thermocouples measured the temperature of the surface of the diffuse ceiling inlet. In addition, air temperatures in the test room were also measured by SensoAnemo 5100F with a precision of 0.2 °C [18]. Thirty-six thermocouples were installed at three different heights in the plenum. HOBO data loggers were used to measure the outside temperature with an accuracy of 0.35 °C [19].

3.1.6 Velocity measurements

Transducers SensoAnemo 5100SF with an accuracy ± 0.02 m/s $\pm 1\%$ of a reading for velocities below 5 m/s were used to measure air velocities in the test room [18]. The measurements took place on the three vertical stands as shown in Figure 4, at heights of 0.1 m, 1.1 m and 1.7 m. Draught rating was used to relate draught magnitude to indoor environment comfort, including the effects of both velocities and temperatures. The recommended standard is to keep the draught rating value below 15% [20]. The maximum velocity in the occupied zone should not exceed 0.19 m/s in a cooling scenario for class B [20]. The draught rating was calculated according to Eq.(1):

$$DR = (34 - t_a) \cdot (v - 0.05)^{0.62} (0.37 \cdot v \cdot T_u + 3.14) \quad \text{Eq.(1)}$$

where: t_a is the temperature of air at the place of measurement [°C], v is the mean air velocity at the place of measurement [m/s], and T_u is the turbulence intensity at the place of measurement [%].

3.2 Numerical simulations

The aim of the development of a CFD model of the test room with the radiant cooling system was to allow for deeper understanding of the system and to facilitate efficient and economical optimization of its design taking into account various parameters. The developed CFD model is depicted in Figure 5. The commercial CFD program Ansys Fluent 14.0 was used for the numerical simulations [21].

3.2.1 The grid creation

A hexahedral grid was created by using a sweep method. The grid was refined in the areas close to the wall surfaces to allow for the correct calculation of heat transfer. The maximum skewness of the model was 0.3 and the average value was less than 0.00045. The mesh had 4,354,482 cells. The grid independence was investigated and the results can be found in [22].

3.2.2 Boundary conditions

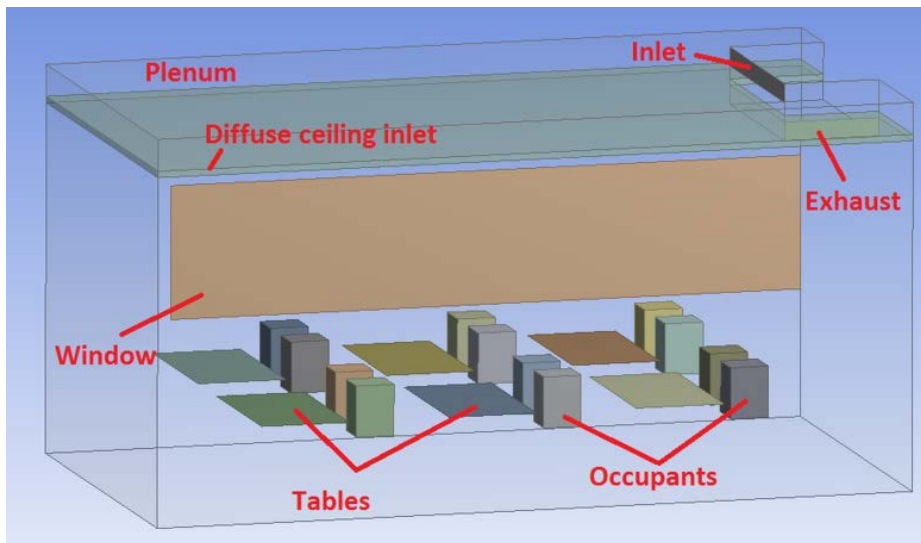


Figure 5: CFD model

The positions of the boundaries in the CFD model are depicted in Figure 5. The inlet boundary, with dimensions of 0.8 m x 0.1 m, was assigned a velocity magnitude of 1.44 m/s and a temperature of 26.6 °C. The exhaust element, with dimensions of 0.45 m x 0.10 m, was defined as a static pressure outlet 0 Pa. The rectangular blocks, with dimensions of 0.25 m x 0.20 m and height of 0.45 m, were used to model the seated occupants and were placed on horizontal plates at a height of 0.55 m representing chairs with dimensions of 0.45 m x 0.40 m. The tables were modeled as horizontal plates with dimensions of 1.3 m x 0.7 m and placed at a height 0.7 m. The boundary conditions of the external wall surfaces were defined with external heat transfer coefficients of 0.18 W/(m²·K) for the roof, 0.19 W/(m²·K) for the walls, 2.47 W/(m²·K) for the floor, and 1.26 W/(m²·K) for the windows, and a surrounding air temperature of 8.5 °C for the roof, walls and windows and 19.8 °C for the floor. The solar radiation from the window was not modeled because the measurements used to validate the CFD model were taken in a period where no sun was present.

3.2.3 Porous zone model

The porous gypsum panels creating the diffuse ceiling inlet were modeled and calculated using a porous zone model in Ansys Fluent. The porous zone model in Fluent is defined as a fluid domain with an added momentum loss equation. The inputs to the model were determined based on the measured pressure drop across the suspended ceiling. The porosity was set as isotropic with a value of 15%, in accordance with the known open area of the perforated gypsum plate. The momentum loss was defined by the viscous and inertial resistance coefficients of $1.306 \times 10^9 \text{ m}^{-2}$ and $1,185,000 \text{ m}^{-1}$, respectively. These values were obtained from quadratic regression analysis of the measured values of the pressure drop and the velocity expressed by Eq. (2):

$$\Delta p = 35554 \cdot v^2 + 1181.8 \cdot v \quad \text{Eq. (2)}$$

where: Δp is the pressure drop measured across the porous suspended ceiling and v is the velocity of the air flowing through porous suspended ceiling.

3.2.4 Turbulence modeling and near wall treatment

It was important to account for buoyancy forces in the CFD model because they influence air movement in rooms equipped with a diffuse ceiling inlet to a considerable degree. A Boussinesq model was used to account for the buoyancy forces. The reference temperature was defined as the average temperature in the calculated domain. The investigations were carried out as steady-state calculations. The semi-empirical, two-equation $k-\xi$ model was used to model the turbulent effects in the test room. The model is normally used for fully developed turbulent flows and is therefore suitable for free stream areas of a domain [23]. The RNG $k-\xi$ model was used because it partly accounts for low Reynolds number effects when combined with optimal near wall treatment [24]. However, the $k-\xi$ turbulence model has its limitations in close-to-the-wall regions, and it very often yields high wall shear stress and high heat transfer rates [23]. That is why the $k-\xi$ turbulent model needed to be combined with proper near wall treatment. The scalable wall function was applied to resolve the area close to the surfaces in the test room. The scalable wall function has the advantage over other types of wall functions in that there is no limitation on the grid spacing close to the wall surface. The limiting value of 11.067 was used to ensure that the first grid point would always be in the logarithmic profile area [23].

4. Results and discussion

4.1 Temperatures

Figure 6 shows the results of the temperature development measured in the test room over a period of 72 hours. The aim was to identify the most stable period which was then used for the validation of the CFD model. The three most stable periods were found each day in the early mornings between 4 a.m. and 7 a.m., as shown by the horizontal red lines with arrows in Figure 6. The measurements from the last of these periods were used for the validation of the CFD model (farthest right in Figure 6). The temperatures and velocities in the test room were measured at the same time. The last period was considered to be in a quasi-steady-state situation because the temperatures did not change markedly. The outside temperature was also rather stable during that period. The occupied hours are shown by the horizontal blue lines with arrows in Figure 6. It can be seen that temperatures in the test room were generally rather low during our measurements. There were two critical positions in the occupied space where occupants could feel thermal discomfort. The first position was close to the two cooling wall, where the occupant might feel too cold as shown by the blue circle in Figure 4. The second position was in the opposite corner of the test room, where the occupant might feel too hot as shown by the red circle in Figure 4, because this position was farthest from the cooled surfaces. The operative temperatures at the two critical points were close to 23 °C and 22 °C for the hot and the cold critical points, respectively, representing environment category classes B and C, respectively [7]. As the main purpose of the experimental investigations was to get reliable data which could be used for the validation of the CFD model, the experiment was not especially controlled to achieve a better indoor environmental category. As can be seen from Figure 6, the influence of the radiant cooling systems on the operative temperature in the test room was rather great. The average temperature of the cooled surfaces was 18.8 °C. Regular small fluctuations in the inlet air temperature were observed as a result of the ON/OFF operation of the electrical heater in the ventilation unit. The irregular larger fluctuations were a result of the algorithm used by the control system of the ventilation unit, which could not be changed.

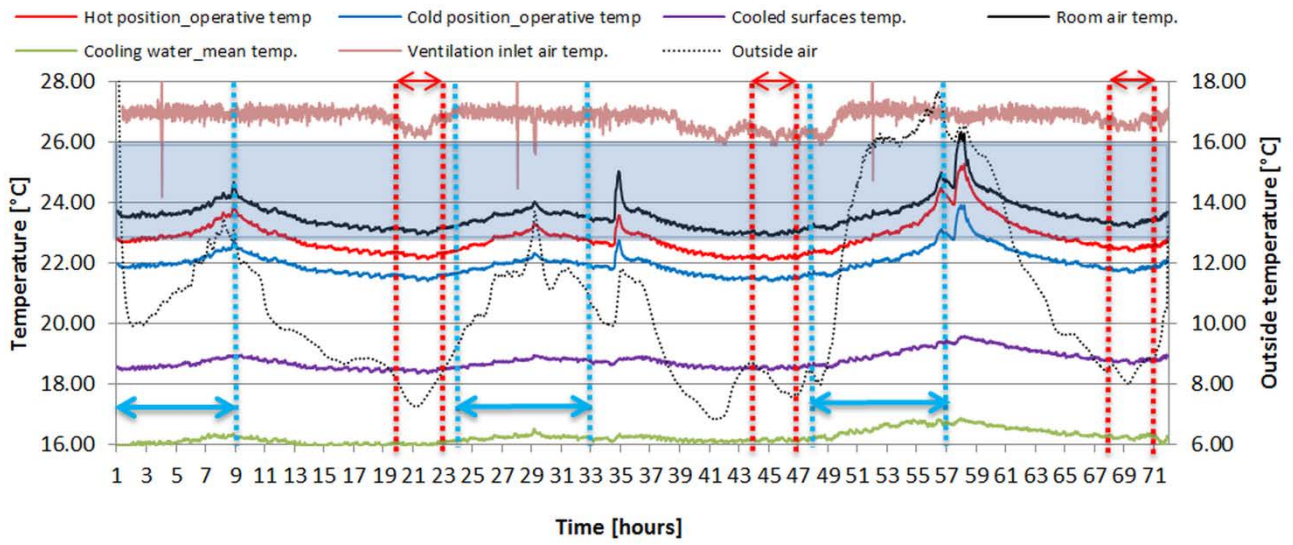


Figure 6: Temperature development from measurement

Table 1: Draught rating values on the different stands

Height [m]	Measured values			CFD original model		
	St1	St2	St3	St1	St2	St3
0.1	0.0	5.1	0.0	0.0	0.0	0.0
1.1	0.0	0.0	0.0	0.0	0.0	0.0
1.7	0.0	0.0	0.0	0.0	0.0	0.0

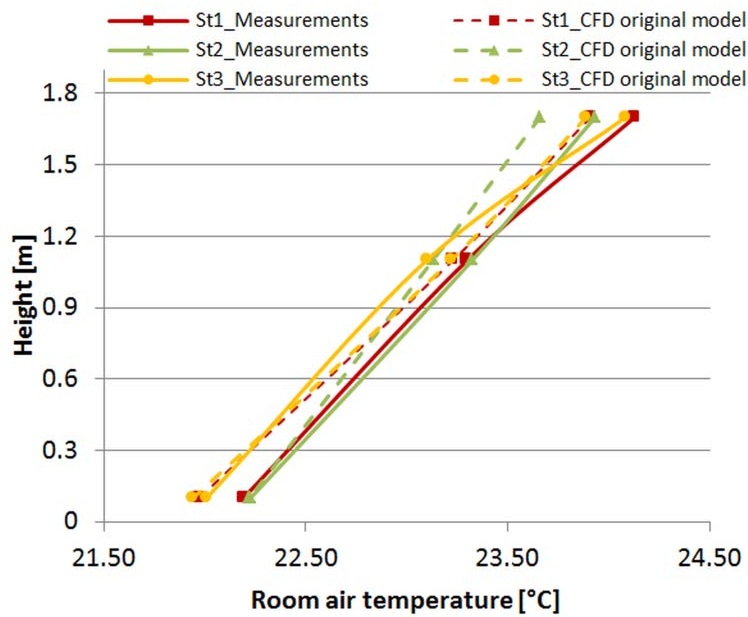


Figure 7: Measured and CFD temperature distribution in the room

Figure 7 shows the measured and the CFD calculated air temperature distribution in the test room in the quasi-steady-state period. The measured vertical temperature difference between the lowest (0.1 m) and the highest (1.7 m) measurement points was 2 K, which is within environmental class A [20]. As can be seen from Figure 7, the room air temperatures calculated by the CFD model were in good agreement with the measured values. The maximum temperature difference between the measurements and the CFD predictions was 0.3 K. In general, the calculated temperatures were slightly lower than the measured values at all heights. The vertical temperature difference obtained from CFD calculations was also consistent with the measurements. A cold draught close to the cold surfaces could create a large vertical temperature difference in the test room, and it is therefore very important that the CFD model was able to capture this behavior.

4.2 Air velocities

As can be seen from Figure 8, the room air velocity magnitudes were generally slightly higher in the lower part of the test room as a result of buoyancy forces induced by the internal heat sources and the vertical walls activated for cooling. It is difficult to obtain good velocity predictions by means of CFD calculations because the air flow in a room is influenced by many different factors. As can be seen from Figure 8, the CFD calculations slightly underestimated the air velocities in the test room. However, the air speed within the test room was generally very low and therefore the differences were actually minor. The results of draught rating for three measuring stands are in Table 1. In conclusion, the CFD model was validated for the investigated case and was considered satisfactory for the subsequent parametrical analysis. The main benefit of CFD velocity predictions is to identify the places with potential for the creation of draught resulting in decreased comfort for occupants. The room air cooled by the cold surfaces moved down towards the floor, as can be seen in Figure 9. This could potentially result in the creation of cold draughts at the height of ankles as result of the acceleration of cold air. However, this did not happen because the velocities measured close to the cold walls were higher at heights of 1.1 m and 1.7 m than at the height of 0.1 m, as can be seen in Table 2. This can be explained by the fact that the falling air accumulated at the bottom of the test room as it hit the floor surface. Local overpressure was created as a result, which did not allow the falling air to reach high velocity at a height of 0.1 m. The down-directed air flow was then partly directed to the center of the test room, as can be seen in Figure 9. The heat sources situated in close proximity to the cooled surfaces could have had influence on the flow pattern close to the cooled walls. The CFD calculations show the area in the test room where the down draughts from

the two cooled walls collided. Here, the air velocity increased and the unique flow pattern was created diagonally across the test room. The result at height 0.1 m is shown in Figure 20 (farthest left). Because the measuring stands were situated in different positions in the test room during our measurements, this diagonal flow pattern was not captured in the measured results.

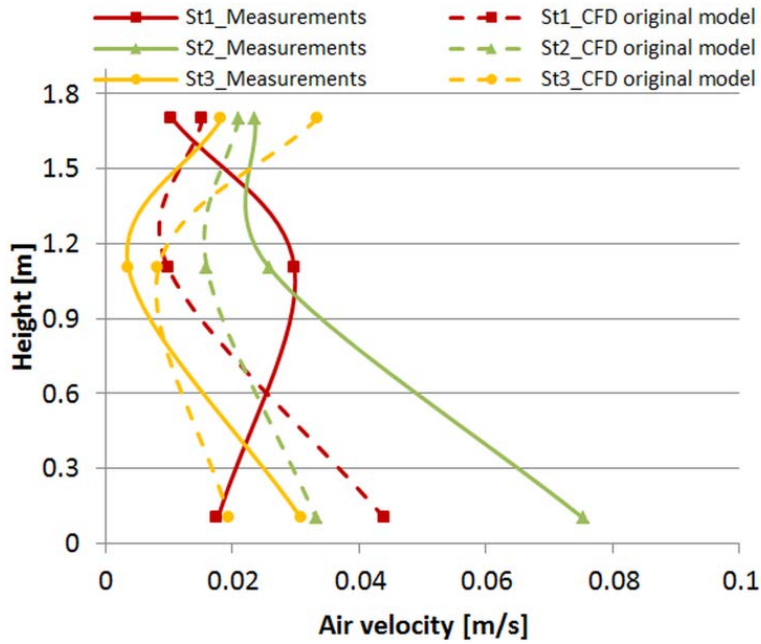


Figure 8: Measured and CFD velocity magnitude distribution in the room

Table 2: Measured velocity magnitude close to the south-eastern wall

Distance from wall [m]	Height		
	1.7[m]	1.1[m]	0.1[m]
0.2	0.11	0.15	0.09
0.05	0.31	0.25	0.15
0.01	0.33	0.28	0.15

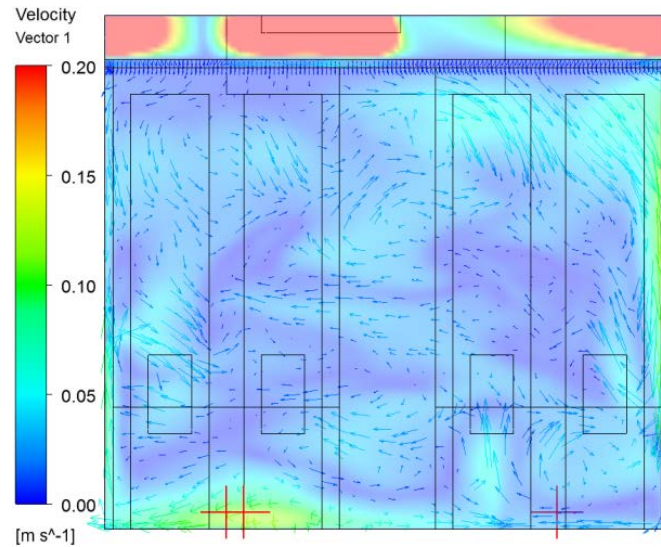


Figure 9: Velocity distribution in transverse plane in the room

4.3 Parametrical analyses

4.3.1 *Reduced area of diffuse ceiling inlet*

To investigate the effect of a different suspended ceiling setup on the indoor climate of the investigated test room, a scenario with a reduced area of the diffuse ceiling inlet was studied using the original CFD model. The area of the diffuse ceiling inlet was reduced to the area of three rectangles situated at positions above the tables. The new supply area is depicted in Figure 10 in green. Each supply rectangle had dimensions of 3.15 m x 0.70 m, giving an overall area of 6.60 m² and corresponding to 35% of the original supply area. The rest of the suspended ceiling was assumed to be covered by solid gypsum through which air could not penetrate – shown in red in Figure 10.



Figure 10: Layout of scenario with reduced area of diffuse ceiling inlet

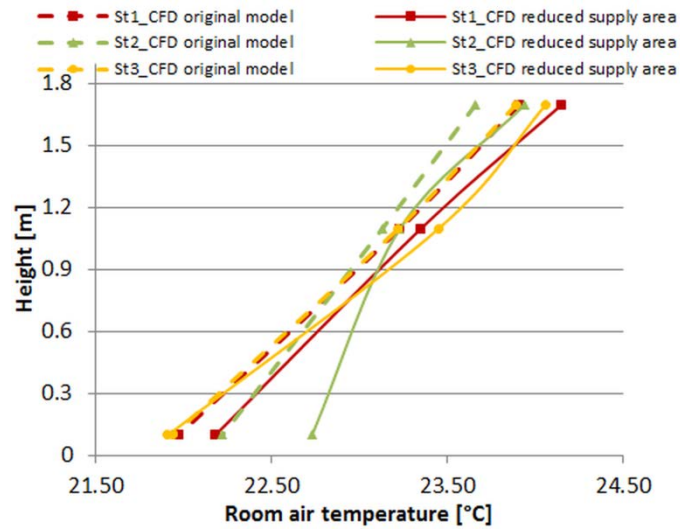


Figure 11: Temperature distribution in scenario with reduced supply area

Figure 11 shows comparison of the temperature distribution in the scenario with a reduced supply area to the original scenario. The temperature of the cooled surfaces was 18.5 °C. The temperature development in the test room was very similar for both scenarios except for the situation on stand 2. A disruption in the general flow pattern occurred in this area, as can also be seen from the velocity development shown in Figure 12.

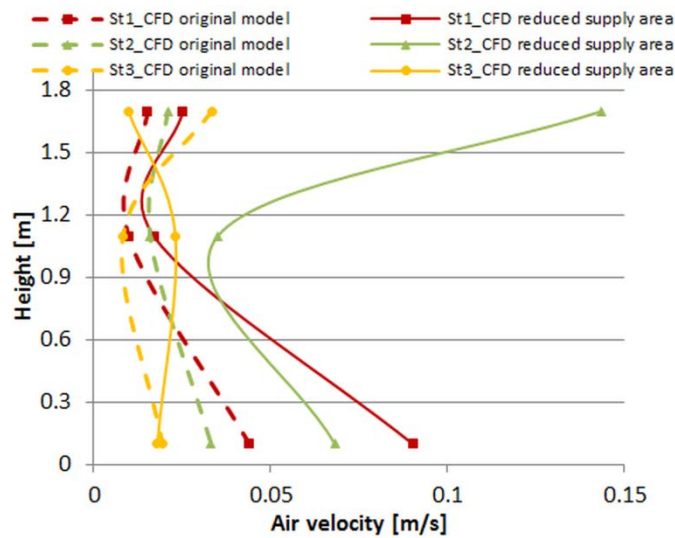


Figure 12: Velocity development in scenario with reduced supply area

The results show that reducing the area of the diffuse ceiling inlet by a factor of 3 did not pose any limitations in terms of temperature and velocity distributions in the test room, because the differences in these were rather small. This is an important finding since in practice it is not always possible to activate the whole area of the ceiling for ventilation.

4.3.2 Various temperatures of cooled surfaces

The temperature distribution within the test room for the two different scenarios and with various cooled wall temperatures is shown in Figure 13. The purpose of the investigations was to find out the effect of various cooled wall temperatures on the temperature and velocity distribution in the test room and on the risk of draught creation. The results are shown for three different cooled surface temperatures: 14 °C, 18.5 °C and 21.5 °C. These temperatures correspond to a power output from the cooled walls of 1200 W, 780 W and 500 W, respectively. The temperature distribution pattern was similar for both scenarios, confirming the previous conclusion that reducing the supply area did not have make much difference to the temperature distribution within the test room. This applies to all three cooled surface temperatures investigated. The vertical temperature difference was slightly higher when the temperature of the cooled surfaces is 14 °C. The explanation is that when the temperature of the cooled walls was low, higher velocity was experienced close to the cooled surfaces and higher volumes of cold air were distributed to lower parts of the test room. The velocity at a height of 0.1 m and at a distance of 0.01 m from the south-eastern wall was 0.05 m/s, 0.04 m/s and 0.03 m/s for cooled surface temperatures of 14 °C, 18.5 °C and 21.5 °C, respectively.

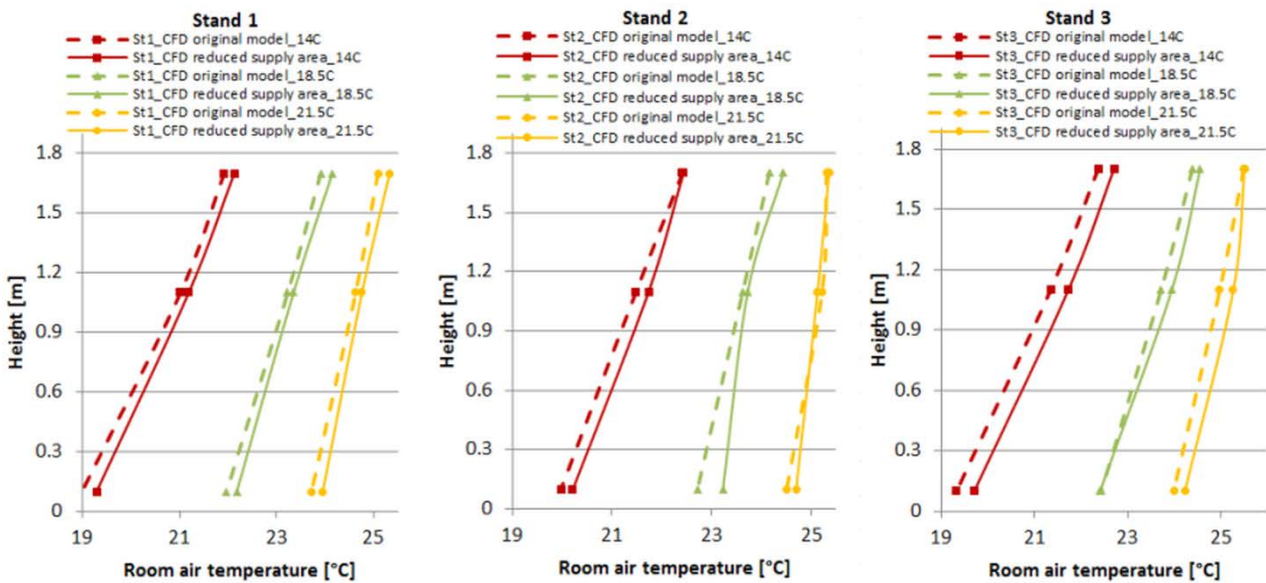


Figure 13: Comparison of temperature distribution between original scenario and scenario with reduced supply area for various wall temperatures

Figure 14 shows the results of the velocity distribution for the two different scenarios and with cooled surface temperatures of 14 °C, 18.5 °C and 21.5 °C, respectively. The velocity distribution within the test room is very similar in both scenarios except on stand 2. The velocity increased in both CFD models at a height of 0.1 m when the cooled wall

temperature was 21.5 °C. The reason can be seen in Figure 15, where a flow pattern with higher velocity was created in the corner of the test room (the upper right-hand corner in Figure 15). The explanation of this phenomenon, however, is not known. A similar flow pattern can be seen when the cooled surface temperature was 14 °C. Here it could be argued that it was a result of the low temperature of the cooled wall surface. Despite this phenomenon, the critical velocities which would result in draught problems were not exceeded with any of the cooled surface temperatures investigated, as can be seen in Table 3 and Table 4.

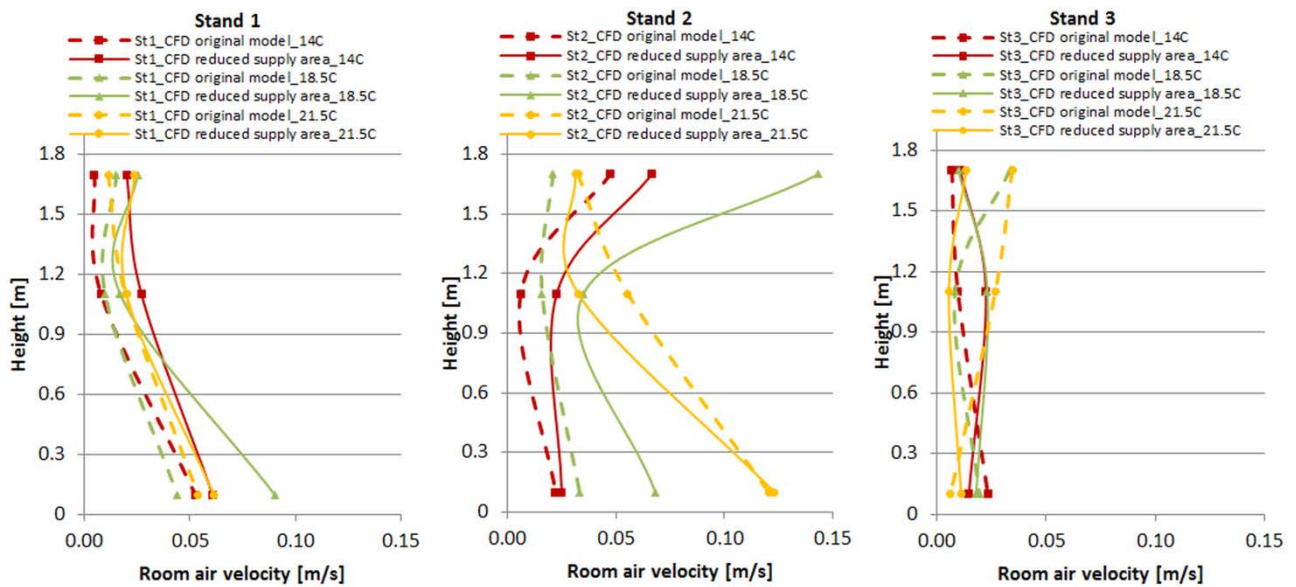


Figure 14: Comparison of velocity magnitude distribution between original scenario and scenario with reduced supply area for various wall temperatures

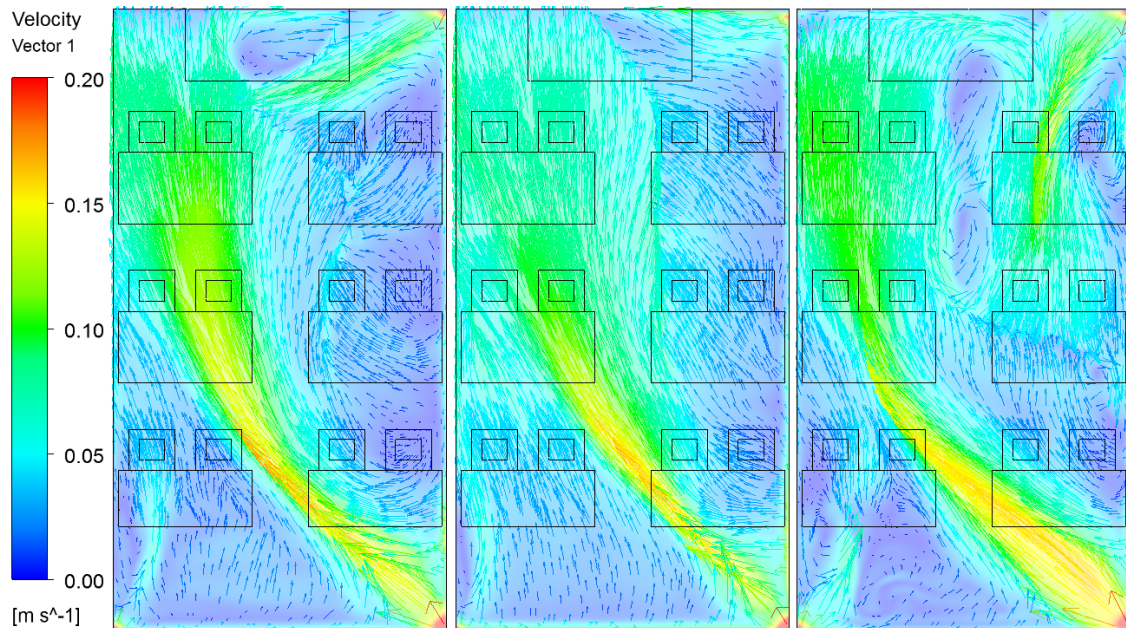


Figure 15: Velocity distribution in the horizontal plane at a height of 0.1 m: 14 °C (left); 18.5 °C (middle); 21.5 °C (right)

Table 3: Draught ratings for cooled wall temperatures of 14 °C, 18.5 °C and 21.5 °C in the original CFD model

CFD original model									
Height	14 deg			18.5 deg			21.5 deg		
m	St1	St2	St3	St1	St2	St3	St1	St2	St3
0.1	1.2	0.0	0.0	0.0	0.0	0.0	1.0	9.5	0.0
1.1	0.0	0.0	0.0	0.0	0.0	0.0	0.0	1.4	0.0
1.7	0.0	0.0	0.0	0.0	0.0	0.0	0.0	0.0	0.0

Table 4: Draught ratings for cooled wall temperatures of 14 °C, 18.5 °C and 21.5 °C in the CFD model with a reduced supply area

CFD model with reduced supply area									
Height	14 deg			18.5 deg			21.5 deg		
m	St1	St2	St3	St1	St2	St3	St1	St2	St3
0.1	2.8	0.0	0.0	5.1	3.9	0.0	2.0	9.6	0.0
1.1	0.0	0.0	0.0	0.0	0.0	0.0	0.0	0.0	0.0
1.7	0.0	3.9	0.0	0.0	12.2	0.0	0.0	0.0	0.0

4.3.3 Heat gains variation

Figure 16 shows the temperature distribution in scenarios with different internal heat loads. The original scenario had an internal heat gain of 1327 W. Two more scenarios were investigated: one with a decreased heat load of 664 W and

one with an increased heat load 2654 W. It can be seen in Figure 16 that the vertical temperature difference increased when internal heat loads were decreased.

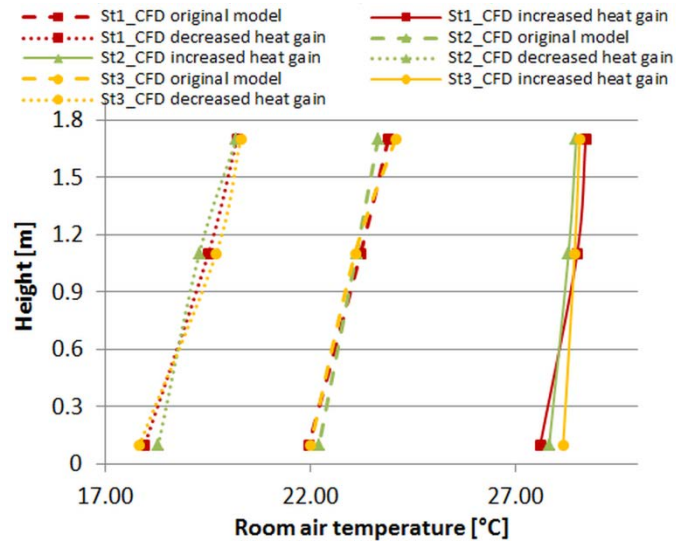


Figure 16: Temperature distribution in scenarios with different heat loads

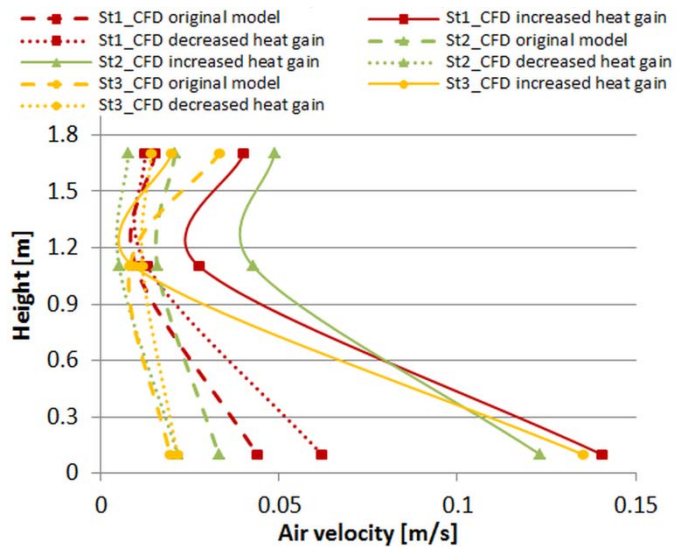


Figure 17: Velocity distribution in scenario with increased and decreased heat load

The velocity distribution in the test room for the scenarios with different internal heat loads is shown in Figure 17. The higher internal heat loads resulted in higher velocities throughout the whole test room, especially in areas close to the floor. The results support the finding that air flows in the test room were significantly influenced by buoyancy forces. The results of draught ratings for the scenarios with various internal heat loads are shown in Table 5.

Table 5: Draught ratings for scenarios with increased and decreased internal heat loads

Height [m]	CFD original model			CFD increased heat loads			CFD decreased heat loads		
	St1	St2	St3	St1	St2	St3	St1	St2	St3
0.1	0.0	0.0	0.0	4.6	6.1	4.0	3.3	0.0	0.0
1.1	0.0	0.0	0.0	0.0	0.0	0.0	0.0	0.0	0.0
1.7	0.0	0.0	0.0	0.0	0.0	0.0	0.0	0.0	0.0

4.3.4 One wall used for cooling

The purpose of this investigation was to find out the effect of activating only one wall for cooling instead of the two walls as in the original scenario. Two scenarios were investigated, where in the first scenario only the south-eastern wall was activated and in the second scenario only the south-western wall was activated for cooling. The same cooling power as in the original scenario was used for both new scenarios to make them comparable.

The surface area of the cooled wall was different in each scenario, so the temperature of the cooled surfaces also differed. The cooled surface temperature was 18.7 °C in the original scenario, 17.8 °C in the scenario with the south-eastern wall, and 12.3 °C in the scenario with the south-western wall.

Figure 18 shows the temperature distribution in the test room for the scenarios with the different surfaces activated for cooling. The temperature development is similar for all scenarios except for the situation on stand 1 at a height of 0.1 m, which was caused by strong flow patterns created along sides of the test room as can be seen in the right-hand picture in Figure 20. The stands are shown by the red crosses in Figure 20 and the positions of the measuring stands are depicted in Figure 4. The vertical temperature differences were slightly higher at all stands for the scenario with the south-western wall activated for cooling.

Different behavior was observed in the case of the velocity development. As can be seen from Figure 19, higher velocity was observed on stand 3 at a height of 0.1 m in the scenario with the south-western wall activated for cooling. This was because the low temperature of the south-western wall created a down draught. The increased velocity in the plane 0.1 m above the floor can be seen in Figure 20, which shows the velocity distribution in the room at a height of 0.1 m for the three different scenarios.

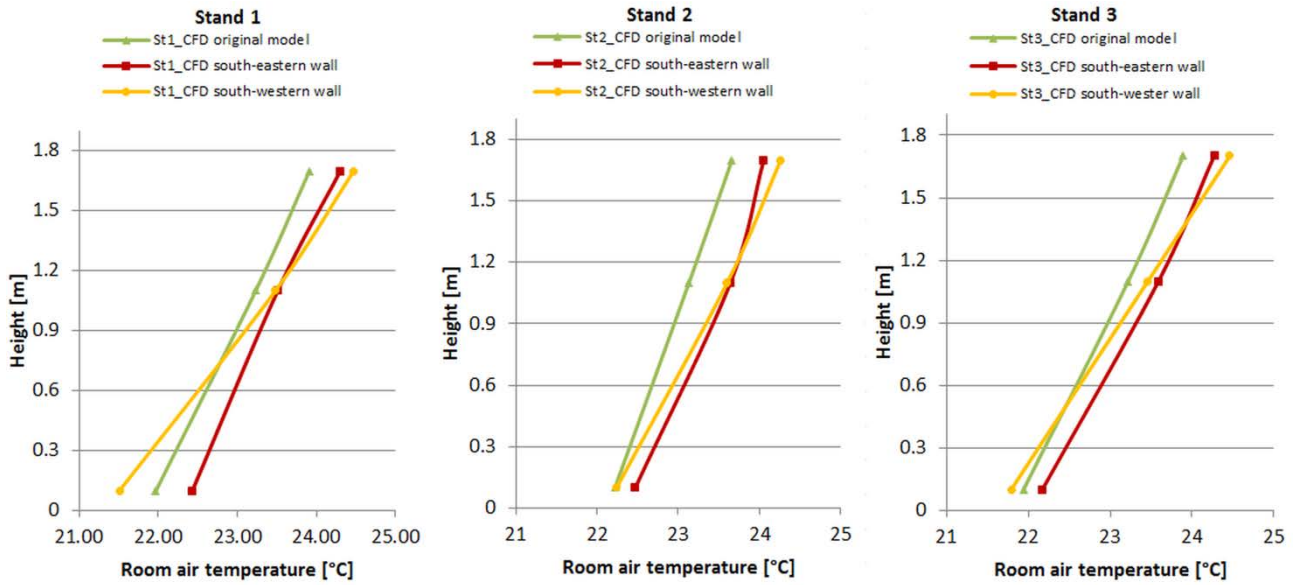


Figure 18: Temperature distribution in scenarios with different surfaces activated for cooling

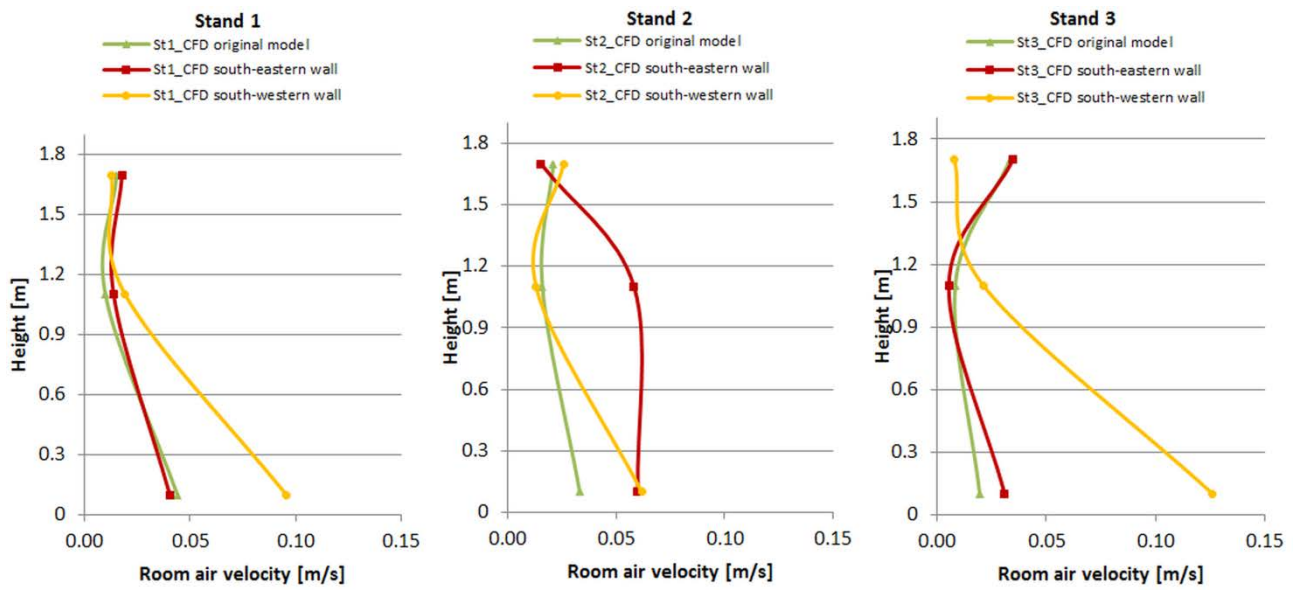


Figure 19: Velocity distribution for scenarios with different surfaces activated for cooling

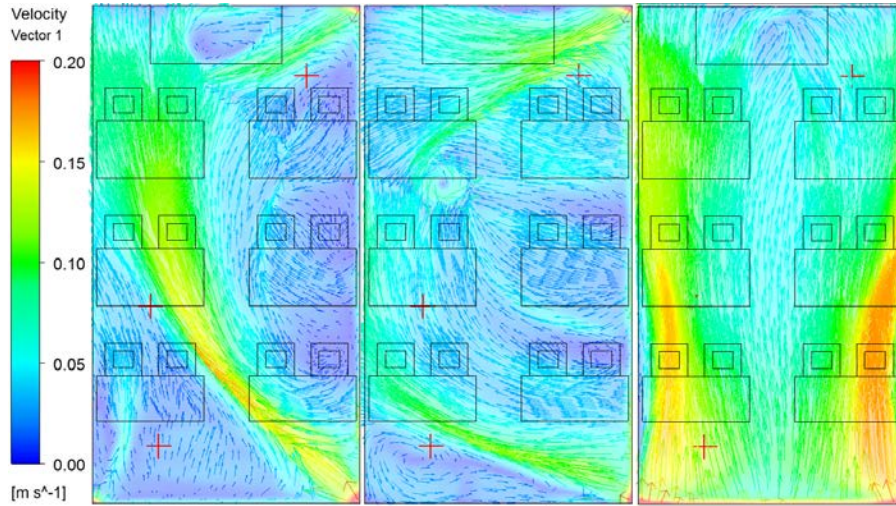


Figure 20: Velocity distribution at height 0.1m for three scenarios: original model (left); south-eastern wall (middle); south-western wall (right)

Rather a strong flow current is observed diagonally through the test room when both walls were activated for cooling, as can be seen in the left-hand picture in Figure 20. This current is in the area where the down flow pattern from the south-eastern wall collides with the down flow pattern from the south-western wall. When only the south-eastern wall is activated for cooling, the flow pattern is not so strong and is situated in a slightly different position in the test room. The recirculated area is in the corner of the test room, as can be seen in the bottom left-hand corner of the middle picture in Figure 20. The activation of only the south-western wall for cooling creates strong flow patterns along the sides of the long walls, as can be seen in the right-hand picture in Figure 20.

The draught ratings for all scenarios are shown in Table 6. As the above investigations have already indicated, the highest draught ratings were found in the scenario with the south-western wall activated for cooling.

Table 6: Draught ratings for scenarios with different walls activated for cooling

Height [m]	CFD original model			CFD south-eastern wall activated			CFD south-western wall activated		
	St1	St2	St3	St1	St2	St3	St1	St2	St3
0.1	0.0	0.0	0.0	0.0	2.7	0.0	5.8	3.0	7.8
1.1	0.0	0.0	0.0	0.0	2.1	0.0	0.0	0.0	0.0
1.7	0.0	0.0	0.0	0.0	0.0	0.0	0.0	0.0	0.0

5. Conclusion

The wall radiant cooling system combined with a diffuse ceiling inlet for ventilation created a comfortable indoor climate in a classroom with a high density of occupants of 0.6 per m² of floor area. The radiant system provided energy for cooling between 29 W/m² and 59 W/m² of floor area with cooling water temperatures of between 21.5 °C and 18.5 °C. The resulting indoor air temperature was between 25 °C and 22 °C. The value 29 W/m² can be assumed as a suitable and sufficient amount of cooling power for the scenarios investigated in the test room which had a ratio of cooling walls to floor area of 1.2. This means that a low temperature difference between cooling water and room air of 4.5 K is sufficient to maintain a comfortable indoor climate. This is favorable for the use of renewable sources of cooling water, such as ground water and sea water. The highest measured draught rating of 5.1% was experienced in the area close to the floor, so the system did not create draught. Our measurements showed that the radiant cooling system had a rather high influence on the operative temperature, which was as much as 2 K lower than the room air temperature. Higher internal heat gains resulted in higher velocities especially in areas close to the floor, which means that the air flows in the test room were governed to a considerable degree by buoyancy forces. Decreasing the area of the diffuse ceiling inlet by a factor of 3 did not pose any limitations in terms of temperature and velocity distribution in the test room.

Bibliography

- [1] P. Wargocki and D. P. Wyon, "Providing Better Thermal and Air Quality Conditions in School Classrooms Would Be Cost-effective," *Building and Environment*, vol. 59, pp. 581-589, 2013.
- [2] D. G. Shendell, W. J. Fisk, M. G. Apte, D. Faulkner, R. Prill and D. Blake, "Associations Between Classroom CO₂ Concentrations and Student Attendance in Washington and Idaho," *Indoor Air*, no. LBNL-54413, 2004.
- [3] M. Turunen , O. Toyinbo, T. Putus, A. Nevalainen, R. Shaughnessy and U. Haverinen-Shaughnessy, "Indoor Environmental Quality in School Buildings, and the Health and Wellbeing of Students," *Int. J. Hyg. Environ. Health*,

2014.

- [4] D. Clements-Croome, "Work Performance, Productivity and Indoor Air," vol. SJWEH Suppl (4), pp. 69-78, 2008.
- [5] H. Levin, "Sick Building Syndrome: Review and Exploration of Causation Hypotheses and Control Methods," in *Proceedings of the ASHRAE/SOEH Conference IAQ*, San Diego, California, April 17-20 1989.
- [6] WHO, "Indoor Air Pollutants: Exposure and Health Effects," World Health Organization, 1983.
- [7] EN 15251:2007, "Indoor Environmental Input Parameters for Design and Assessment of Buildings Addressing Indoor Air Quality, Thermal Environment, Lighting and Acoustics," European Committee for Standardization, 2007.
- [8] S. A. Mumma, "Designing Dedicated Outdoor Air Systems," *Ashrae Journal*, 2001.
- [9] B. W. Olesen, "Radiant Floor Cooling Systems," *Ashrae Journal*, 2008.
- [10] P. Jacobs, E. C. van Oeffelen and B. Knoll, "Diffuse Ceiling Ventilation, a New Concept for Healthy and Productive Classrooms," TNO Built Environment and Geosciences, Delft, 2008.
- [11] C. A. Hviid and S. Svendsen, "Experimental and Numerical Analysis of Perforated Suspended Ceiling as Diffuse Ventilation Air Inlets".
- [12] C. A. Hviid and S. Terkildsen, "Experimental Study of Diffuse Ceiling Ventilation in a Classroom," Technical University of Denmark.
- [13] T. Mikeska and S. Svendsen, "Study of Thermal Performance of Capillary Micro Tubes Integrated into the Building Sandwich Element Made of High Performance Concrete," *Applied Thermal Engineering*, no. 52, pp. 576-584, 2013.
- [14] P. Simmonds, S. Reuss and W. Gaw, "Using Radiant Cooled Floors to Condition Large Spaces and Maintain Comfort Conditions," *Ashrae Journal*, 2000.

- [15] S. A. Mumma, "Ceiling Panel Cooling Systems," *Ashrae Journal*, 2001.
- [16] J. Dieckmann, K. W. Roth and J. Brodrick, "Radiant Ceiling Cooling," *Ashrae Journal*, 2004.
- [17] A. Heller, "Large-Scale Solar Heating- Evaluation, Modelling and Designing," Technical University of Denmark, 2000.
- [18] Sensor-electronic, "AirDistSys 5000 product datasheet," [Online]. Available: http://www.sensor-electronic.pl/pdf/KAT_AirDistSys5000.pdf. [Accessed 1 July 2014].
- [19] Onset, "HOBO Data Loggers Product Datasheet," [Online]. Available: <http://www.onsetcomp.com/products/data-loggers/u12-012>. [Accessed 1 July 2014].
- [20] EN ISO 7730:2005, "Ergonomics of the Thermal Environment: Analytical Determination and Interpretation of Thermal Comfort Using Calculation of the PMV and PPD Indices and Local Thermal Comfort Criteria," International Organization for Standardization, Geneva, 2005.
- [21] Ansys Fluent, "Product Datasheet," [Online]. Available: <http://ansys.com/Products/Simulation+Technology/Fluid+Dynamics/Fluid+Dynamics+Products/ANSYS+Fluent> . [Accessed 1 July 2014].
- [22] T. Mikeska and J. Fan, "Full Scale Measurements and CFD Simulations of Diffuse Ceiling Inlet for Ventilation and Cooling of Densely Occupied Rooms," *Energy and Buildings*, 2014.
- [23] W. Vieser, T. Esch and F. Menter, "Heat Transfer Predictions Using Advanced Two-equation Turbulence Models," Ansys, CFX Validatin Report.
- [24] Ansys 14.5, "Fluent Theory Guide 4.3.2".

Paper IV

Dynamic behavior of radiant cooling system based on capillary tubes in walls made of high performance concrete

Mikeska T., Svendsen S.

Accepted with minor revision in Energy and Buildings (2014)

Dynamic behavior of radiant cooling system based on capillary tubes in walls made of high performance concrete

Tomas Mikeska, Svend Svendsen*

Department of Civil Engineering, Technical University of Denmark, Brovej, Building 118 DK-2800 Kgs. Lyngby, Denmark

Abstract

Rooms with a high density of occupants inevitably have high internal heat gains. It is possible to remove large sensible internal heat gains solely by radiant cooling systems if large areas of internal surface can be activated for radiant cooling. The ventilation system then only has to supply the small amount of fresh air required by standards to provide a healthy indoor environment.

This paper reports on experimental analyses evaluating the dynamic behavior of a test room equipped with a radiant cooling system composed of plastic capillary tubes integrated into the inner layer of sandwich wall elements made of high performance concrete. The influence of the radiant cooling system on the indoor climate of the test room in terms of the air, surface and operative temperatures and velocities was investigated.

The results show that the temperature of the room air can be kept in a comfortable range using cooling water for the radiant cooling system with a temperature only about 4 K lower than the temperature of the room air. The relatively high speed reaction of the designed system is a result of the slim construction of the sandwich wall elements made of high performance concrete.

*Corresponding author: Tel.: +4527338619, E-mail: tommi@byg.dtu.dk

1. Introduction

Low-energy buildings can result in greater cooling demand than heating demand. This is especially true in low-energy buildings with a high occupant density, such as classrooms, which inevitably have high internal heat gains. It can be a challenge to cool down such spaces using conventional ventilation systems because they can result in reduced occupant comfort by creating draughts. The installation of a diffuse ceiling inlet can improve the cooling capacity of a ventilation system because it allows the supply of large volumes of air into a room. In principle, the air comes from the ventilation unit into a space between a concrete slab and a suspended ceiling, and then it is supplied into the room through a perforated area of the suspended ceiling. Since a large area of a ceiling is used, large volumes of air can be supplied into a room without causing any discomfort for occupants. Nielsen and Jakubowska investigated the concept of the diffuse ceiling inlet in a laboratory environment [1]. Their results showed that a diffuse ceiling inlet was able to handle higher thermal loads and higher flow rates than five conventional ventilation diffusers.

Radiant cooling systems have an advantage over full-air conditioning systems because they make use of large surface areas in a building structure, which gives them high cooling capacity. Radiant cooling systems are therefore suitable for spaces with a high occupant density such as classrooms. The cooling capacity of a radiant cooling system may be limited by the dew-point temperature, the vertical air temperature, radiant asymmetry or an acceptable temperature of the cooled surfaces [2].

Radiant cooling systems greatly influence the operative temperature in a room because radiation becomes the dominant heat transfer principle [2]. Higher temperature supply air can be used for the ventilation while keeping the same comfort for occupants. This saves energy otherwise needed to precondition supply air. Radiant cooling systems will also have an influence on the surface temperature of the diffuse ceiling inlet, precooling the incoming air as a result. Another benefit of radiant cooling systems lies in the small difference required between the temperatures of the cooling water and the room air. Thanks to this phenomenon, low-grade heat sources can be used, such as ground water and sea water in case of cooling, and solar energy, wind energy and geothermal energy in case of heating [2]. Radiant systems have a high degree of self-regulation if they work with small temperature differences between the heating/cooling water and the room air. This high degree of self-regulation can be often achieved in low-energy buildings when using radiant heating, because heat losses from such a building are generally low. The heat flux from the radiant heating system decreases as the indoor temperature increases until heat transfer totally ceases [3]. A

different situation can arise in the case of a radiant cooling system in low-energy buildings, since the good thermal insulation of a building envelope keeps more heat inside. Larger areas of surface need to be activated for the radiant cooling system to allow the small temperature difference between the cooling water and the room air that gives a good degree of a self-regulation.

The slow response to a control system is regarded as a major drawback of conventional radiant cooling systems. This slow response is mostly due to the activation of a large volume in a building structure, e.g. a floor. The reaction time of radiant systems can therefore be somewhat longer than with full-air conventional cooling systems. This can become an issue in cases where changes in internal thermal loads occur too quickly, which could be the case in classrooms. In such a situation, an increase of temperature in a room can be very rapid and the system is not able to react sufficiently quickly, resulting in overheating of the occupied space. The slim construction of the inner layer (30 mm) of a sandwich wall component made of high performance concrete presented in this paper was designed to eliminate a slow response of the radiant cooling system to the control system. On the other hand, the activation of a large amount of thermal mass can reduce the peak cooling load and also move a part of the load outside of occupant hours [2]. Weitzmann in his thesis investigated both the steady-state and the dynamic cooling behavior of a thick concrete slab with plastic pipes installed for cooling purposes [4]. His main focus was on the precooling of the concrete slab during the night time. His results showed that the concrete deck can absorb heat during occupied hours, and remove it through the pipes during the night. Instantaneous cooling can be a problem when a thick concrete slab is used because it is difficult to control, and uncomfortable temperatures in the room can be reached as a result [4].

If a space is equipped with a radiant system, large savings can be made on the ventilation system because the radiant system can handle all the sensible heat loads in a room [5]. Smaller volumes of air are handled by the ventilation system, which means smaller ducts can be used, because only latent cooling loads are covered by the ventilation system. The ventilation system can then be designed just for the necessary air flow based on the health and comfort requirements stated in the relevant standards [6], [7]. The ventilation unit should be designed to condition only supply air, which means covering heat loss/gain from the ventilation. Transmission losses/gains are covered by the radiant system. Simmonds *et al.* in their paper described the development and performance of a radiant cooled floor combined with displacement ventilation [8]. The system created a comfortable indoor climate with high thermal

stratification in the space. The amount of ventilated air needed was reduced and the overall energy consumption was decreased [8].

As previous text suggests, the combination of different solutions for cooling and ventilation can possibly lead to the better overall performance of the building. The classroom is a good example where integration of various systems can be even necessary to achieve acceptable comfort within the investigated space. The integration approach brings further advantages (besides good quality indoor climate) such as lowering the price of the whole system, improvement of overall design of the interior as the installations are not visible and availability of larger surfaces in the space for air conditioning purposes. Additionally, an integration of the cooling system into the prefabricated construction takes place in the controlled environment of assembly hall, which should eventually lead to better quality assurance.

The literature review did not reveal any case where plastic capillary tubes were installed in a layer of high performance concrete and used as the radiant cooling system. New knowledge about the performance of radiant cooling systems made of plastic capillary tubes cast in a thin layer of high performance concrete is presented in this paper. The aim was to analyze the dynamic behavior of a test room cooled down by the installed radiant cooling system using cooling water with different temperatures. The test room investigated is densely occupied to analyze the performance of radiant wall cooling under extreme conditions, which can be interpreted as the worst case scenario.

The experimental measurements were carried out in a newly constructed test building with inbuilt plastic capillary tubes allowing the thermal activation of two vertical surfaces as the radiant system.

2. Methods of investigation

The investigations described in this paper were carried out as experimental measurements in a test building constructed specially for the purposes of our investigations. The test building is a real, full-scale house built outside and was therefore subject to constant changes in weather. This had an influence on our measurements, but at the same time provided us with valuable information on the behavior of the systems under real operating conditions. The main focus was on the dynamic effects and the response to changes in the control system of the test room built with sandwich wall elements made of high performance concrete with an inbuilt system of radiant cooling based on plastic capillary tubes.

3. Test room and measurements

3.1 Test room

The experimental measurements were carried out in the full scale test building built with the sandwich elements made of two layers of high performance concrete and a thermal insulation in between (see Figure 1). The test room used during our investigations was 6.05 m long and 3.25 m wide, giving a floor area of 19.66 m². The ceiling deck was constructed from pre-stressed hollow core concrete panels 0.2 m thick. Two windows with dimensions of 2.5 m x 1.1 m were installed in the wall facing north-west giving a total area of 5.5 m² (see Figure 2). A partition wall separated the test room from an entrance space, which also served as a small technical room. Its purpose was purely to divide the two spaces in terms of air flow. The partition wall was made of wood and gypsum board.



Figure 1: Full scale test house used for experiments

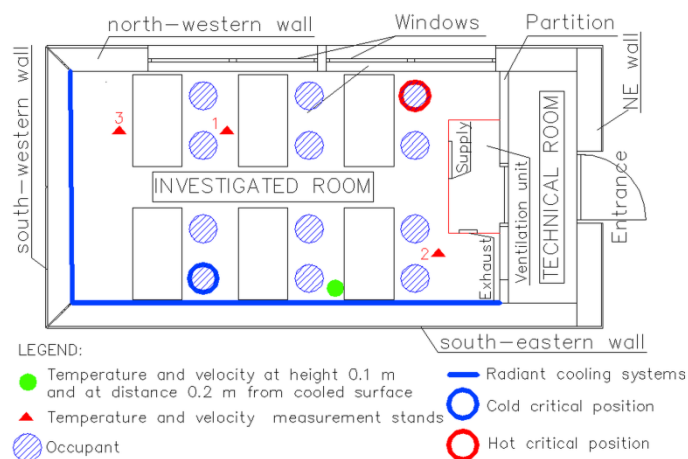


Figure 2: Layout and description of the room in the test house

3.2 Diffuse ceiling inlet

The diffuse ceiling inlet was constructed so as to allow the whole area of a suspended ceiling to act as a supply diffuser (see Figure 3). The diffuse ceiling inlet was made from large perforated gypsum boards with dimensions of 0.9 m x 2.7 m. The connections between the gypsum boards were sealed with silicone paste to prevent any unwanted flow through the joints. The total perforated area was 15.5%. The perforated suspended ceiling was built 0.28 m below the concrete ceiling slab to separate the inlet and the exhaust openings of the ventilation unit. The resulting height of the test room was 2.65 m. The ventilation unit reduced the surface area of the diffuse ceiling inlet to an area of 18.6 m². The volume of the test room was 52.9 m³. The additional functions of the perforated suspended ceiling construction included acoustic regulation in the test room and a cover of the installations.

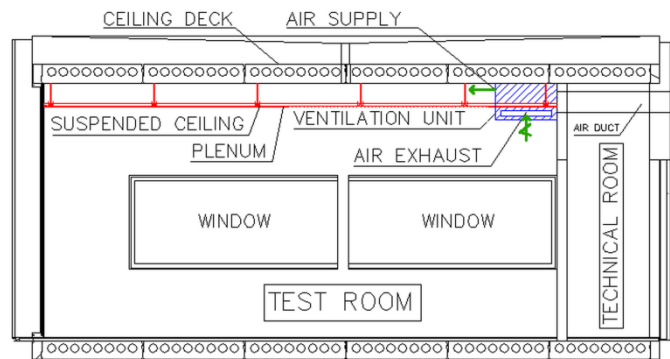


Figure 3: Diffuse ceiling inlet construction and ventilation unit position

The ventilation unit was installed below the concrete deck close to the technical room. The ventilation unit was partly in the test room (1/3) and partly in a plenum (2/3) (see Figure 3). Figure 4 shows the supply of fresh air from the ventilation unit into the plenum, which was realized by an opening 0.05 m below the ceiling deck with dimensions of 0.8 m x 0.1 m. The exhaust opening was on one side of the ventilation unit, just below the perforated suspended ceiling in the test room, as can be seen in Figure 4. The dimensions of the exhaust opening were 0.15 m x 0.1 m.



Figure 4: The view into ventilation unit with uncovered lid after installation

3.3 Radiant cooling systems

The radiant cooling system made use of 50% of the area of the vertical surfaces within the test room. The inner layers of the south-eastern and the south-western walls were equipped with the radiant systems and are shown by the blue lines in Figure 2. The walls were constructed with the sandwich elements composed of two layers of high performance concrete (20 mm outside layer and 30 mm inside layer) with a layer of a thermal insulation in the middle (300 mm). The radiant cooling system was based on capillary mats made of polypropylene capillary tubes and it was cast in the inner layer of high performance concrete as shown in Figure 5. The outer diameter of the tubes was only 4.3 mm and the wall thickness of the tubes was 0.8 mm. Such small dimensions allowed integration of the radiant cooling systems into the 30 mm thick layer of high performance concrete. Each wall panel contained several capillary mats with the dimensions of 2.7 m x 1.0 m. The two activated walls had a total of 10 capillary mats providing a radiant area of 27 m² and containing 4.32 l of cooling water. The capillary mats were connected to polypropylene manifold pipes by flexible hoses (see Figure 6).



Figure 5: Capillary mats casted into the layer of concrete



Figure 6: Connections of capillary mats in the wall to the main manifold with flexible pipes

3.4 Other appliances installed in test room

The test room was equipped with 12 metal barrels painted black, which simulated sedentary occupants. They had a cylindrical shape with a diameter of 0.35 m and a height of 0.45 m. There were 12 chairs to accommodate the barrels. Six classroom tables with dimensions of 1.2 m x 0.7 m and a height of 0.7 m were situated in the test room and their positions are shown in Figure 2.

3.5 Scenarios investigated

3.5.1 *Dynamic behavior of the test room during a pre-cooling period*

The ability of the radiant cooling system to condition the test room before occupancy was investigated. The test room was overheated on purpose to an air temperature of 32.5 °C to test the performance of the radiant cooling systems and the whole room in this extreme situation. Such a situation could happen, for example, in the early morning before

the start of a working week after a very hot and sunny weekend. Therefore it is relevant to investigate how long it takes for the radiant cooling systems to condition the test room to an acceptable temperature. The aim was to achieve a temperature in the upper part of a range meeting the comfort requirements (for indoor environment class B [7]) and at the same time to use just the necessary amount of energy during the pre-cooling period. There were no heat gains, ventilation or lighting during this investigation representing the room with no occupants present. The temperature of the cooling supply water was kept around 15 °C (± 0.5 K). A flow rate of 0.125 l/sec was maintained in the cooling water loop.

3.5.2 *Dynamic behavior of the test room in occupied hours*

Here we investigated the dynamic behavior of the radiant cooling systems and the whole test room at the beginning of the occupied hours, when people have entered the room. Three different scenarios were investigated to test the dynamic behavior under different operational conditions (see Table 1). The internal heat gains were measured with the energy meter. The ventilation system, the water cooling system and internal heat gains were all started at the same time.

Table 1: The three scenarios investigated

Scenario	Internal heat gains [W]	Temperature of cooling water [°C]	Weather
1	1530	15.5	Overcast
2	1530	18.5	Overcast
3	1530	21.5	Overcast

A constant flow rate of 0.125 l/sec was maintained in the cooling water loop during all of the measurements. The ventilation flow rate was also kept constant with a value of 415 m³/h, corresponding to an air change rate of 7.8 h⁻¹. The precision of the ventilation flow rate was checked with CO₂ measurements using an air flow meter with an accuracy of $\pm 3\%$ [9]. The CO₂ was dosed in the duct delivering outside air to the ventilation unit, before the supply fan. The measurements took place at a position after the fan and close to the inlet to the plenum using four CO₂ sensors. The dosing position is shown by the green dot in Figure 7, the measuring position by the blue dot, and the black dot shows the position of the fan. The resulting ventilation flow rate was calculated as $q = p/c_1 - c_2$; where p is the CO₂ flow rate [m³/s], c_1 is the measured CO₂ concentration after the fan [m³/m³], and c_2 is the measured CO₂

concentration of outside air [m^3/m^3]. The air flow rate used is between class B and A, according to the relevant standard [6].

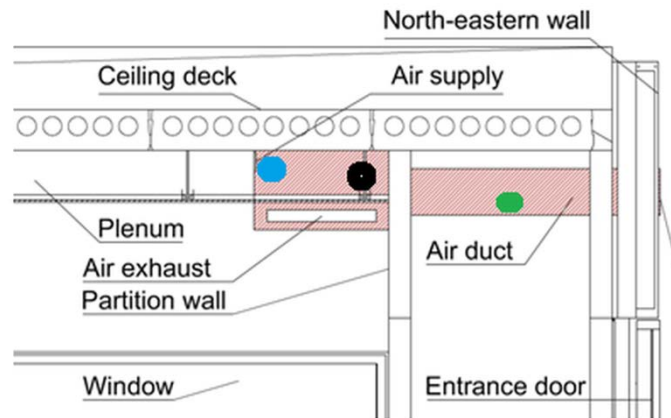


Figure 7: CO2 measurements

3.6 Temperature measurements

The operative temperature, a parameter expressing the combined effect of room air temperature and the mean radiant temperature, was used for an evaluation of indoor climate in the test room. The operative temperature was calculated as an average of the air temperature and the mean radiant temperature because air velocities in the test room were less than 0.2 m/s and the differences between the air temperature and the mean radiant temperature were less than 4 K [10]. Operative temperatures were calculated for the two critical points which are shown by the blue and red circles in Figure 2. The blue circle is the position of an occupant who might feel too cold. This assumption is based on the distance from the cooled surfaces and on the view factors to the cooled surfaces. In contrast, an occupant in the red circle might feel too hot, again based on the distance and the view factors.

Thermocouple readings were taken using the acquisition/switch unit Agilent 34970A [11]. T-type thermocouples were used for the measurements. Their accuracy for indoor measurements ranges from 0.7 °C to 1 °C, involving a voltage to temperature conversion [12]. However, the temperature difference across the whole multiplexer card (used with Agilent unit) can be as much as 1 K. This brings some uncertainty into the measurements. To improve the accuracy of our measurements, the reference temperature was not measured at each multiplexer card, but at the common cold junction reference point in the separate thermally insulated box. The reference temperature was measured with a T-type thermocouple and its precision was compared with the readings of the Pt100 sensors for better precision of

the measurements. All the measurements at the points of interest in the test room were then made by the connected T-type thermocouples. The precision of the measurements with the thermocouples was 0.3 K [12].

The wall surface temperatures were measured with 12 thermocouples attached to the walls by use of a special thermally conductive paste enhancing heat transfer between the surface of the wall and the thermocouple. The surface thermocouples were shielded against the effects of thermal radiation by aluminum tape. Fifteen thermocouples on the three vertical stands measured the room air temperature, as shown in Figure 2. The thermocouples were positioned at height levels of 0.1 m, 0.6 m, 1.1 m, 1.7 m and 2.1 m, respectively, in order to reveal the vertical temperature profile, which is used as a factor in local thermal comfort evaluation in [7]. The temperatures were measured continuously for the entire period of the experiment and were recorded in minute intervals. The thermocouples measuring the air temperature were shielded against thermal radiation by aluminum cylinders. Twelve thermocouples were used to measure the temperature of the bottom side of the perforated suspended ceiling, four thermocouples were placed on the floor, and two thermocouples measured the temperature of the surface of the windows. Thirty-six thermocouples were installed in the plenum at three different heights. Furthermore, air temperatures in the test room were also measured on the moveable stands by SensoAnemo5100SF transducers with an accuracy of measurement of 0.2 K [13].

The outside air temperature measurements were made by sets of HOBO Data loggers (model U12) with a temperature accuracy ± 0.35 K [14].

3.7 Air velocity measurements

The floor area close to cold vertical surfaces is a critical area for the comfort of occupants. The test room air adjacent to the cold vertical surfaces is cooled down and due to buoyancy effects starts to drop down to the floor. When the air hits the floor surface, even higher speed can then be experienced as a result of the building up of momentum close to the floor. The combination of high velocity and low temperature of air could result in the creation of a draught, which could be very uncomfortable for occupants, so it was very important to investigate this phenomenon in test room. The velocities of air were measured at a height of 0.1 m and at a distance of 0.2 m from the cooled south-eastern wall for all the scenarios investigated (see Figure 2). The room air velocities were measured using SensoAnemo5100SF transducers with an accuracy of ± 0.02 m/s $\pm 1\%$ for velocities below 5 m/s [13]. The air velocities were also measured on the three stands at heights of 0.1 m, 1.1 m and 1.7 m.

Draught rating was used to measure the critical areas in the test room where a draught could bother occupants. Draught is the most common cause of local discomfort, and it is recommended to be kept below the value of 15% [7]. The draught rating was calculated according to Eq.(1).

$$DR = (34 - t_a)(v - 0,05)^{0,62}(0,37 * v * Tu + 3,14) \quad \text{Eq.(1)}$$

where: t_a is the air temperature at the point of measurement [$^{\circ}C$], v is the mean air velocity at the point of measurement [m/s], and T_u is the turbulence intensity at the point of measurement [%].

The general velocities in the occupied zone should not exceed 0.16 m/s in winter or 0.19 m/s in summer (environmental class B [7]). These values can be adjusted according to the activity and clothing level of the occupants.

3.8 Thermo-graphic investigation of radiant cooling system

Thermo-graphic investigation using a radiometric thermal camera [15] was carried out to check the proper functioning of the radiant cooling systems. The rather large temperature differences between the walls with activated radiant systems and other internal surfaces allowed us to uncover any problematic areas.

4. Results analysis and discussion

4.1 Dynamic behavior of room during pre-cooling period

Figure 8 shows the cooling down period before occupants enter the test room. The test room was overheated on purpose to test the performance of the radiant cooling systems and the whole room in an extreme situation. The results in Figure 8 show how much time it took to cool the test room to an acceptable temperature. It can be seen that the temperature of the cooled surfaces started to drop immediately after activating the circulating pump, and this can be attributed to the rather thin layer of concrete which was being cooled. The room air temperature started to decrease after about 20 minutes. The reason for the delay is the need for sufficient temperature difference between the cooled surface and the room air to allow for heat exchange between them. The knowledge gained from the pre-cooling investigation will be useful for the future design of buildings using the same radiant cooling technology.

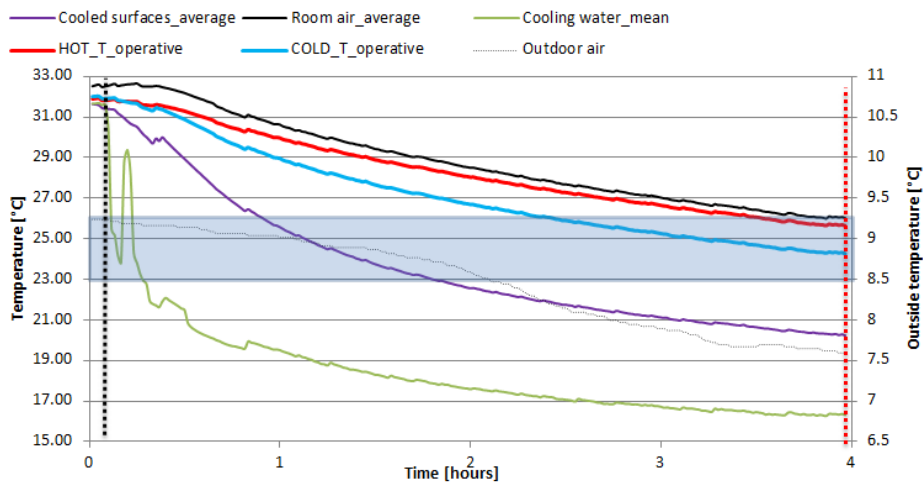


Figure 8: Cooling down the room before presence of occupants

4.2 Dynamic behavior of room in occupied hours

Figures 9-11 show the dynamic behavior of the test room after people entered the room and the radiant cooling systems were activated for scenarios 1, 2, and 3 respectively. The time in Figures 9-11 is shown with a logarithmic scale in order to expand the most relevant part of the measurements. The situation before the activation of the ventilation unit, the internal heat gains, and the water cooling system is shown in the left-hand part of Figures 9-11 (left of the black dotted line). We can see that the measured temperatures fluctuated modestly in this period. The fluctuation was a result of the ON/OFF control of a heater situated in the room. The purpose of the heater was to keep the temperature in the test room around 26 °C in periods when no experiments were being carried out. The reason a value of 26 °C was chosen is that it is the highest acceptable indoor temperature for the chosen environmental class (environmental class B [7]). In this way, very similar starting temperatures were established for all the scenarios measured, as can be seen in Figures 9-11.

The outside temperature was rather stable during the investigation of scenario 1 (between 11 °C and 12 °C), reaching its peak around 3 pm. The mean temperature of the cooling water (calculated as an average of the supply and return water in the cooling loop) dropped substantially right after the start of the system (the vertical black dotted line in Figure 9). The valve regulating temperature of the supply cooling water was set to 15 °C. However, the temperature of the supply cooling water was about 16.5 °C at the start of the experiment as a result of an imprecise functioning of a valve and also rather fast changes in the temperature of the return cooling water after the start of the experiment. The decrease was gradual in later stages of measurements, reaching 15.4 °C.

The temperature of the inlet air coming from the ventilation unit into the plenum fluctuated around a preset temperature of 27 °C due to the ON/OFF control of the heater installed in the ventilation unit. The air temperature in the test room went above 26 °C for the first half an hour after the start of the experiment as a result of the activation of the internal heat gains and supplying the outdoor air with higher temperature into the test room. However, this caused no occupant discomfort, because operative temperatures at this time were in the comfort range of 23-26 °C.

The surface temperature of the cooled walls in scenario 1 decreased rapidly after the start of the measurements. The temperature of the cooled surfaces dropped from 26 °C to 20 °C in the first 4 hours of the experiment. Such a fast reaction from the installed radiant cooling systems can be attributed to the use of the plastic capillary tubes with a small spacing and a rather slim layer of high performance concrete where the plastic capillary tubes were imbedded, as described in section 3.3. The room air temperature and the operative temperature at the two critical positions (see section 3.6 for further description) started to decrease after 20 minutes from the beginning of the experiment. The temperatures stabilized four hours after the start of the experiment, and a small increase in temperatures followed, most probably as a result of an increase in the outside temperature, as can be seen in Figure 9. The temperatures were within the lower part of the comfort range (for an environmental class B [7]) during the whole experiment (running for 5.5 hours).

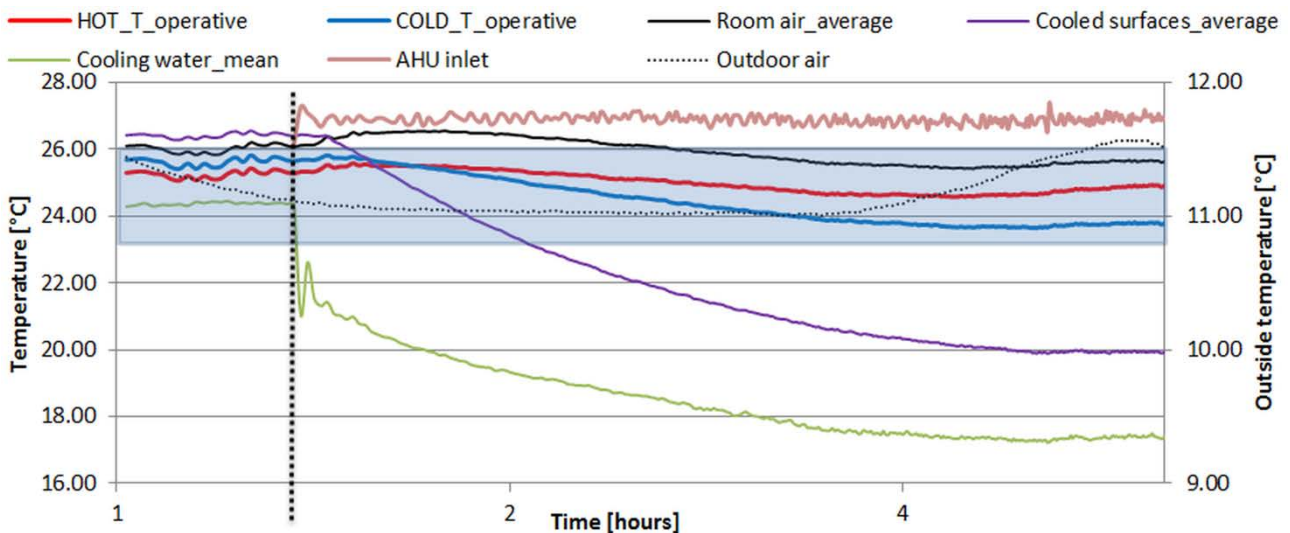


Figure 9: Measured temperature development for scenario 1

In scenario 2, the temperature of the cooled surfaces dropped about 4 K after 4 hours of the experiment and was maintained around 21.5 °C with modest fluctuation, as can be seen from Figure 10. The operative temperatures at the

two critical points were kept around 25 °C for most of the time of the experiment, even though the room air temperature was slightly above 26 °C for most of the time of the experiment. The possibility of having higher air temperatures in the room is one of the advantages of using radiant cooling systems. A slight increase in temperatures was experienced after 4 hours of the experiment. One possible explanation for this situation is an increase in the outside air temperature (as in scenario 1). The temperatures in scenario 2 were kept in the middle part of the comfort range the whole time of the experiment. The temperature of the supply cooling water was kept close to 18.2 °C in later stages of the experiment (in contrast to scenario 1 where the temperature of the supply cooling water was 15.2 °C). Scenario 2 would therefore be preferred, considering energy conservation benefits.

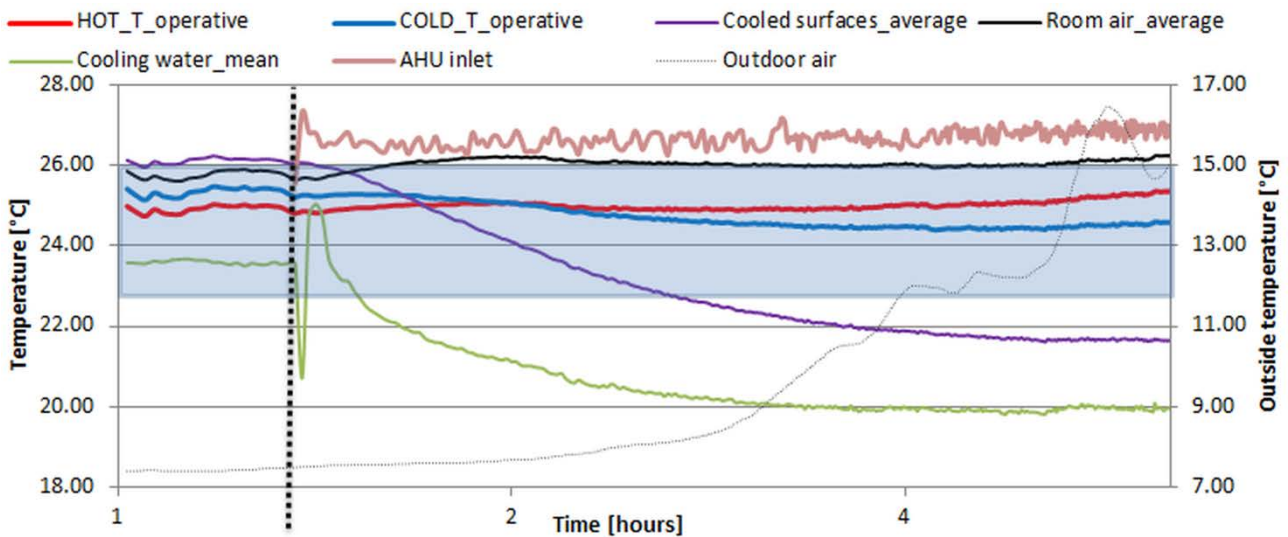


Figure 10: Measured temperature development for scenario 2

In scenario 3, the temperature of the supply cooling water was around 21.5 °C in later stages of the measurement (see Figure 11). The surface temperature of the cooled walls decreased from 26 °C to only 23.5 °C. The larger and longer fluctuation in the supply cooling water was experienced at the beginning of the measurement (in contrast to scenarios 1 and 2). One reason for this could be the rather high temperature of the supply cooling water. The opening valve had difficulty in adjusting the flow rate of the cooling water in a secondary loop because the temperature difference between the return cooling water and the required supply cooling water was too small. One could argue that the reaction of the radiant cooling systems and the whole test room would be faster if the valve reacted briskly. The room air temperature was above 26 °C most of the time, peaking around 27 °C in later stages of the measurement. The operative temperatures at both critical points were kept below 26 °C, and therefore within the comfort range for

design class B. The results show that occupant comfort can be achieved with the designed and installed solution even when the temperature of the available cooling water is only 4 K lower than the operative temperature in the test room. The interesting finding is that there is a very small difference in operative temperatures in the test room between scenario 1, with a cooling water temperature of 15.5 °C, and scenario 3, with a cooling water temperature of 21.5 °C. More precisely, a difference of 1 °C in operative temperature is compared to a 6 °C difference in cooling water temperature. In other words, rather a small influence on indoor comfort can have substantial consequences for the design of the cooling system in a building and on efficient use of the sources of cooling power.

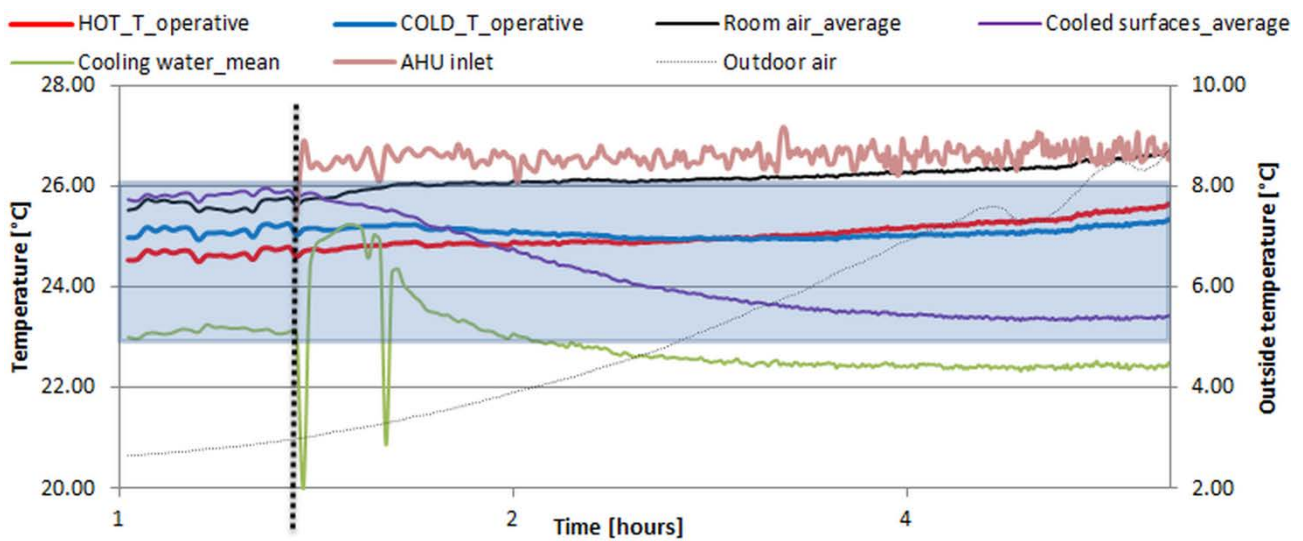


Figure 11: Measured temperature development for scenario 3

The measurements have been carried out in autumn as a result of the delays in construction of experimental facilities. The outside temperatures are therefore lower than would be during summer. It is however believed that the influence on the results is not very high based on following facts: The ventilation inlet air was heated up to the temperature of about 26°C to simulate the summer conditions in Denmark. The window was situated to the North and the solar radiation would be therefore limited also during the summer months. Furthermore, it was the intention to exclude the solar radiation, as the main assumption is that the properly functioning external solar shading is on place before any further means of active cooling are used. Concerning the transitional heat losses/gains, those can be nearly disregarded as the walls in experimental building were well insulated (thickness of wall insulation was 250 mm with λ -value of 0.035 W/mK).

4.3 Velocities in the room

Figure 12 shows the results for room air velocities and temperatures measured at a height of 0.1 m and at a distance of 0.2 m from the cooled walls. Figure 12 also shows the average surface temperatures. The velocity of room air at a height of 0.1 m in the proximity of the cooled surfaces was very much dependent on the temperatures of the cooled surfaces. Room air velocities increased close to the floor when the cooled surface temperature decreased. The velocity fluctuated around 0.11 m/s in scenario 1, around 0.1 m/s in scenario 2, and around 0.07 m/s in scenario 3. The velocities did not reach the threshold for the maximum velocity in the room of 0.19 m/s for summer conditions [7] in any of the scenarios investigated.

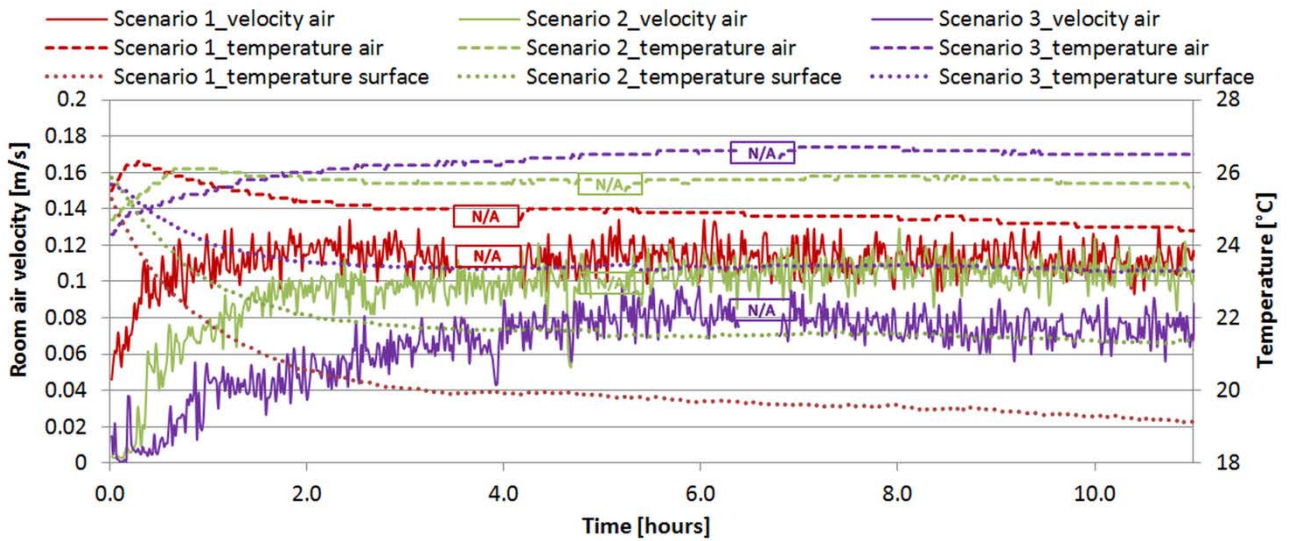


Figure 12: Comparison of velocity measurements at a height of 0.1 m and at a distance of 0.2 m from cooled surfaces for the three scenarios

The draught rating results are shown in Figure 13. The results are in good correlation with the results of velocities. The highest values of draught rating were experienced in scenario 1 where the highest room air velocities were combined with the lowest room air temperatures.

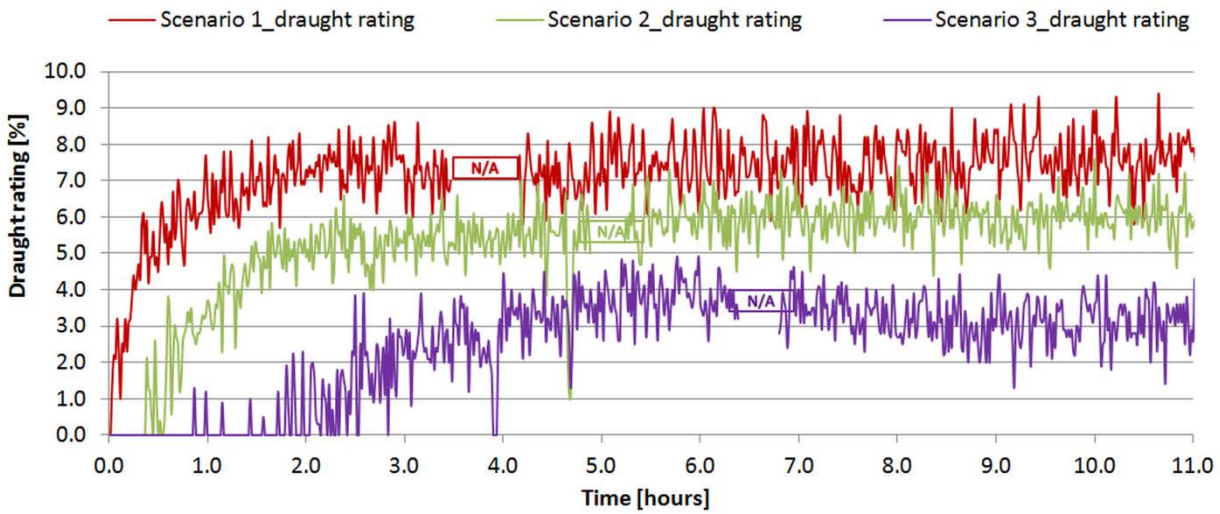


Figure 13: Draught rating results for the three scenarios at a distance of 0.2 m from the cold surfaces

Figure 14 shows the results of room air velocities measured on the three stands (see Figure 2 for the positions of the stands). Air velocities in a room are not easily predictable because the flow of air in a room is a complex phenomenon dependent on many different factors. The highest air velocities at a height of 0.1 m were experienced in scenario 1, followed by scenarios 2 and 3. Higher above the floor, the situation was a bit different because velocities were generally rather low and similar in all the scenarios investigated. The velocities measured on all three stands were below the maximum air velocity for comfort in a room. The draught rating results were reasonably low at all measured points, as can be seen in Table 2.

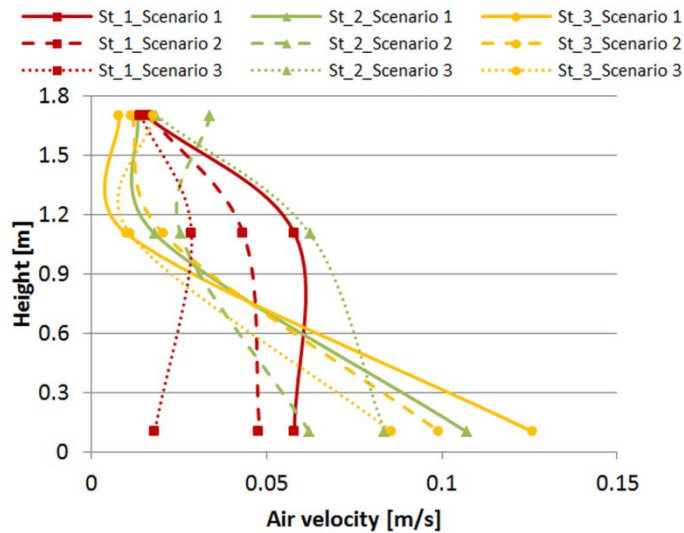


Figure 14: Velocities in the room

Table 2: Draught rating for three stands

Height [m]	Scenario 1			Scenario 2			Scenario 3		
	Stand 1	Stand 2 [%]	Stand 3	Stand 1	Stand 2 [%]	Stand 3	Stand 1	Stand 2 [%]	Stand 3
0.1	1.8	6.3	7.5	1.1	2.3	4.9	0.0	3.9	3.7
1.1	1.8	0.1	0.0	0.8	0.6	0.3	0.3	1.7	0.0
1.7	0.0	0.0	0.0	0.1	0.4	0.1	0.1	0.1	0.1

4.4 Temperatures in the room

Figure 15 shows the results of room air temperature measurements on the three stands in the test room. The room air temperatures were highest on all three stands in scenario 3 as a result of the use of the highest temperature cooling water. In contrast, the lowest room air temperatures were experienced in scenario 1 as a result of the use of the lowest temperature cooling water. The highest vertical temperature difference was also found in the case of scenario 1: a value of 1.2 K. The vertical temperature difference was 0.9 K in scenario 2 and 0.7 K in scenario 3. The vertical temperature differences were within the comfort range in all scenarios [7].

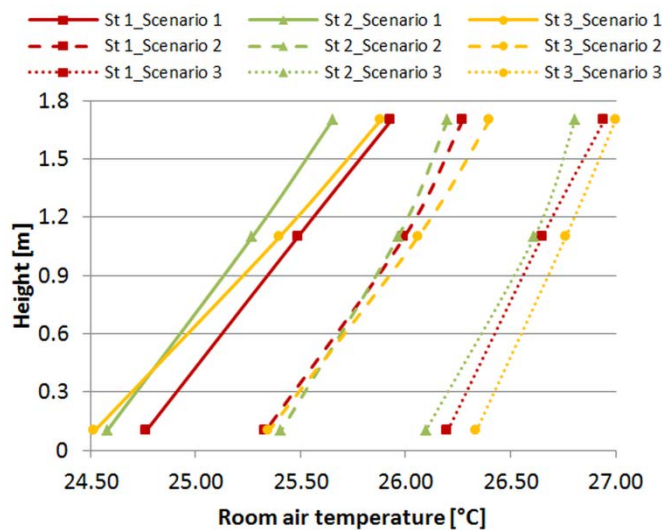


Figure 15: Temperatures in the room

4.5 Thermo-graphic investigation results

Figure 16 shows thermo-graphic pictures of the corner where the two walls used for the cooling purposes joined the diffuse ceiling inlet when the room was heated up. The lower temperature measured at the join of the two walls and the diffuse ceiling inlet was a result of a thermal bridge at this place. Figure 17 shows the same area during the period

when water with a temperature of 15.5 °C was supplied to the radiant systems installed in the two walls. It can be seen that the temperature of the two cooled walls is about 6 K lower than the temperature of the diffuse ceiling inlet. One can also see that a vertical strip about 0.5 m wide has a much higher temperature than the rest of the surface of the two cooled walls. The reason for this was a non-functioning part of the south-west wall, which may have been due to clogging of the plastic capillary tubes by impurities present in the cooling water. This suggests that further filtering and cleaning of the cooling water might be necessary when such tiny tubes are used for the radiant systems.

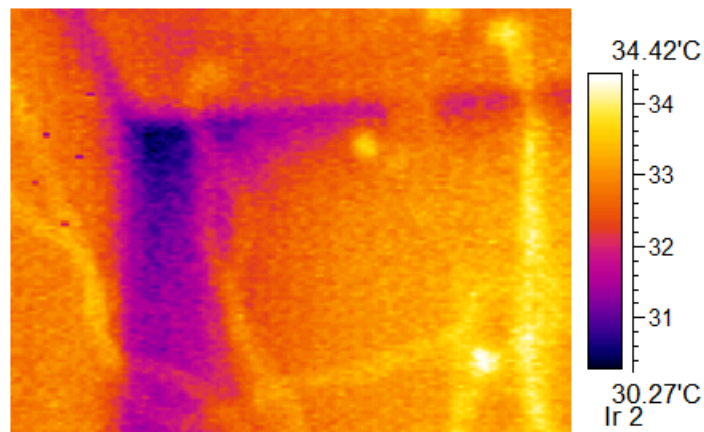


Figure 16: Corner where the two walls join the diffuse ceiling inlet when room was heated

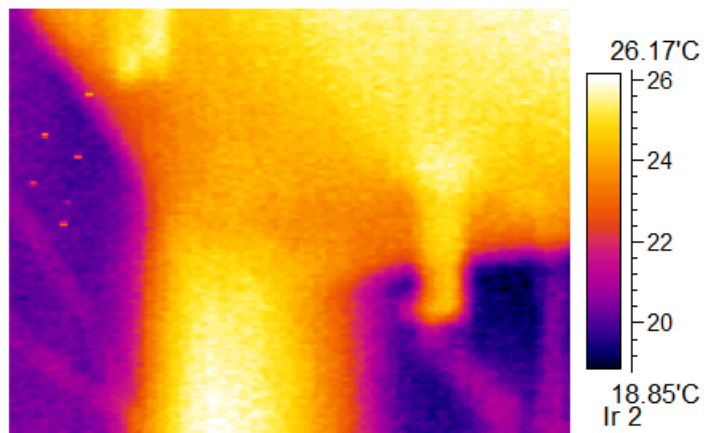


Figure 17: Corner where the two cooled walls join the diffuse ceiling inlet after activation of cooling

5. Conclusion

The results of our investigations show that radiant cooling systems integrated into a thin layer of interior walls made of high performance concrete can provide a comfortable indoor climate in a room with a high density of occupants, without creating any local discomfort. The scenarios investigated showed that the designed solution of wall radiant

cooling does not greatly benefit from substantial lowering of the temperature of cooling water. Comfortable temperatures can be achieved in the room with a supply cooling water temperature only 4 K lower than the average operative temperature in the room. This allows the use of renewable sources of cooling water such as ground water or sea water. The maximum measured vertical temperature difference was 1.2 K. Higher air velocities were measured at ankle height in the proximity of the cooled walls, but the values were below the critical threshold and did not cause any local discomfort. The use of plastic capillary tubes can bring practical challenges with clogging of the radiant cooling system, as was experienced during our investigations. The installation of a proper filtering system is recommended to avoid such complications with the system in practice.

Acknowledgement

This research came to existence thanks to kind sponsorship of companies Airmaster[®], Knauf Danoline[®], and Connovate A/S.

Bibliography

- [1] P. V. Nielsen and E. Jakubowska, The Performance of Diffuse Ceiling Inlet and Other Room Air Distribution Systems, COLD CLIMATE HVAC 2009: Sisimiut Greenland, 16-19 March 2009. 2009.
- [2] B. W. Olesen, Radiant Floor Cooling Systems, *Ashrae Journal*, 2008.
- [3] H. Karlsson, Self-Regulating Floor Heating Systems in Low Energy Buildings, in *Building Physics Nordic Symposium*, 2008.
- [4] P. Weitzmann, Modelling Building Integrated Heating and Cooling Systems, Technical University of Denmark, 2004.
- [5] S. A. Mumma, Designing Dedicated Outdoor Air Systems, *Ashrae Journal*, 2001.
- [6] EN 15251:2007, Indoor Environmental Input Parameters for Design and Assessment of Energy Performance of Buildings - Addressing Indoor Air Quality, Thermal Environment, Lighting and Acoustics, European Committee for

Standardization, 2007.

- [7] EN ISO 7730:2005, Ergonomics of the Thermal Environment: Analytical Determination and Interpretation of Thermal Comfort Using Calculation of the PMV and PPD Indices and Local Thermal Comfort Criteria, International Organization for Standardization, Geneva, 2005.
- [8] P. Simmonds, S. Holst, S. Reuss and W. Gaw, Using Radiant Cooled Floors to Condition Large Spaces and Maintain Comfort Conditions, *Ashrae Journal*, 2000.
- [9] Key Instruments Series FR4000. [Online]. Available: www.keyinstruments.com. [Accessed 1 July 2014].
- [10] EN ISO 7726, Ergonomics of the Thermal Environment - Instruments for Measuring Physical Quantities, International Organization for Standardization, Geneva, 1998.
- [11] Agilent 34970A, Data Acquisition/Switch Unit Family Datasheet, 1 July 2014. [Online]. Available: <http://www.amplicon.com/data/34972a.pdf>.
- [12] A. Heller, Large-Scale Solar Heating - Evaluation, Modelling and Designing, Technical University of Denmark, 2000.
- [13] Sensor-electronic, AirDistSys 5000 product datasheet, [Online]. Available: http://www.sensor-electronic.pl/pdf/KAT_AirDistSys5000.pdf. [Accessed 1 July 2014].
- [14] Onset, HOBO Data Loggers Product Datasheet, [Online]. Available: <http://www.onsetcomp.com/products/data-loggers/u12-012>. [Accessed 1 July 2014].
- [15] SDS-Infrared, "HotFind-D," [Online]. Available: http://www.emtamericas.com/pdf/Satir_Hotfind.pdf. [Accessed 1 July 2014].

The thesis reports on the behaviour of wall elements made of high performance concrete with an integrated water-based radiant cooling and heating system and solution for ventilation based on a diffuse ceiling inlet for mechanical ventilation made of perforated gypsum boards. Methods applied in this work included measurements and numerical simulations. Measurements were carried out in the full scale test building. The test room represented a classroom with a high density of occupants. Theoretical investigations were carried out with a CFD model of the test room.

DTU Civil Engineering
Department of Civil Engineering
Technical University of Denmark

Brovej, Building 118
2800 Kgs. Lyngby
Telephone 45 25 17 00

www.byg.dtu.dk

ISBN: 9788778774217
ISSN: 1601-2917